Pacific Community
Communauté du Pacifique

TSUNAMI HAZARD ASSESSMENT
SAMOA CASE STUDY

Judith Giblin and Herve Damlamian
Pacific Community

Australian Aid
Australian Government
Geoscience Australia
PCRAFI PROGRAM
GEM
Geoscience, Energy and Maritime Division

TSUNAMI HAZARD ASSESSMENT
SAMOA CASE STUDY

Judith Giblin and Herve Damlamian
Pacific Community

Suva, Fiji, 2022

Original text: English

Pacific Community Cataloguing-in-publication data

Giblin, Judith

Tsunami Hazard Assessment: Samoa Case Study / Judith Giblin and Herve Damlamian

(SPC Technical Report SPC00069 / Pacific Community)

1. Tsunamis – Risk assessment – Samoa.
2. Natural disasters – Risk assessment – Samoa.
3. Sea level – Samoa.
4. Climatic changes – Samoa.
5. Coastal zone management – Samoa.
6. Cyclones – Samoa.
7. Ocean waves – Samoa.

I. Giblin, Judith II. Damlamian, Herve III. Title IV. Pacific Community

551.4637099614 AACR2

ISBN: 978-982-00-1445-9

Prepared for publication at SPC's Suva Regional Office, Private Mail Bag, Suva, Fiji, 2022
www.spc.int | spc@spc.int

Table of Contents

Glossary

Amplitude	Height of the tsunami wave crest above mean sea level.
Bathymetry	Measurement of water depth.
Deformation grid	Geospatial grid of the water surface deformation caused by the initial conditions of a tsunami generated from an earthquake.
Exceedance rate	The average frequency of occurrence. For instance, a tsunami with a return period of 100 years has a 1-in-100-year (0.01 or 1%) chance of being exceeded in one year (refer to return period).
Flow depth	Relates to the tsunami depth of water measured onshore in different locations.
Hazard point	Set of points in the ocean that PTHA18 has site-specific hazard information.
Inundation	Horizontal distance inland that a tsunami travels, measured perpendicular to the shoreline.
Maximum stage or Maxstage	Maximum water level that a particular tsunami attains at a particular location, ignoring tidal variation and assuming constant MSL.
Maximum stage exceedance rate	Describes 'how often' tsunamis occur with a maximum stage.
Mean sea level (MSL)	Averaged highest and lowest tides over a long period (usually at least 19 years). An important reference level as heights on land are measured in metres above MSL.
PCRAFI	Pacific Catastrophe Risk Assessment and Financing Initiative
PTHA18	Probabilistic Tsunami Hazard Assessment 2018
Return period	The average estimated length of time between hazardous events, such as earthquakes and tsunamis. For instance, 100-year return period. It is the inverse of the average frequency of occurrence (refer to *exceedance rate*).
Runup	Elevation of water reached by the tsunami, measured relative to datum such as MSL.
Source zone	The trenches and faults where earthquakes originate from.
Tsunami	Wave generated by a sudden disturbance of water. It is fast moving with a small amplitude in deep water but slows down and increases in height as it reaches shallow water.
Tsunamigenic	Earthquake capable of producing a tsunami (commonly along major subduction zone plate boundaries).
Wave time series	A series of tsunami waves that depict wave heights and arrival times for a given earthquake scenario at a particular hazard point.

Acknowledgements

This report was prepared under the PCRAFI project funded by the World Bank.
The report was prepared with contributions from many people who assisted during data processing.

The authors would like to express their appreciation and gratitude to the following organisations and individuals:

- Gareth Davies (GA), Cyprien Bosserelle (NIWA), Rikki Webber (GA), Kaya Wilson (GA), Antonio Hermosa (SPC), Moritz Wandres (SPC) and Naomi Jackson (SPC)
- Samoa Airborne Light Detection and Ranging (LIDAR) data availability.

Executive summary

The Pacific region faces risk of tsunami inundation due to its location within the Ring of Fire, a path of active volcanoes and frequent earthquakes caused by tectonic plate movement along the rim of the Pacific Ocean. Caused by earthquakes, submarine landslides, volcanic eruptions, explosions and meteorites, tsunamis are series of ocean waves generated by large disturbances of the ocean. Tsunamis have wavelengths ranging from 10 km to 500 km, with wave periods lasting five minutes to two hours. Tsunami waves become dangerous once they reach shallow waters near the coast as they go through the shoaling process where the oncoming tsunami wave slows down dramatically, becomes compressed and grows steeper due to the decreasing shoreline depth, sometimes creating 30-metre-high waves (SMS Tsunami Warning 2018; Bureau of Meteorology 2021).

Under the Pacific Catastrophe Risk Assessment and Financing Initiative (PCRAFI), a probabilistic tsunami inundation hazard assessment was carried out for Samoa. This tsunami hazard inundation assessment is restricted to tsunamigenic earthquake events. Utilising the 2018 regional Probabilistic Tsunami Hazard Assessment (PTHA18) database (Davies 2021) and the PCRAFI regional tsunami inundation assessment guidelines (Giblin et al. 2022), 68 events covering four return periods (100 years, 500 years, 1000 years and 2500 years 84th percentile) were extracted from the PTHA18 database. These events were modelled using BG-Flood (Block-adaptive on Graphics processing unit Flood model; Bosserelle 2021), a numerical model for simulating shallow water hydrodynamics on graphics processing units (GPUs). Prior to modelling these events, a sensitivity analysis was done to determine the resolution of the first level of bathymetry resolution, followed by validation of the model using the historical tsunami events of Samoa in 2009 and Japan in 2011.

The tsunami model has five levels of resolution (5 km, 1 km, 50 m, 10 m and 5 m, with the exception of the Kermadec-Tonga events as computation began at 1 km resolution grid due to Samoa's close proximity). Model computation took approximately two months to complete, with inundation output data at a national scale computed and stored with a 50 m resolution, community-scale output at 10 m resolution (South East Upolu) and urban-scale output at 5 m resolution (Apia, the capital city). The inundation data were then processed to generate six different types of information products to support risk-informed decision-making.

The first product type provides the aggregated maximum flow depth for a set of return periods (100 years, 500 years, 1000 years and 2500 years 84th percentile). This option is useful for future urban planning and evacuation planning purposes as it reveals heavily inundated coastal areas according to the likelihood of a tsunami occurring. The second product type provides the aggregated maximum flow depth for the four return periods inclusive of projected sea-level rise (projected 2100 level at shared socioeconomic pathway [SSP]5-8.5, with mean high spring water). The sea level inclusions are important for any key infrastructure development as the future likely impact of climate change on coastal zones will need to be considered.

The third product type provides the aggregated inundation extent for each trench/source and return period. The results reveal that the majority of highest flow depths for Samoa (50 m) and South East Upolu (10 m) are from scenarios that originate from the Kermadec-Tonga Trench. For Apia (5 m), the source giving the highest flow depth varies depending on the return period. For the 100-year return period, the majority of highest flow depths originate from Izu Mariana, for the 500-year return period, it is Alaska Aleutians, and for 1000-year and 2500-year (84th percentile) return periods, it is from the South America trench/source. This product type could support response planning by making provision for areas that are likely to be impacted depending on the origin and magnitude of the tsunamigenic earthquake.

The fourth product type provides possible damage grades for building structures depending on the flow depth by using a standard vulnerability scale, the Integrated Tsunami Intensity Scale (ITIS-2012) developed by Lekkas et al. (2013). The series of flow depth ranges (0.5–1 m, 1–2 m, 2–5 m, 5–7 m, 7–10 m and greater than 10 m) categorises the maximum grade of damage for building structures within the inundation areas. The fifth product type is designed to complement the first product type, providing the percentage of events that inundate an onshore location. An area that provides 100% event coverage reveals the location that holds the return period probability. Due to aggregating the events for each return period, determining probability becomes difficult as each event aggregated has that return period's chance. For instance, there are 15 events for a 1-in-2500-year return period. If all 15 events inundate a particular location, that location has an event percentage of 100% and truly reflects a 2500-year return period. Areas with an event percentage less than 100% do not share the same probability of 1-in-2500-year chance of tsunami inundation. The sixth product type provides the aggregated maximum flux at the national scale of Samoa (50 m resolution) for each return period.

Samoa's national tsunami hazard assessment study is the first for the Pacific under guidelines developed by PCRAFI and Geoscience Australia (GA) using the PTHA18 database. The inundation maps reveal that Samoa is exposed to a high inundation hazard level from tsunami events that originate from both near and distant sources. The modelled tsunami inundation results will be used to cross-check Samoa's evacuation procedures to verify that evacuation routes and assembly points are in the most appropriate locations. This assessment and its information products increase Samoa's tsunami risk knowledge and in turn, contribute to strengthening Samoa's tsunami preparedness.

Unsplash: Matt Paul Catalano

1.0 INTRODUCTION

1.1 Background

The Pacific Catastrophe Risk Assessment and Financing Initiative (PCRAFI) provides climate and disaster risk insurance to Pacific Island countries (PICs). The primary aim of PCRAFI is to assist participating governments to swiftly deliver relief efforts following a natural hazard event. The World Bank began implementing PCRAFI as a regional technical assistance activity in 2010 to provide a foundation for a regional catastrophe risk pool for PICs. A key component of PCRAFI is the Pacific Risk Information System (PacRIS), a regional hazard and national exposure data repository for disaster risk across 14 PICs. The second phase of PCRAFI involves updating the 2010 PacRIS datasets, ensuring the information remains accurate to protect household, business and government assets from exposure to disaster-related risks. The tsunami hazard work detailed in this paper aligns to the update of data in PacRIS.

1.2 Project objective

The objective of this technical component of the PCRAFI project is to improve and update PacRIS, thereby strengthening the capacity of PICs for disaster risk management. In contributing to this objective, a component under PCRAFI seeks to enable improvements in country-scale hazard information. Thus, the Pacific Community (SPC) proposed updating the tsunami inundation hazard information for Samoa, chiefly due to the availability of data from Samoa's country-scale comprehensive light detection and ranging system (LiDAR).

The tsunami inundation hazard mapping for Samoa draws on the regional 2018 Probabilistic Tsunami Hazard Assessment (PTHA18) database developed by Geoscience Australia (GA). PTHA18 provides the Pacific region with a catalogue of over 1 million possible tsunamigenic earthquake events/scenarios and associated return periods based on their inherent offshore tsunami wave heights around key locations throughout the region. PTHA18 data is freely accessible (Geoscience Australia 2021).

The Geoscience, Energy and Maritime Division of SPC conducted a probabilistic tsunami inundation hazard assessment for Samoa to support increased risk knowledge. More importantly, this study also aims to showcase the leap in increased risk knowledge and opportunity for risk-based decision-making available to countries that are investing in high-resolution and high-quality baseline data, such as LiDAR data. SPC aims to produce hazard maps to identify high hazard-prone areas, update the tsunami exposure data for Samoa, and deliver training to disseminate this risk knowledge to government decision-makers.

1.3 Purpose of this report

This report describes the methodology and results of the probabilistic tsunami inundation hazard assessment for Samoa. The tsunami inundation modelling was computed using BG-Flood (Block-adaptive on Graphics processing unit Flood model), a graphics processing unit (GPU)-based numerical model for simulating shallow water hydrodynamics (Bosserelle 2021). Based on earthquake deformation grids obtained using the PTHA18 database (Davies 2021) and following the regional guidelines for tsunami hazard assessment methodology (Giblin et al. 2022), 68 tsunamigenic earthquake events were identified and modelled using BG-Flood. This report outlines the tsunami scenario selection methodology, the tsunami software parameters used, and the data processing and analysis of the tsunami inundation outputs.

2.0 SAMOA TSUNAMI THREAT PROFILE

Located in the Pacific Ocean, Samoa comprises two main islands, Upolu and Savai'i. The capital city, Apia, is located on the central north coast of Upolu (Figure 1). According to the 2016 Census, the Samoan population reached 195,979, with approximately 78% residing in Upolu and 22% in Savai'i (Samoa Bureau of Statistics 2017).

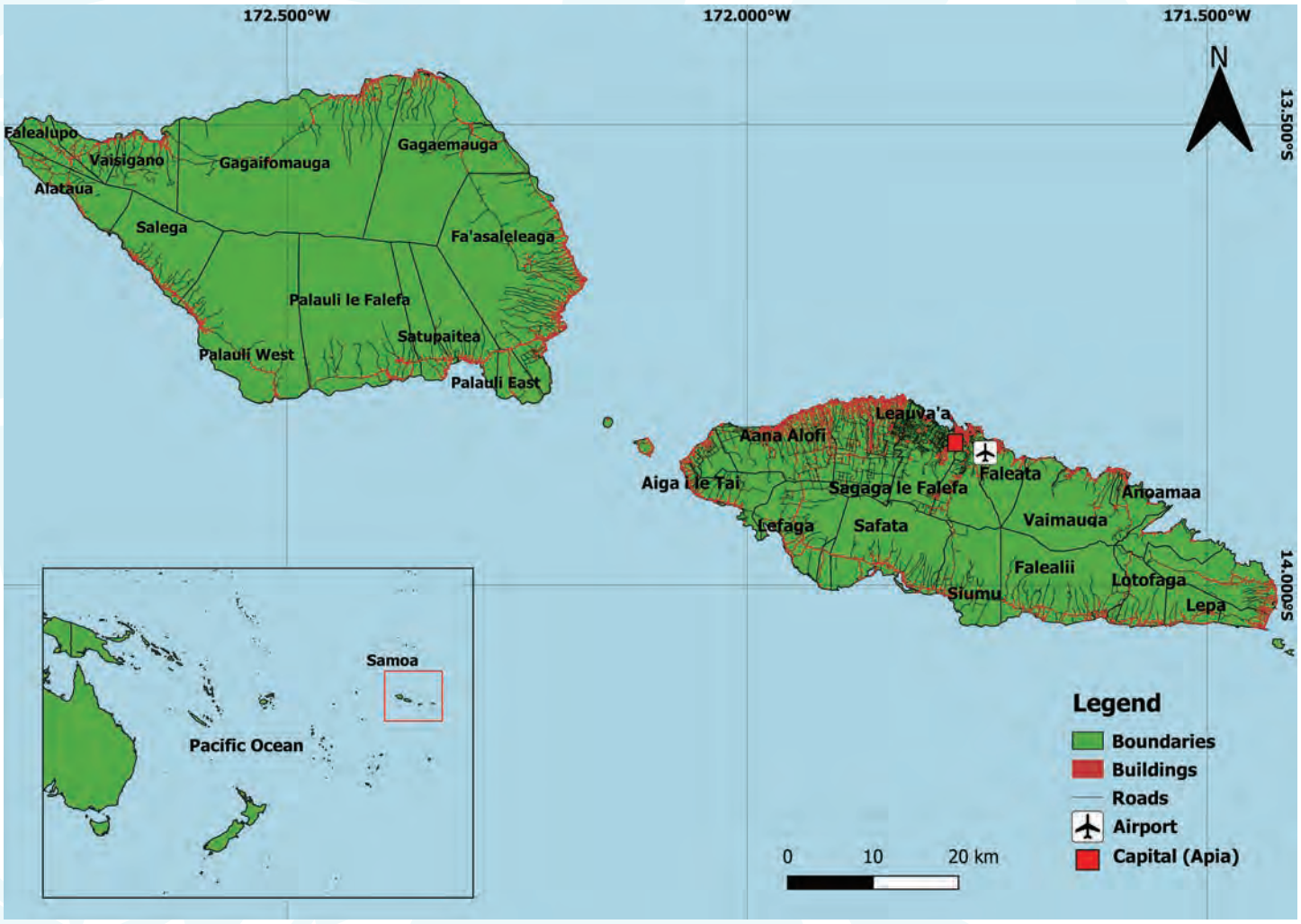

Figure 1: Map of Samoa

Samoa is located about 100 km north of the Kermadec-Tonga Trench, one of the most seismically active areas in the world (NCEI et al. 2017; Bosserelle et al. 2020). In the Kermadec-Tonga Trench, the Pacific Plate subducts beneath the Australia Plate at a rate of 6–9 cm/year (NCEI et al. 2017). The trench is oriented south–north and curves westward into the northern Lau Basin. Earthquakes occur along the subducting Pacific Plate on both sides of the trench, with focal depths extending to more than 600 km (NCEI et al. 2017).

In Samoa, the threat of inundation-related hazards such as tsunamis is extreme as approximately 70% of Samoa's population resides within coastal zones (Disaster Management Office 2017). The 2009 earthquake-generated tsunami that hit Samoa, American Samoa and Tonga led to widespread destruction and 149 fatalities in Samoa, highlighting the high risk of tsunami hazard to Samoa (Disaster Management Office 2017). The event was the most devastating tsunami in modern history for American Samoa, Samoa and Tonga, costing Samoa an estimated USD 166 million in damages (Table 1). Samoa also experienced a minor tsunami in 1981 and a volcanic eruption in 1907 (NCEI et al. 2017).

Historical tsunami records of damage and deaths in American Samoa, Samoa and Tonga

Date	Location	EQ Mag[1]	Tide Gauge[2] (m)			Eyewitness & Field Survey[3] (m)			Damage (in $million[4]) in			Deaths in		
			Am. Samoa	Samoa	Tonga	Am. Samoa	Samoa	Tonga	Am. Samoa	Samoa	Tonga	Am. Samoa	Samoa	Tonga
1865	Tonga Islands	8.0									Y			
1868	Northern Chile	8.5					1-3.0			Y			2	
1877	Northern Chile	8.3					0.9	3.6		Y				
1907	Matavanu Volcano						3.6			Y				
1917	Samoa Islands	8.3		0.3		2.4	0.4-12	4.2	Y	Y	Y		2	
1922	Northern Chile	8.7				0.9			Y					
1946	Unimak Island	8.6		0.3		0.8	1.2		Y					
1952	Kamchatka	9.0	0.9	0.9			1.4			Y				
1957	Andrean of Islands	8.6	0.2	0.2		1-2				Y				
1960	Southern Chile	9.5	0.8			1-2	4.9		0.4					
1981	Samoa Islands	7.7	0.1	0.1			1.0			Y			Y	
2009	Samoa Islands	8.1	2.7	0.8	0.2	1-18	0.4-15	1-22	140	166	10.5	34	149	9

1 Earthquake magnitudes (Ms or Mw) are instrumental (from USGS) or estimated based on intensity before 1900 (from NCEI).
2 Half of the maximum height (minus the normal tide) of a tsunami wave recorded at the coast by a tide gauge. Also called the amplitude.
3 The height of the tsunami at the point of maximum inundation above the state of the tide at the time. The measured value may be from eyewitness or field survey.
4 Adjusted for inflation to 2016 dollars.

Table 1: Historical tsunami records of damage and deaths in American Samoa, Samoa and Tonga (above). Historical tsunami observation comparison between maximum runup height for American Samoa, Samoa and Tonga with all the other events, obtained by tide gauge, eyewitnesses and field surveys (NCEI et al. 2017) (below).

Historical tsunami observations near the Tonga Trench

Location	29 September 2009			All Other Events			
	Maximum Runup Height (m)		Total Number of Runups	Maximum Runup Height (m)		Total Number of Runups	Total Number of Events
	Tide Gauge (m)	Eyewitness & Field Survey (m)		Tide Gauge (year)	Eyewitness & Field Survey (year)		
American Samoa	2.7	17.6	219	0.9 (1952)	2.4 (1917 & 1960)	74	68
Samoa	0.8	14.5	168	0.9 (1952)	12.2 (1917)	63	44
All of Tonga	0.2	22.4	74	0.6 (2011)	4.2 (1917)	24	21
Northeastern Tonga	-	22.4	68	-	2.7 (1917)	1	1

Local and regional tsunami source locations causing damage and/or deaths in American Samoa, Samoa and Tonga

Table 1 (top of previous page) provides a list of historical tsunamis that have caused damage and/or deaths in American Samoa, Samoa and Tonga with the year, location and earthquake magnitude. In the bottom table is a comparison of the catastrophic 2009 tsunami with all other tsunami events.

Figure 2 (right) provides the tsunami source locations of the historical events of 1865, 1917, 1981 and 2009. The 1907 event is the Matavano Volcano eruption on Savai'i Island, Samoa. Historical tsunami runup observations are presented on the following page in the figure on the left. Figure 3 (on the following page, right) illustrates the runup heights in metres for the 2009 tsunami that impacted Samoa, with the highest runup for Savai'i and Upolu at 8.2 m and 14.5 m, respectively.

The majority of tsunami waves observed in Samoa are from tsunamis that originate from distant sources, further than 1000 km from Samoa. Although the 2009 tsunamigenic earthquake event that originated at the Kermadec-Tonga Trench has been the most devastating tsunami, far distant sources such as Alaska Aleutians pose a tangible threat to Samoa as well.

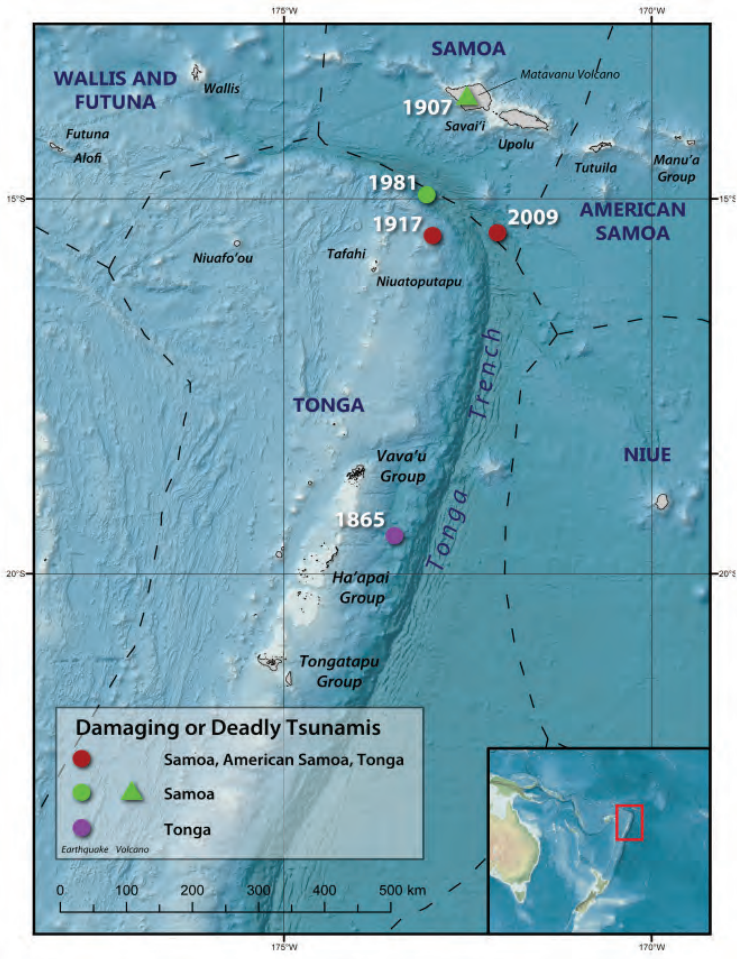

Figure 2: The source locations of the historical tsunamis in 1865, 1917, 1981 and 2009 that impacted American Samoa, Samoa and Tonga. A volcanic eruption was recorded in 1907 at Matavanu Volcano, Savai'i, Samoa (above). Historical runup height tsunami observations from the recorded events (NCEI et al. 2017) (right).

Historical tsunami observations near the Tonga Trench

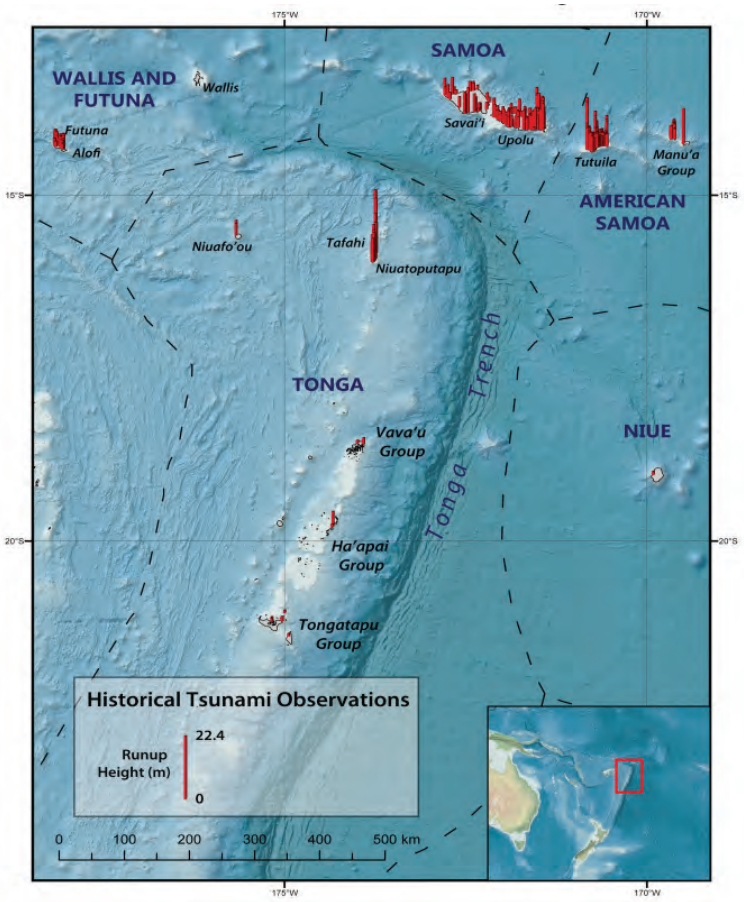

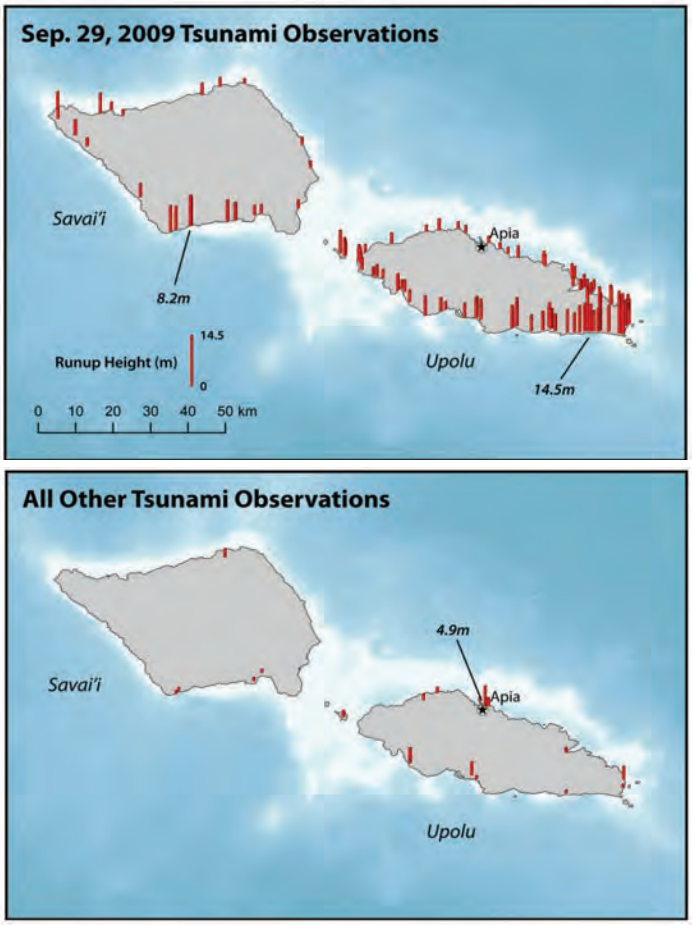

Figure 3: The September 29, 2009 runup height in metres according to observations obtained from the tide gauge, eyewitnesses and field surveys (top). Other tsunami observations acquired from the Apia tide gauge from the 1952 event and from eyewitnesses and field surveys for the 1917 event (NCEI et al. 2017) (bottom).

3.0 METHODOLOGY

3.1 PTHA18 database and scenario selection

PTHA18 estimates the likelihood of the maximum wave height (or stage) generated by potential (synthetic) tsunamigenic earthquakes around the Ring of Fire. PTHA18 has simulated hundreds of thousands of possible tsunamigenic earthquake scenarios from key sources within the Pacific and Indian Oceans, and these scenarios are freely accessible (Davies and Griffin 2018). Earthquake scenario data provided by PTHA18 include initial sea surface deformation and the resulting wave time series at a set of predefined 'hazard points'. Importantly, for each hazard point, PTHA18 also provides an estimate of the wave height's average-return-interval (Davies 2021).

Regional guidelines for applying the PTHA18 database in probabilistic tsunami inundation hazard assessment were finalised through a partnership between GA and SPC (Giblin et al. 2022). The guidelines aim to standardise probabilistic tsunami inundation hazard assessment within the Pacific region to enable PICs to better understand and mitigate tsunami risk. A regional tsunami hazard assessment scenario-based methodology utilising the PTHA18 database is included in the guidelines (Giblin et al. 2022). This methodology was applied to the Samoa case study. The PTHA18 instructions and code to undertake this assessment are located at the PTHA18 Github Repository (Davies 2021).

3.1.1 Probabilistic tsunami hazard assessment scenario selection

Two methods for probabilistic tsunami inundation hazard assessment are outlined in the regional guidelines (Giblin et al. 2022). The scenario-based approach was selected as the modeller has more control over the selected scenarios and thus it is less computationally intensive. This methodology searches the PTHA18 scenarios that satisfy the exceedance-rate criteria at one or more hazard points while producing smaller waves at the remaining sites. By combining multiple scenarios, a set of scenarios is generated for which the largest waves meet the exceedance rate at every hazard point of interest. After simulating the tsunami inundation for a set of scenarios, the inundation maxima are used to create inundation maps with a specified exceedance rate (Giblin et al. 2022).

The flowchart below summarises the recommended steps for undertaking a scenario-based approach using PTHA18 (Figure 4). The methodology requires access to the PTHA18 open-source database as well as expert judgement to tune the user-defined parameters to fit the purpose of the assessment. The tutorial on this methodology (multi-gauge scenario-selection) provides documentation and codes in detail.

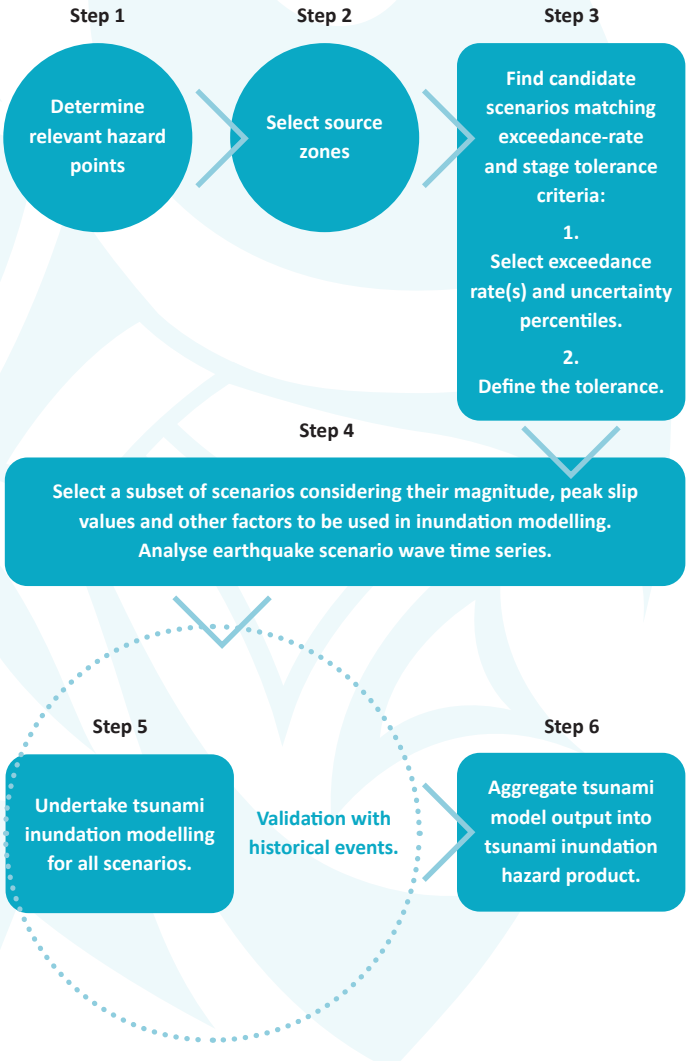

Figure 4: Summary of the tsunami inundation hazard assessment methodology. The beginning two steps requires researchers to access the PTHA18, while the remaining steps require user/experts decision gate (Giblin et al. 2022).

Step 1: Determine relevant hazard points

The first step is to identify the hazard point(s) closest to the study site. Global hazard point locations are available in PTHA18 (as csv or shapefile format). PTHA18 provides site-specific information for each hazard point, including tsunami wave time series for every corresponding earthquake scenario and initial sea surface deformation. Multiple hazard points are preferable for localised studies to ensure scenario selection is not reliant on a single site. Shallow water points (less than 100 m) or points close to the coast were avoided as the PTHA18 coarse-grid linear tsunami solver is not well suited for modelling shallow sites. In the case of Samoa, the PTHA18 database has 11 hazard points surrounding Samoa (Figure 5). Table 2 provides the geographical location and elevation of each point.

Point ID	Longitude	Latitude	Elevation
3097.3	187.029	-13.46	-3599.16
3098.3	187.354	-13.32	-3581.93
3099.3	187.746	-13.26	-1153.97
3100.3	187.990	-13.58	-1622.93
3101.3	188.341	-13.68	-2565.69
3102.3	188.698	-13.85	-3599.46
3103.3	188.658	-14.21	-2318.08
3093.3	188.274	-14.22	-3149.01
3094.3	187.898	-14.09	-1733.98
3095.3	187.553	-13.97	-2896.96
3096.3	187.212	-13.79	-2585.94

Table 2: Hazard point identification number with geographical location and elevation.

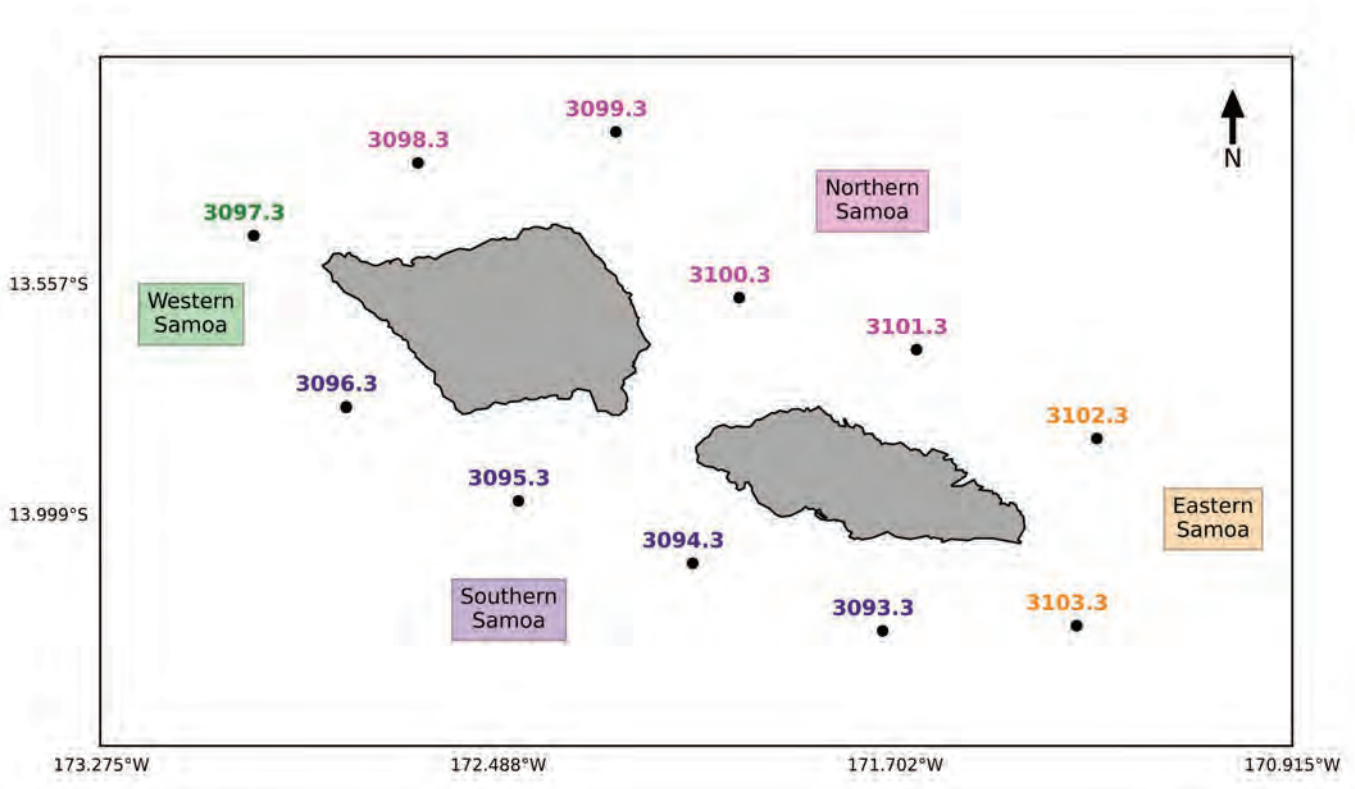

Figure 5: Location and identification number of the hazard points surrounding Samoa.

Step 2: Identify relevant source zones and choose earthquake slip type

The next step involves identifying and selecting the source zones most likely to contribute to the tsunami hazard. PTHA18 models the contribution of a major tsunami source zone to every offshore hazard point and through pre-computed source deaggregation plots (Figure 6). Source deaggregation plots are provided for each hazard point and can be downloaded as described. It is recommended that a conservative approach is taken by considering multiple source zones to account for island scale or inherent nearshore processes that may potentially be poorly resolved through the regional tsunami study. For instance, while assessing the probabilistic tsunami hazard for Apia, Outerrise Kermadec-Tonga was not shown as dominant in the pre-computed source deaggregation plots. With uncertainty in the ability of the regional model (due to coarse resolution) to adequately account for wave refraction around Upolu, the Outerrise Kermadec-Tonga source was included as a relevant source in the assessment. After reviewing each source deaggregation plot for the 11 hazard points and considering other source zones, a total of eight sources were identified as possibly providing a tsunami hazard to Samoa. These sources were Alaska Aleutians, Izu Mariana, Kermadec-Tonga, Kurils Japan, Mexico, New Hebrides, Outerrise Kermadec-Tonga and South America (Figure 7; Table 3).

In the multi-gauge scenario-selection script, each identified source zone is searched with a heterogenous-slip (HS) type. HS scenarios have a variable rupture area (similar to variable-area-uniform-slip [VAUS]) as well as spatially variable slip. Real earthquakes exhibit spatially variable slip, and the HS model aims to simulate that. The script also supports VAUS type. VAUS scenarios have uniform slip but a stochastic rupture area, which aims to represent the observation variability in earthquake magnitude-vs-area relationships. A given magnitude would have a range of existing scenarios varying between compact-area-high-slip scenarios to large-area-low-slip scenarios.

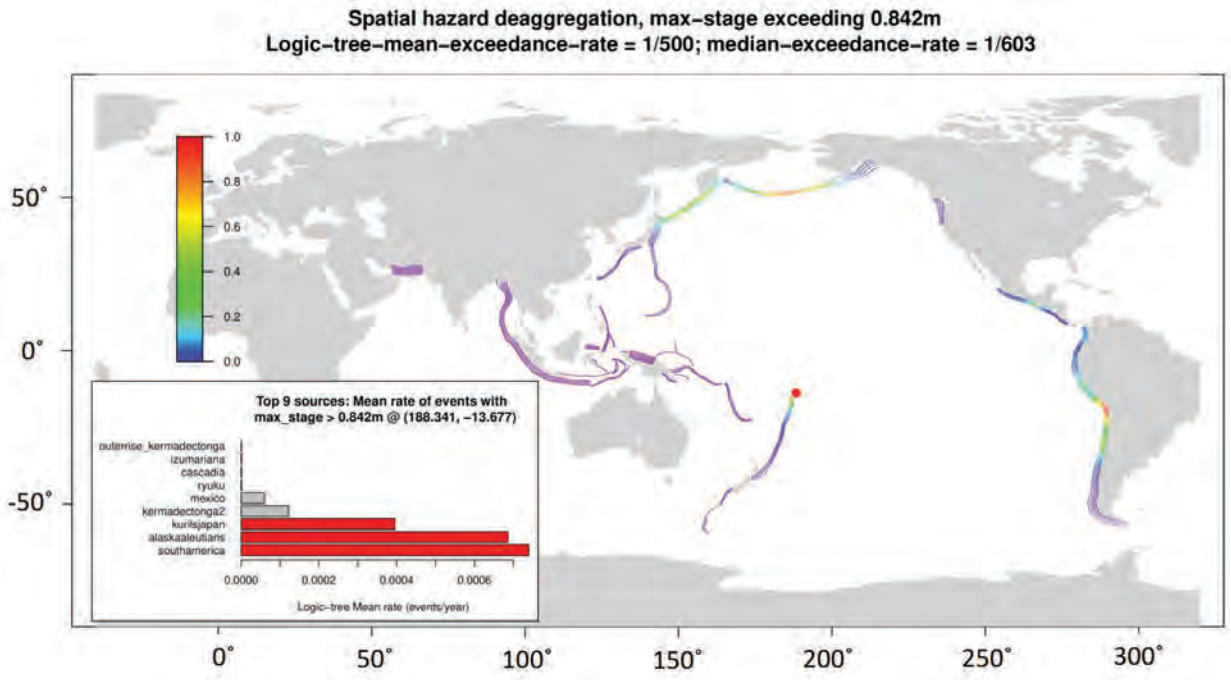

Figure 6: PTHA18 source deaggregation plot for hazard point 3101.3. The top six sources are identified as Alaska Aleutians, South America, Kurils Japan, Kermadec-Tonga, Mexico and Outerrise Kermadec-Tonga.

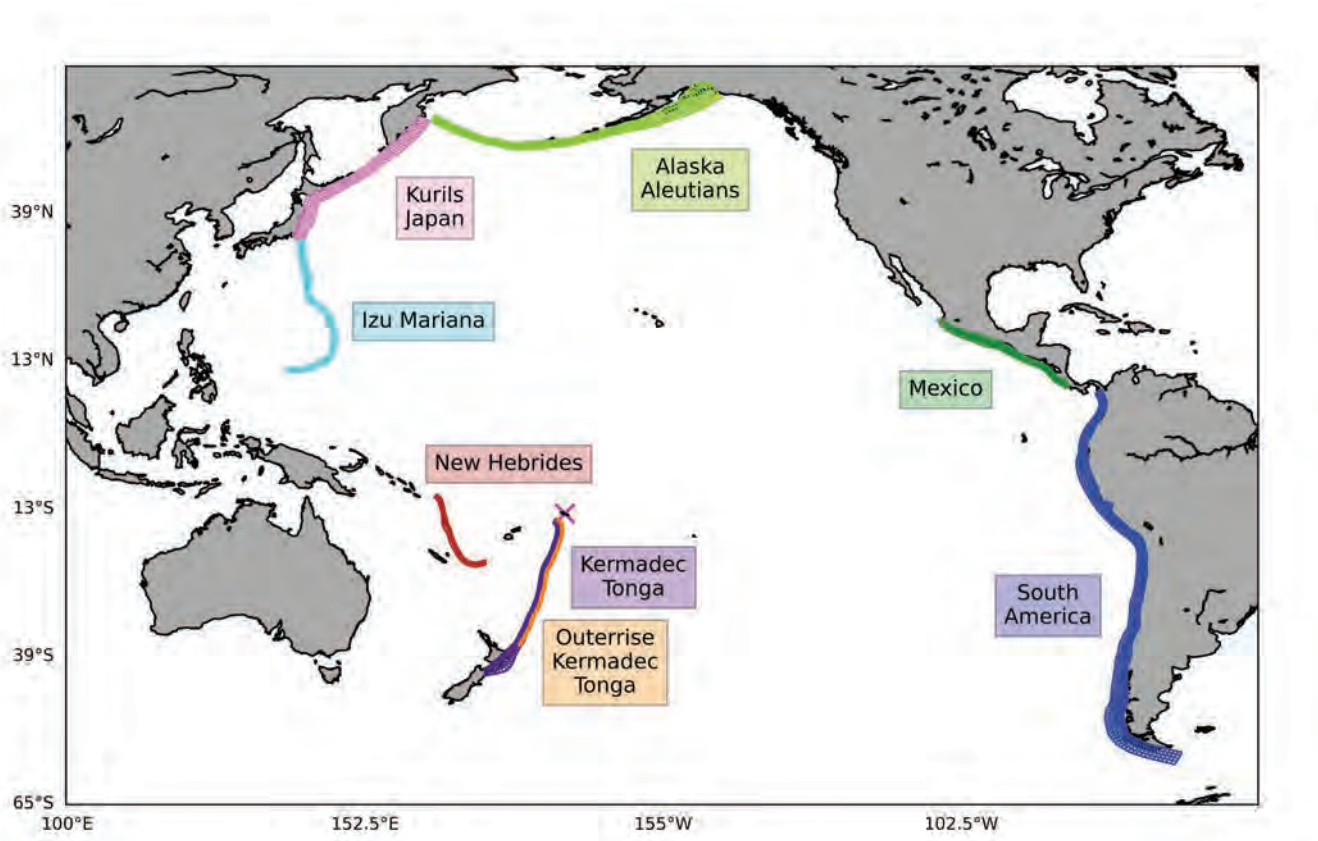

Figure 7: The source zones identified to provide the most tsunami hazard to the 11 hazard points surrounding Samoa. The sources are Alaska Aleutians, Izu Mariana, Kermadec-Tonga, Kurils Japan, Mexico, New Hebrides, Outerrise Kermadec-Tonga and South America.

No.	Source zone	Identification
1	Alaska Aleutians	PTHA18 source deaggregation identified for most of the 11 hazard points.
2	Izu Mariana	Orientation of the source zone is facing west Samoa.
3	Kermadec-Tonga	PTHA18 source deaggregation for southern hazard points and identified as a nearby source zone south of Samoa.
4	Kurils Japan	PTHA18 source deaggregation identified for most of the 11 hazard points.
5	Mexico	PTHA18 source deaggregation for one hazard point (3099.3).
6	New Hebrides	Located near Samoa.
7	Outerrise Kermadec-Tonga	PTHA18 source deaggregation for three hazard points (3093.3, 3095.3 & 3101.3).
8	South America	PTHA18 source deaggregation identified for most of the 11 hazard points.

Table 3: List of tsunamigenic earthquake source zones that will provide tsunami scenarios hazardous to Samoa.

Step 3: Identify candidate scenarios matching the exceedance rates of interest and stage tolerance criteria

1. Choose exceedance rate(s) of interest

The next step is to select a list of exceedance rates relevant to the assessment being undertaken. For each hazard point, the source deaggregation plots mentioned above include a tsunami maximum-stage exceedance rate curve and the associated uncertainty (Figure 8, bottom). The maximum stage exceedance rate describes how often a tsunami occurs with the maximum stage above a particular threshold value. The tsunami maximum stage is the maximum water level of a tsunami at a hazard point. Figure 8 below illustrates the maximum stage exceedance rate curve for hazard point 3101.3. This step was carried out on all 11 points surrounding Samoa. Generally, using the median is recommended, however if conservatism is desired, the 84th percentile is best.

PTHA18 provides an exceedance rate ranging from a 1/10-year event to 1/10,000-year event. For the Samoa case study, we selected four exceedance rates relevant to our assessment. Table 4 shows the exceedance rate and associated return period.

Exceedance rate (events/year)	Return period (year)
0.01	100
0.002	500
0.001	1000
0.0004 (84th percentile)	2500 (84th percentile)

Table 4: Exceedance rate and corresponding return period values selected for this assessment.

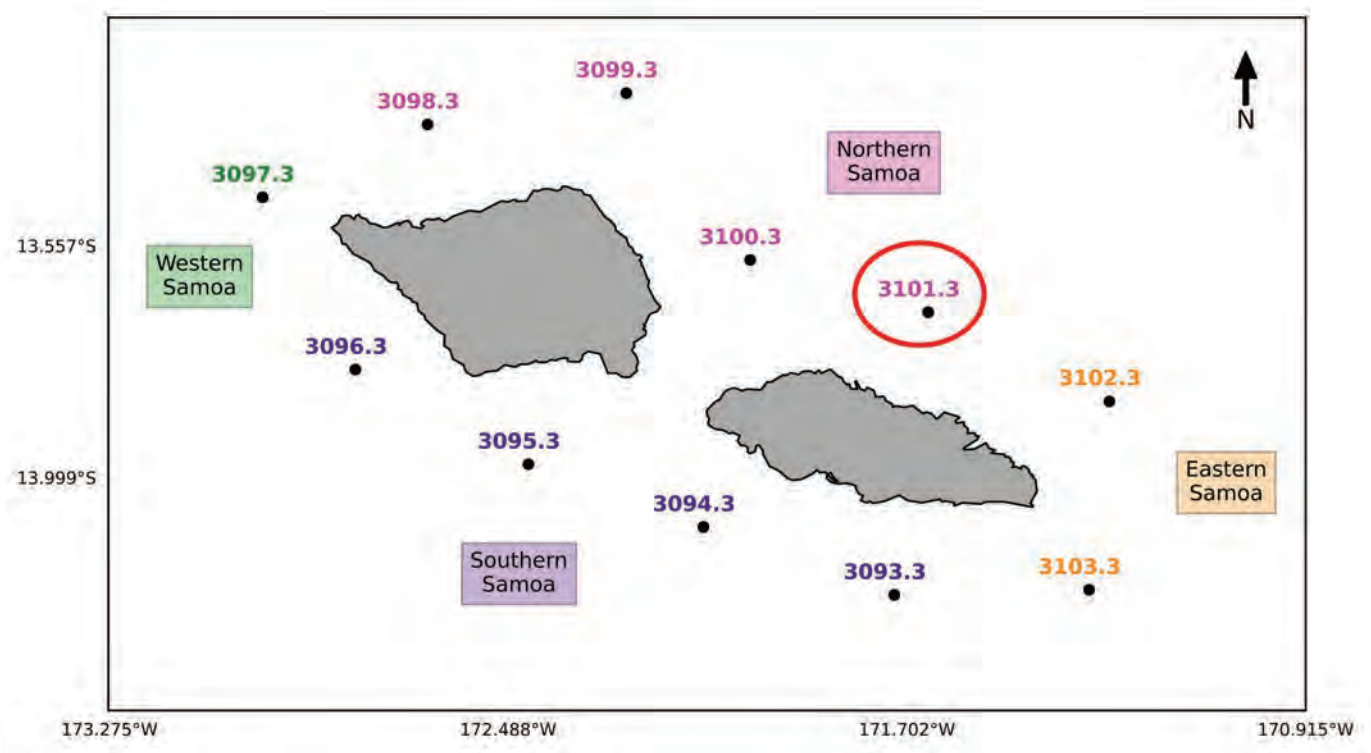

Figure 8: Location of hazard point 3101.3 (above). Maximum stage exceedance rate curve for hazard point 3101.3 (right).

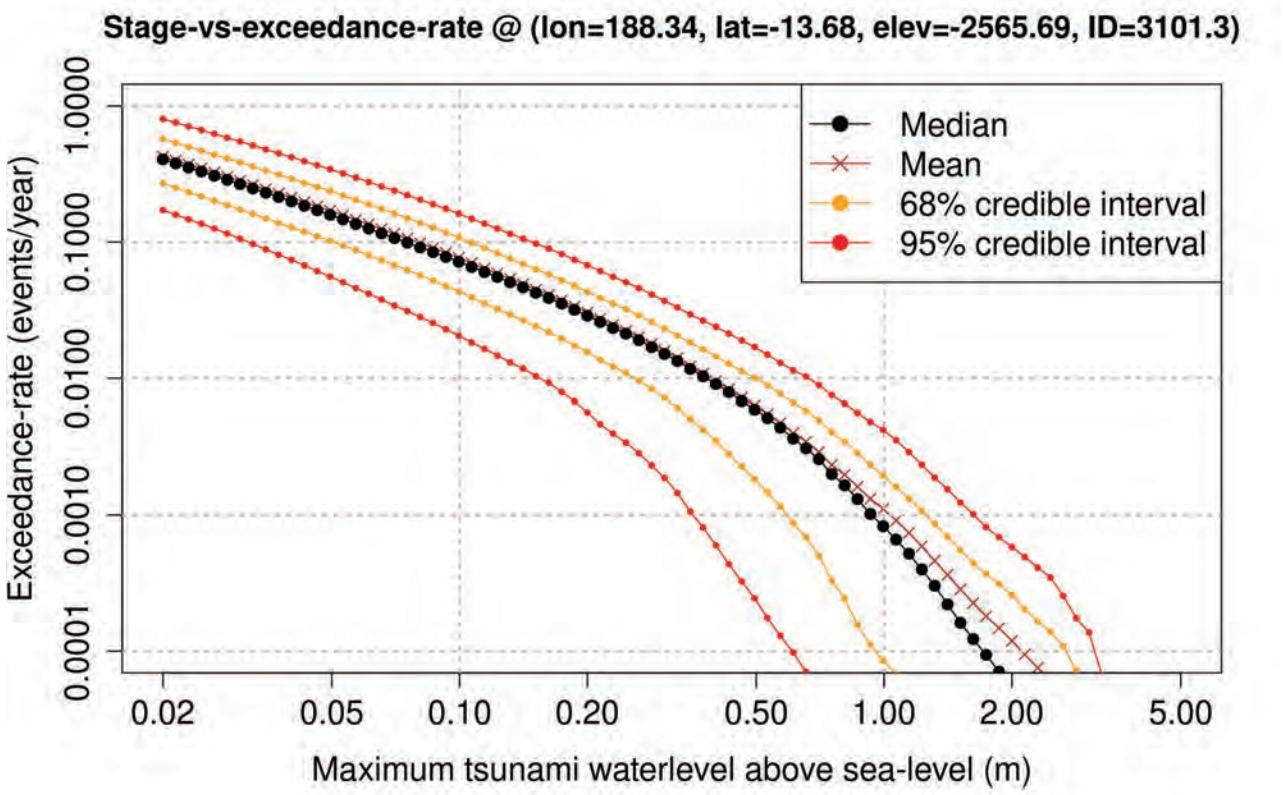

2. Produce a set of candidate scenarios by defining tolerance stage interval

For each exceedance rate, multiple scenarios from multiple source zones are selected, such that all offshore hazard points/gauges have at least one scenario with tsunami maxima close to the desired exceedance rate. Ultimately, through the collective scenarios, the maximum inundation from these scenarios should give an indication of inundation depths at the target exceedance rate.

It is unlikely to have scenarios that match exactly the desired exceedance rate, particularly with multiple gauges. Thus, a user-defined tolerance is specified by the researcher to determine how many scenarios are within a desired stage level. Table 5 provides the 500-year return period stage interval set at a user-defined 4% tolerance range for each of the 11 hazard points identified earlier. This tolerance value can be increased (or decreased) to generate more (or fewer) candidate scenarios. To ensure the offshore tsunami maxima is close to the target stage, it is recommended scenario tolerance values of 4–10% are considered.

Point ID	ER	Return period	Stage (m)	+/- 4% Stage interval
3093.3	0.002	500 years	0.962	0.924–1.000
3094.3	0.002	500 years	1.004	0.964–1.044
3095.3	0.002	500 years	0.949	0.911–0.987
3096.3	0.002	500 years	0.866	0.831–0.901
3097.3	0.002	500 years	0.737	0.708–0.766
3098.3	0.002	500 years	0.772	0.741–0.803
3099.3	0.002	500 years	0.748	0.718–0.778
3100.3	0.002	500 years	0.941	0.903–0.979
3101.3	0.002	500 years	0.803	0.771–0.835
3102.3	0.002	500 years	0.767	0.736–0.798
3103.3	0.002	500 years	0.903	0.867–0.939

Table 5: Stage interval of 4% for the exceedance rate of 0.002 or return period of 500 years.

The multi-gauge scenario-selection script is used to filter PTHA18 scenarios based on the chosen exceedance rate and tolerance interval for the selected source zone. Figure 9 is a graphical summary of various statistics to describe the scenarios originating from the Alaska Aleutians source at a 500-year return period and a 4% tolerance interval. The script is designed so that the filtered scenarios will not greatly exceed the desired stage level for any of the gauges/hazard points. Some scenarios may produce smaller than desired stage level (depicted in Figure 9b). Another feature in the script is specifying the minimum number of gauges/hazard points that must match the desired stage level. For this example, the minimum number of gauges/hazard points specified to match the desired stage level was three. At this stage of analysis, there is a reasonable set of candidate scenarios observed through the graphical summary to assist with further reduction of scenarios based on the researcher's subjective judgement in the next step.

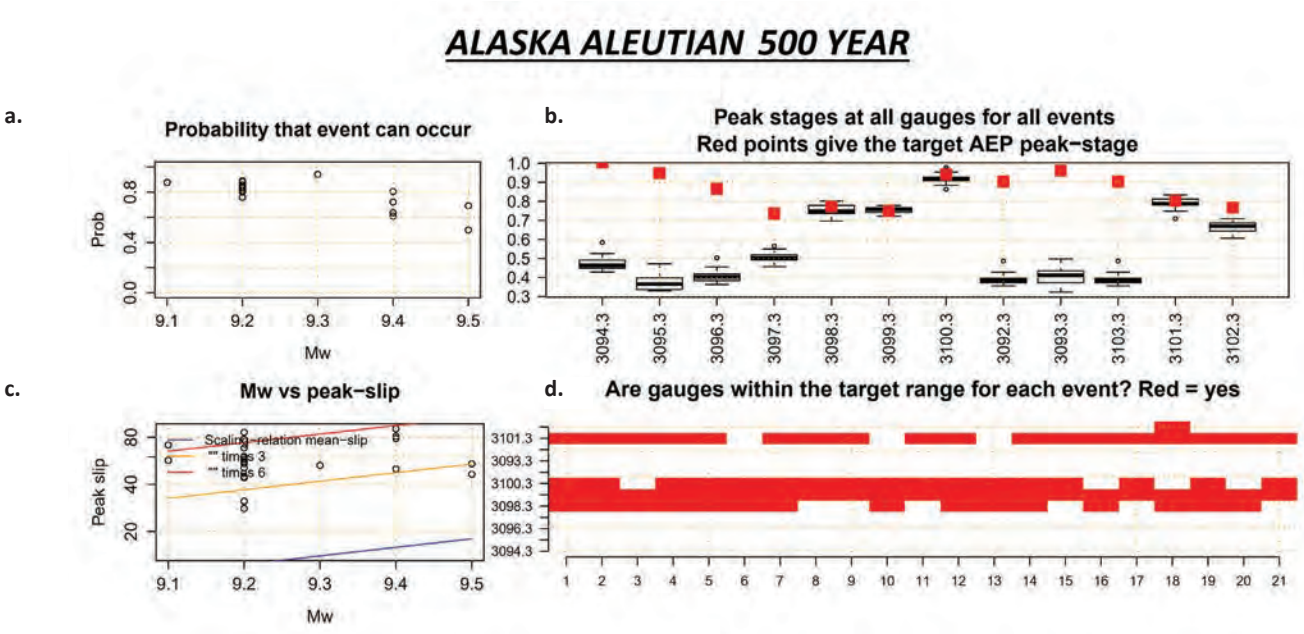

Figure 9: PTHA18 events/scenarios for the Alaska Aleutians source at a 500-year return period and a stage tolerance interval of 4%. a) Probability of the selected scenarios' event magnitudes occurring, Mw 9.1–9.5; b) Peak stage at all hazard points for all events. The hazard points 3083.3, 3099.3, 3100.3 and 3101.3 have peak stages within the interval; c) Event magnitude against peak slip; d) Events that have gauges/hazard points within the target stage interval; there are 21 events with a majority satisfying stage interval criteria for hazard points 3083.3,3099.3, 3100.3 and 3101.3.

Step 4: Subjective selection of the final set of scenarios to be used for inundation modelling

Selecting the final scenarios to be used for tsunami inundation modelling requires the researcher's judgement. The candidate scenarios identified in the previous step are available in the form of a graphical summary that provides various statistics for the candidate scenarios (further details are provided in the online tutorial). With the researcher's judgement, the scenarios are further refined by reviewing the scenario magnitude vs the probability that the scenario is possible according to PTHA18 (Figure 9a). As the maximum magnitude of any particular source zone is uncertain, it is generally not known whether large magnitude scenarios are even possible. Based on the Figure 9a plot, for the Alaska Aleutians 500-year return period, magnitudes less than 9.4 are considered plausible (> 50%), whereas scenarios with a magnitude of 9.5 are less favoured as PTHA18 suggests they have a less than 50% chance of occurring.

The scenarios identified are also refined by viewing their peak-slip and magnitude (Figure 9c). Figure 9c uses coloured lines for comparative purposes, with the blue line showing the average slip for a hypothetical uniform-slip earthquake, and orange and red lines showing the average slip multiplied by 3 and 6, respectively. For variable-area-uniform-slip earthquakes, high peak slip values correspond to compact earthquakes and vice versa. The heterogeneous-slip earthquake high peak slip values are also often associated with compact earthquakes but more generally indicate that the slip is concentrated on an asperity. In PTHA18, peak-slip values greater than 7.5 times the average blue slip line are not permitted, however, there is much uncertainty around this threshold. It is recommended that the researcher choose scenarios between the blue and red lines, depending on research preference.

It is recommended researchers favour an optimized set of scenarios for each source zone and return period that when combined, meet the stage interval requirement for all hazard points. To ensure majority/all the hazard points are included in the assessment, multiple events/scenarios may be selected. For instance, in Figure 9d, the Alaska Aleutians 500-year return period events/scenarios covered mainly four hazard points (3098.3, 3099.3, 3100.3 and 3101.3). The events in table 6 were selected based on their probability of event magnitude and on peak slip value.

Alaska Aleutian events – Northern point coverage

Source	Return period	Event ID	Mw	Slip peak	3098.3 (N)	3099.3 (N)	3100.3 (N)	3101.3 (N)
Alaska	500	58769	9.2	31.22				
Aleutians	500	57981	9.1	56.96				

Table 6: Alaska Aleutians 500-year return period events selected based on the probability of the event magnitude, peak slip value, and hazard point coverage. The two events covered the northern hazard points 3098.3, 3099.3, 3100.3 and 3101.3.

The wave time series for each event selected is analysed, ensuring the largest wave is at the beginning (Figure 10). This needs to be considered as the PTHA18 wave time series are derived using a frictionless linear model with 1 arcmin cell size (approximately 1.8 x 1.8 km^2 at the equator) and due to the coarseness, there are limitations and uncertainty in reliably simulating waves nearshore and thus it does not capture the slow dissipation of real tsunamis at a global scale (Davies 2021).

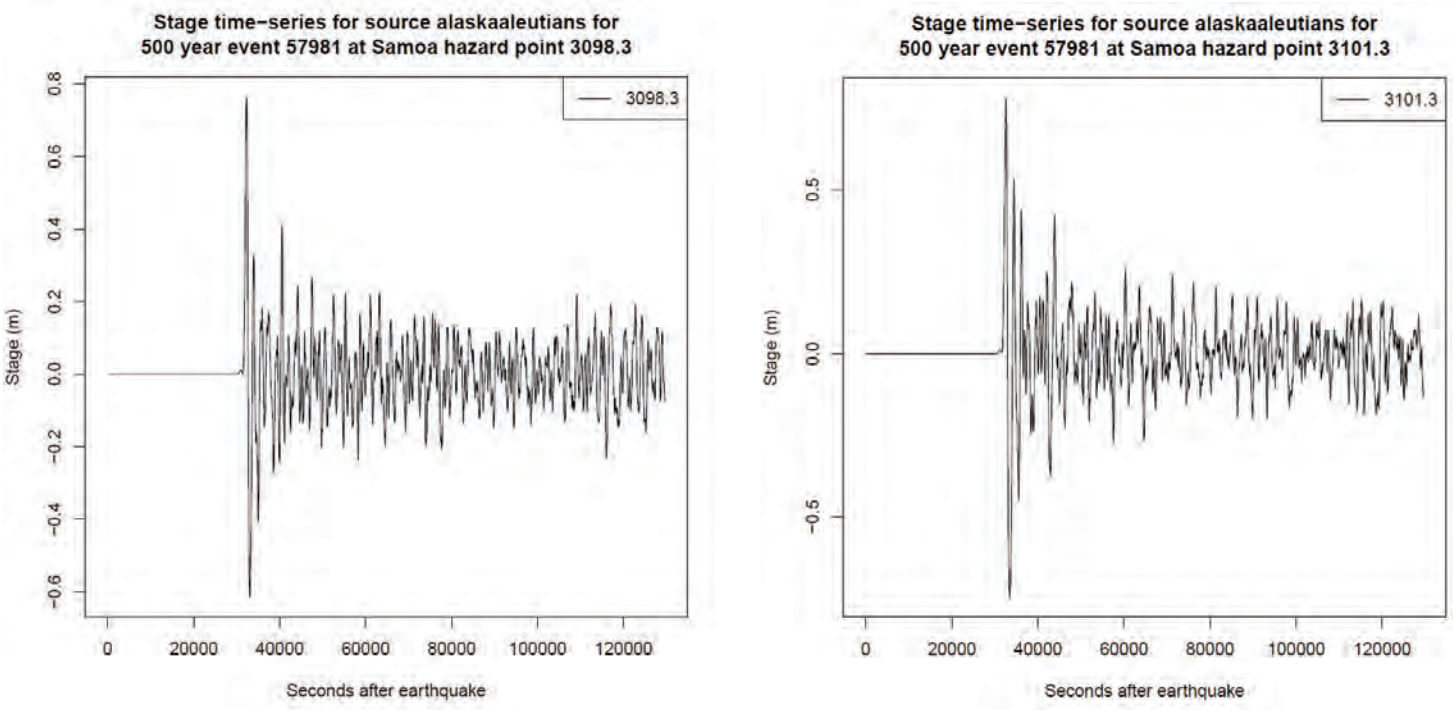

Figure 10: Wave time series plots for the Alaska Aleutians 500-year event number 57981 for hazard points 3098.3 (left) and 3101.3 (right).

The deformation grids for the selected scenarios/events are then extracted (Figure 11). Using the national scale tsunami hazard assessment methodology, 68 tsunami events were selected to provide probabilistic tsunami inundation hazard information for Samoa. Upon acquiring the tsunami events for the northern, eastern, southern and western hazard points around Samoa, it became apparent that certain source zones were dominant and provided events that covered the hazard points well, such as Alaska Aleutians and South America. However, there were other source zones, such as New Hebrides and Outerrise Kermadec-Tonga, that did not provide probable events that fit our selection criteria.

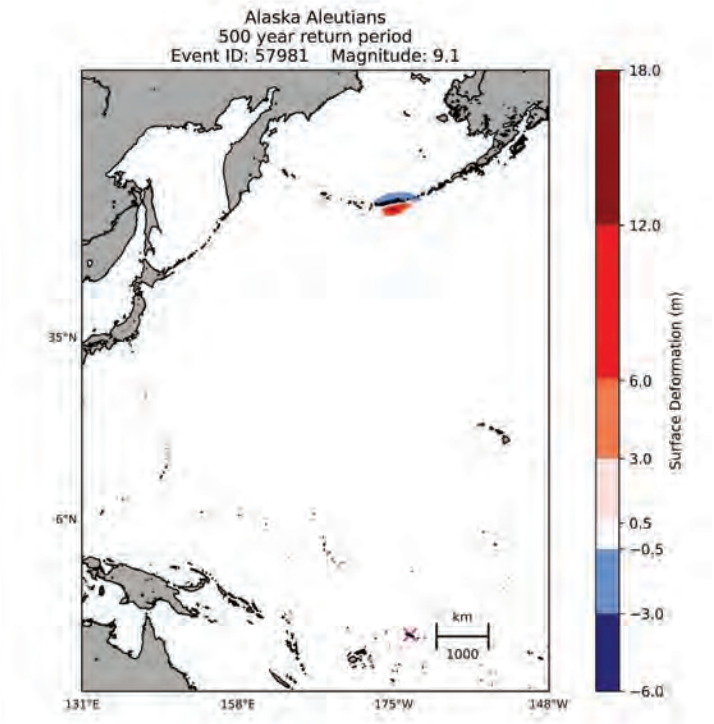

Figure 11: Earthquake scenario deformation grid for Alaska Aleutians 500-year event number 57981. Deformation grid orientation is towards Samoa. The pink cross marks the location of Samoa.

The dominant source zones identified were Alaska Aleutians, Kermadec-Tonga and South America, all of which provided events for each of the four return periods. Kurils Japan has events covering all the return periods except for 2500-year return period 84th percentile. Other sources, such as Izu Mariana and Mexico, only had probable events for 100-year and 500-year return periods. The remaining sources, New Hebrides and Outerrise Kermadec-Tonga, provided no realistic events meeting the stage interval requirement for 100-year return period, 500-year return period, 1000-year return period and 2500-year return period (84th percentile) events. The New Hebrides and Outerrise Kermadec-Tonga events that were within the 100-year return period stage interval revealed low probabilities (< 40%) and were thus considered unlikely to occur (Figure 12). As a result, no events/scenarios for those return periods were extracted for New Hebrides and Outerrise Kermadec-Tonga.

Samoa should still consider that earthquakes originating from New Hebrides and Outerrise Kermadec-Tonga could pose a risk and follow evacuation procedures. However, for this assessment, the PTHA18-based analysis indicated that Alaska Aleutians, Izu Mariana, Kurils Japan, Kermadec-Tonga, Mexico and South America would provide the set of conditions needed to assess tsunami hazard across Samoa for all selected return periods.

Table 7 provides a summary of the selected PTHA18 events for Samoa per source zone for each return period. The 68 events identified for Samoa using the probabilistic tsunami selection methodology are enumerated in Table 8 in accordance with their return period and source. More detailed information on these 68 events is available in Annex A.

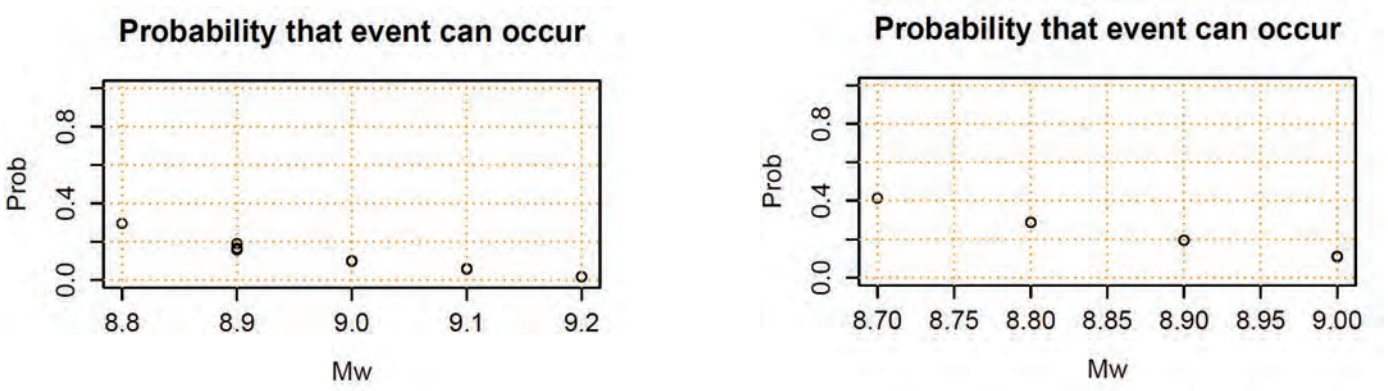

Figure 12: Plots that show the scenario magnitude versus the probability that the scenario is possible for events to occur at a 100-year return period for New Hebrides (left) and Outerrise Kermadec-Tonga (right). All possible 100-year return period events for these two sources had magnitudes with a low probability (< 40%) and were considered unlikely to occur.

Source	Return period (RP)	Notes
Alaska Aleutians	2500 years 84th percentile	Events cover northern and eastern Samoa for all RPs except 1000-year events which cover only northern Samoa. No events cover southern and western Samoa.
	1000 years	
	500 years	
	100 years	
Izu Mariana	2500 years 84th percentile	No events lie within the stage tolerance interval < 40%.
	1000 years	No events as they have a low probability of occurring.
	500 years	Events cover northern and western Samoa.
	100 years	Events cover northern, western and eastern Samoa.
Kermadec-Tonga	2500 years 84th percentile	Events cover southern, eastern and western Samoa for all RPs except 1000-year events which only have southern and eastern events. The 1000-year scenario covering western Samoa has a very low probability of occurring. No events for northern Samoa.
	1000 years	
	500 years	
	100 years	
Kurils Japan	2500 years 84th percentile	No events as they have a low probability of occurring. Events cover northern, western and eastern Samoa. No events for southern Samoa.
	1000 years	
	500 years	
	100 years	
Mexico	2500 years 84th percentile	No events as they have a very low probability of occurring.
	1000 years	
	500 years	Events cover only northern Samoa
	100 years	
New Hebrides	All RPs	No events as they have a very low probability of occurring.
Outerrise Kermadec-Tonga	All RPs	No events as they have a very low probability of occurring.
South America	2500 years 84th percentile	Events cover all of Samoa (northern, eastern, southern and western Samoa).
	1000 years	
	500 years	
	100 years	

Table 7: PTHA18 event summary for each source zone around Samoa per return period.

Source	100 years	500 years	1000 years	2500 years 84th percentile	Total (per source)
Alaska Aleutians	3	3	2	3	11
Izu Mariana	2	1	0	0	3
Kermadec-Tonga	4	5	3	3	15
Kurils Japan	4	3	3	0	10
Mexico	2	1	0	0	3
South America	6	5	6	9	26
Total (per RP)	**21**	**18**	**14**	**15**	**68**

Table 8: Number of events for each source per return period identified using probabilistic tsunami hazard assessment methodology for Samoa.

3.2 Tsunami modelling

The next step in the probabilistic tsunami inundation hazard assessment methodology is to undertake tsunami inundation modelling for the selected tsunamigenic earthquake events/scenarios. Prior to modelling inundation from the selected scenarios, the tsunami inundation model must be adequately set up and validated. To do so, a sensitivity analysis focusing on grid resolution as well as a model validation based on historical tsunami events were carried out.

For tsunami inundation modelling, the shock-capturing hydrodynamic model BG-Flood was used to simulate tsunami scenarios for Samoa (Bosserelle 2021). In its current version, BG-Flood computes shallow water hydrodynamic on GPUs with a nested grid system. BG-Flood documentation and codes are available here.

3.2.1 Model parameters

The BG-Flood model is configured using a 5 km coarse grid and four nested grids (1 km, 50 m, 10 m, 5 m) to simulate the PTHA18 68 tsunamigenic events. For each modelled event, simulation began with a 5 km resolution grid containing the earthquake deformation (Figure 13), with the exception of Kermadec-Tonga, which began at 1 km resolution due to its close proximity to Samoa (Figure 13c). The 5 km grid range was designed for each source zone to include the earthquake deformation and the four nested grids (Table 9). The output from the 5 km resolution tsunami simulation was fed into a 1 km resolution model surrounding Samoa (Figure 14a). The 5 km resolution and 1 km resolution were obtained from the ETOPO1 Global Relief Model.

The modelled events were further downscaled to a 50 m resolution for Samoa (Figure 14b). The 50 m grid was created with the 2012 LiDAR 5 m resolution bathymetry and topography data, and multibeam echosounder (MBES) 70 m grid from a 2004 bathymetry survey of Samoa conducted by the Pacific Islands Applied Geoscience Commission (SOPAC). ETOPO1 bathymetry was also used for the deep-water ocean. These datasets were merged at a 50 m resolution using Quickin software from Deltares.

The model was further nested at 10 m resolution for South East Upolu (Figure 14c) and 5 m resolution over Apia City, the capital of Apia (Figure 14d). The South East Upolu and Apia grids were created by merging the LiDAR and MBES data at their respective resolutions of 10 m and 5 m using Quickin software. In addition, the Manning's friction coefficient for land used in the 10 m and 5 m resolution models was set to a conservative value, meaning that the land was represented as bare land with no buildings or vegetation. This was chosen as a larger Manning's friction coefficient causes a delay in the tsunami arrival time for areas sheltered by vegetation or urban areas, and arrival time is an important aspect to consider for evacuation preparedness (Bricker et al. 2015). The conservative approach set elevation above -15 m to a friction coefficient of 0.01, while remaining elevation lower than -15 m was set to 0.0001.

Grids	Resolution	Lower	Upper	Lower	Upper
Alaska Aleutians	5 km	156.483	222.513	-28.513	68.517
Izu Mariana	5 km	130.483	198.513	-25.013	42.017
Kermadec-Tonga	1 km	162.495	198.505	-48.505	-7.495
Kurils Japan	5 km	130.983	197.013	-23.013	64.017
Mexico	5 km	181.483	285.513	-19.513	27.517
South America	5 km	179.983	305.013	-65.013	15.017
Ocean surrounding Samoa	1 km	173.495	203.505	-28.005	0.005
National Samoa	50 m	186.926	188.883	-14.392	-13.051
South East Upolu	10 m	188.291	188.603	-14.080	-13.968
Apia	5 m	188.184	188.284	-13.863	-13.771

Table 9: The bathymetry grid extents used in the BG Flood simulations.

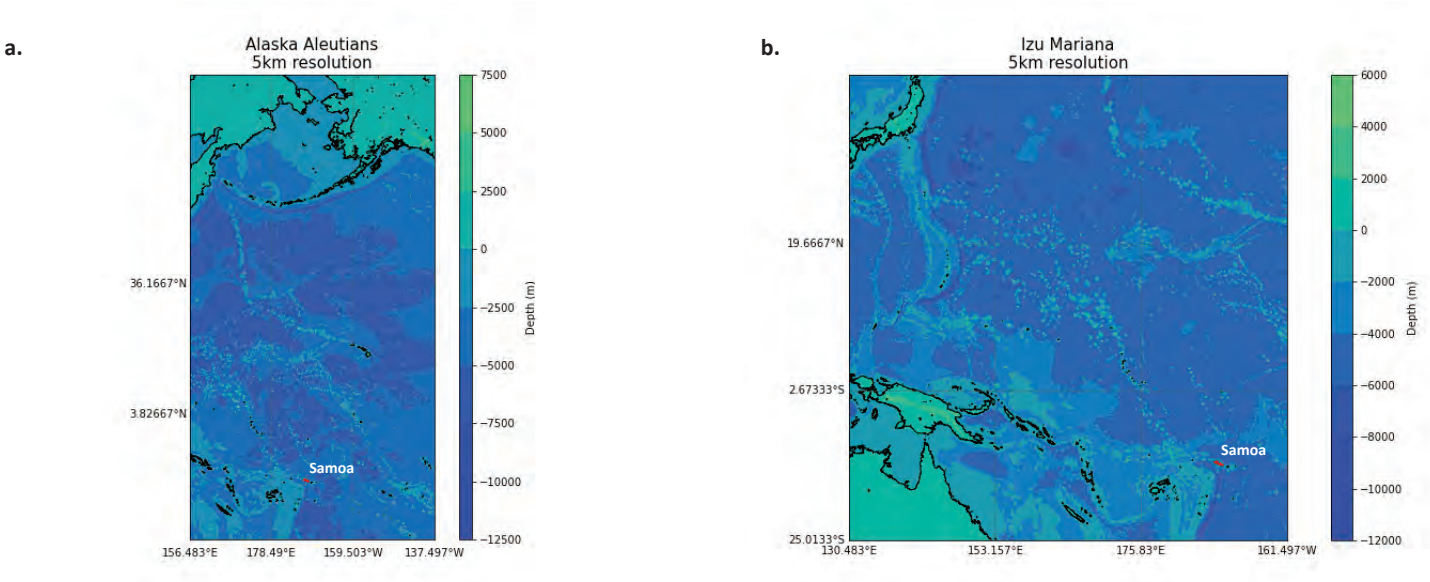

Figure 13: Bathymetry grids used for the computation of tsunamis in deep water for the following tsunamigenic sources: a) Alaska Aleutians 5 km, b) Izu Mariana 5 km (above), c) Kermadec-Tonga 1 km, d) Kurils Japan 5 km, e) Mexico 5 km and f) South America 5 km (right). Samoa is outlined in red in each of the plots.

c.

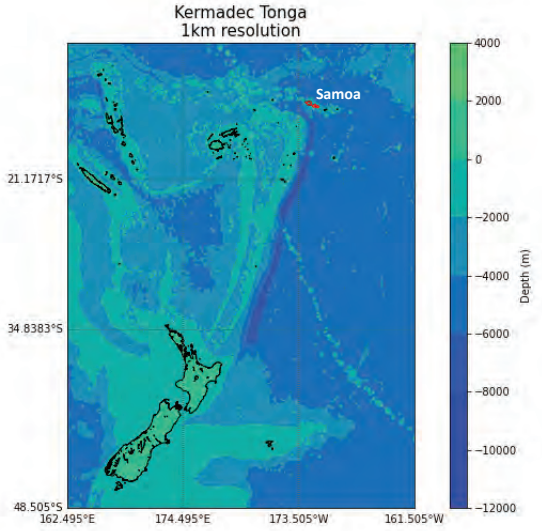
Kermadec Tonga
1km resolution
Samoa
21.1717°S
34.8383°S
48.505°S
162.495°E
174.495°E
173.505°W
161.505°W
4000
2000
0
−2000
−4000
−6000
−8000
−10000
−12000
Depth (m)

d.

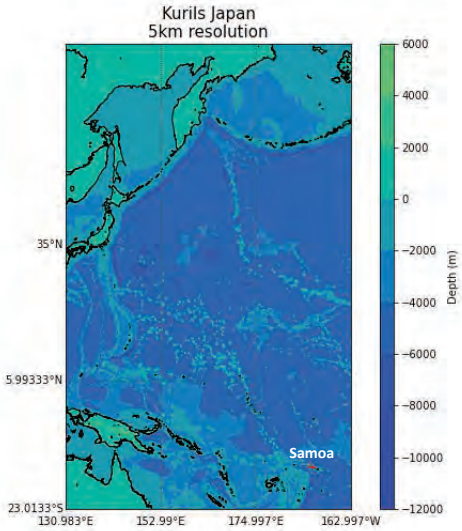
Kurils Japan
5km resolution
35°N
5.99333°N
23.0133°S
130.983°E
152.99°E
174.997°E
162.997°W
Samoa
6000
4000
2000
0
−2000
−4000
−6000
−8000
−10000
−12000
Depth (m)

e.

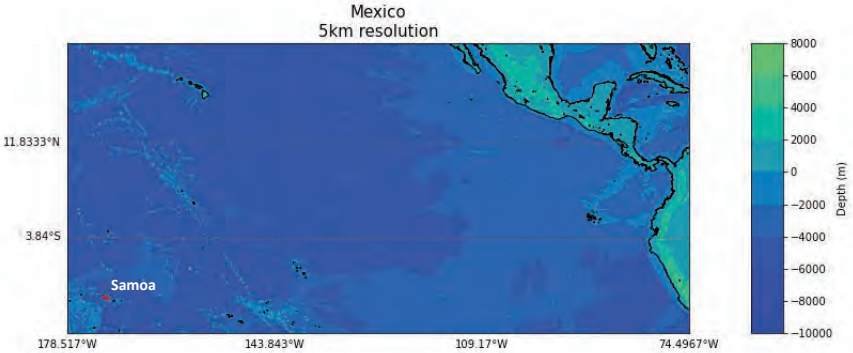
Mexico
5km resolution
11.8333°N
3.84°S
Samoa
178.517°W
143.843°W
109.17°W
74.4967°W
8000
6000
4000
2000
0
−2000
−4000
−6000
−8000
−10000
Depth (m)

f.

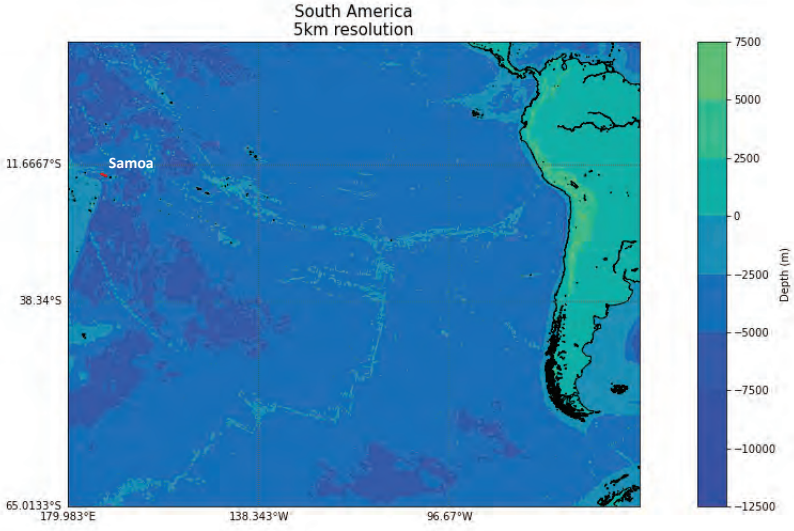
South America
5km resolution
11.6667°S
38.34°S
65.0133°S
179.983°E
138.343°W
96.67°W
Samoa
7500
5000
2500
0
−2500
−5000
−7500
−10000
−12500
Depth (m)

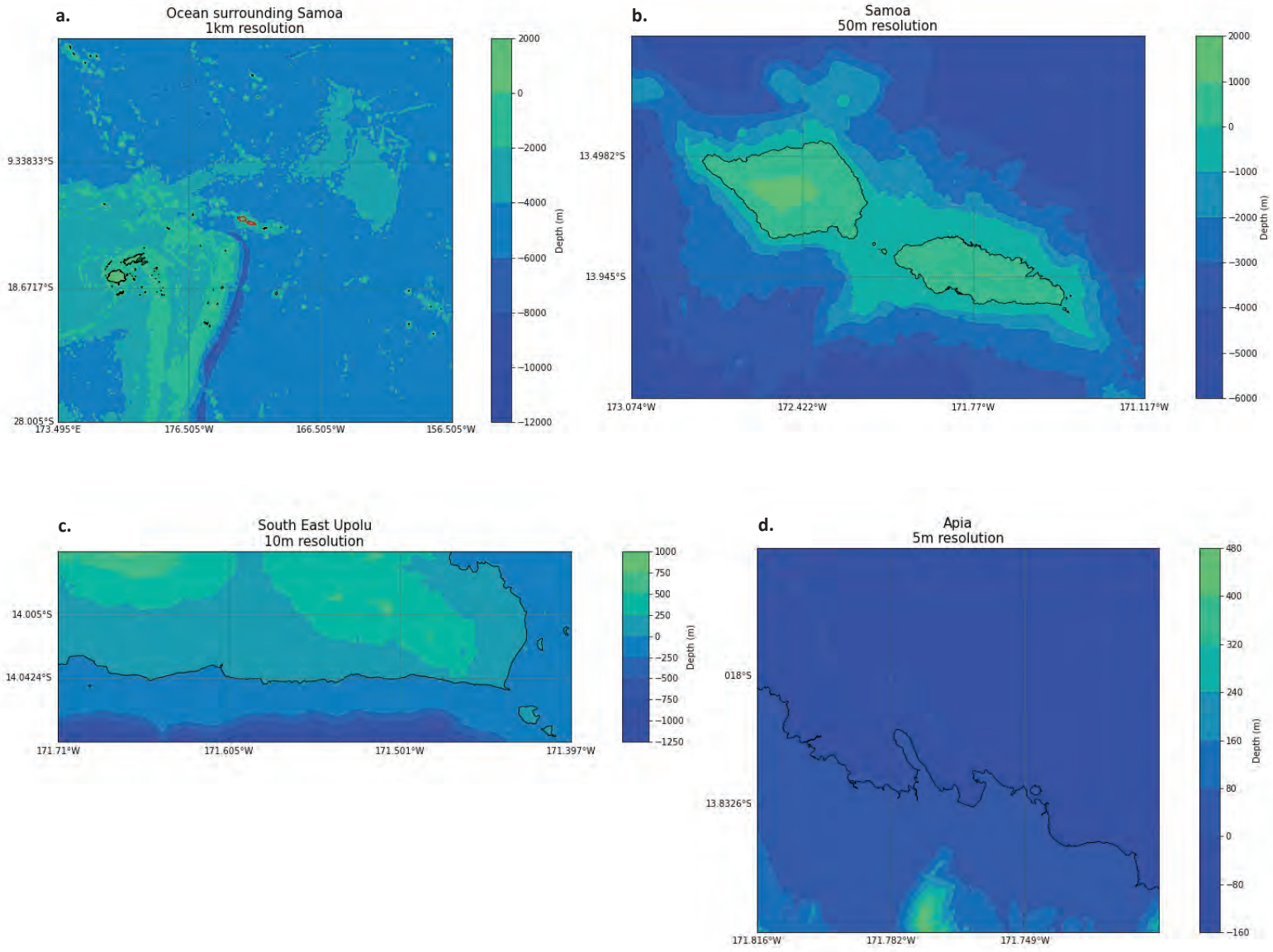

Figure 14: Nested bathymetry grids used in this study. a) Ocean surrounding Samoa 1 km (Samoa is outlined in red), b) Samoa 50 m, c) South East Upolu 10 m and d) Apia 5 m.

For 5 km, 1 km and 50 m resolution, the model was set to output relevant tsunami parameters every 60 seconds. The computation on the remaining nested grids (i.e., 10 m and 5 m resolution) was set up to output the parameters at the end of the model simulation to reduce the required storage space. The output parameters were specified in the model and used to determine the resulting flow depth and flow velocity (Table 10).

Output parameters	Definition	Unit
zs	Water level elevation above datum	Metres
zsmax	Maximum water level elevation above datum	Metres
uu	U velocity (at cell centre) zonal velocity positive right	Metres/second
vv	V velocity (at cell centre) meridional velocity positive right	Metres/second
hh	Water depth at cell centre	Metres
zb	Topography elevation above datum	Metres

Table 10: Output parameters and their definitions for zs, zsmax, uu, vv, hh and zb.

3.2.2 Sensitivity analysis

A sensitivity analysis was carried out to determine the most appropriate coarse grid resolution. The nested grids were fixed around Samoa at 1 km, 50 m, 10 m and 5 m, but a coarser grid is necessary as deformations occur at far distant sources, such as Alaska Aleutians and South America trenches which are located approximately 7300 km and 10,300 km away from Samoa. The coarse grid is required to propagate the tsunami wave from the earthquake source to the vicinity of Samoa. The sensitivity analysis identified the coarse grid resolution that could provide the best compromise on accuracy of wave propagation and the required storage space for the nested grid simulations. By comparing model output with resolutions ranging from 40 km all the way to 3 km, it was determined that a 5 km resolution would provide reasonable accuracy while utilising our maximum storage capacity. Figure 15 gives the wave time series for a modelled event with various computational grid (7 km, 6 km, 5 km and 3 km) resolutions. The wave time series was extracted for a location north of Samoa from the coarse grid simulation of the PTHA18 event from Alaska Aleutians, event identification number 60559, magnitude 9.4 and return period of 1000 years. The 3 km computational grid shows more detail than the 5 km, however, the 5 km was chosen as it depicts the wave time series well and takes less storage space than 3 km.

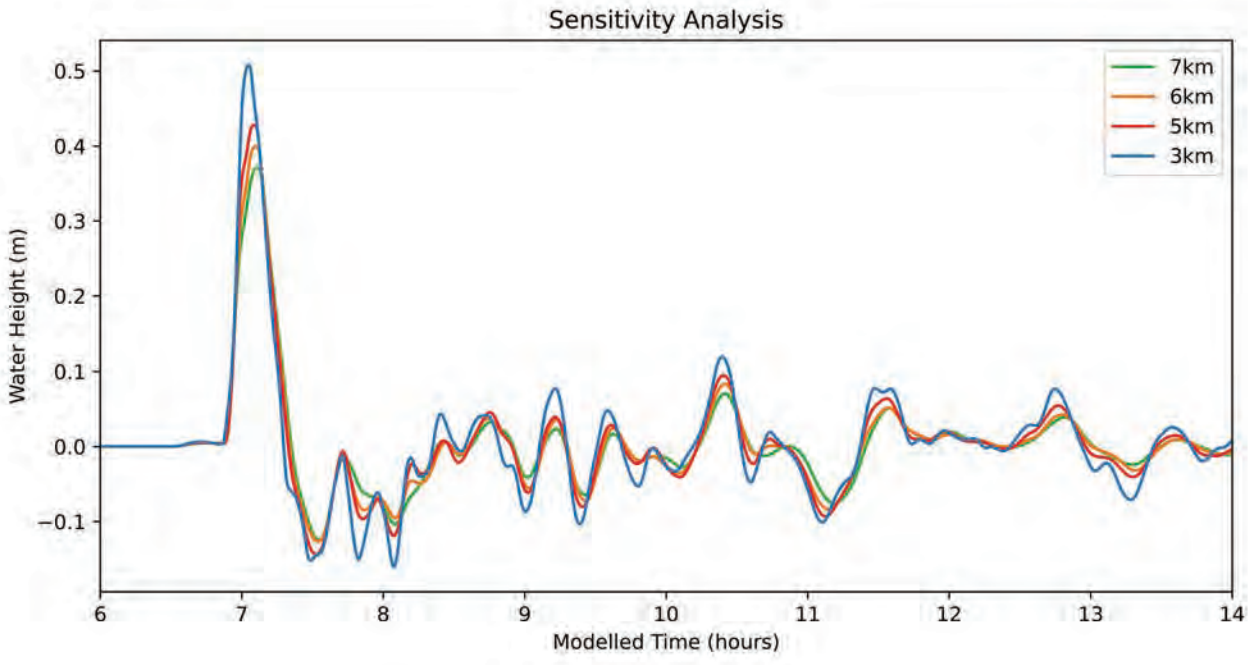

Figure 15: Sensitivity analysis plot for the wave time series extracted at a location north of Samoa at a 7 km, 6 km, 5 km and 3 km grid resolution. Simulation of PTHA18 event 60559 from Alaska Aleutians source, magnitude 9.4 and return period 1000 years.

3.2.3 Model validation

The BG-Flood tsunami model was validated using two historical events:

1. The September 29, 2009 magnitude 8.1 Samoa tsunami event.
2. The March 11, 2011 magnitude 9.1 Tohoku, Japan tsunami event.

On September 29, 2009 a tsunami wave was generated by a Mw 8.1 earthquake sequence near the northern end of the Kermadec-Tonga subduction zone, east of the Kermadec-Tonga Trench (USGS 2021). This earthquake sequence was initiated by an intraplate normal faulting in the outer rise oceanic plate and a major interplate reverse faulting that occurred nearly simultaneously (within two minutes of each other) (Beavan et al. 2010; Bosserelle et al. 2020; Fan et al. 2016; Hossen et al. 2017; Lay et al. 2010). The combined faulting caused a tsunami that inundated American Samoa, Samoa and Tonga, with 149 fatalities and USD 166 million in economic loss reported for Samoa (Hossen et al. 2017). Table 1 provides 2009 tsunami data for Samoa gathered from various sources, including tide gauges, eyewitness and field surveys. Figure 3 shows the 2009 Samoa tsunami runup heights in metres.

The other tsunami used for model validation is the March 11, 2011 Tohoku earthquake that occurred northeast of Honshu, Japan. This earthquake resulted from a shallow thrust faulting on the subduction zone plate boundary between the Pacific and North America Plates. A tsunami was generated by the earthquake, arriving at the northeast Honshu coast within 30 minutes. The Great East Japan earthquake and tsunami resulted in over 15,899 deaths, 2527 missing and presumed dead, and 6157 injuries. A maximum wave height of almost 40 m was reported in Iwate Prefecture, with a 2000-km stretch of Japan's coast impacted by the tsunami. Damages associated with the Japan tsunami were estimated at USD 220 billion (NCEI 2021).

3.2.3.1 Samoa 2009 tsunami

For the 2009 Samoa tsunami model validation, 12 events were extracted from the PTHA18 database that best fit the historical 2009 tsunami earthquake event (Table 11). The 12 events were selected based on their goodness-of-fit with historical Deep-ocean Assessment and Reporting of Tsunamis (DART) buoy data. These scenarios were first simulated at a 1 km resolution to compare modelled data with tsunami observations. The 1 km resolution was chosen due to the proximity of Kermadec-Tonga events to Samoa and is consistent with our modelling approach.

Further simulations were also carried out following three other earthquake parameters provided in Hossen et al. (2017), Lay et al. (2010), and Zhou et al. (2012). The earthquake parameters in Zhou et al. (2012) included three thrust faulting and two normal faulting unit sources (Table 12). The parameters selected by Hossen et al. (2017) and Lay et al. (2010) Version C were based on BG-Flood simulations by Bosserelle et al. (2020), who found that these two sources were most consistent with the 2009 post-disaster survey data.

Historical event	Source	Slip type	Event identification
2009 Samoa Tsunami	Kermadec-Tonga	Heterogeneous slip (HS)	24563
		HS	28606
		HS	28678
		Heterogeneous slip model with variable shear modulus (HSvaryMu)	30715
		HSvaryMu	32759
		HSvaryMu	32783
		Variable area uniform slip (VAUS)	26557
		VAUS	26623
		VAUS	28657
		Variable area uniform slip model with variable shear modulus (VAUSvaryMu)	30747
		VAUSvaryMu	32752
		VAUSvaryMu	32755

Table 11: PTHA18 scenarios best fit to the historical 2009 Samoa tsunamigenic event.

Table 11 provides the 12 PTHA18 scenarios with their respective slip type and event identification number, and Table 12 lists the source parameters from the articles by Hossen et al. (2017), Lay et al. (2010) Version C and Zhou et al. (2012). These PTHA18 events and the source parameters from the three articles were used to create a deformation grid that was input into BG-Flood to simulate the tsunami propagation. From these simulations, the simulated wave time series for the Apia tide gauge and DART buoy (identification numbers 51425 and 51426) data were extracted and compared with the 2009 observations of Apia tide gauge and DART buoy data 51425 and 51426. In addition, the model output runup and flow depth heights were compared to 2009 field survey and eyewitness accounts.

Article		Length (km)	Width (km)	Strike (deg)	Dip (deg)	Rake (deg)	Slip (m)	Depth (km)	Longitude	Latitude	Rupture initiation	Rise time (s)
Hossen et al. (2017)	1	130	50	315	25	-99	6.1	18	199	-15.5	3	60
	2	50	50	180	29	90	7.9	18	187.6	-16	49	40
Lay et al. (2010) Version C	1	130	50	324	65	-85	10.2	18	188	-15.5	3	60
	2	50	50	175	29	90	4.7	18	187.6	-16	49	40
	3	50	50	180	29	90	4.7	18	187.6	-16	90	40
Zhou et al. (2012)	S1	100	50	182.13	15	90	4.7	13.41	186.78	16.26		
	S2	100	50	182.13	9.68	90	6.5	5	187.23	16.28		
	S3	100	50	149.85	8.24	90	4.5	5	187.19	15.64		
	S4	100	50	7.62	57.06	-90	1.5	6.57	187.97	16.50		
	S5	100	50	342.45	57.06	-90	3.6	6.57	186.88	15.63		

Table 12: Tsunamigenic earthquake parameters from Hossen et al. (2017), Lay et al. (2010) Version C, and Zhou et al. (2012) used for historical validation for the 2009 Samoa tsunami.

3.2.3.2 Samoa 2009 tsunami historical data comparison

The model validation simulations output water levels at the Apia tide gauge location and at DART buoy locations 51425 and 51426, including flow depth heights for South Upolu, that can be compared with historical in-situ tsunami observations. The 12 PTHA18 scenarios and the earthquake parameters from the three articles (15 scenarios in total) were first simulated at 1 km resolution. Following the 1 km simulation, a nested grid of 50 m resolution was used to simulate the 2009 tsunami wave at the Apia tide gauge for all scenarios. Of the 12 PTHA18 events, a root mean square error (RMSE) was calculated to determine the five PTHA18 events that best match the historical in-situ observations. These five PTHA18 events were heterogeneous slip (HS) event ID 28606, HS event ID 28678, heterogeneous slip model with variable shear modulus (HSvaryMu) event ID 30715, HSvaryMu event ID 32759 and HSvaryMu event ID 32783 (Figure 16).

Figure 16 below shows the five PTHA18 events that best fit the Apia tide gauge observations. Figure 16 reveals that the PTHA18 modelled scenarios do not exactly reflect the intricacies of the tsunamigenic events. Although they represent the arrival time and wave period well, the fit with wave amplitudes is not as good. The HSvaryMu events ID 32759 and 32783 best fit the arrival time and wave period for the initial three waves that were recorded in the historical 2009 in-situ Apia tide gauge observations.

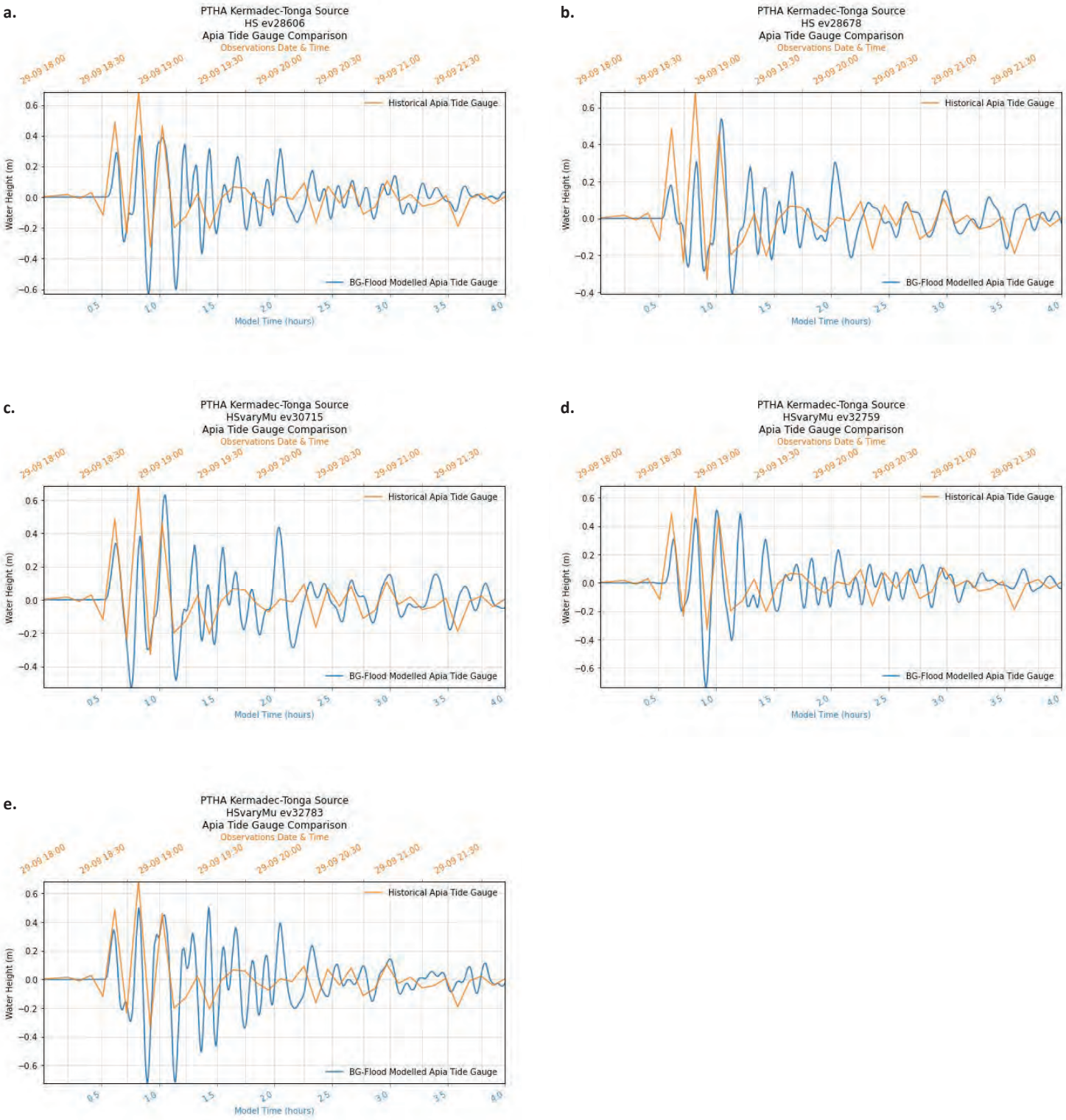

Figure 16: Apia tide gauge comparison of the five best PTHA18 modelled events against the historical observations for the 2009 Samoa tsunami. The five PTHA18 events originated from the Kermadec-Tonga source. The slip type and event identification (ID) numbers were: a) heterogeneous slip with constant shear modulus (HS) event ID 28606, b) HS event ID 28678, c) heterogeneous slip with variable shear modulus (HSvaryMu) event ID 30715, d) HSvaryMu event ID 32759 and e) HSvaryMu event ID 32783.

A nested grid of 50 m resolution was also used to simulate the 2009 tsunami wave at the Apia tide gauge. The modelled Apia tide gauge and historical in-situ observation comparison is provided in Figure 17. The figure shows that even though the results do not match exactly, three peaks in Hossen et al. (2017), Lay et al. (2010) Version C and Zhou et al. (2012) align with the historical data.

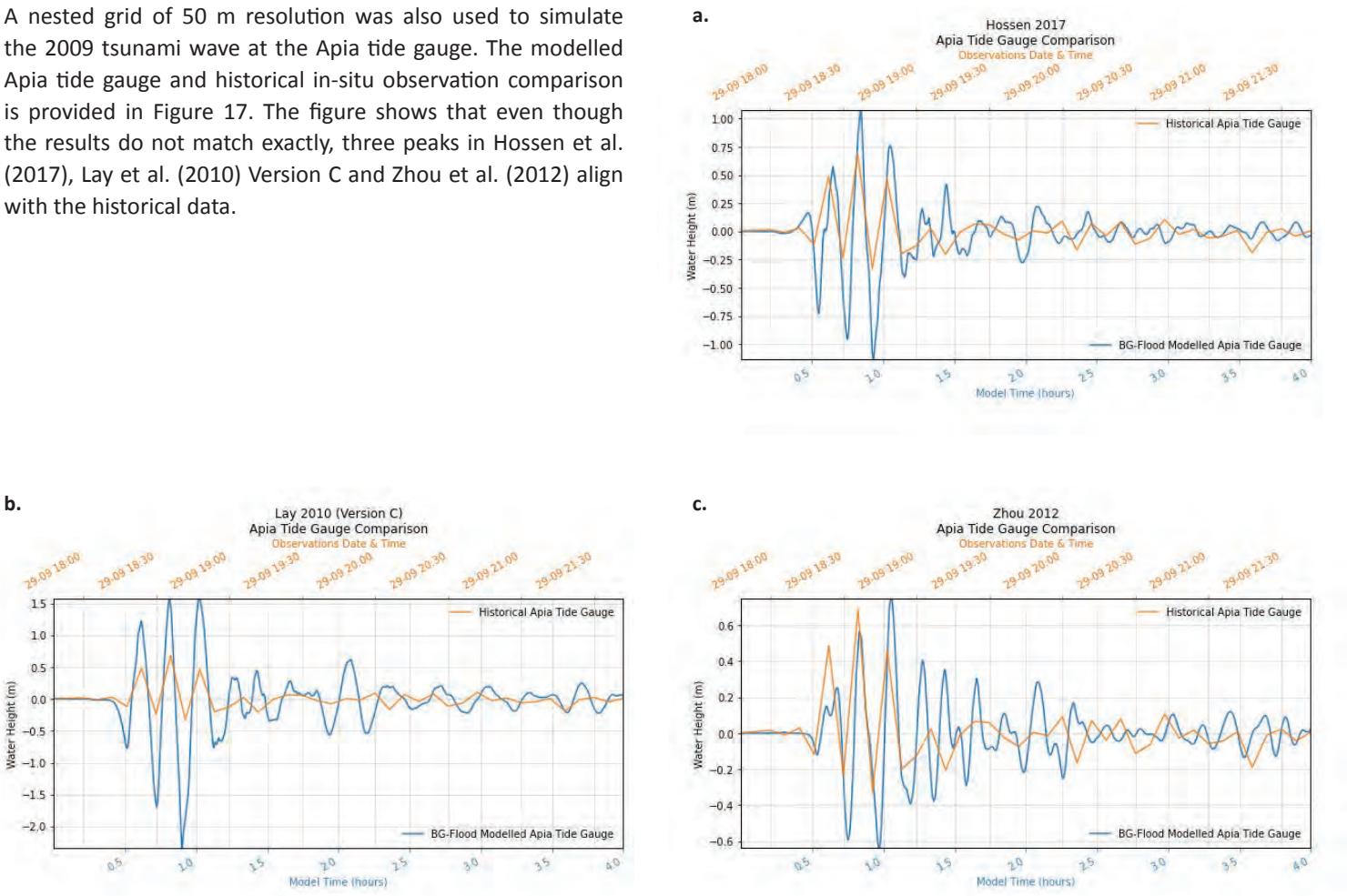

Figure 17: Apia tide gauge comparison of the historical 2009 Samoa tsunami tide gauge observations against the BG-Flood simulated Apia tide gauge readings for a) Hossen et al. (2017), b) Lay et al. (2010) Version C and c) Zhou et al. (2012). The modelled Apia tide gauge data was obtained from a nested grid simulation of 50 m resolution.

The model was also validated with DART buoy data using the output from the coarse (1 km resolution) simulation. Figure 18 below provides a comparison between the simulated and in-situ DART buoy observations for the five best PTHA18 events. The modelled DART 51425 for all five PTHA18 events portrays a leading peak, whereas the historical DART buoy observations describe a leading trough. This trough is also reflected in the Apia tide gauge observations. Other PTHA18 events, such as HSvaryMu 30715 and 32783, are characterised by a prominent trough but only after the first wave peak. Figure 19 shows that the modelled DART 51425 data by Hossen et al. (2017) and Lay et al. (2010) Version C best depict the leading trough (even though it is overpredicted) with the first peak of the tsunami wave.

The modelled and observational data were further analysed using the RMSE and Pearson correlation coefficient (Pearson's R). RMSE is a method that measures the error of a model of the predicted quantitative data from the actual values in the dataset. RMSE is a measure of how concentrated the data is around the line of best fit (also known as a regression line). A small RMSE value, close to zero, indicates the predicted errors are small and that the predicted/modelled data are close to the regression line (Moody 2011).

The Pearson correlation coefficient measures the statistical relationship, or association, between two continuous variables. The coefficient values range from +1 to -1, where +1 indicates a perfect positive relationship, -1 indicates a perfect negative relationship, and zero indicates no relationship exists between the two variables. Coefficient values below 0.29 indicate a small correlation, values between 0.30 and 0.49 a moderate correlation, and values between 0.50 and 1 a strong correlation (Statistics Solutions 2021).

As shown by the Pearson's R and RMSE values in Table 13, the three scenarios with the strongest correlation for the Apia BG-Flood modelled and in-situ observational data for the 2009 Samoa tsunami were HS event 28606, HSvaryMu event 32759 and HSvaryMu event 32783. The Pearson's R values of the three PTHA18 events were 0.70, 0.64 and 0.67, respectively. The corresponding RMSE values for the best three scenarios were 0.13, 0.14 and 0.13, respectively, indicating the predicated/ modelled values lie close to the regression line. The Lay et al. (2010) Version C scenario gives a Pearson's R value of 0.75, revealing a strong correlation; however, the RMSE value of 0.46 reveals that the predicted value errors do not lie close to the regression line compared to the other three PTHA18 scenarios.

For the DART buoy data, the RMSE and Pearson's R values are both close to zero for all of the scenarios (Table 13). The Pearson's R values close to zero reveal that there is no correlation between the modelled BG-Flood scenarios and 2009 Samoa tsunami observational DART buoy data. The RMSE values close to zero reveal that the predicted value lies close to the regression line.

Scenario	Gauge	Resolution	RSME (root mean square error)	Pearson correlation coefficient (Pearson's R)
PTHA18 HS event 28606	DART 51425	1 km	0.03	0.00
	DART 51426	1 km	0.07	-0.05
	Apia	50 m	0.13	0.70
PTHA18 HS event 28678	DART 51425	1 km	0.03	-0.02
	DART 51426	1 km	0.07	0.05
	Apia	50 m	0.16	0.48
PTHA18 HSvaryMu event 30715	DART 51425	1 km	0.03	0.03
	DART 51426	1 km	0.07	0.01
	Apia	50 m	0.17	0.43
PTHA18 HSvaryMu event 32759	DART 51425	1 km	0.03	0.04
	DART 51426	1 km	0.07	0.05
	Apia	50 m	0.14	0.64
PTHA18 HSvaryMu event 32783	DART 51425	1 km	0.03	-0.03
	DART 51426	1 km	0.07	0.00
	Apia	50 m	0.13	0.67
Hossen et al. (2017)	DART 51425	1 km	0.03	0.08
	DART 51426	1 km	0.07	-0.06
	Apia	50 m	0.17	0.46
Lay et al. (2010) Version C	DART 51425	1 km	0.04	0.06
	DART 51426	1 km	0.08	-0.01
	Apia	50 m	0.46	0.75
Zhou et al. (2012)	DART 51425	1 km	0.03	0.00
	DART 51426	1 km	0.07	-0.02
	Apia	50 m	0.18	0.14

Table 13: Root mean square error (RMSE) and Pearson correlation coefficient (Pearson's R) values for the 15 scenarios used for validation of the model.

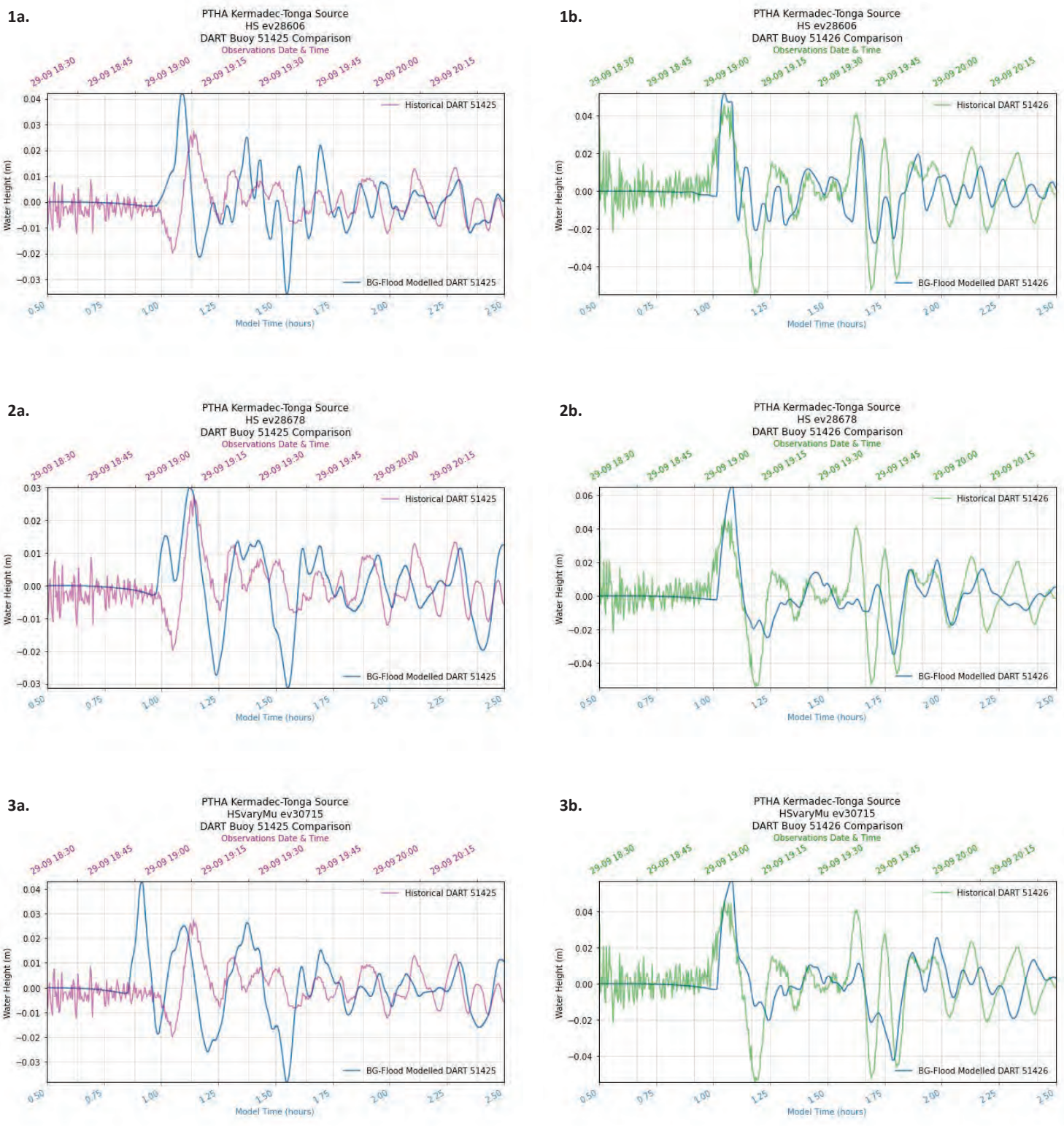

Figure 18: DART buoy data comparison of modelled and in-situ historical 2009 Samoa tsunami DART 51425 and 51426 observations for PTHA18 events: 1) HS event ID 28606, 2) HS event ID 28678, 3) HSvaryMu event ID 30715, (next page) 4) HSvaryMu event ID 32759 and 5) HSvaryMu event ID 32783. DART 51425 buoy data (a) is shown in magenta and DART 51426 buoy data (b) is shown in green. The modelled DART buoy data was obtained from a 1 km resolution simulation.

4a.

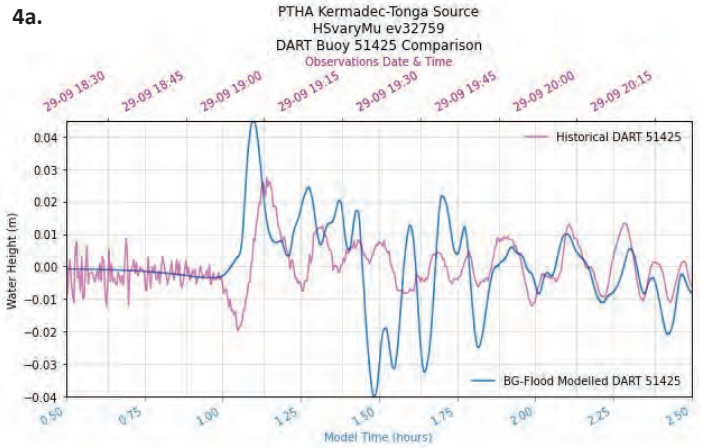
PTHA Kermadec-Tonga Source
HSvaryMu ev32759
DART Buoy 51425 Comparison
Observations Date & Time
29-09 18:30
29-09 18:45
29-09 19:00
29-09 19:15
29-09 19:30
29-09 19:45
29-09 20:00
29-09 20:15
Historical DART 51425
BG-Flood Modelled DART 51425
Water Height (m)
Model Time (hours)

4b.

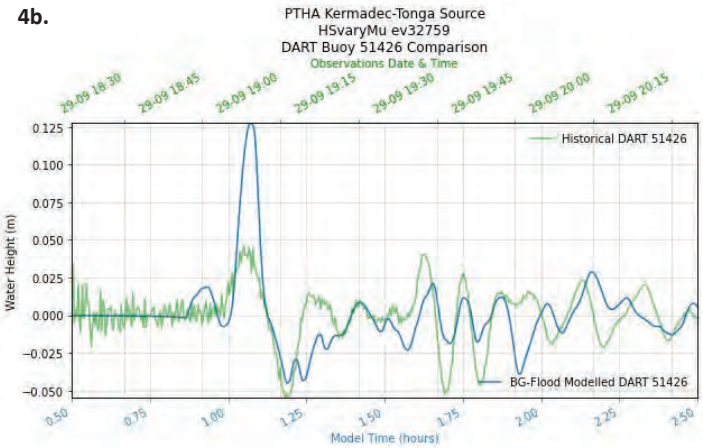
PTHA Kermadec-Tonga Source
HSvaryMu ev32759
DART Buoy 51426 Comparison
Observations Date & Time
29-09 18:30
29-09 18:45
29-09 19:00
29-09 19:15
29-09 19:30
29-09 19:45
29-09 20:00
29-09 20:15
Historical DART 51426
BG-Flood Modelled DART 51426
Water Height (m)
Model Time (hours)

5a.

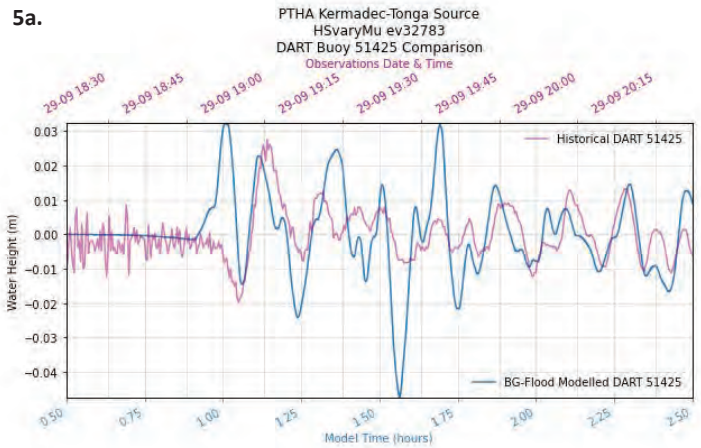
PTHA Kermadec-Tonga Source
HSvaryMu ev32783
DART Buoy 51425 Comparison
Observations Date & Time
29-09 18:30
29-09 18:45
29-09 19:00
29-09 19:15
29-09 19:30
29-09 19:45
29-09 20:00
29-09 20:15
Historical DART 51425
BG-Flood Modelled DART 51425
Water Height (m)
Model Time (hours)

5b.

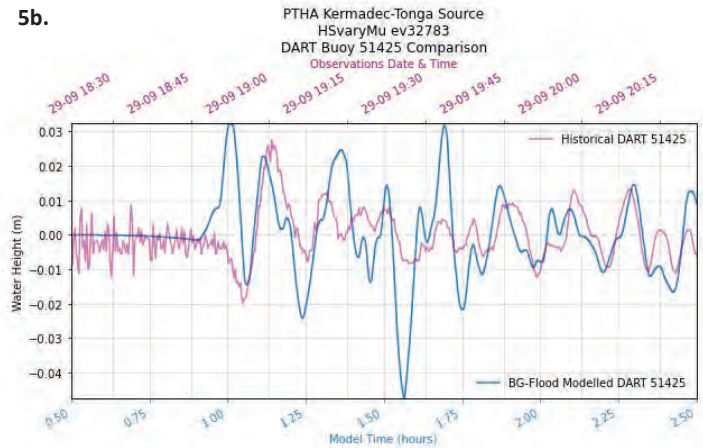
PTHA Kermadec-Tonga Source
HSvaryMu ev32783
DART Buoy 51425 Comparison
Observations Date & Time
29-09 18:30
29-09 18:45
29-09 19:00
29-09 19:15
29-09 19:30
29-09 19:45
29-09 20:00
29-09 20:15
Historical DART 51425
BG-Flood Modelled DART 51425
Water Height (m)
Model Time (hours)

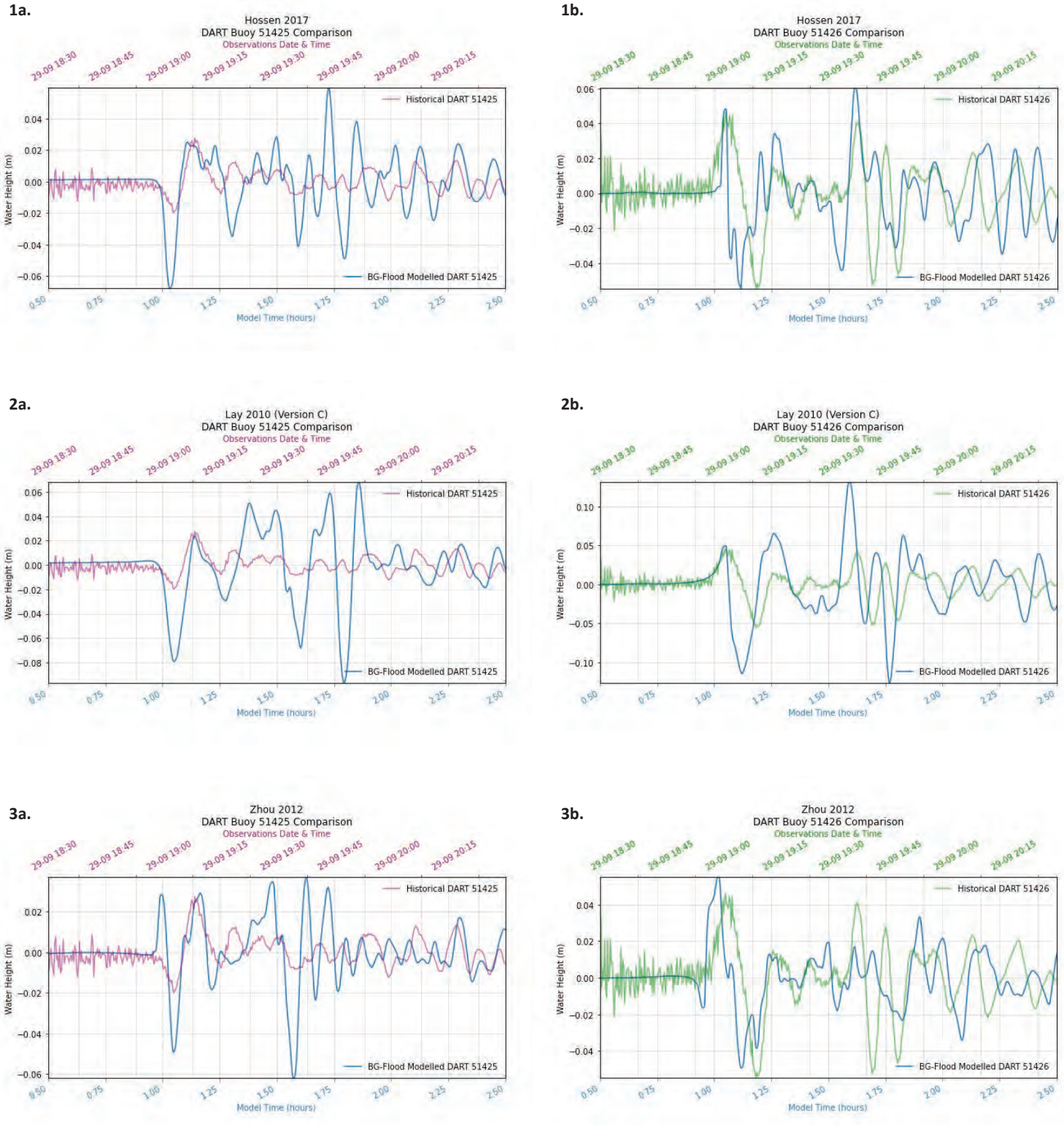

Figure 19: DART buoy data comparison of modelled and in-situ historical 2009 Samoa tsunami DART 51425 and 51426 observations for 1) Hossen et al. (2017), 2) Lay et al. (2010) Version C and 3) Zhou et al. (2012). DART 51425 buoy data (a) is shown in magenta and DART 51426 buoy data (b) is shown in green. The modelled DART buoy data was obtained from a 1 km resolution simulation.

After reviewing the modelled Apia tide gauge and DART buoy data with the 2009 tsunami in-situ observations, the next step was to compare the field survey data and eyewitness accounts of runup and flow depth collected along South East Upolu. For the eight scenarios (five best PTHA18 events and three earthquake parameters), a 10 m resolution simulation was carried out focusing on South East Upolu. The simulated runup and flow depth were compared with the in-situ field survey and eyewitness accounts (Figures 20 and 21).

Figure 20 shows the runup height comparison for the eight scenarios (five PTHA18 events and three source parameters). Based on Pearson's R, a strong correlation (R = 0.7) was found between the in-situ runup data and the simulated runup from the five PTHA18 events and the earthquake parameter in Zhou et al. The runup height comparison for Hossen et al. (2017) and for Lay et al. (2010) Version C show the highest Pearson's R values, 0.78 and 0.79, respectively, and the lowest RMSE values, 2.68 and 2.63, respectively.

The flow depth height, also known as the inundation depth, is the depth of water measured on land. The flow depth height is obtained by subtracting the maximum water level elevation (BG-Flood zsmax variable) with the topography elevation (BG-Flood zb variable). Only Hossen et al. (2017) and Lay et al. (2010) Version C had locations where water depth was recorded at comparable locations to the 2009 Samoa in-situ field survey flow depth heights. Figure 20 shows that Hossen et al. (2017) and Lay et al. (2010) Version C have a moderate to strong Pearson's R value (0.56 and 0.6, respectively) and RMSE values of 1.97 and 1.84, respectively.

Of the 15 scenarios (12 PTHA18 events and 3 earthquake parameters), those best depicting the complexity of the 2009 Samoa tsunami event are reflected in a variety of different events. The PTHA18 HS event 28606, HSvaryMu event 32759 and HSvaryMu event 32783 best represent the Apia tide gauge comparison, while Hossen et al. (2017) and Lay et al. (2010) Version C best reflect the runup and flow depth height comparison. This is supported by Bosserelle et al. (2020), who states that the source parameters in Hossen et al. (2017) and Lay et al. (2010) Version C most consistently fit the 2009 Samoa tsunami observed data.

Bosserelle et al. (2020) further states that the source models published by Hossen et al. (2017) and Lay et al. (2010) Version C were suitable for reproducing the large inundation in Samoa, although none reproduced the extreme runup of 10–15 m observed in areas more severely impacted on the southeast Upolu coast. These extreme runups occurred east of Lepa, at Saleapaga bay and on Lalomanu cliffs. The distribution and intensity of the runup and inundation for Samoa were dependent on source model, local topographic and bathymetric features, regional coastal geomorphology, and the short-period waves trapping over the reef flats. According to Bosserelle et al. (2020), the computed maximum runup for the scenarios by Hossen et al. (2017) and Lay et al. (2010) Version C are consistent with recorded observations and eyewitness accounts in southeast Upolu where the second and third waves were observed to be the largest and that the simulation confirms the large variation observed in runups and flow depths along the shore at Lepa and Saleapaga.

a.

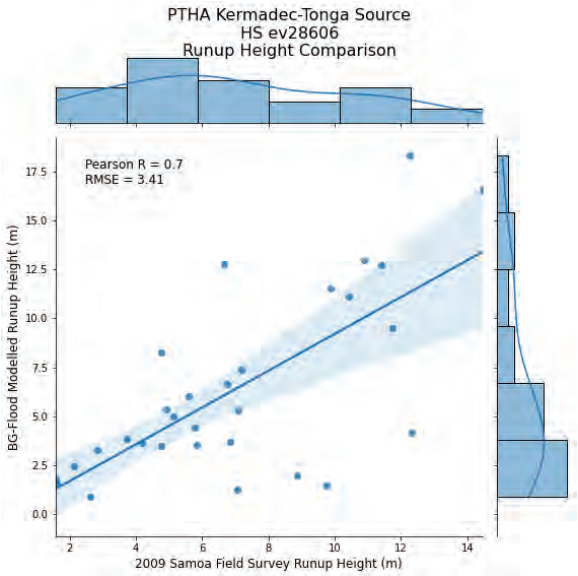

b.

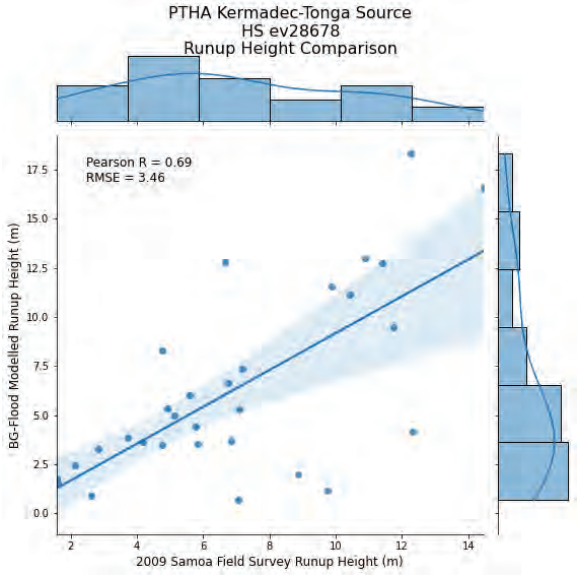

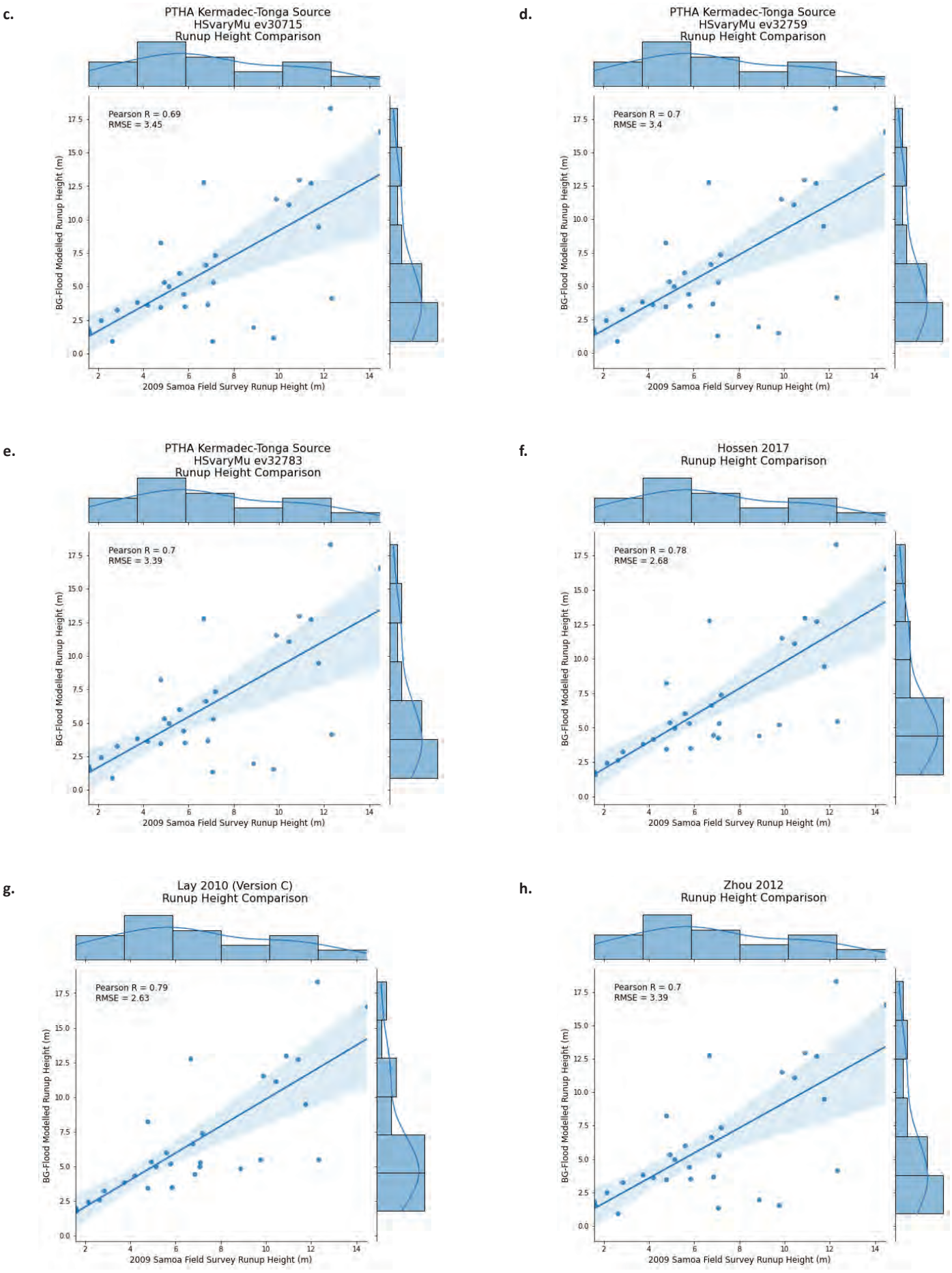

Figure 20: Field survey and eyewitness runup height (m) observations against modelled PTHA18 events: (left) a) HS event ID 28606, b) HS event ID 28678, (above) c) HSvaryMu event ID 30715, e) HSvaryMu event ID 32759 and e) HSvaryMu event ID 32783; and the article source parameters: f) Hossen et al. (2017), g) Lay et al. (2010) Version C and h) Zhou et al. (2012).

a.

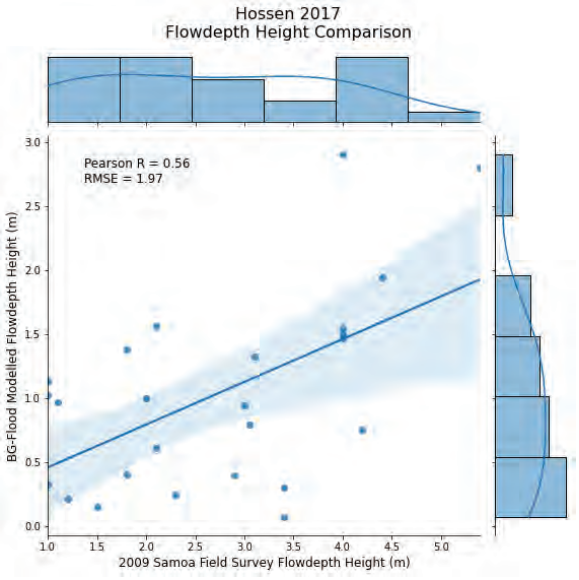

b.

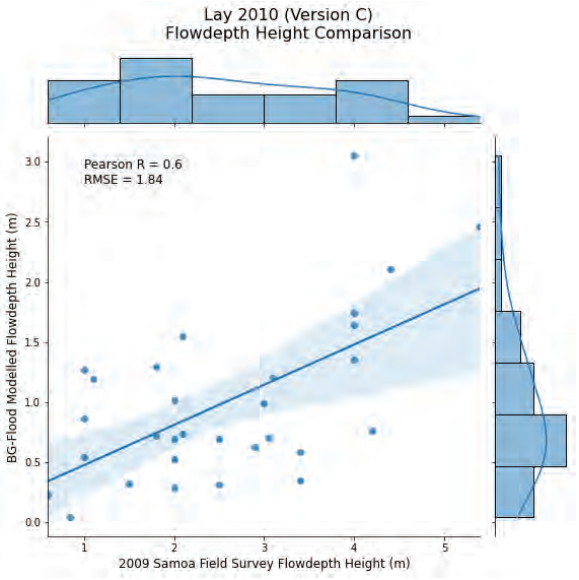

Figure 21: Field survey and eyewitness flow depth height (m) observations against earthquake parameters: a) Hossen et al. (2017) and b) Lay et al. (2010) Version C.

3.2.3.3 Japan 2011 tsunami

The BG-Flood model was further validated using the 2011 Japan tsunamigenic event. Unfortunately, the Apia tide gauge was not operational on March 11, 2011 so validation was solely done by comparing the 13 DART buoy historical observations situated within the coarse bathymetry grid extents (Figure 22). Table 14 provides the DART ID and geographic location of the 13 DART buoys. The PTHA18 database provided six event scenarios that had the best fit to the historical DART buoy data for the 2011 Japan Tsunami (Table 15).

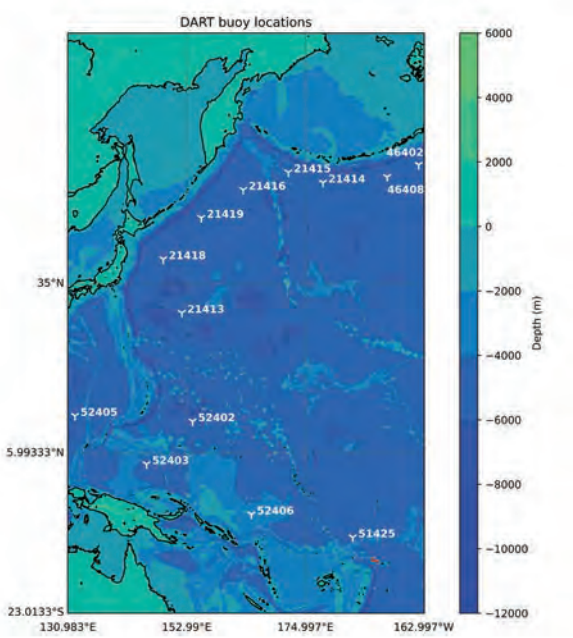

Figure 22: Bathymetry grid (5 km resolution) used for the Japan tsunamigenic event simulation. The grid also shows the location of the DART buoys used for the 2011 Japan tsunami.

DART Buoy ID	Longitude	Latitude
21413	152.123	30.528
21414	178.251	48.937
21415	171.849	50.176
21416	163.486	48.042
21418	148.698	38.718
21419	155.735	44.455
46402	-164.005	51.068
46408	-169.853	49.624
51425	-176.230	-9.504
52402	154.111	11.822
52403	145.596	4.032
52405	132.334	12.881
52406	165.002	-5.294

Table 14: Geographical location of the DART buoys for the 2011 Japan tsunami model validation.

Historical event	Source	Slip type	Event identification
2011 Japan Tsunami	Kurils Japan	Heterogeneous slip (HS)	46994
		HS	47004
		HS	47004
		Variable area uniform slip (VAUS)	47635
		VAUS	47746
		VAUS	48324

Table 15: PTHA18 scenarios best fit to the historical 2011 Japan tsunamigenic event.

3.2.3.4 Japan 2011 tsunami DART buoy data comparison

The six PTHA18 scenarios were simulated at a 5 km resolution to extract the wave time series at the 13 DART buoy locations (Table 15). Table 16 provides the RMSE values, while Table 17 provides the Pearson's R values for the comparison of 13 historical DART buoy observations against the BG-Flood modelled wave time series. According to the RMSE values, the three scenarios that had modelled data closest to the regression line (or line of best fit) were HS event 46994, HS event 47004 and HS event 47634, with a mean RMSE value of 0.05 for all three events (Table 16). The Pearson's R values revealed that the same three events had a moderate to strong correlation, with values of 0.55, 0.55 and 0.52, respectively (Table 17). Figure 23 shows the HS event ID 46994 modelled DART buoys that had the closest relation to the DART tsunami observations.

DART ID	HS ev46994	HS ev47004	HS ev47634	VAUS ev47635	VAUS ev47746	VAUS ev48324
21413	0.08	0.09	0.08	0.18	0.11	0.14
21414	0.03	0.04	0.03	0.05	0.04	0.05
21415	0.03	0.03	0.03	0.06	0.04	0.06
21416	0.05	0.05	0.05	0.07	0.06	0.08
21418	0.17	0.18	0.16	0.32	0.19	0.26
21419	0.07	0.07	0.07	0.11	0.08	0.11
46402	0.02	0.03	0.03	0.04	0.03	0.03
46408	0.03	0.03	0.03	0.05	0.04	0.05
51425	0.02	0.02	0.02	0.04	0.03	0.03
52402	0.05	0.04	0.05	0.08	0.05	0.06
52403	0.03	0.03	0.03	0.04	0.03	0.04
52405	0.03	0.03	0.03	0.04	0.03	0.03
52406	0.03	0.03	0.04	0.05	0.03	0.05
Total	**0.64**	**0.67**	**0.65**	**1.13**	**0.76**	**0.99**
Mean	**0.05**	**0.05**	**0.05**	**0.08**	**0.06**	**0.08**

Table 16: RMSE (root mean square error) values for the 13 DART buoys of the modelled PTHA18 scenarios against the DART observations for 2011 Japan Tsunami.

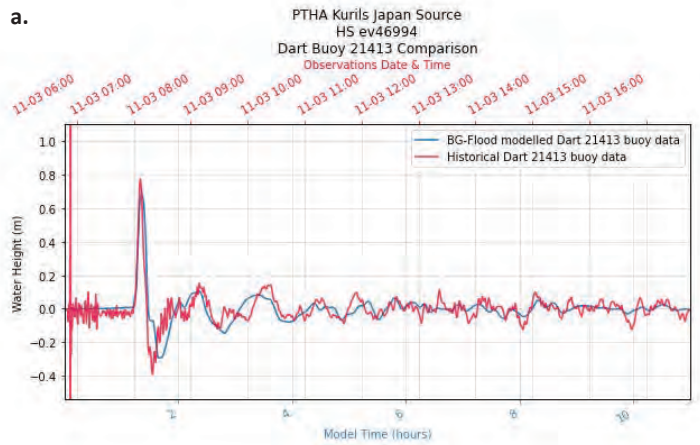

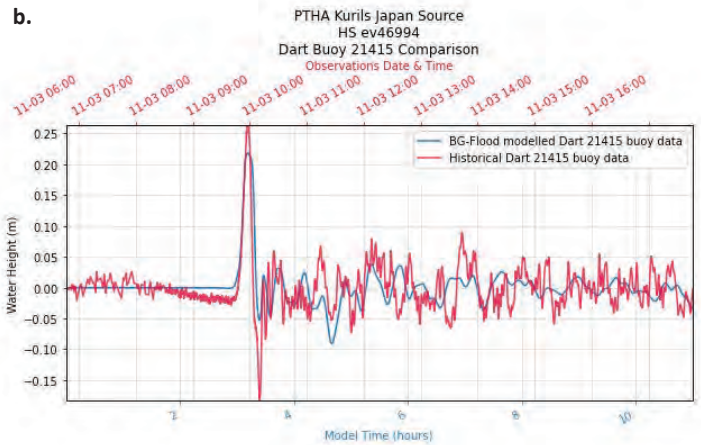

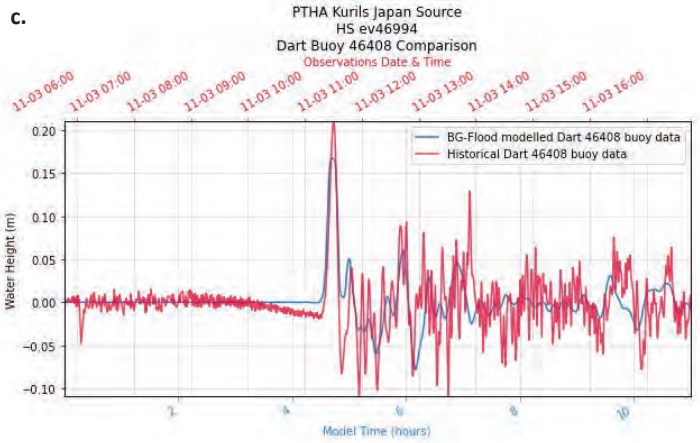

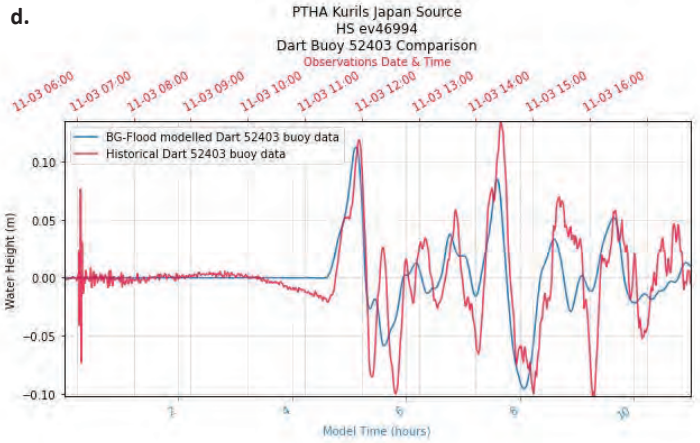

Figure 23: DART buoy comparison of modelled PTHA18 HS event ID 46994 with the historical DART buoy observations for DART: a) 21413, b) 21415, c) 46408 and d) 52403.

Pearson correlation coefficient

DART	HS ev46994	HS ev47004	HS ev47634	VAUS ev47635	VAUS ev47746	VAUS ev48324
21413	0.67	0.56	0.70	0.04	0.45	0.54
21414	0.60	0.54	0.54	0.53	0.50	0.54
21415	0.60	0.62	0.58	0.52	0.48	0.50
21416	0.50	0.49	0.49	0.46	0.39	0.39
21418	0.32	0.49	0.41	0.11	0.22	0.19
21419	0.54	0.57	0.54	0.55	0.51	0.47
46402	0.54	0.47	0.49	0.43	0.42	0.49
46408	0.62	0.56	0.54	0.44	0.43	0.54
51425	0.50	0.38	0.50	0.13	0.40	0.47
52402	0.50	0.65	0.43	0.10	0.58	0.57
52403	0.69	0.70	0.62	0.46	0.69	0.71
52405	0.50	0.49	0.46	0.20	0.51	0.51
52406	0.58	0.61	0.45	0.33	0.62	0.61
Total	**7.16**	**7.13**	**6.75**	**4.30**	**6.20**	**6.53**
Mean	**0.55**	**0.55**	**0.52**	**0.33**	**0.48**	**0.50**

Table 17: Pearson's R correlation values for the 13 DART buoys of the modelled PTHA18 scenarios against the DART observations for 2011 Japan Tsunami.

3.2.3.5 BG-Flood validation decision

The BG-Flood model was used to simulate scenarios best fit to the historical 2009 Samoa tsunami and the 2011 Japan tsunami. For the 2009 Samoa tsunami, PTHA18 HS event 28606, HSvaryMu event 32759, HSvaryMu event 32783 and Lay et al. (2010) Version C had the highest Pearson correlation coefficient with the Apia tide gauge observations (R values of 0.70, 0.64, 0.67 and 0.75, respectively). The field survey runup heights revealed that Hossen et al. (2017) and Lay et al. (2010) Version C gave the highest Pearson's R value of 0.78 and 0.79, respectively. Following these were PTHA18 HS event 28606, HSvaryMu event 32759, HSvaryMu event 32783 and Zhou et al. (2012) (R values of 0.70 for all). The field survey flow depth heights were only applicable to Hossen et al. (2017) and Lay et al. (2010) Version C as these scenarios had locations where water depth was recorded at the comparable locations of the 2009 in-situ field survey flow depth heights, while the other scenarios didn't have any comparable simulated flow depth data. The flow depth heights in Hossen et al. (2017) and Lay et al. (2010) Version C showed strong correlation, with R values of 0.56 and 0.6, respectively. The DART buoy data, on the other hand, revealed no correlation between the modelled and historical DART 51425 and 51426 observations.

According to Bosserelle et al. (2020), the scenarios in Hossen et al. (2017) and Lay et al. (2010) Version C were generally consistent with recorded observations and eyewitness accounts in southeast Upolu, where the second and third waves were generally observed to be the largest. These simulated scenarios also confirmed the large variation observed in runups and flow depths along the shore of Lepa and Saleapaga. The inability of the source models to reproduce the extreme runup of 10–15 m peaks could be from various causes. Bosserelle lists the causes as:

1. Potential limitations of a 10 m resolution for southeast Upolu to represent the 2009 topography and bathymetry for nearshore and onshore inundation,
2. Complexity in the source mechanism is not captured using uniform heterogenous slip models,
3. Dispersion of propagating waves that aligns its resonance periods of the locations with the extreme runup, and/or
4. Vertical flow inertia needed to dynamically model the drawdown and runup process on the steep slopes of southeast Upolu.

Due to the lack of records for the Apia tide gauge during the 2011 Japan tsunami event, only DART buoy observations were compared with modelled PTHA18 events. Thirteen DART buoy observations were analysed against the PTHA18 best fit scenarios. The three PTHA18 events best fit to the 2011 tsunami were PTHA18 HS event 46994, HS event 47004 and HS event 47634 (R values 0.55, 0.55 and 0.52, respectively).

The BG-Flood model simulated scenarios that satisfactorily reproduced the 2009 Samoa and 2011 Japan tsunamigenic earthquake events. The model simulated scenarios that had moderate to strong correlation with DART buoys for the 2011 Japan tsunami and strong correlation with the Apia tide gauge, runup and flow depth field survey heights for the 2009 Samoa tsunami. Conversely, the DART buoy data for the 2009 Samoa tsunami revealed no correlation, further endorsing the complexity of the earthquake source for this event, which still remains unknown.

3.2.4 Model simulation

After gaining confidence in the model's ability to satisfactorily reproduce real events, the 68 PTHA18 scenarios were simulated. A total of 325 tsunami simulations were carried out, that is 68 scenarios at 5 levels of resolutions (5 km, 1 km, 50 m, 10 m and 5 m, with the exception of Kermadec-Tonga, which started at 1 km). In addition, an extra 136 tsunami simulations were done to include the projected 2100 sea-level rise (SLR) at mean high-water spring (MHWS) for the 68 scenarios at 10 m and 5 m resolution. According to the Intergovernmental Panel on Climate Change Assessment Report 6 (IPCC AR6, 2021), global mean sea level (GMSL) is projected to rise (with medium confidence, relative to 1995–2014 GMSL) 0.77 m, with a likely range of 0.63–1.02 (based on shared socioeconomic pathway [SSP]5-8.5). The MHWS, the averaged highest level of spring tides, is reported to be 0.485 m at the Apia tide gauge. Thus, the projected SLR with MHWS value added to the extra scenarios is 1.255 m.

The BG-Flood parameters were set with the specified resolution and model simulation time duration (incorporating the tsunami initiation and wave propagation), with the specified output variables. Table 18 shows the source, resolution of the simulation and the model time duration specified for each scenario. Each source had a different model time duration specified, with 5 km, 1 km and 50 m resolution outputting every 60 seconds and 10 m and 5 m resolution outputting once at the end of the simulation. Overall, the 68 scenarios took more than 52 days of computation to fully compute.

Source	Resolution	Model time duration
Alaska Aleutians	5 km 1 km 50 m	12-hour (43,200 seconds) simulation, output every 60 seconds.
	10 m 5 m	Output once at 12-hour mark. Another simulation was done for SLR inclusion at MHWS.
Izu Mariana	5 km 1 km 50 m	11-hour (39,600 seconds) simulation, output every 60 seconds.
	10 m 5 m	Output once at 11-hour mark. Another simulation was done for SLR inclusion at MHWS.
Kermadec Tonga	1 km 50 m	4-hour (14,400 seconds) simulation, output every 60 seconds.
	10 m 5 m	Output once at 4-hour mark. Another simulation was done for SLR inclusion at MHWS.
Kurils Japan	5 km 1 km 50 m	13-hour (46,800 seconds) simulation, output every 60 seconds.
	10 m 5 m	Output once at 13-hour mark. Another simulation was done for SLR inclusion at MHWS.
Mexico	5 km 1 km 50 m	16-hour (57,600 seconds) simulation, output every 60 seconds.
	10 m 5 m	Output once at 16-hour mark. Another simulation was done for SLR inclusion at MHWS.
South America	5 km 1 km 50 m	16-hour, 40-minute (60,000 seconds) simulation, output every 60 seconds.
	10 m 5 m	Output once at 16-hour, 40-minute mark. Another simulation was done for SLR inclusion at MHWS.

Table 18: Model time duration specified for each source with their corresponding output times.

4.0 RESULTS

The last step in the tsunami hazard assessment methodology, step 6, is to aggregate all the inundation outputs to obtain a maximum inundation map for each return period. After running the simulations for each of the scenarios, only the 50 m, 10 m and 5 m resolution inundation outputs were stored for data analysis and inundation aggregation. The 50 m resolution was stored as it is key for informing the national-scale inundation hazard assessment of Samoa. Similarly, the 10 m resolution is designed to provide inundation hazard information for communities and high-value tourism facilities on the South East of Upolu. Finally, the 5 m resolution output will be used to provide high-resolution hazard information for Apia City, the capital of Samoa. Output data from a total of 340 inundation scenarios were analysed (68 scenarios with 3 resolution outputs at present mean sea level and 68 scenarios with sea level inclusion at 2 resolution outputs). To make this data digestible and increase its uptake by government and stakeholders, the inundation data were processed into six types of aggregated outputs (Figure 24). The full collection of these maps is available in Annex B (Supplementary material).

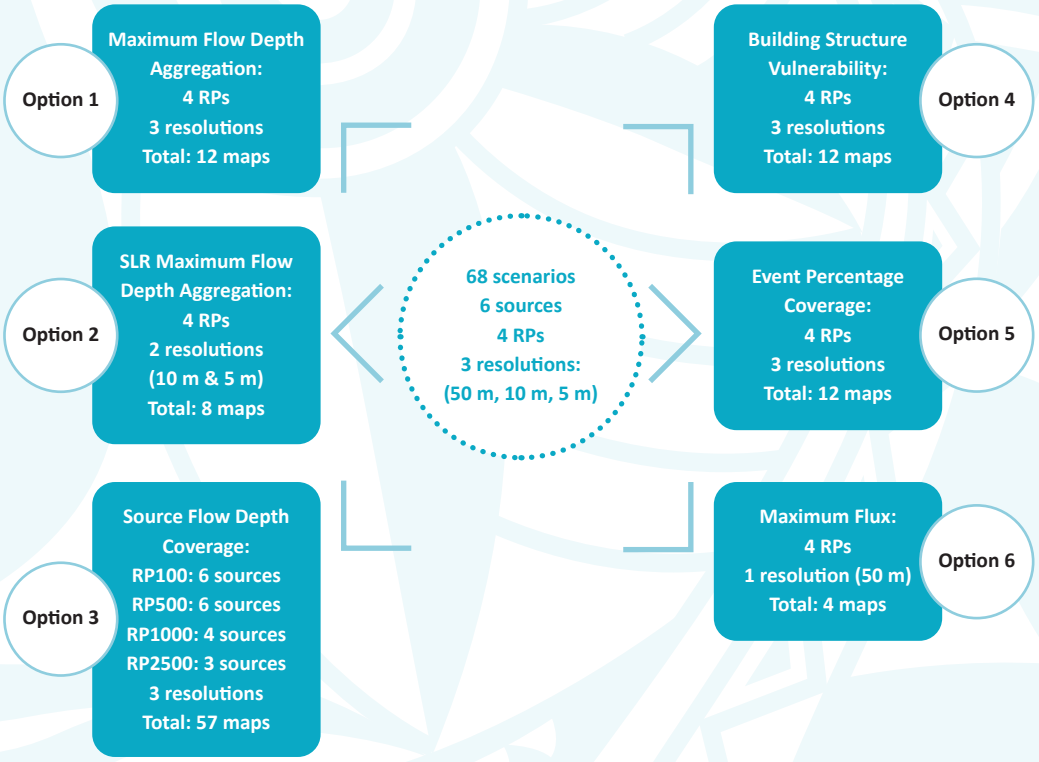

Figure 24: Summary of the six types of aggregated inundation maps that was assembled from the 340 inundation output data that covers 68 scenarios/events, six sources, four return periods and three resolutions.

4.1 Maximum flow depth aggregation

The first product type aggregates all maximum flow depth inundation data according to their return period. For instance, all outputs that fall under the 2500-year return period and have a resolution of 50 m were aggregated. This aggregation was also done for the South East Upolu 10 m and Apia 5 m outputs (Figures 25–27). As there are four return periods (100 years, 500 years, 1000 years and 2500 years) and three output resolutions, a total of 12 inundation maps were produced. These aggregated maps show the maximum values of flow depth in metres for each grid cell.

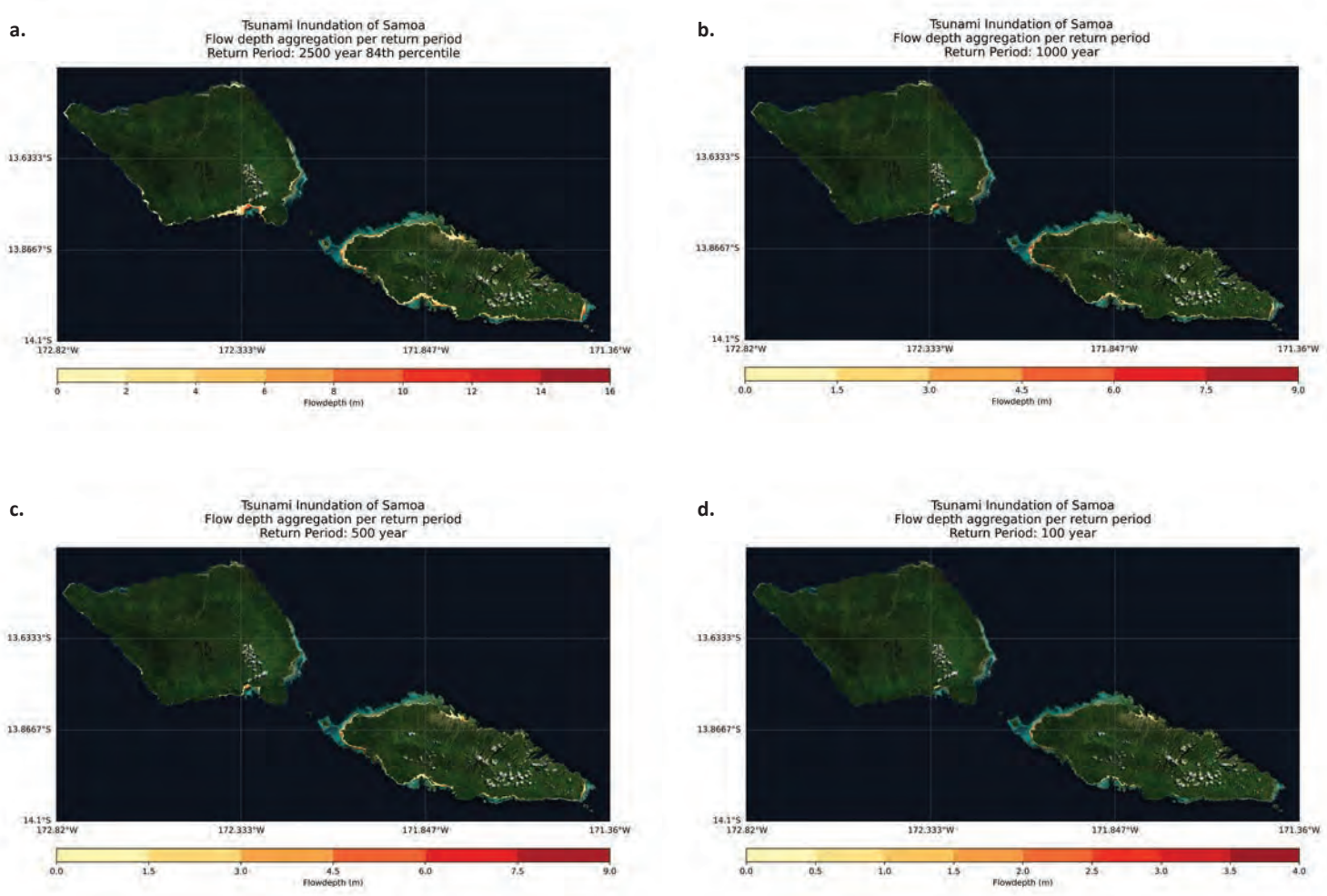

Figure 25: Maximum flow depth aggregation of Samoa at 50 m resolution for four return period aggregations: a) 2500 years 84th percentile, b) 1000 years, c) 500 years and d) 100 years.

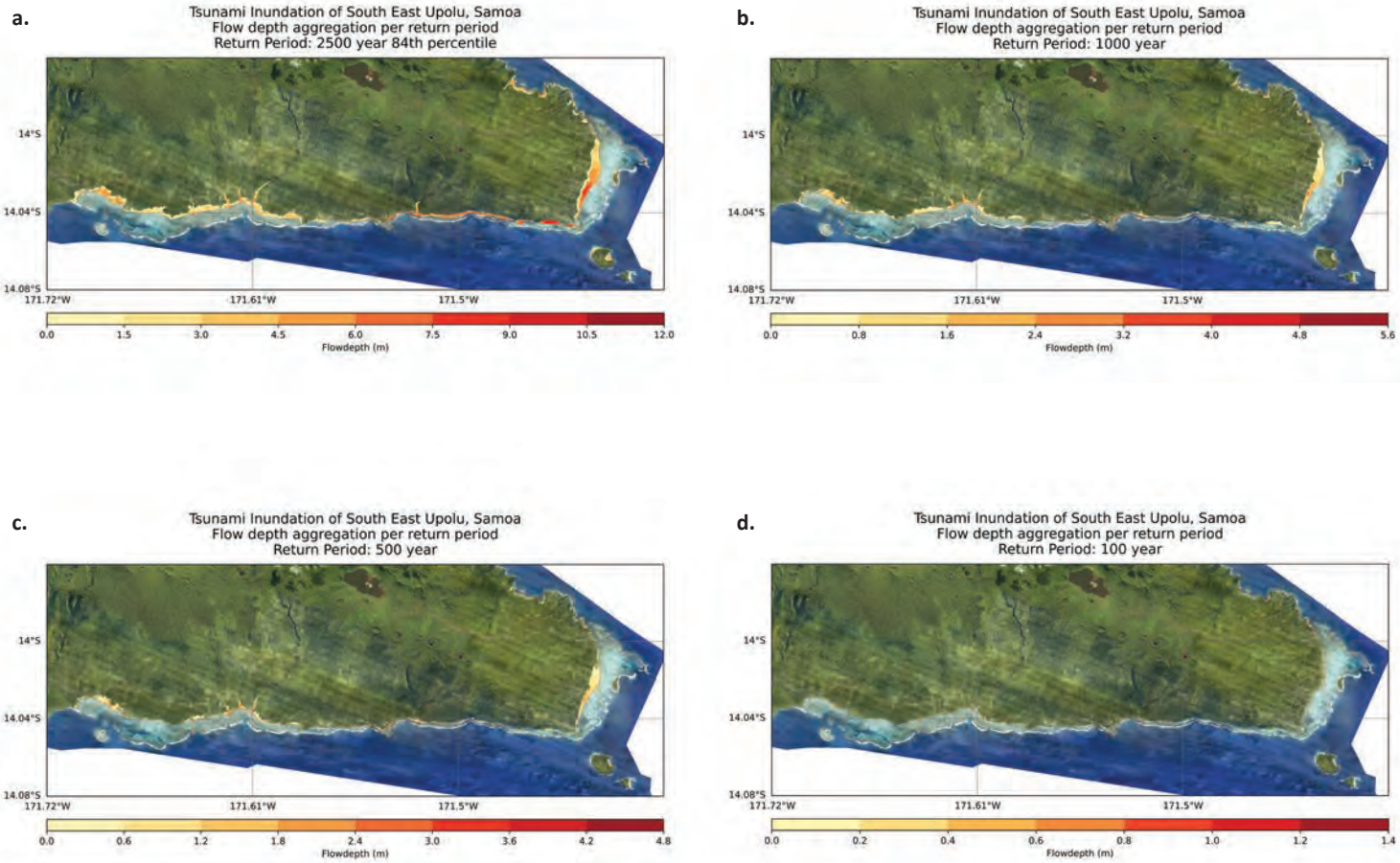

Figure 26: Maximum flow depth aggregation of South East Upolu at 10 m resolution for four return period aggregations: a) 2500 years 84th percentile, b) 1000 years, c) 500 years and d) 100 years.

a.

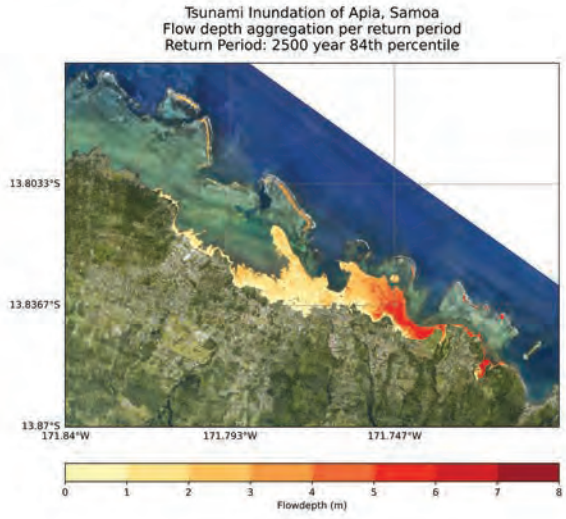

b.

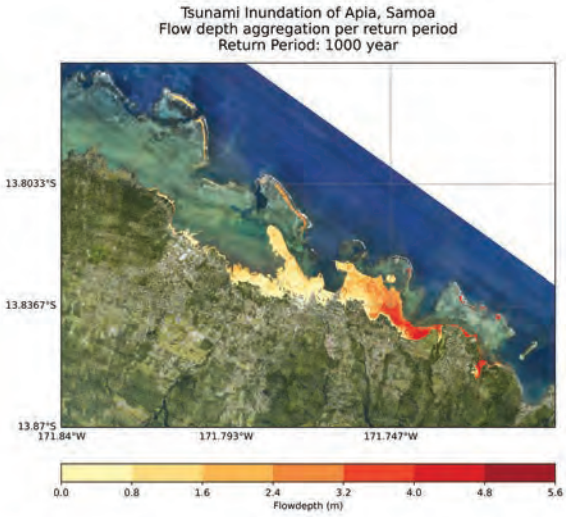

c.

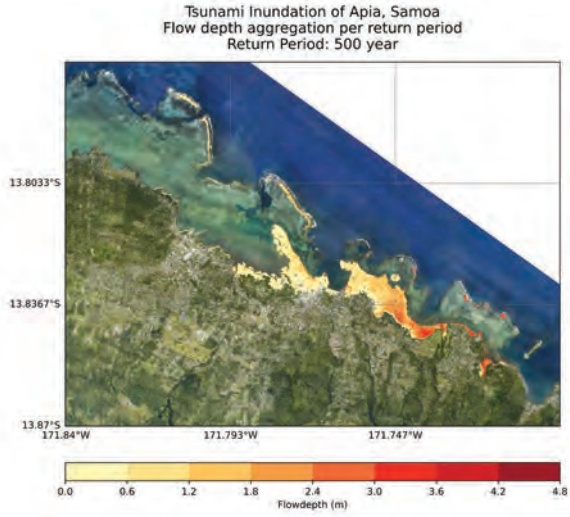

d.

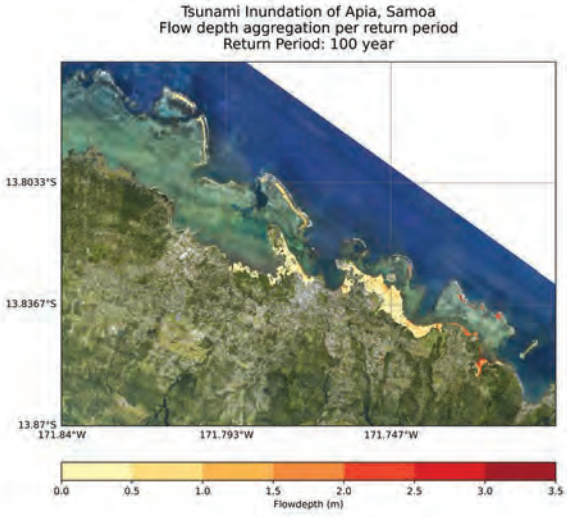

Figure 27: Maximum flow depth aggregation of Apia at 5 m resolution for four return period aggregations: a) 2500 years 84th percentile, b) 1000 years, c) 500 years and d) 100 years.

4.2 Sea-level rise inclusive maximum flow depth aggregation

The second product type aggregates all sea-level rise inclusive maximum flow depth inundation data according to their return period. An additional 1.255 m water depth was included to the mean sea level to reflect projected 2100 sea-level rise at MHWS. The aggregation of the flow depth height was done for the four return periods (100 years, 500 years, 1000 years, and 2500 years 84th percentile) at two output resolutions (southeast Upolu 10 m and Apia 5 m), and a total of 8 inundation maps were produced. Figure 28 shows the projected 2100 sea-level rise with MHWS inclusions at 2500 years 84th percentile flow depth aggregated maps. Refer to Annex B supplementary material for the full collection of inundation maps.

a.

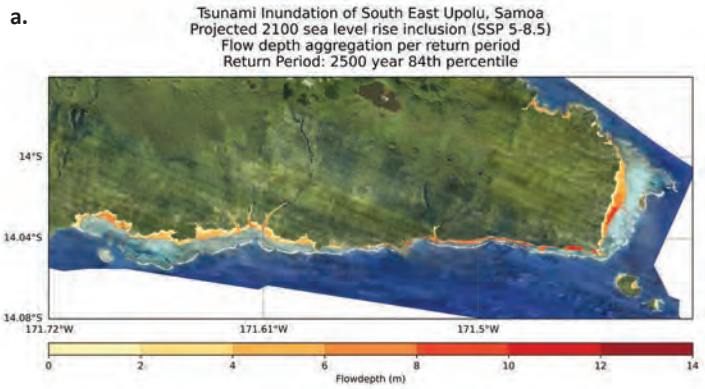

b.

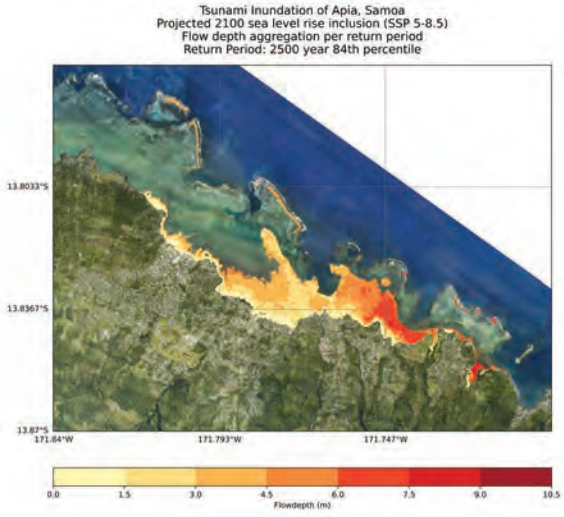

Figure 28: Projected sea-level rise inclusions (SSP 5-8.5) maximum flow depth aggregation at return period of 2500 years 84th percentile for: a) South East Upolu 10 m resolution and b) Apia 5 m resolution.

4.3 Source flow depth coverage

The third product type provides inundation coverage of the flow depth from each source zone separately per return period. This map is to be overlaid on the maximum flow depth aggregation from the first product type. This aggregated map complements the outputs described in 4.1 as it provides insights into the inundation hazard contribution from each source. Figure 29 provides the source coverage for Alaska Aleutians at a return period of 2500 years (84th percentile). The red areas indicate the coverage from that targeted source. For each resolution, the return period of 100 years and 500 years have scenarios from all six sources, however, the 1000-year return period has scenarios from only four sources and the 2500-year return period has only three sources. Overall, a total of 57 aggregated source inundation coverage maps are available for this output type.

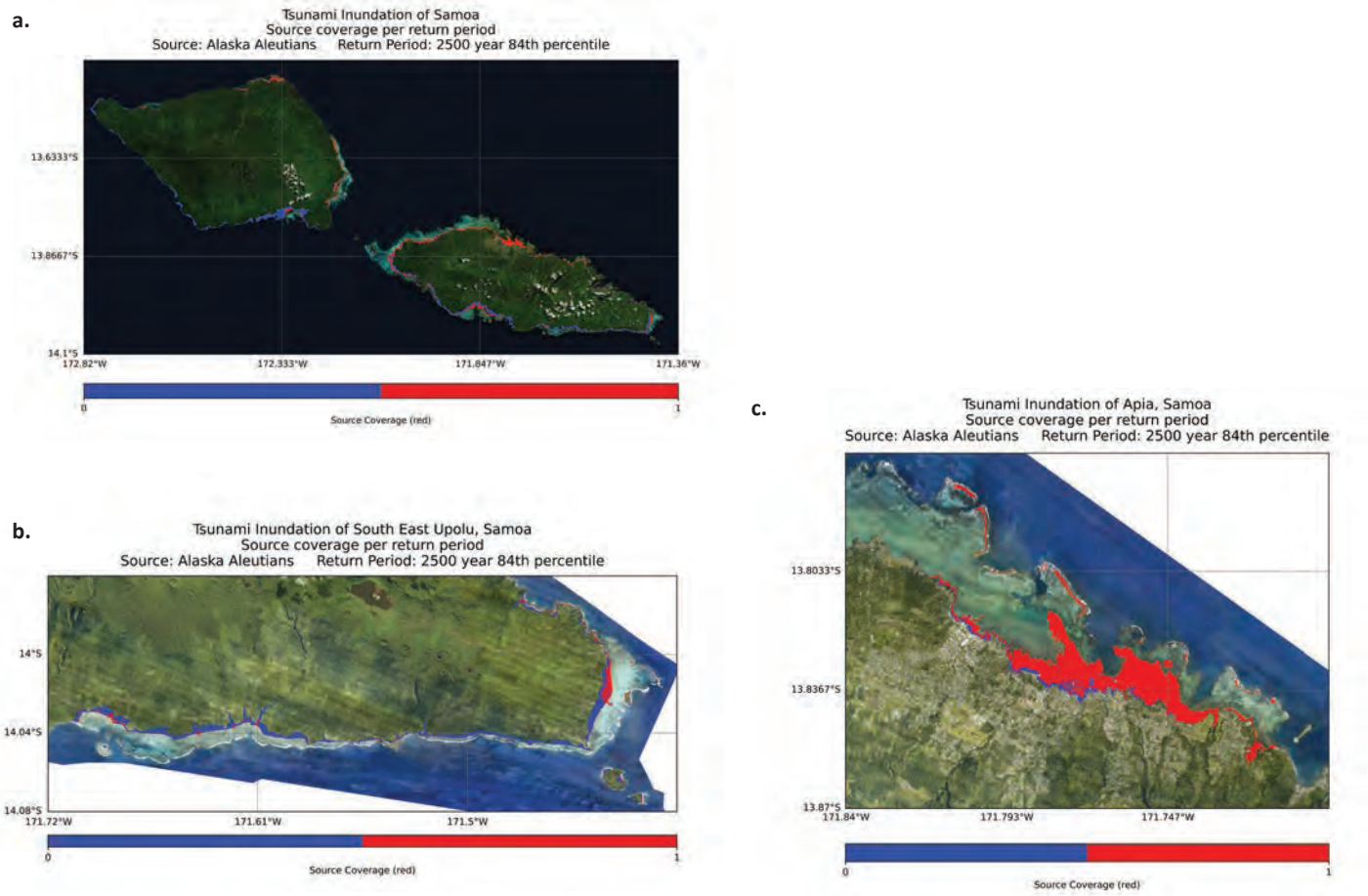

Figure 29: Source coverage aggregation map for Alaska Aleutians at a return period of 2500 years 84th percentile for: a) Samoa 50 m resolution, b) South East Upolu 10 m resolution and c) Apia 5 m resolution.

4.4 Building structure vulnerability scale

The fourth product type provides insights into the expected impact based on the aggregated maximum flow depth using a common vulnerability scale, the Integrated Tsunami Intensity Scale (ITIS-2012) proposed by Lekkas et al. (2013). The 12-grade scale is based on data collected from two mega-tsunamis in the Indian Ocean in 2004 and northeast Japan in 2011. Among many other variables, ITIS-2012 classification considers flow depth heights and impact on structures (inclusive of buildings). In Lekkas et al. (2013), structure types are categorised according to vulnerability class A–F (Table 19) and grade of damage caused by the tsunami for each structure type (Table 20). Table 21 shows the maximum grade of damage by vulnerability class for various tsunami flow depths.

Based on ITIS-2012, a series of flow depth levels (0.5–1 m, 1–2 m, 2–5 m, 5–7 m, 7–10 m and greater than 10 m) was used to categorise the maximum aggregation flow depth. These ranges correspond to ITIS-2012 categories V, VII, VIII, IX, X and XII, respectively (Table 21). The scale provides the damage grade of structures (Grade 1–5) for the vulnerability class of the structure (Class A–F). Overall, 12 maps were produced for this study output (four return periods and three resolutions).

Figure 30 illustrates the ITIS-2012 categories V, VII, VIII, IX, X and XII according to flow depth ranges (0.5–1 m, 1–2 m, 2–5 m, 5–7 m, 7–10 m and greater than 10 m) for the 2500-year 84th percentile return period. These maps complement the other outputs as they indicate which building structure types are vulnerable to tsunami flow depth heights for 100-year, 500-year, 1000-year and 2500-year (84th percentile) return periods, providing the possible damage grade to these building structures based on the vulnerability class.

Vulnerability class	Type of structure
A	**Masonry:** rubble, fieldstone, adobe (earth brick) **Reinforced concrete:** frame without earthquake resistant design (ERD) **Wood:** timber structures
B	**Masonry:** adobe (earth brick), simple stone, massive stone, unreinforced manufactured stone units, unreinforced with reinforced concrete floors **Reinforced concrete:** frame without ERD, walls without ERD **Wood:** timber structures
C	**Masonry:** massive stone, unreinforced with reinforced concrete floors **Reinforced concrete:** frames with moderate ERD, walls without ERD **Steel:** steel structures **Wood:** timber structures
D	**Masonry:** reinforced or confined **Reinforced concrete:** frames with moderate ERD, frames with high ERD, walls with moderate ERD **Steel:** steel structures
E	**Masonry:** reinforced or confined **Reinforced concrete:** frames with moderate ERD, frames with high ERD, walls with moderate ERD, walls with high ERD
F	**Reinforced concrete:** frames with high ERD, walls with high ERD

Table 19: Structure type categorized according to their vulnerability class for ITIS-2012 (Lekkas et al. 2013).

Grade	Timber structures	Steel structures	Masonry structures	Reinforces concrete structures
Grade 1	Slight damage: Perimetrical imprints of water level. Slight abrasions. Light objects overturn.	Slight damage: Perimetrical imprints of water level. Slight abrasions. Light objects overturn.	Slight damage: Perimetrical imprints of water level. Slight abrasions on walls. Light objects overturn outwards.	Slight damage: Perimetrical imprints of water level. Slight abrasions on walls. Light objects overturn outwards.
Grade 2	Moderate damage: Extensive external abrasions. Windows break. Decorative elements detachment.	Moderate damage: Extensive external abrasions. Windows break. Decorative elements detachment.	Moderate damage: External erosion. Extensive external abrasions. Windows break. Decorative elements detachment.	Moderate damage: Extensive perimetrical abrasions. Windows break. Decorative elements detachment.
Grade 3	Heavy damage: Walls fracture, roof damage. Doors break. Small deformations.	Heavy damage: Deformation and detachment of frame elements. Doors break.	Heavy damage: Partial wall collapse. Roof damage, tiles are detached, or extensive wall damage from object impact. Doors and shutters break.	Heavy damage: Masonry wall damage. Masonry wall damage due to object impact.
Grade 4	Very heavy damage: Extensive fracture on walls and roof. Detachment and small movement of the construction.	Very heavy damage: Extensive detachment of wall elements. Load bearing structure exposure.	Very heavy damage: Partial building collapse. Partial/total roof collapse.	Very heavy damage: Extensive damage on masonry walls, masonry walls blow up. Reinforced masonry walls suffer damage. Load bearing elements are destroyed, few buildings collapse.
Grade 5	Destruction: Total fracture and collapse of the construction. Detachment of whole construction and transportation at sufficient distance.	Destruction: Extensive load bearing structure deformation. Buildings are possible to be detached and carried away at great distances.	Destruction: Total collapse of most of the buildings. Debris is carried away. Buildings disappear. Buildings are uprooted.	Destruction: Total destruction of most of the buildings. Construction elements are carried away.

Table 20: Damage classification (Grade 1–5) for each structure type (Lekkas et al. 2013). The structure type and corresponding damage grade are based on the observed damage from the two tsunami events of 2004 and 2011.

ITIS $_{2012}$	Tsunami Height/Tsunami Flow Depth	Maximum Grade of Damage by Vulnerability Class					
		A	B	C	D	E	F
I	–						
II	–						
III	–						
IV	<0.5						
V	0.5-1	1	1				
VI	<1	2	2	1			
VII	1-2	4	3	2	1		
VIII	2-5	5	4	3	2		
IX	5-7	5	5	4	3	2	
X	7-10	5	5	5	4	3	2
XI	<10	5	5	5	5	4	3
XII	>10				5	5	5

Table 21: The tsunami flow depth height and corresponding maximum damage grade for each building vulnerability class according to ITIS-2012 (Lekkas et al. 2013).

a.

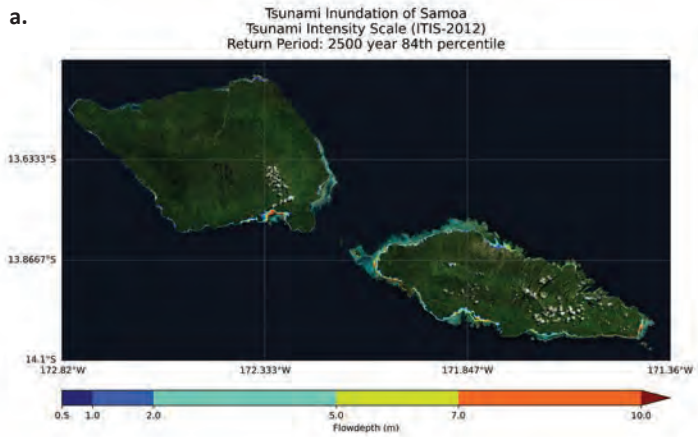

b.

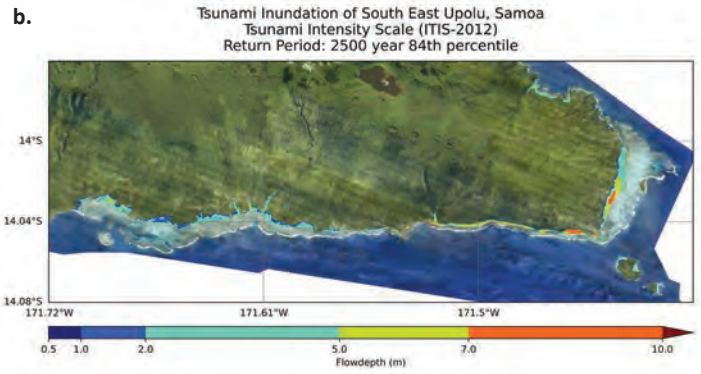

c.

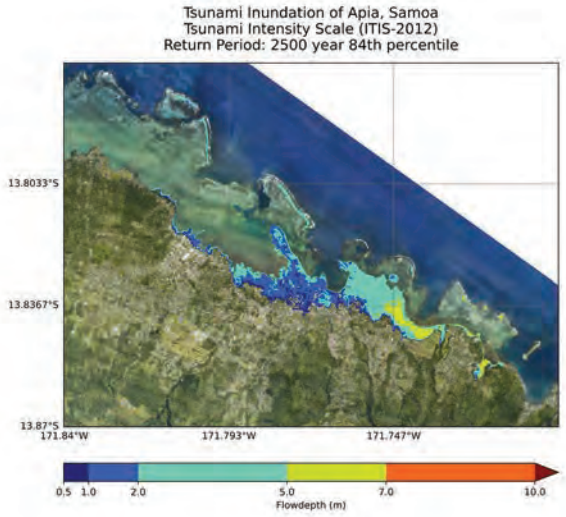

Figure 30: Tsunami inundation flow depth height (m) categorised according to the Integrated Tsunami Intensity Scale (ITIS-2012) flow depth ranges of 0.5–1 m, 1–2 m, 2–5 m, 5–7 m, 7–10 m and greater than 10 m for return period of 2500 years 84th percentile: a) Samoa 50 m resolution, b) South East Upolu 10 m resolution and c) Apia 5 m resolution.

4.5 Event percent coverage per return period aggregation

The fifth product type is designed to complement the flow depth aggregation of the first product type as it provides the percentage of events that cover onshore inundation. Flow depth aggregation per return period loses its probability of inundation due to the numerous events aggregated to give the maximum flow depth value. For instance, for the return period of 2500 years 84th percentile, a total of 15 events are aggregated, but since each event has a 1-in-2500-year (0.0004) chance of the tsunami event occurring, the aggregated inundation does not hold that return period probability any more. This event percent coverage map is a way to view the percentage of events that inundate onshore. Areas with an inundation percentage of 100% indicate that all events inundate that area, revealing that it holds the return period probability for that location. Figure 31 provides the event percentage of a 1-in-2500-year return period for 15 events. The areas in red reveal the locations that have a return probability of 2500 years for all 15 events (Figure 31). Overall, a total of 12 maps were developed for this output (four return periods and three resolutions).

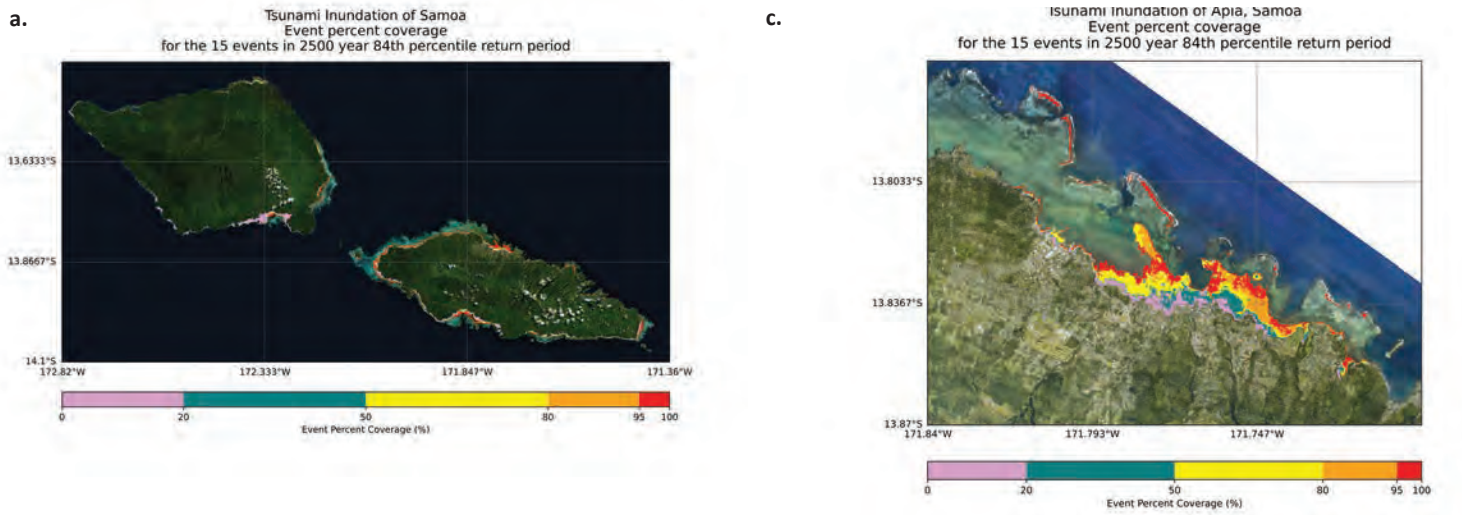

Figure 31: Event percent coverage for the 68 events for return period aggregation of 2500 years 84th percentile: a) Samoa 50 m resolution, b) South East Upolu 10 m resolution and c) Apia 5 m resolution.

4.6 Maximum flux

The sixth and final output type is the aggregated maximum flux per return period. Flux is determined from the total water flow depth (m) and the flow velocity (m/s) per unit width (1 m). The flux is expressed as volume per time (m^3/s). For the national Samoa 50 m resolution scale, flux was calculated from each time step output recorded every 60 seconds, and the maximum value of the flux was aggregated for each return period.

Figure 32 provides the aggregated maximum flux for return period 2500 years 84th percentile at a national Samoa 50 m resolution scale. A high flux may be attributed to a high flow depth inundation or a high velocity, or both (Kaiser et al. 2011).

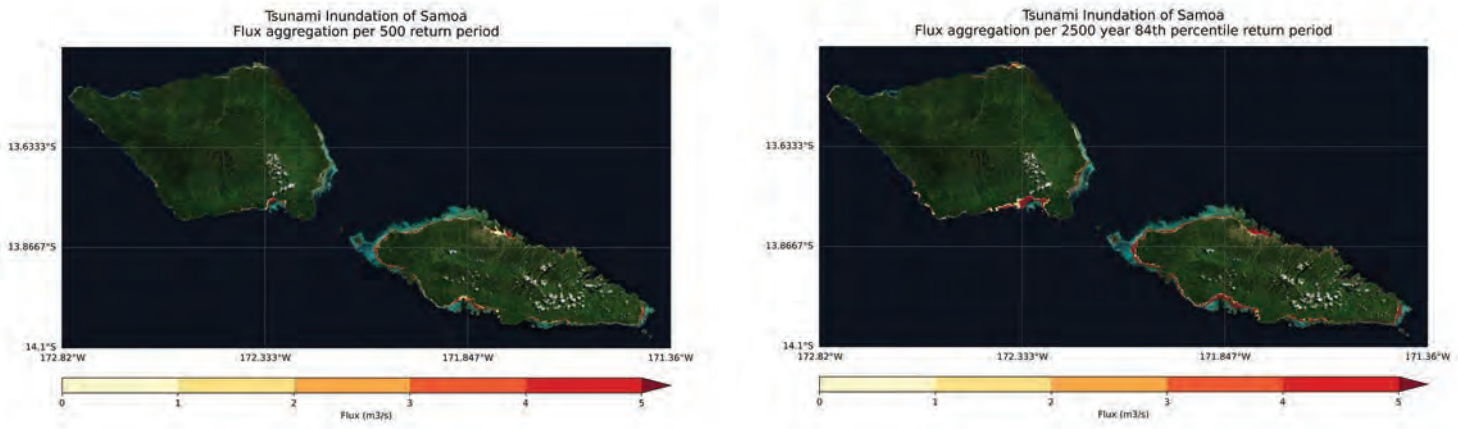

Figure 32: Maximum flux for return period aggregation of 500 years (left), and 2500 years 84th percentile (right) for Samoa 50 m resolution.

5.0 DISCUSSION

A total of 461 tsunami simulations were completed for the 68 designed scenarios covering the four return periods (100 years, 500 years, 1000 years and 2500 years, 84th percentile) and computed for five levels of resolution (5 km, 1 km, 50 m, 10 m and 5 m, with the exception of Kermadec-Tonga scenarios, which started at 1 km) with the projected sea-level rise inclusions (at 10 m and 5 m resolutions for all 68 scenarios). From these simulations, only the 50 m, 10 m, and 5 m resolution tsunami outputs were stored for data analysis. National Samoa (50 m resolution), South East Upolu (10 m) and Apia (5 m) inundation outputs were aggregated to represent six output types. The full collection of these six inundation map types is available in Annex B (Supplementary material).

The first output type reveals the aggregated maximum flow depth height. The lower return period flow depth aggregation maps, such as 100 years and 500 years are useful for urban planning as they outline areas that probabilistically will get inundated by a tsunami that is moderate/less extreme. It is also important to note that due to aggregating the scenarios per return period, the probability of these events occurring are no longer 1-in-100 year (0.01) and 1-in-500 year (0.002) as these aggregated scenarios are a compilation of each event's probability. For example, there are 18 events within the 500-year return period aggregation, and each one is a 1-in-500-year event. By providing the event percent coverage, the maps produced in the fifth product type are useful for retaining the probability for each return period. If an event percent coverage is 100%, those onshore locations that are inundated have the full probability of those return periods.

For 100-year and 500-year return period aggregated maximum flow depth, the national Samoa maximum flow depth map (Annex B) reveals the areas that are inundated in Savai'i and Upolu at a 50 m resolution. Notable inundation areas in Savai'i are the along the coasts of Palauli East district. For Upolu, the inundated areas are the southern coasts for the districts of Safata, Siumu, Falealili, Lepa, eastern coasts of Aleipata Itupa i Lalo and Aleipata Itupa i Luga, western coast of Upolu (Falelatai & Samatau, Lefaga & Faleseela, Aiga i le Tai and Aana Alofi 3), and the capital city, Apia.

Figure 34 shows the maximum flow depth inundation for South East Upolu and Apia for a return period of 500 years with 5 m contour line intervals ranging 0–15m. This inundation map is a useful tool for urban planning and for deciding on alternative locations for special infrastructure. In South East Upolu, the 500-year return period inundation covers topography below 5 m elevation. The areas most affected are the eastern coast of Aleipata Itupa i Lalo and Aleipata Itupa i Luga Districts, the southern coast of Falealili and Lepa District on Upolu. The greatest flow depth heights are located at the bay in Lepa and the bay in Falealili, with flow depth heights of more than 1.8 m.

For Apia City, the 500-year return period inundation covers the majority of Apia below 5 m elevation (Figure 34). The greatest flow depth heights are located at a bay beside Fagali'i and Moataa and at western Vailele Bay, with flow depth heights of more than 3 m. Located within the inundation areas is Apia Wharf, which has a flow depth height of roughly less than 1.8 m.

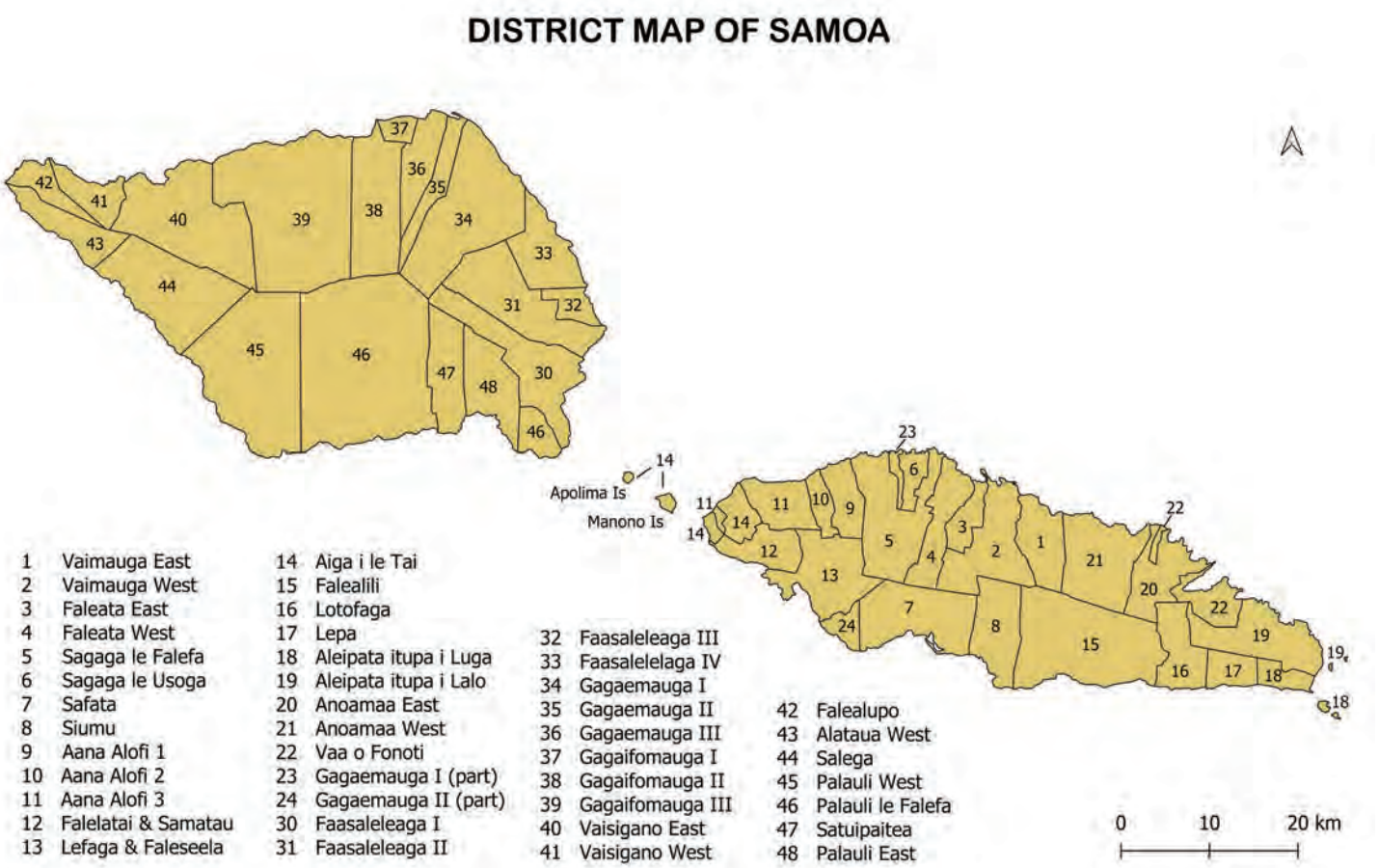

Figure 33: District map of Samoa (Samoa Bureau of Statistics 2016).

Inundation maps with higher return periods, such as 1000 and 2500 years, show the more extreme cases. The higher return period maps are most useful for planning the development of key and expansive infrastructure. The use of 2500 years at 84th percentile return period is recommended as it includes large subduction interface earthquakes, including events comparable to the earthquake that caused the 2011 Great East Japan tsunami. It is not the absolute 'worst case' but a compromise for very low probability of larger events. It also evaluates the risks and issues associated with mass evacuation after a powerful earthquake. The 84th percentile is used to be conservative (i.e., cautious) due to unknown or uncertain factors as the 84th percentile is similar to the upper bound of an error bar (Ministry of Civil Defence & Emergency Management 2016). It is recommended that extreme scenarios be used for evacuation mapping to ensure evacuation centres are away from any known tsunami threat.

For the 2500-year return period maximum flow depth for Samoa at 50 m resolution (Annex B), the maps portray similar locations of inundation as the 500-year return period but with greater flow depth heights due to the steep topography marking the boundary of the coastal zone. Figure 35 shows the 2500-year return period maximum flow depth inundation of South East Upolu and Apia with 5 m contour lines. For the 2500-year return period, the inundation of South East Upolu and Apia covers mostly topography below 10 m. However, in Apia, these locations are mainly the coasts of Vaimauga West District (the rest of the inundation in Apia, Vaimauga East and Faleata East districts are below 5 m elevation). For South East Upolu, the area of highest inundation is located along the coasts of districts Lepa and Aleipata Itupa i Luga. For Apia, the highest flow depths are situated at the bay beside Fagali'i and Moataa and at western Vailele Bay. The Apia Wharf is inundated with flow depth heights of less than 3 m.

a.

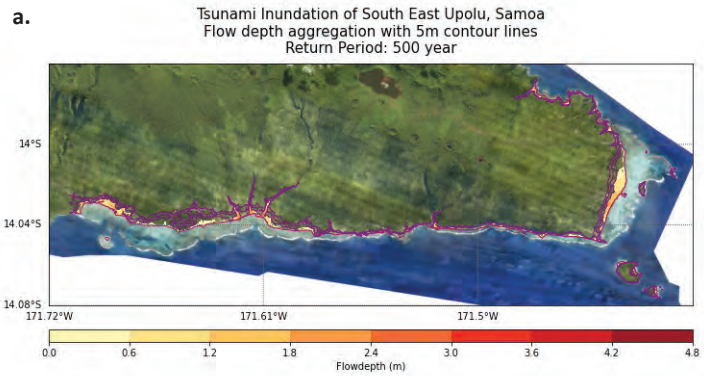

b.

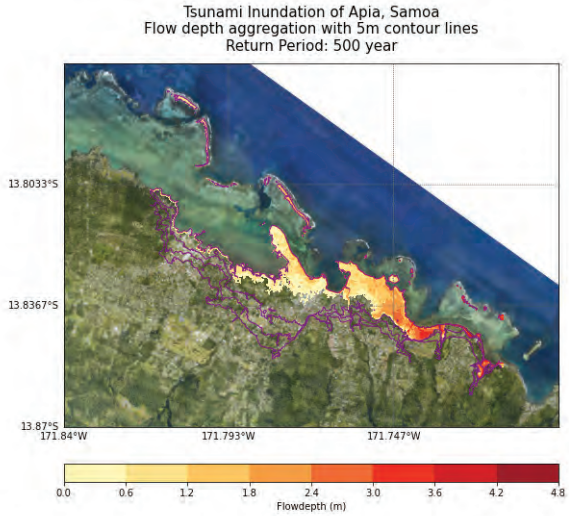

Figure 34: Maximum flow depth heights (m) with 5 m contour interval lines ranging from 0–15 m for a) South East Upolu at 10 m resolution and b) Apia at 5 m resolution for the 500-year return period.

a.

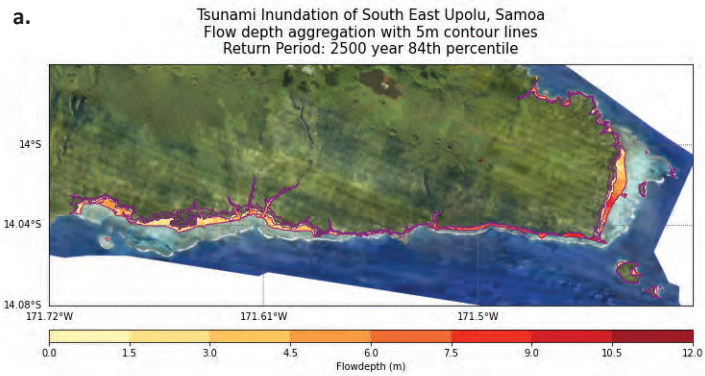

b.

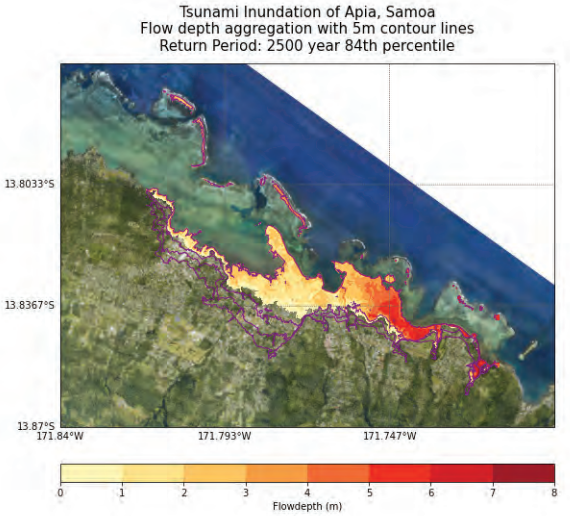

Figure 35: Maximum flow depth heights (m) with 5 m contour interval lines ranging from 0–15 m for a) South East Upolu at 10 m resolution and b) Apia at 5 m resolution for the 2500-year return period (84th percentile).

The second product type provides the aggregated flow depth with sea-level rise inclusions projected for 2100 (SSP 5-8.5) at MHWS for South East Upolu (10 m resolution) and Apia (5 m resolution) for the four return periods: 100 years, 500 years, 1000 years and 2500 years (84th percentile). The inundation maps show a further inundation coverage than the aggregation from the first product type. Figure 36 reveals the inundation extent reaches the 5 m contour line and, in some locations, surpasses it. The maps also reveal that the most heavily inundated areas match that with Figure 35, however, Figure 36 has higher flow depth height than Figure 35. These maps are a useful tool for any key infrastructure development with respect to longevity as climate change factors such as sea-level rise will need to be considered when developing along coastal zones. The full collection of these maps is available in Annex B.

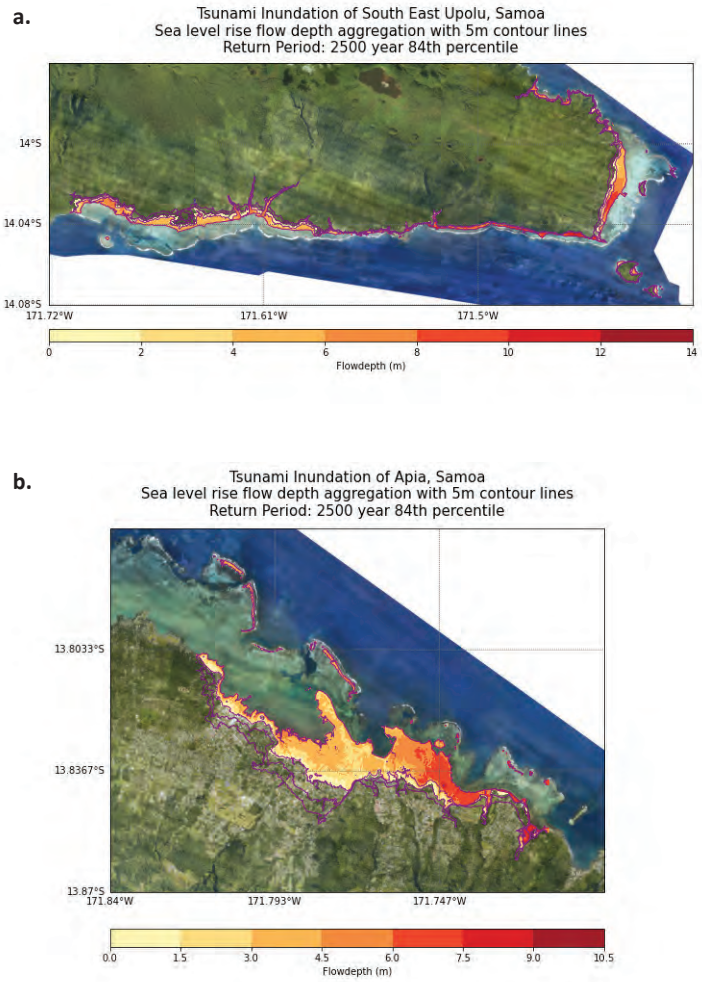

Figure 36: Maximum sea-level rise flow depth heights (m) with 5 m contour interval lines ranging from 0–15 m for a) South East Upolu at 10m resolution and b) Apia at 5 m resolution for the 2500-year return period (84th percentile).

The third product type provides the source coverage for each return period. With a total of 57 maps, this product has the largest quantity of maps (Annex B). The majority of the greatest flow depth heights for Samoa (50 m) and South East Upolu (10 m) are from scenarios that originate from the Kermadec-Tonga source. For Apia (5 m), the source for the greatest flow depth height varies depending on the return period. At 100 years, the majority of the highest flow depth originates from the Izu Mariana source; for 500 years, it is the Alaska Aleutians source; and for 1000 years and 2500 years, it is from the South America source. Due to Apia's location north of Upolu and the city's orientation of bays, probabilistically, the most extreme cases are from far distant sources such as Alaska Aleutians, Izu Mariana and South America. However, it is important not to disregard Kermadec-Tonga inundation in Apia. All tsunami warnings should be acknowledged with appropriate action as a tsunami wave has the potential to generate widespread inundation that can be imminent.

The fourth product type provides the vulnerability and possible damage to building structures within a particular flow depth category based on ITIS-2012. A series of flow depth ranges (0.5–1 m, 1–2 m, 2–5 m, 5–7 m, 7–10 m and greater than 10 m) is used to categorise the maximum grade of damage (Grade 1–5; Table 20) for building vulnerability class (Class A–F; Table 19). For instance, for a flow depth height range of 2–5 m, building structure types listed in vulnerability Class A (including masonry structures [rubble stone], fieldstone, adobe [earth brick], reinforced concrete [frame without earthquake resistant design (ERD)], and wood [timber]) have a maximum damage grade of 5. Damage grade 5 lists the damage according to building structure. For timber structures, grade 5 indicates destruction with total fracture and collapse of construction. The ITIS-2012 maps are available in Annex B (Supplementary material). While this product provides insights into the tsunami risk for Samoa, capitalising on the PCRAFI exposure dataset, further work will be done to transform the tsunami hazard information produced in this study into a tsunami risk assessment product.

The fifth product type is the event percent coverage, designed to provide percentages of events that cover onshore inundation. This product type is a complement to the first product type as the aggregation per return period loses the probability due to the numerous events per return period that are aggregated to contain the maximum flow depth height value. The event percent coverage maps reveal the percentage of events that cover a particular onshore location. The areas that have 100% event percent coverage are considered to contain the return period's probability. For instance, Figure 31c and Figure 37a (below) show the event percent coverage for Apia at a 2500-year return period for 15 events simulated at present mean sea level. The areas with 100% event coverage are locations that have all 15 events inundating that area and thus have the probability of a 1-in-2500-year chance of occurring. The areas with percentages below 100% do not share the same probability of a 1-in-2500-year chance. Figure 37b (next page) provides the sea-level rise inclusions for Apia at a 2500-year return period (IPCC AR6 2100 SSP 5-8.5 projection and MHWS), revealing that with sea-level rise projections, the number of areas with 100% event coverage increases, and the probability of 1-in-2500-year tsunami inundation coverage becomes more likely.

a.

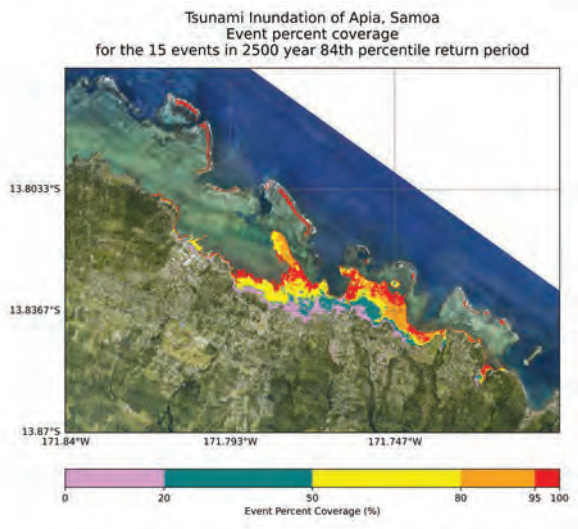

Figure 37: Event percent coverage at 2500 years (84th percentile) return period (above) for events simulated at present mean sea level and (next page) events simulated with sea-level rise at IPCC SSP5-8.5 2100 projection and at mean high spring water (MHWS).

The sixth product type provides the maximum flux for each return period for Samoa at 50 m resolution. The maximum flux is mapped for both Savai'i and Upolu. At higher return periods, the flux values are higher and have a greater coverage. A high flux may be attributed to a high flow depth inundation or a high velocity, or both (Kaiser et al. 2011). At a return period of 500 years, areas affected in Savai'i include the bay located along the coast of Satuipaitea and Palauli East districts. For Upolu, areas affected are Apia, eastern and western Upolu, and the coasts along Safata, Falealili and Lepa districts (Figure 32 [left]). At higher return periods of 1000 years and 2500 years, higher flux and greater coverage are observed along north and south Savai'i and the majority of the Upolu coasts (Figure 32 [right]).

b.

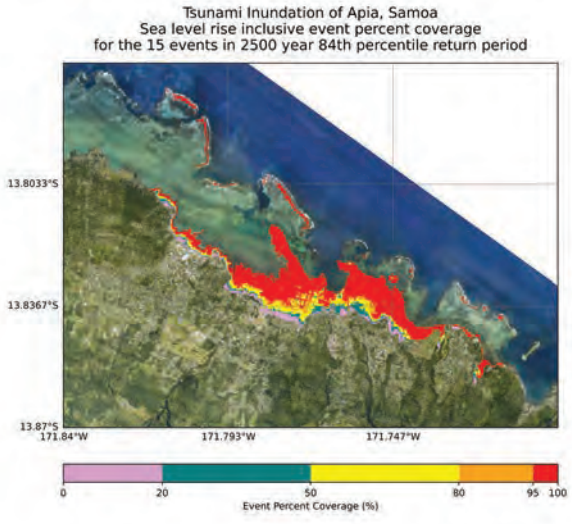

It is important to note that there are limitations to tsunami modelling. For instance, the friction coefficient for land used in the model was set to a conservative value. This value portrays the topography as bare land and disregards buildings, infrastructure and vegetation that may contribute to the tsunami wave energy dissipation. This conservative approach was sought as the friction coefficients that would best depict the bottom friction of Samoa's reef to the shoreline topography have not yet determined. Another limitation is the large uncertainty of the tsunami probabilities as dangerous tsunamis occur infrequently compared to other natural hazards. There is difficulty in representing tsunami sources and their frequencies due to fundamental limitations in present scientific knowledge of how often large magnitude earthquakes occur.

The PTHA18 database provides national-level understanding of tsunami inundation hazards but does not define onshore tsunami impact or tsunami effect on communities. In addition, high-resolution bathymetry and elevation data is important for local tsunami inundation models to best derive evacuation plans to improve community safety. The outputs of local tsunami inundation models like South East Upolu (10 m resolution) and Apia (5 m resolution) can indicate high-risk areas and prioritise further analysis to improve risk mitigation and community safety.

With the uncertainty in tsunami likelihood and its associated widespread impact, there is a need for high-resolution tsunami inundation early warning systems (EWS) to support effective emergency response and relevant preparatory action by communities before and during the event. Under the Pacific Resilience Programme (PREP), the National Institute of Water and Atmospheric Research (NIWA), in collaboration with the University of Cantabria and SPC, is developing a metamodel-based tsunami inundation forecast system for Samoa and Tonga that capitalises on the PTHA18 database and BG-Flood modelling software.

6.0 CONCLUSION

To conclude, a national tsunami hazard assessment was carried out for Samoa using the PCRAFI regional guidelines for tsunami inundation modelling with PTHA18 scenarios (Giblin et al. 2022). From this methodology, 68 events were selected for Samoa, covering six sources (Alaska Aleutians, Izu Mariana, Kermadec-Tonga, Kurils Japan, Mexico and South America) and four return periods (100 years, 500 years, 1000 years and 2500 years [84th percentile]). The BG-Flood model was used to simulate the scenarios using GPU and a nested grid system. The model setup had bathymetry from a coarse grid of 5 km resolution that contained the earthquake deformation for each source (with the exception of Kermadec-Tonga, which began at 1 km). The next nested grid of 1 km resolution that surrounded Samoa was simulated, followed by a national Samoa 50 m resolution, then a 10 m South East Upolu resolution, and finally a 5 m Apia resolution.

Before beginning the tsunami modelling for the 68 identified PTHA18 scenarios, sensitivity analysis and BG-Flood model validation were undertaken. The sensitivity analysis revealed that the best coarse resolution to begin the simulation was at 5 km, before nesting the other higher resolution bathymetry grids. Model validation was performed to ensure the model was calibrated properly using historical events of Samoa in 2009 and Japan in 2011. The 2009 Samoa tsunami was a unique tsunamigenic event with a complex combined faulting causing widespread inundation, damage and loss of life on the southern coasts of Upolu, Samoa. This complexity was best depicted by the comparison of the Apia gauge and DART buoy data of Hossen et al. (2017) and Lay et al. (2010) Version C model validation. This was also supported by Bosserelle et al. (2020), who states that while imperfect, these two source parameters are most consistent with the observed tsunami data. Further model validation using PTHA18 events was undertaken with the 2011 Japan tsunami. Unfortunately, the Apia tide gauge had no observational data for comparison with this tsunamigenic event. The main comparison was done with modelled DART buoy data that validated the observational DART buoy offshore water depths.

The model parameters and resolution levels of the 68 scenarios were set for Bash script running that took approximately two months to complete. Only outputs from the national Samoa (50 m), South East Upolu (10 m) and Apia (5 m resolution) scales were analysed. The Samoa 50 m resolution inundation map provides inundation hazard information at a national scale that is useful for determining the areas at risk of tsunami inundation. The South East Upolu 10 m and Apia 5 m resolution maps are designed to provide high-resolution hazard information to communities and high-value tourism facilities. From the 340 tsunami simulation inundation outputs, six types of aggregated maps were assembled (Annex B Supplementary material).

The first product map type gives the aggregated maximum flow depth inundation height for each return period. Due to the conservative approach of aggregating the maximum values, the maps' probabilities do not give an actual representation of each return period. For example, a 2500-year return period has 15 events aggregated that on their own have a 1-in-2500-year probability, while the aggregation is a culmination of the 1-in-2500-year chances of all 15 events. It is important to note that even though the events reflect a similar maximum stage on offshore points, the onshore inundation from each event differ. The fifth product map type addresses this probability dilemma as it maps the percentages of events that overlap. The events with a percent coverage revealing 100% overlap are a true representation of that return period aggregation. Flow depth aggregation maps for lower return periods (100 years and 500 years) are useful for urban planning as they outline areas that probabilistically will get inundated by a tsunami that is moderate to less extreme. Inundation maps with higher return period flow depth aggregation (1000 years and 2500 years) reveal more extreme events and are useful for development planning of key and expansive infrastructure. At a 50 m national Samoa scale, notable inundated areas in Savai'i are along the coasts of Palauli East, Faasaleleaga I and Gagaemauga III districts, while for Upolu, the inundated areas are Apia city and the coasts for the districts of Safata, Siumu, Falealili, and Lepa, eastern coasts of Aleipata Itupa i Lalo and Aleipata Itupa i Luga, and western coast of Upolu (Falelatai & Samatau, Lefaga & Faleseela, Aiga i le Tai and Aana Alofi 3). At 10 m resolution for South East Upolu, the areas most affected are the eastern coast of Aleipata Itupa i Lalo and Aleipata Itupa i Luga Districts, and the southern coast of Falealili, and Lepa District on Upolu. For Apia at 5 m resolution, the highest flow depths are located at a bay beside Fagali'i and Moataa and at western Vailele Bay.

At a return period of 500 years, the inundation is below the 5 m elevation contour line, whereas for 2500 years, the heavily inundated parts of South East Upolu and Apia are below the 10 m elevation contour line.

The second product map type involves sea-level rise inclusions based on IPCC AR6 projected 2100 SSP 5-8.5 sea-level rise and MHWS for South East Upolu (10 m resolution) and Apia (5 m resolution) for four return periods. The sea-level rise inclusions reveal similar areas of inundation identified in the first product type map but with further inundation extents and at higher flow depth heights. These maps are important for any key infrastructure as climate change factors such as sea-level rise need to be considered while developing along coastal zones.

The third product map type provides coverage of the flow depth based on the earthquake source for each return period. The majority of the greatest flow depth heights for Samoa (50 m) and South East Upolu (10 m) are from tsunamis that originate from the Kermadec-Tonga Trench. For Apia (5 m), due to its location and orientation, the source of the greatest flow depth height varies depending on the return period. For a 100-year return period for Apia, the highest flow depth originates from the Izu Mariana source; for 500 years, it is Alaska Aleutians; and at 1000 years and 2500 years, it is from South America source. However, it is important not to disregard tsunamis that originate at Kermadac-Tonga for Apia. It is expected that all tsunami warnings follow appropriate evacuation procedures.

The fourth map type gives the vulnerability of building structures to flow depth ranges based on ITIS-2012. Building structures are assigned a vulnerability class (Class A–F) and a grade (Grade 1–5) for the damage the building structure class may incur at a certain flow depth range. These maps are useful for determining the possible damage a building may sustain according to the flow depth height range it lies within. These maps give homeowners, prospective businesses and land planning initiatives an indication of the damage that might incur at a 100-year, 500-year, 1000-year and 2500-year (84th percentile) return period.

The fifth product type reveals the percentage of events that are inundating a particular onshore location. Locations that provide 100% event coverage have the return period's probability. For example, 15 events were aggregated for the 2500-year return period. An area that has an event percentage of 100% reveals the onshore locations that truly reflect a 2500-year return period. This map product was designed to assist the first product type, which gives the aggregated maximum flow depth heights. Due to aggregating the flow depth of events, the probability of that return period becomes more difficult if event percentages are less than 100%. While considering development along coastal zones, locations with an inundation event percentage of 100% share the probability of the return period, and this needs to be considered along with the maximum flow depth heights.

The sixth product type provides the maximum flux for each return period at a 50 m Samoa resolution. The maximum flux is mapped to areas that have a high flow depth inundation or high velocity, or both. High flux values are observed on Upolu with the majority of its coastlines affected.

Samoa's tsunami inundation hazard assessment was developed under a Pacific regional tsunami guideline using the PTHA18 database. These six inundation map types reveal that Samoa is susceptible to tsunamis from near and distant sources. The return period aggregation reveals the likelihood and flow depth heights that coastal areas may be flooded in a 100-year, 500-year, 1000-year and 2500-year (84th percentile) return period. This study also plans to compare the modelled inundation results with Samoa's tsunami hazardous zones to verify evacuation routes and assembly points, and to possibly propose more tsunami warning signage in areas that appear heavily inundated according to the maps. This project study was undertaken to provide Samoa government officials knowledge and understanding of the risk of tsunami inundation hazard to their coastal zones.

7.0 REFERENCES

BEAVAN, J., WANG, X., HOLDEN, C., WILSON, K., POWER, W., PRASETYA, G., BEVIS, M. & KAUTOKE, R. 2010. Near-simultaneous great earthquakes at Tongan megathrust and outer rise in September 2009. Nature, 466, 959-963.

BOSSERELLE, C. 2021. BG-Flood Wiki [Online]. Available: https://github.com/CyprienBosserelle/ BG_Flood/wiki [Accessed 18 May 2021].

BOSSERELLE, C., WILLIAMS, S., CHEUNG, K. F., LAY, T., YAMAZAKI, Y., SIMI, T., ROEBER, V., LANE, E., PAULIK, R. & SIMANU, L. 2020. Effects of Source Faulting and Fringing Reefs on the 2009 South Pacific Tsunami Inundation in Southeast Upolu, Samoa. Journal of Geophysical Research: Oceans, 125, e2020JC016537.

BRICKER, J. D., GIBSON, S., TAKAGI, H. & IMAMURA, F. 2015. On the Need for Larger Manning's Roughness Coefficients in Depth-Integrated Tsunami Inundation Models. Coastal Engineering Journal, 57, 1550005.

BUREAU OF METEOROLOGY. 2021. Tsunami Facts and Information [Online]. Commonwealth of Australia. Available: http://www.bom.gov.au/tsunami/info/index.shtml [Accessed 9 July 2021].

DAVIES, G. 2021. PTHA18 Github Repository [Online]. Available: https://github.com/GeoscienceAustralia/ptha [Accessed 21 May 2021].

DAVIES, G. & GRIFFIN, J. 2018. The 2018 Australian probabilistic tsunami hazard assessment: hazard from earthquake generated tsunamis. Canberra, Australia: Geoscience Australia.

DISASTER MANAGEMENT OFFICE. 2017. National Disaster Management Plan 2017-2020. Apia, Samoa: Ministry of Natural Resources and Environment, Government of Samoa.

FAN, W., SHEARER, P. M., JI, C. & BASSETT, D. 2016. Multiple branching rupture of the 2009 Tonga-Samoa earthquake. Journal of Geophysical Research: Solid Earth, 121, 5809-5827.

GEOSCIENCE AUSTRALIA. 2021. Probabilistic Tsunami Hazard Assessment (PTHA) [Online]. Available: https://www.ga.gov.au/about/projects/safety/ptha [Accessed 18 May 2021].

GIBLIN, J., DAVIES, G., DAMLAMIAN, H., WEBER, R., & WILSON, K. 2022. Earthquake Scenario Selection for Tsunami Hazard Assessment: Guidelines on using the 2018 Probabilistic Tsunami Hazard Assessment in the Pacific. Technical Report in preparation.

HOSSEN, M. J., GUSMAN, A., SATAKE, K. & CUMMINS, P. R. 2018. An Adjoint Sensitivity Method Applied to Time Reverse Imaging of Tsunami Source for the 2009 Samoa Earthquake. Geophysical Research Letters, 45, 627-636.

IPCC 2021. Climate Change 2021: The Physical Science Basis. Contribution of Working Group I to the Sixth Assessment Report of the Intergovernmental Panel on Climate Change. In: MASSON-DELMOTTE, V., P. ZHAI, A. PIRANI, S.L. CONNORS, C. PÉAN, S. BERGER, N. CAUD, Y. CHEN, L. GOLDFARB, M.I. GOMIS, M. HUANG, K. LEITZELL, E. LONNOY, J.B.R. MATTHEWS, T.K. MAYCOCK, T. WATERFIELD, O. YELEKÇI, R. YU, B. ZHOU (ed.). Cambridge University Press. In Press.

KAISER, G., SCHEELE, L., KORTENHAUS, A., LØVHOLT, F., RÖMER, H. & LESCHKA, S. 2011. The influence of land cover roughness on the results of high resolution tsunami inundation modeling. Nat. Hazards Earth Syst. Sci., 11, 2521-2540.

LAY, T., AMMON, C. J., KANAMORI, H., RIVERA, L., KOPER, K. D. & HUTKO, A. R. 2010. The 2009 Samoa–Tonga great earthquake triggered doublet. Nature, 466, 964-968.

LEKKAS, E. L., ANDREADAKIS, E., KOSTAKI, I. & KAPOURANI, E. 2013. A Proposal for a New Integrated Tsunami Intensity Scale (ITIS-2012). Bulletin of the Seismological Society of America, 103, 1493-1502.

MINISTRY OF CIVIL DEFENCE & EMERGENCY MANAGEMENT 2016. Tsunami Evacuation Zones: Director's Guideline for Civil Defence Emergency Management Groups [DGL 08/16]. Wellington: Ministry of Civil Defence & Emergency Management. ISBN 978-0-478-43515-3

MOODY, J. 2021. What does RMSE really mean? [Online]. Available: https://towardsdatascience.com/what-does-rmse-really-mean-806b65f2e48e [Accessed 3 August 2021].

NCEI. 2021. On this day: 2011 Tohoku Earthquake and Tsunami [Online]. Available: https:// www.ncei.noaa.gov/news/day-2011-japan-earthquake-and-tsunami [Accessed 29 July 2021].
NCEI, WDS & ITIC. 2017. Historical Tsunami Events near the Tonga Trench (1837-2015). Honolulu, U.S.A.

SAMOA BUREAU OF STATISTICS. 2016. Samoa Socio-Economic Atlas 2016 [Online]. Available: https://www.sbs.gov.ws/images/sbs-documents/Population_and_Demography/SOCIO_ECONOMIC_Atlas2016.pdf.

SAMOA BUREAU OF STATISTICS. 2017. 2016 Census Brief No.1. Revised version: Population Snapshot and Household Highlights. Apia, Samoa.

SMS TSUNAMI WARNING. 2018. Tsunamis: main features [Online]. Available: https://www.sms-tsunami-warning.com/pages/tsunami-features [Accessed 9 July 2021].

STATISTICS SOLUTIONS. 2021. Pearson's Correlation Coefficient [Online]. Available: https:// www.statisticssolutions.com/free-resources/directory-of-statistical-analyses/pearsons-correlation-coefficient/ [Accessed 3 August 2021].

USGS. 2021. M 8.1 - Samoa Islands region [Online]. Available: https://earthquake.usgs.gov/earthquakes/eventpage/usp000h1ys/executive [Accessed 25 May 2021].

ZHOU, H., WEI, Y. & TITOV, V. V. 2012. Dispersive modeling of the 2009 Samoa tsunami. Geophysical Research Letters, 39.

ANNEX A

Source	Return period	Event ID	Mw	Peak slip	Max stage
Alaska Aleutians	2500 years				
	84th percentile	61102	9.5	66.46	0.9666497
		60657	9.4	68.83	0.9553607
		60536	9.4	47.86	0.9197771
	1000 years	60559	9.4	49.48	0.5986628
		59627	9.3	37.3	0.5940279
	500 years	60525	9.4	81.34	0.5838252
		58769	9.2	31.22	0.4531334
		57981	9.1	56.96	0.4490869
	100 years	58228	9.1	43.46	0.2318573
		57279	9	56.25	0.2493708
		57165	9	38.08	0.2260948
Izu Mariana	500 years	28225	9.3	72.37	0.5011606
	100 years	28268	9.3	64.15	0.290757
		27463	9.2	79.2	0.2558099
Kermadec-Tonga	2500 years				
	84th percentile	41316	9.1	35.04	1.896666
		40430	9	45.07	1.92158
		37655	8.7	45.42	1.73144
	1000 years	42747	9.3	44.45	1.366749
		42071	9.2	34.66	1.226913
		39613	8.9	36.4	1.204324
	500 years	43041	9.3	83.49	0.8069231
		40488	9	26.55	1.012366
		39608	8.9	38.38	0.8619965
		38729	8.8	50.93	0.9329659
		34737	8.5	17.44	0.9817109
	100 years	41376	9.1	38.86	0.3286293
		40477	9	31.72	0.4651025
		39733	8.9	32.23	0.4855594
		34773	8.5	20.03	0.476863
Kurils Japan	1000 years	49923	9.6	94.5	0.6758353
		49533	9.5	59.47	0.5629229
		49497	9.5	76.25	0.7250311
	500 years	49953	9.6	88.64	0.6199597
		49228	9.4	65.44	0.4862833
		49158	9.4	64.68	0.4793799
	100 years	49278	9.4	60.71	0.2709512
		48714	9.3	77.48	0.2692837
		47931	9.2	41.56	0.2618724
		47859	9.2	50.36	0.2256674
Mexico	500 years	30053	9.1	76.18	0.4512498
	100 years	28642	8.9	25.28	0.2363083
		28004	8.8	38.08	0.2306855

Source	Return period	Event ID	Mw	Peak slip	Max stage
South America	2500 years				
	84th percentile	147944	9.6	130.7	2.085454
		147771	9.6	56.69	2.023661
		147727	9.6	85.18	1.857057
		147715	9.6	124.5	1.584987
		147548	9.6	98.12	1.966608
		146242	9.5	90.74	1.786048
		146024	9.5	133.2	2.064196
		145867	9.5	101.4	2.098882
		144206	9.4	97.58	1.865142
	1000 years	148217	9.6	85.24	1.264794
		147826	9.6	62.98	1.386427
		145931	9.5	49.2	1.110762
		144019	9.4	69.88	1.334338
		144004	9.4	53.61	1.215989
		143811	9.4	75.37	1.193918
	500 years	148123	9.6	85.87	0.8110231
		146157	9.5	28.42	1.004214
		145942	9.5	45.53	0.8211437
		144162	9.4	43.52	0.9762511
		142072	9.3	54.73	0.7495269
	100 years	144507	9.4	50.86	0.4348389
		141862	9.3	34.5	0.4119683
		141545	9.3	63.99	0.4429784
		139943	9.2	57.63	0.3670495
		139865	9.2	34.69	0.4845489
		137616	9.1	25.67	0.4702698

ANNEX B SUPPLEMENTARY MATERIAL

Inundation Output Maps Per Return Period

Table of Contents

1.0 Maximum flow depth aggregation

a. Return period (RP) 100 year

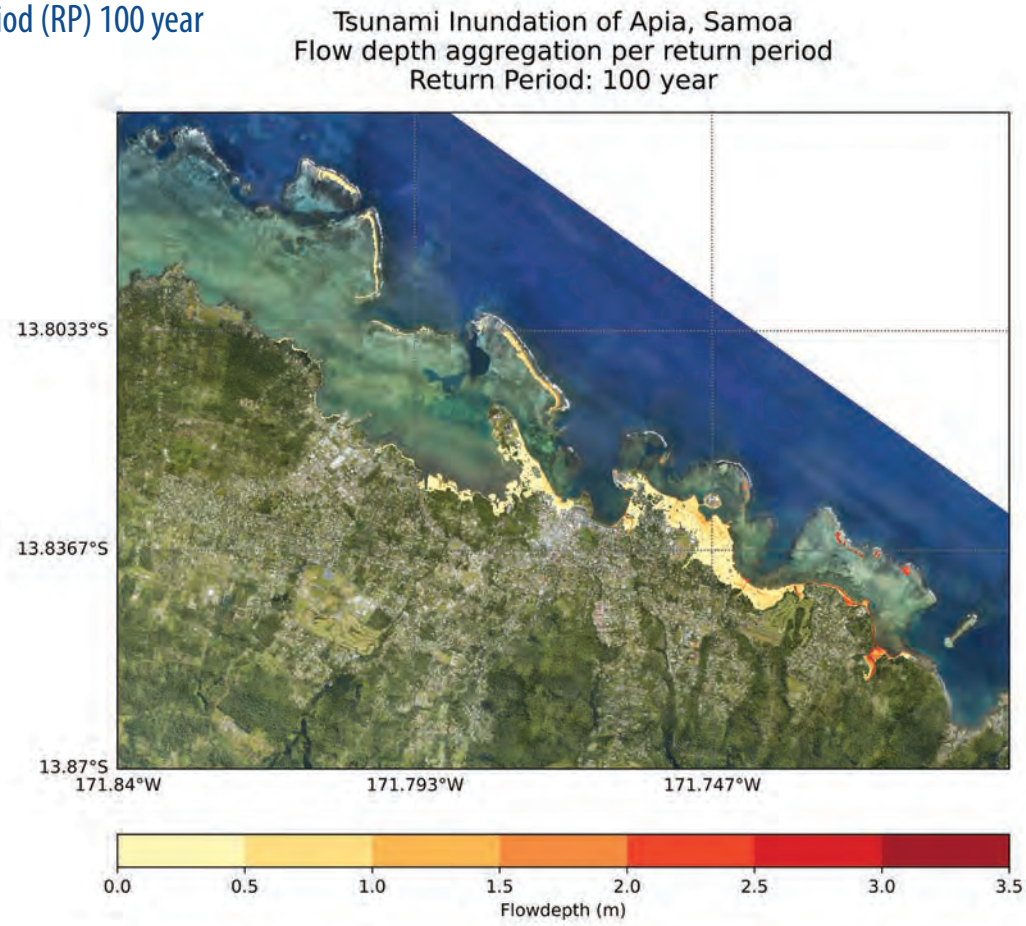

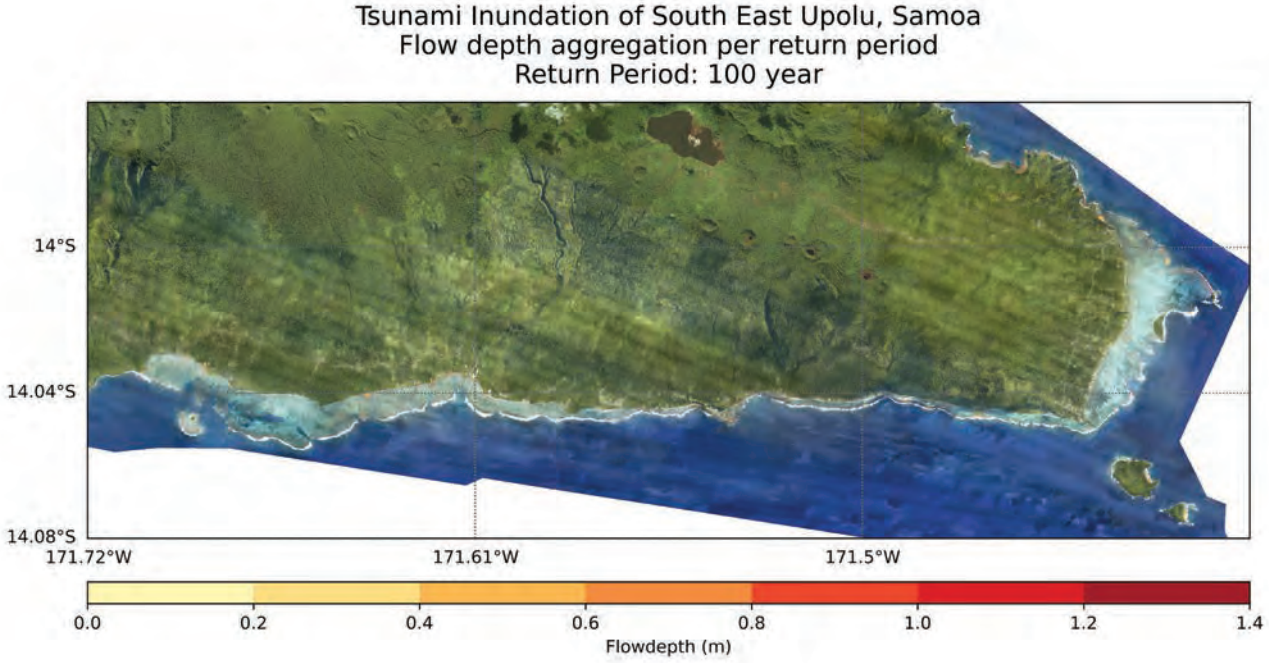

a. RP 100 year

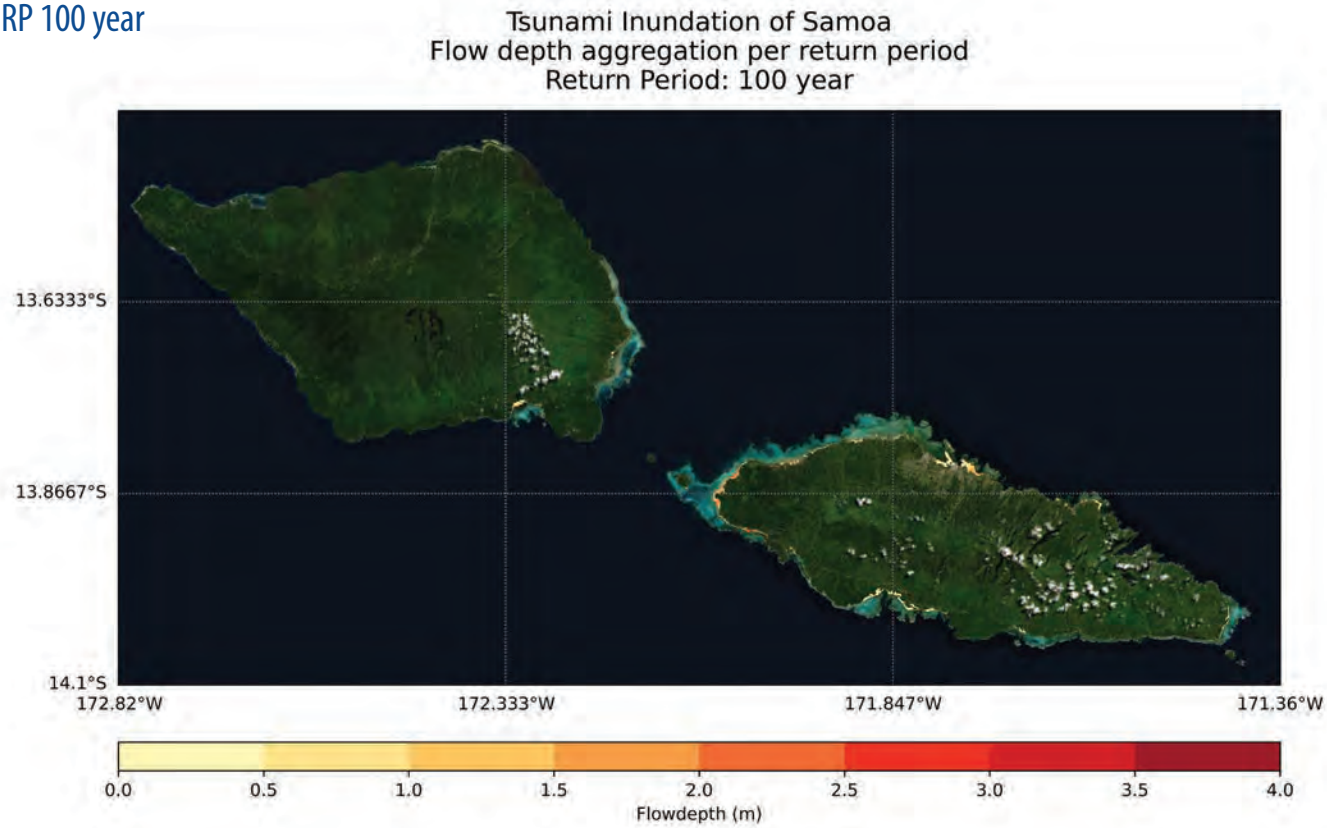

b. RP 500 year

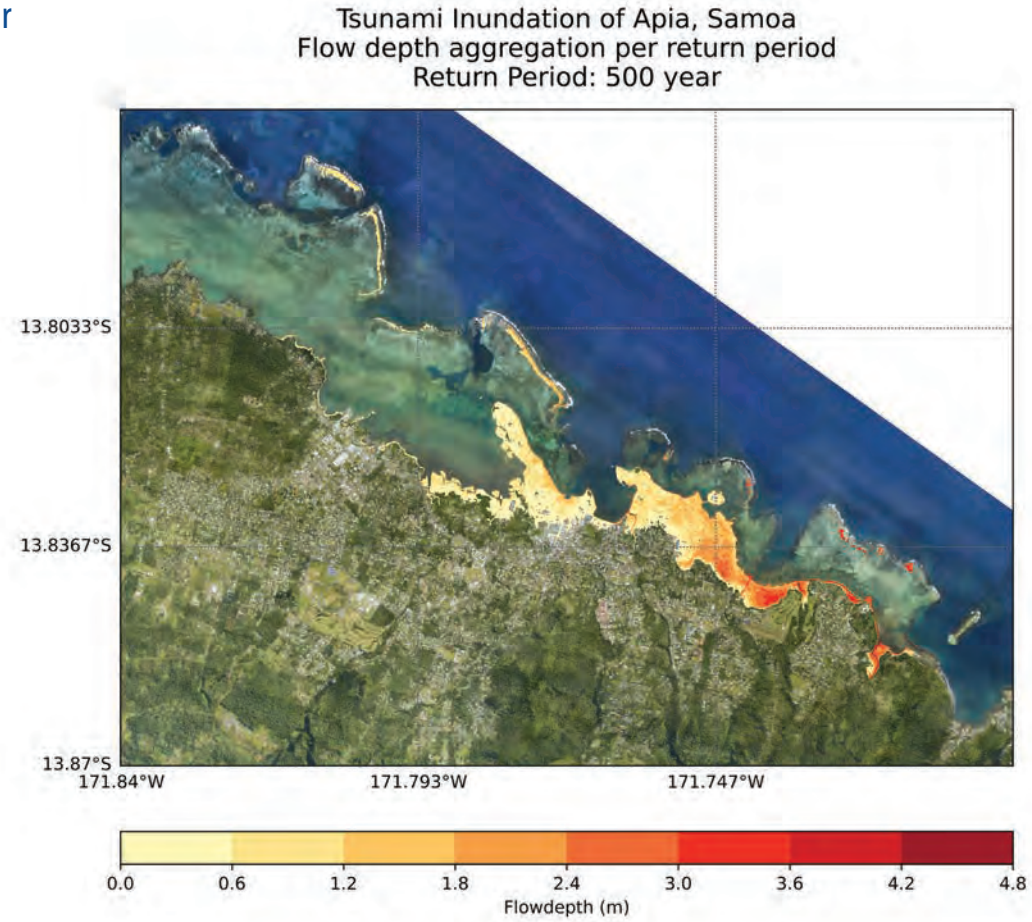

b. RP 500 year

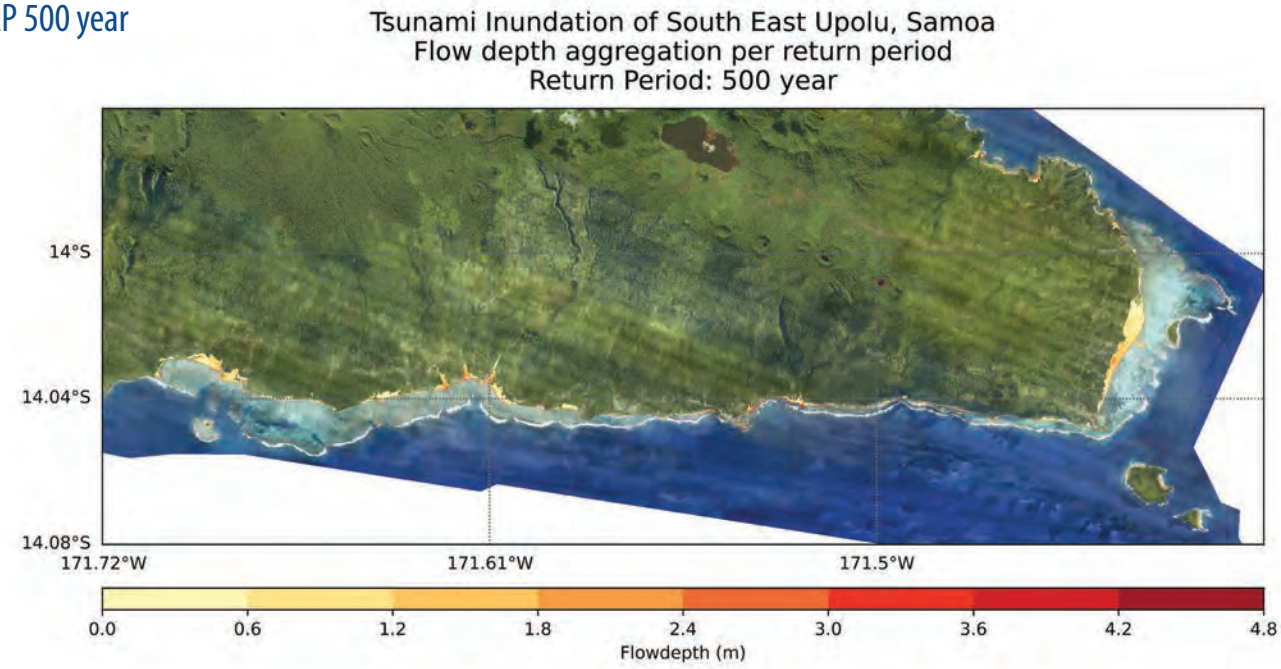
Tsunami Inundation of South East Upolu, Samoa
Flow depth aggregation per return period
Return Period: 500 year
14°S
14.04°S
14.08°S
171.72°W
171.61°W
171.5°W
0.0
0.6
1.2
1.8
2.4
3.0
3.6
4.2
4.8
Flowdepth (m)

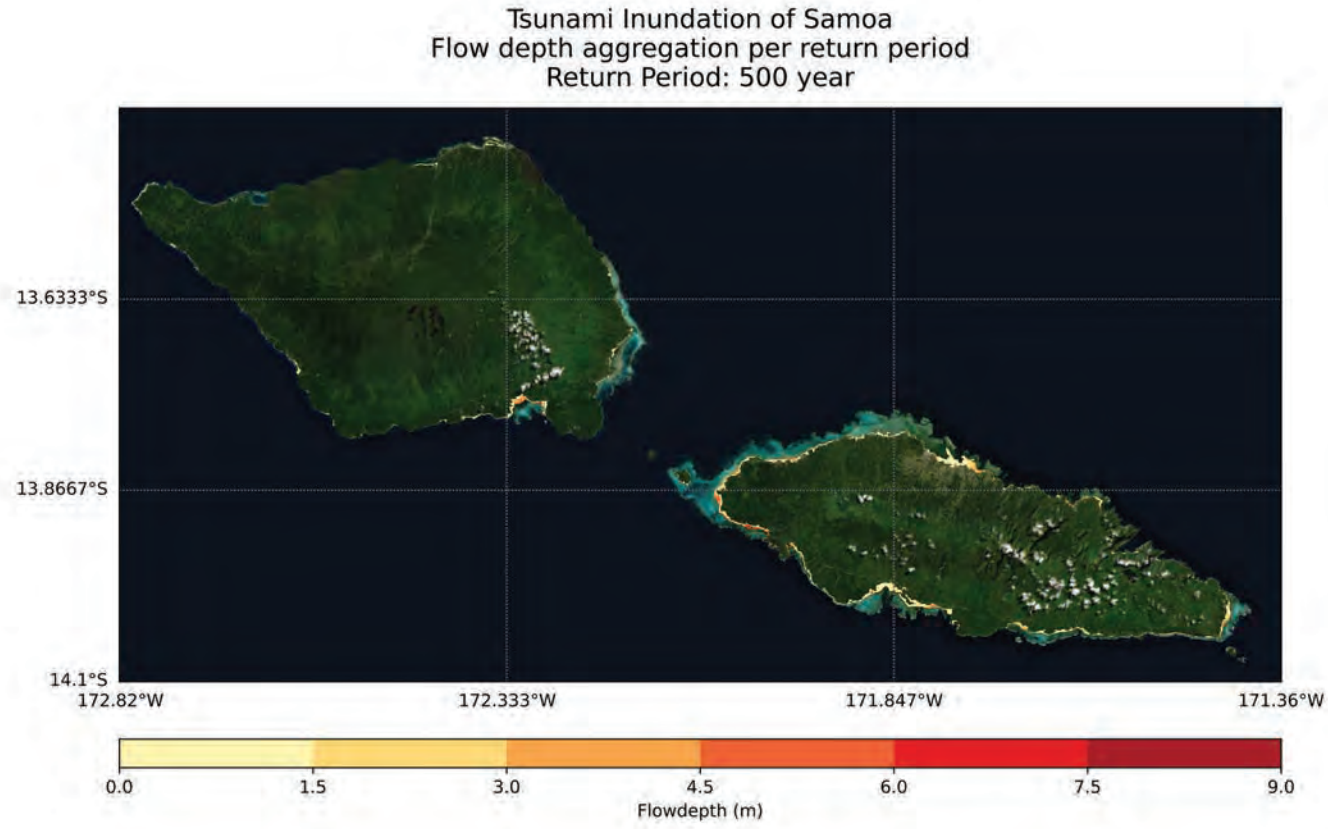
Tsunami Inundation of Samoa
Flow depth aggregation per return period
Return Period: 500 year
13.6333°S
13.8667°S
14.1°S
172.82°W
172.333°W
171.847°W
171.36°W
0.0
1.5
3.0
4.5
6.0
7.5
9.0
Flowdepth (m)

c. RP 1000 year

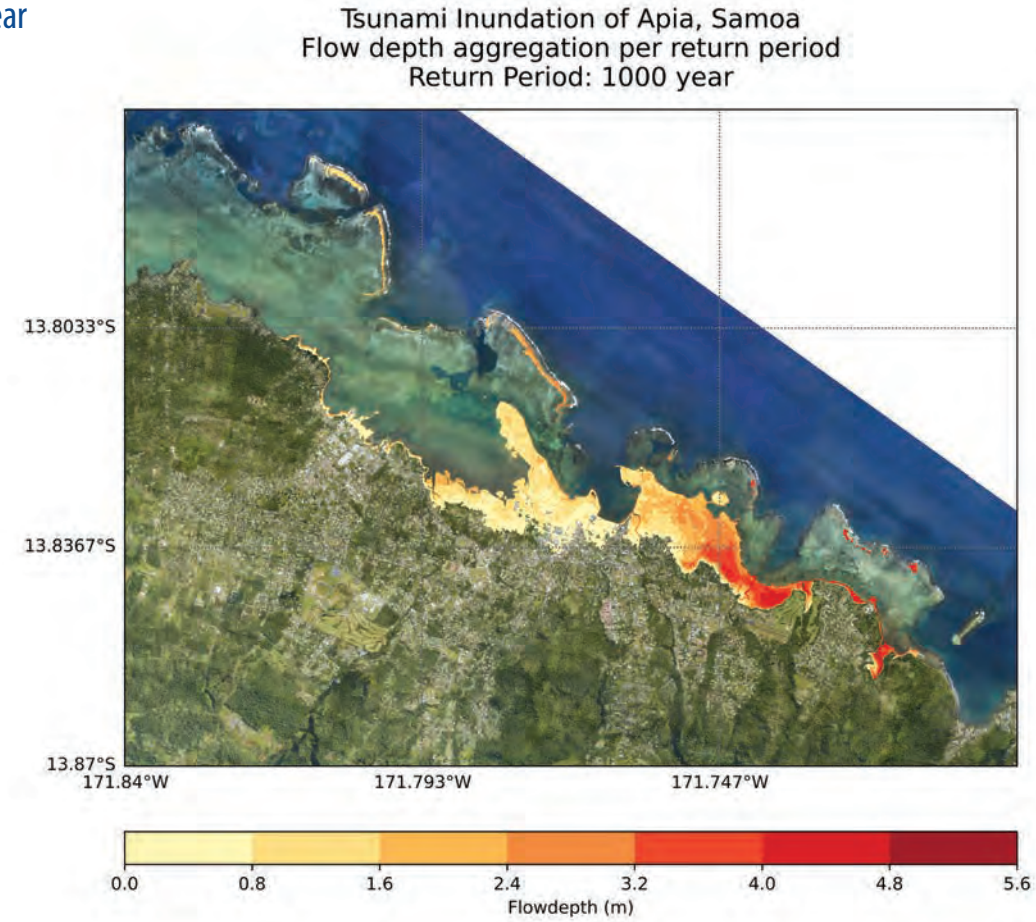

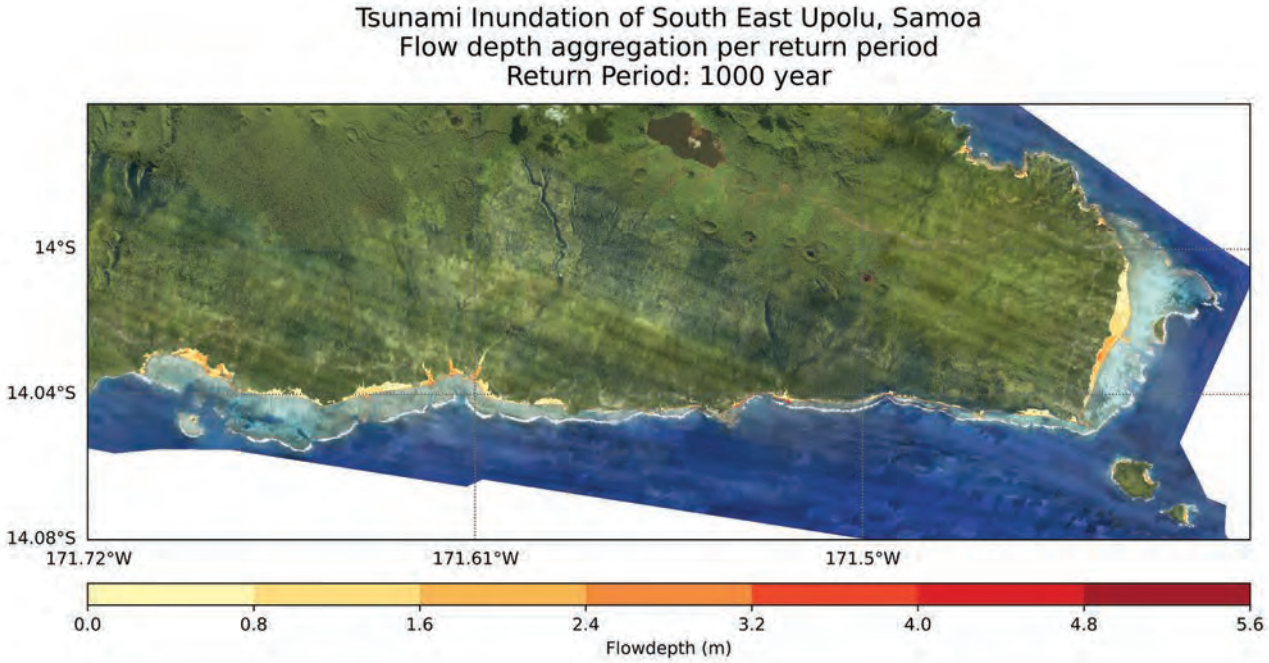

c. RP 1000 year

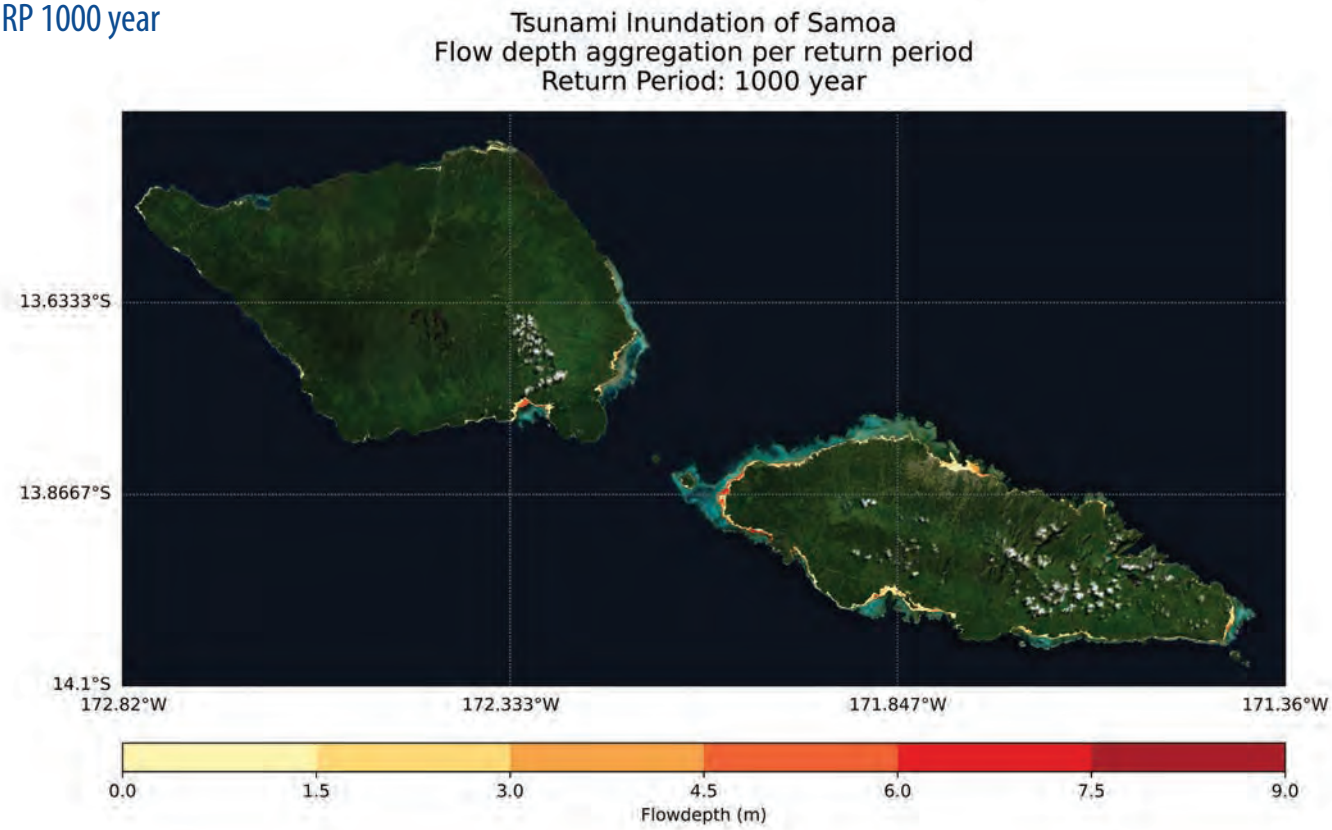

d. RP 2500 year 84th percentile

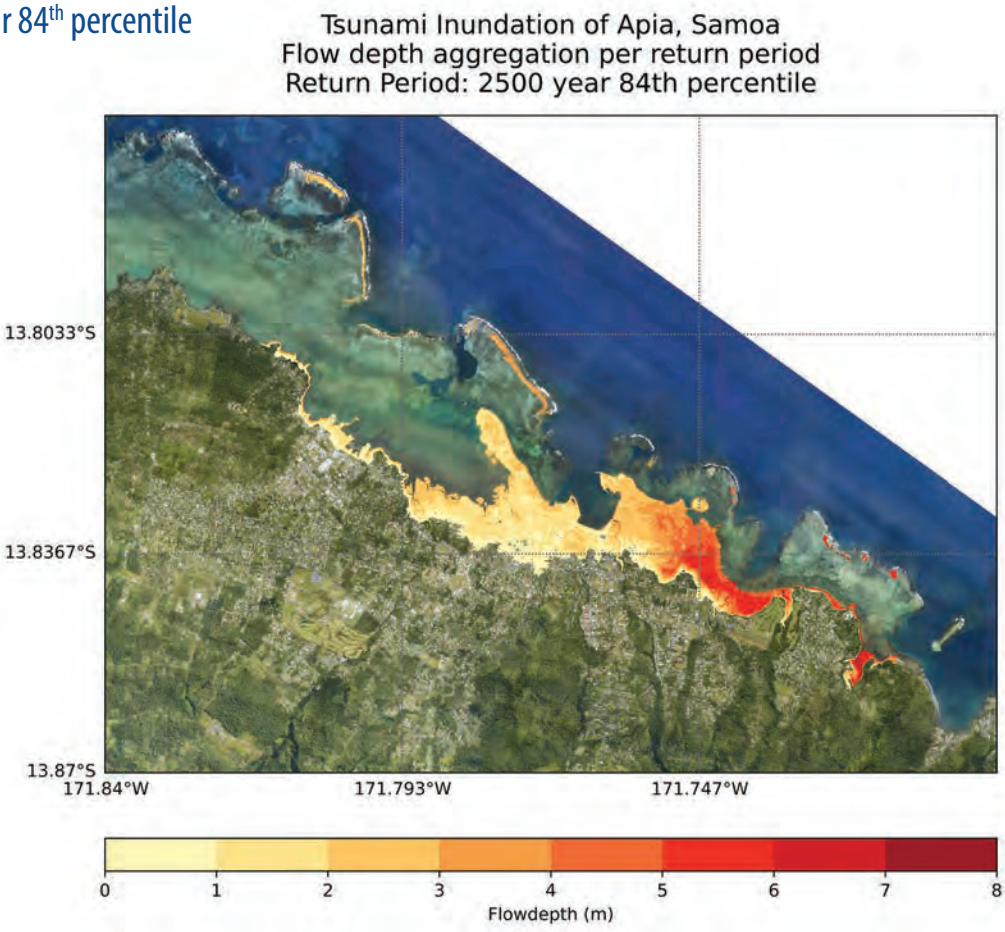

d. RP 2500 year 84th percentile

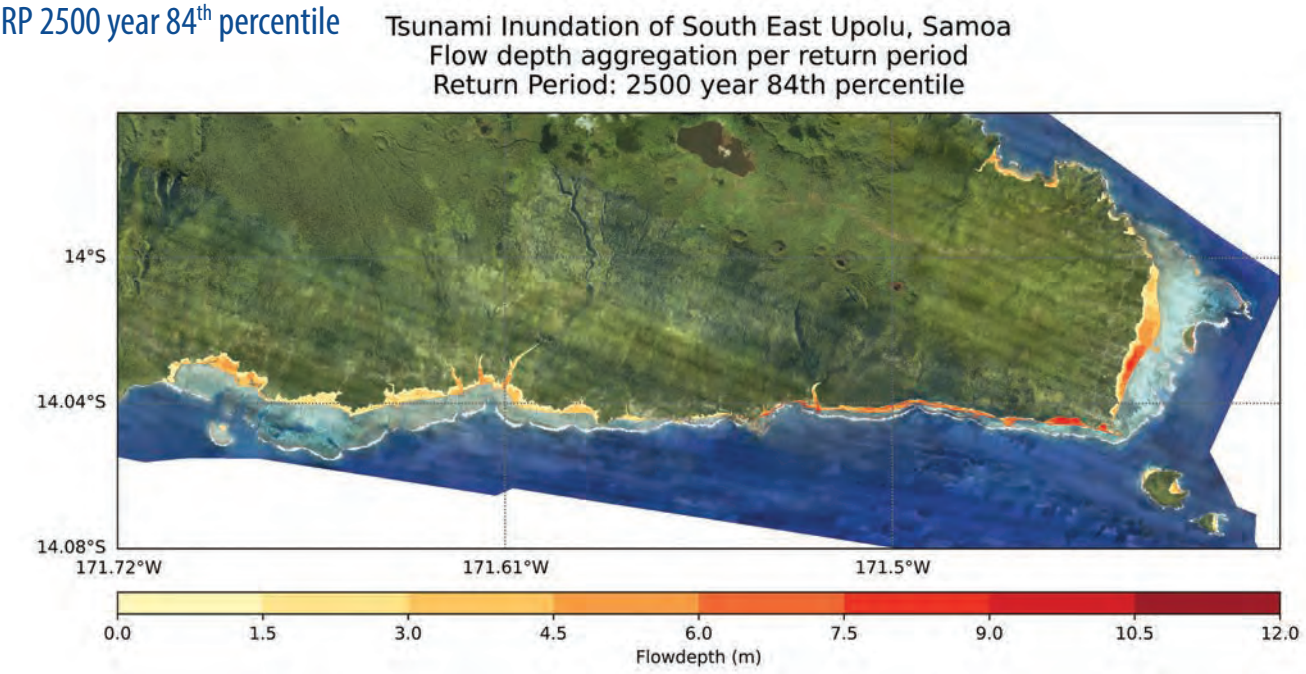

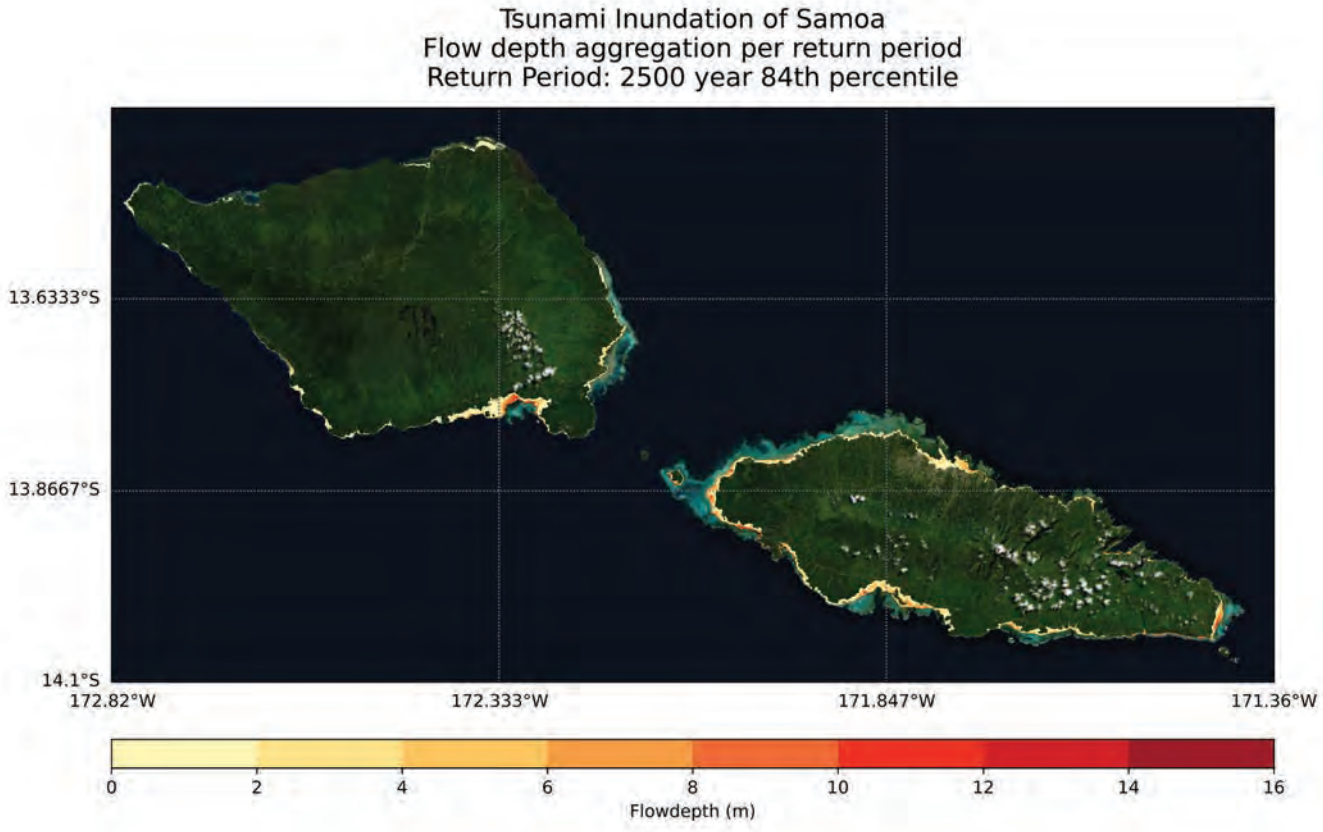

2.0 Sea-level rise inclusive maximum flow depth aggregation

a. RP 100 year

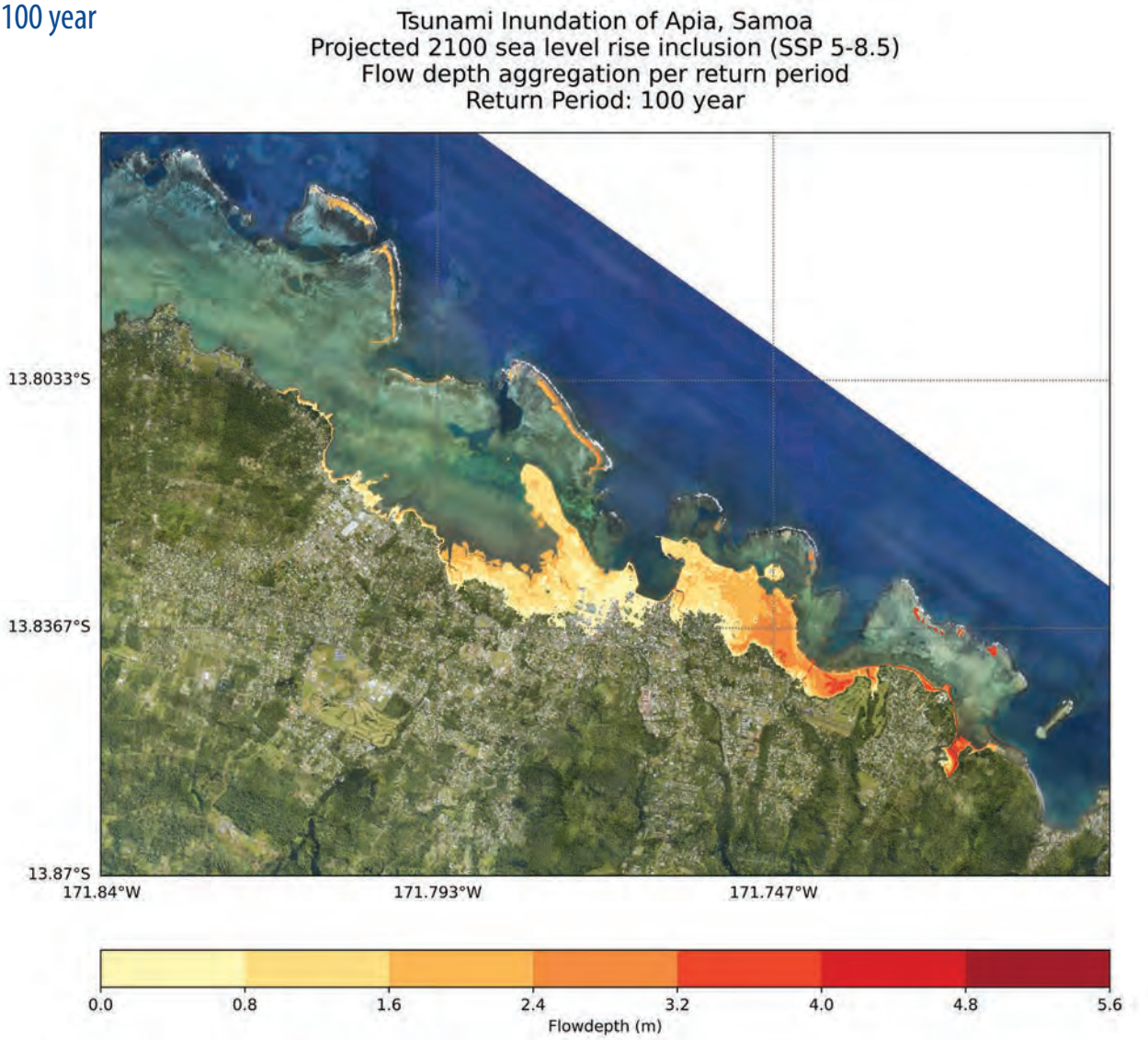

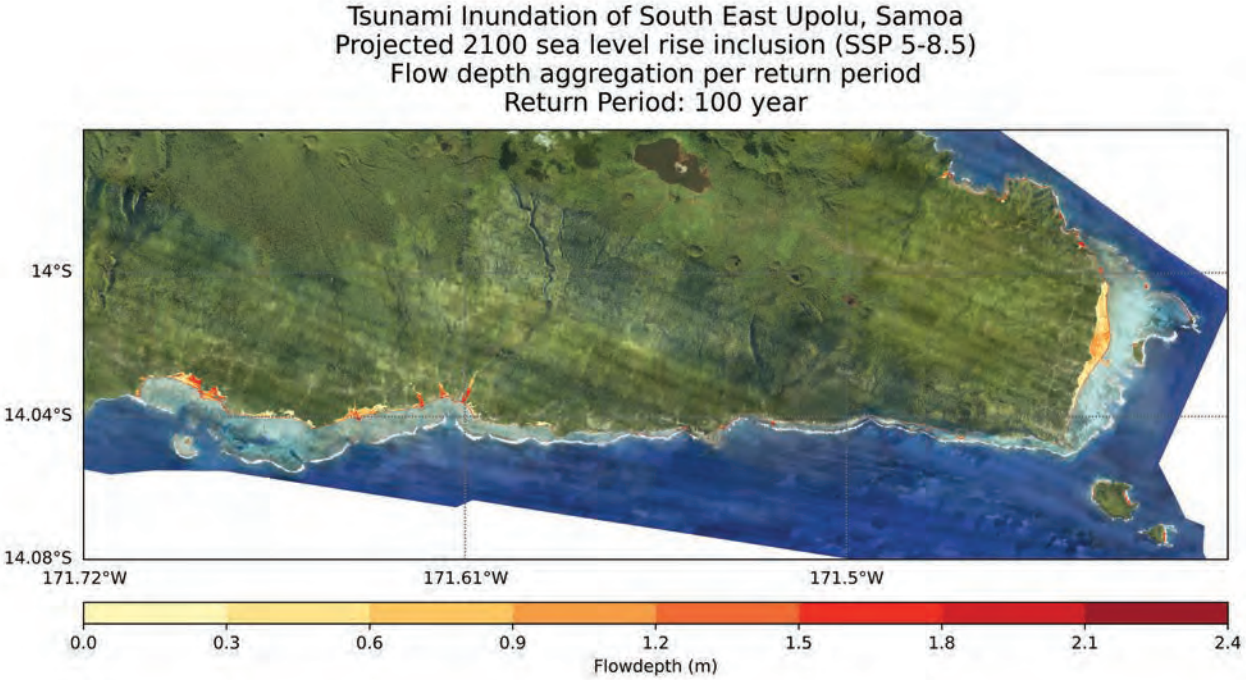

b. RP 500 year

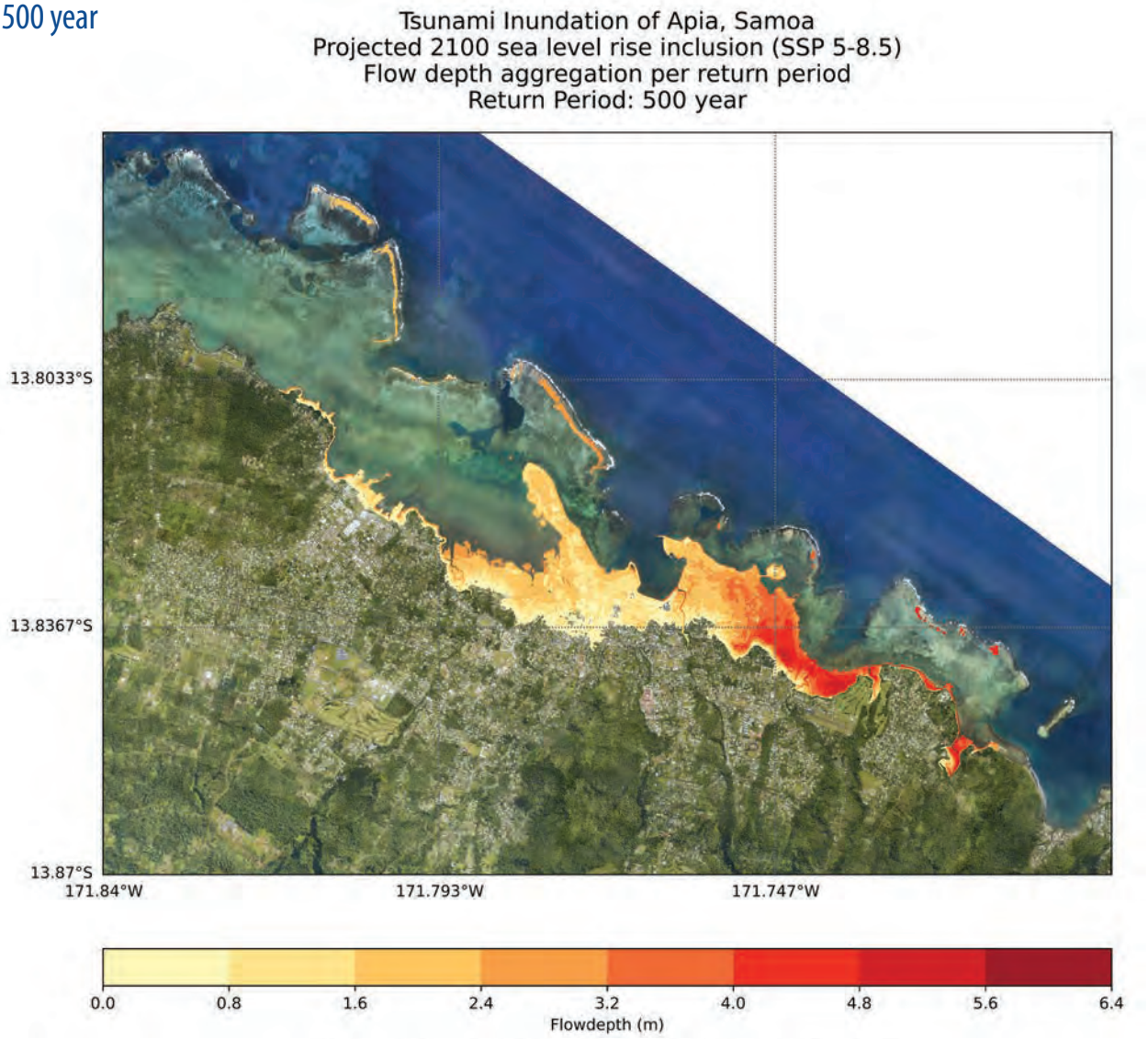
Tsunami Inundation of Apia, Samoa
Projected 2100 sea level rise inclusion (SSP 5-8.5)
Flow depth aggregation per return period
Return Period: 500 year
13.8033°S
13.8367°S
13.87°S
171.84°W
171.793°W
171.747°W
0.0
0.8
1.6
2.4
3.2
4.0
4.8
5.6
6.4
Flowdepth (m)

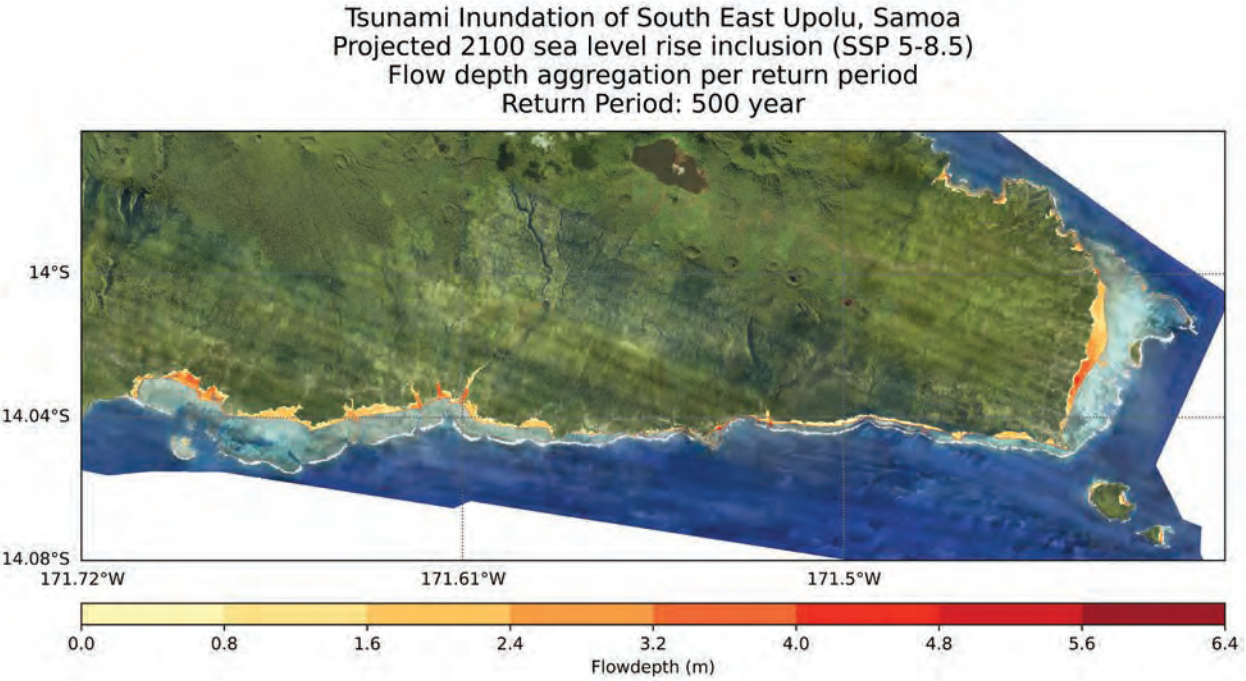
Tsunami Inundation of South East Upolu, Samoa
Projected 2100 sea level rise inclusion (SSP 5-8.5)
Flow depth aggregation per return period
Return Period: 500 year
14°S
14.04°S
14.08°S
171.72°W
171.61°W
171.5°W
0.0
0.8
1.6
2.4
3.2
4.0
4.8
5.6
6.4
Flowdepth (m)

c. RP 1000 year

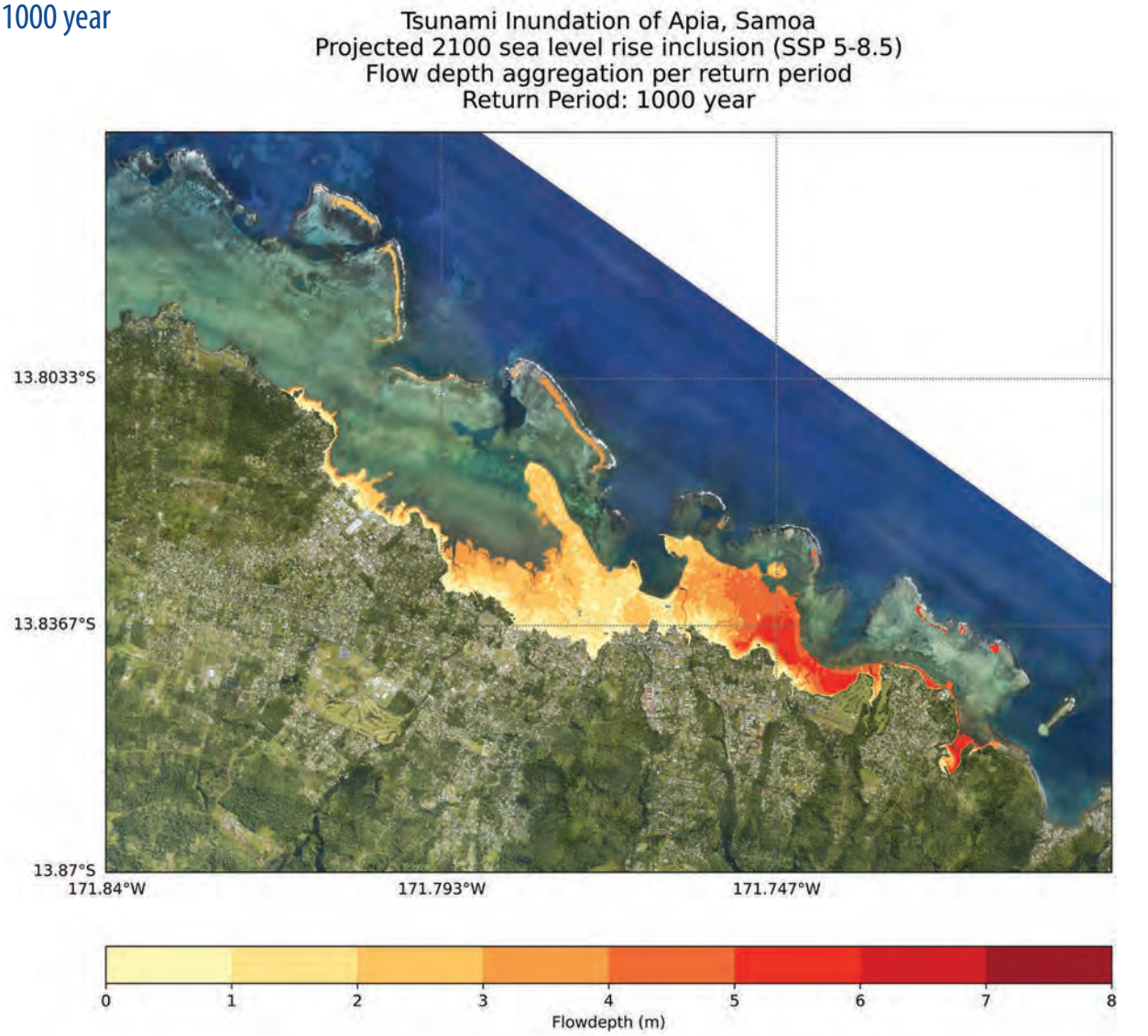

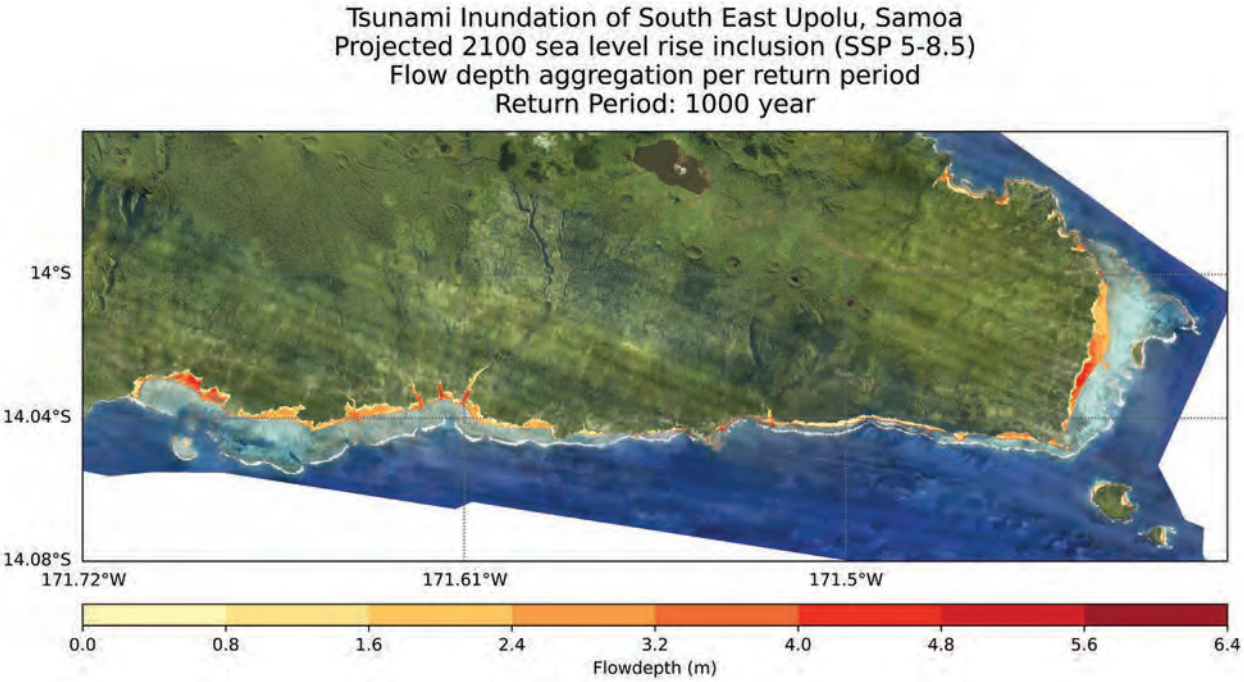

d. RP 2500 year 84th percentile

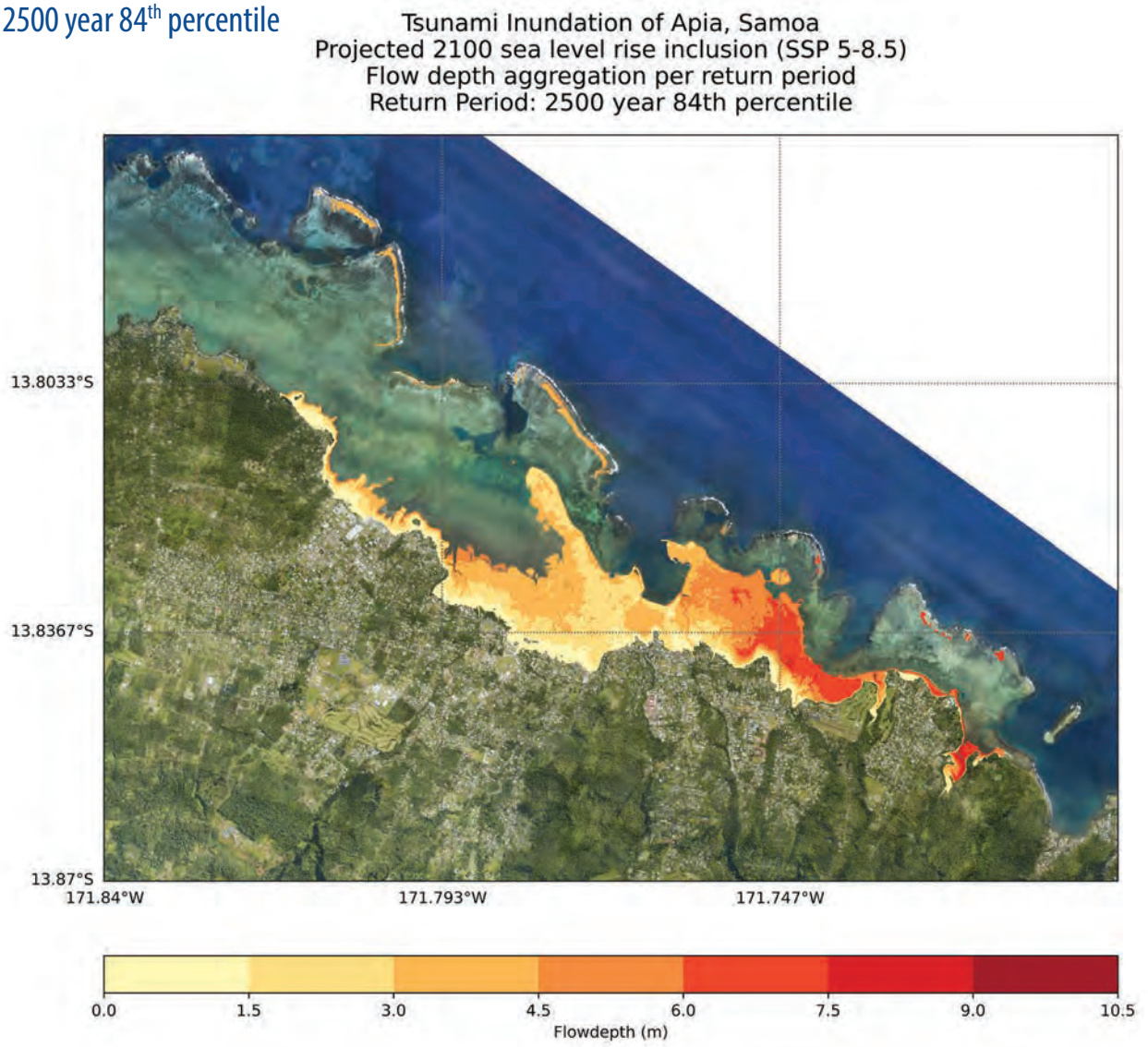

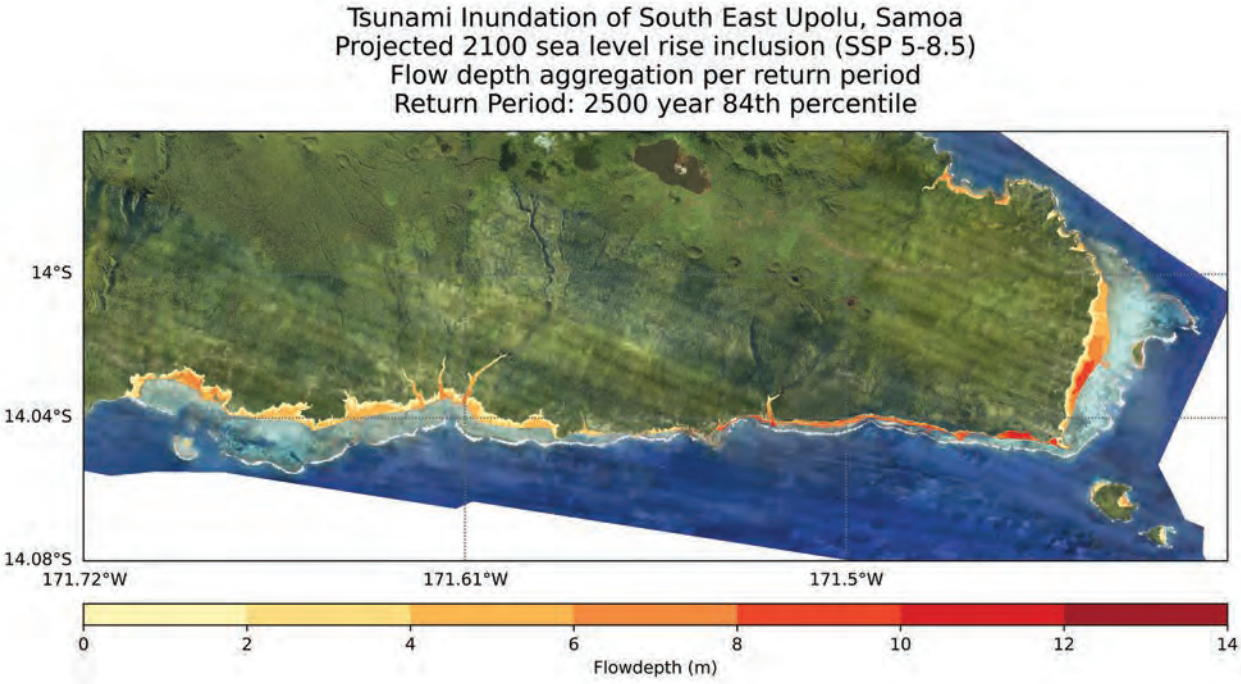

3.0 Source flow depth aggregation

a. RP 100 year

i. Alaska Aleutians

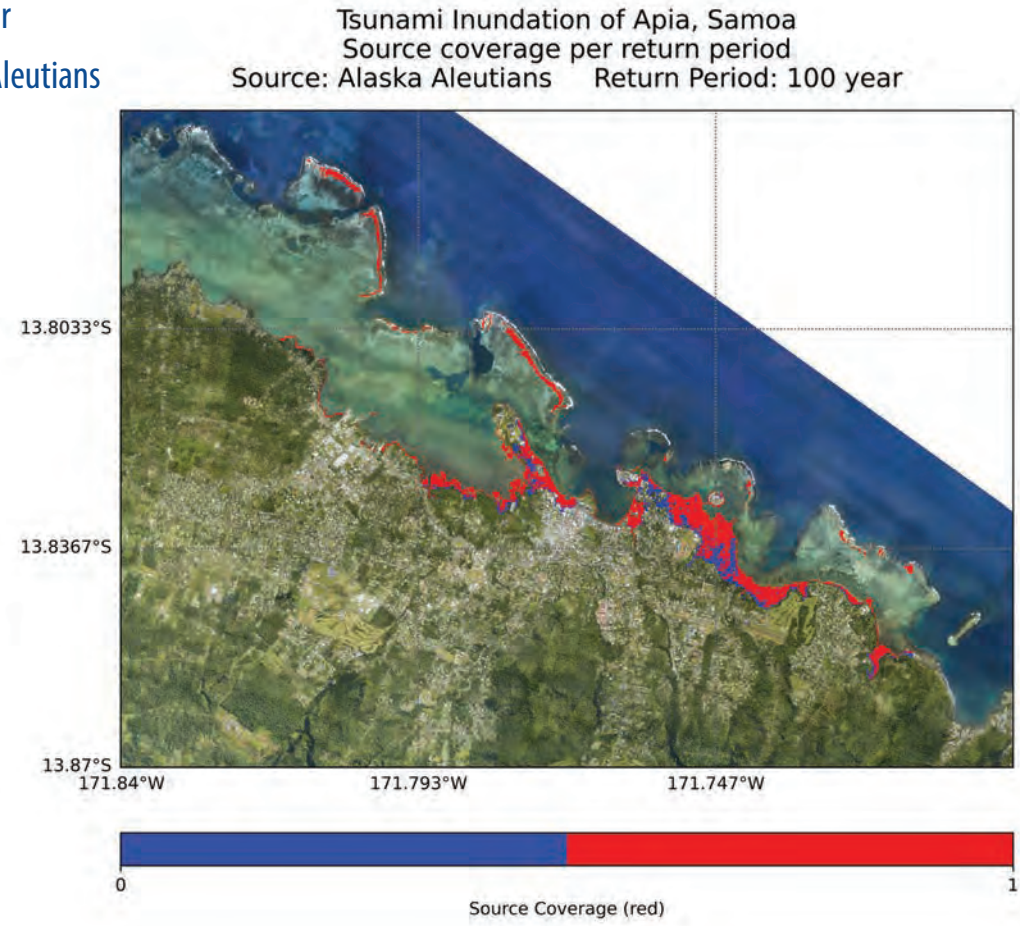

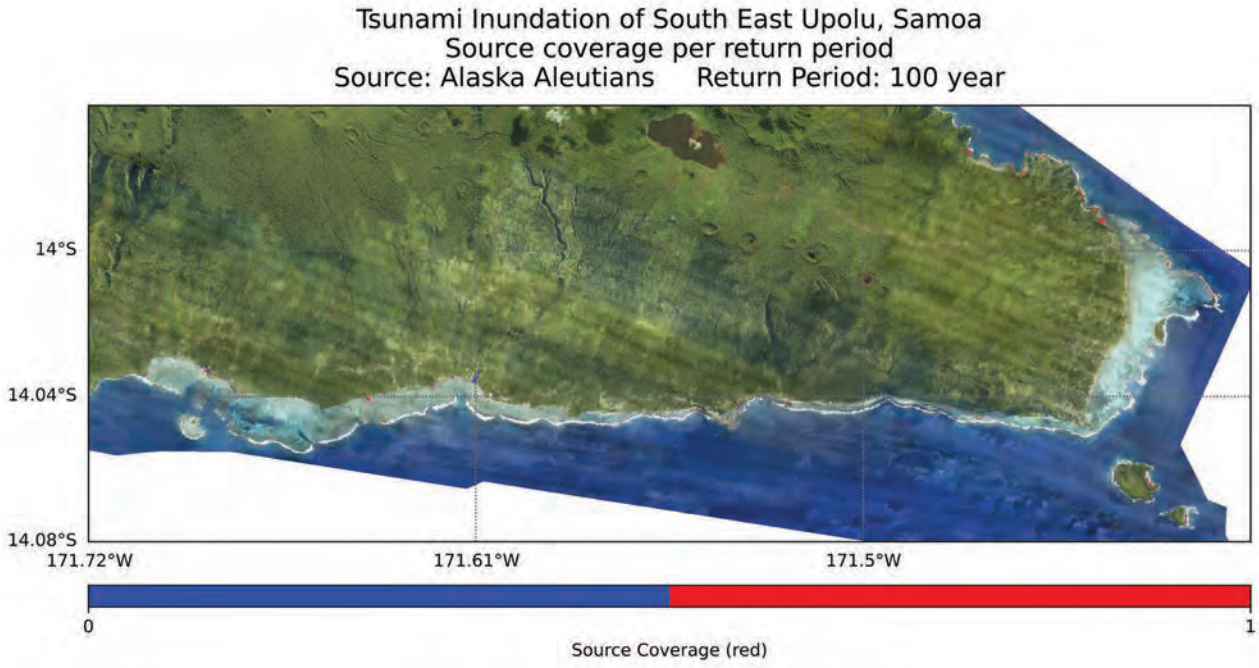

a. RP 100 year

i. Alaska Aleutians

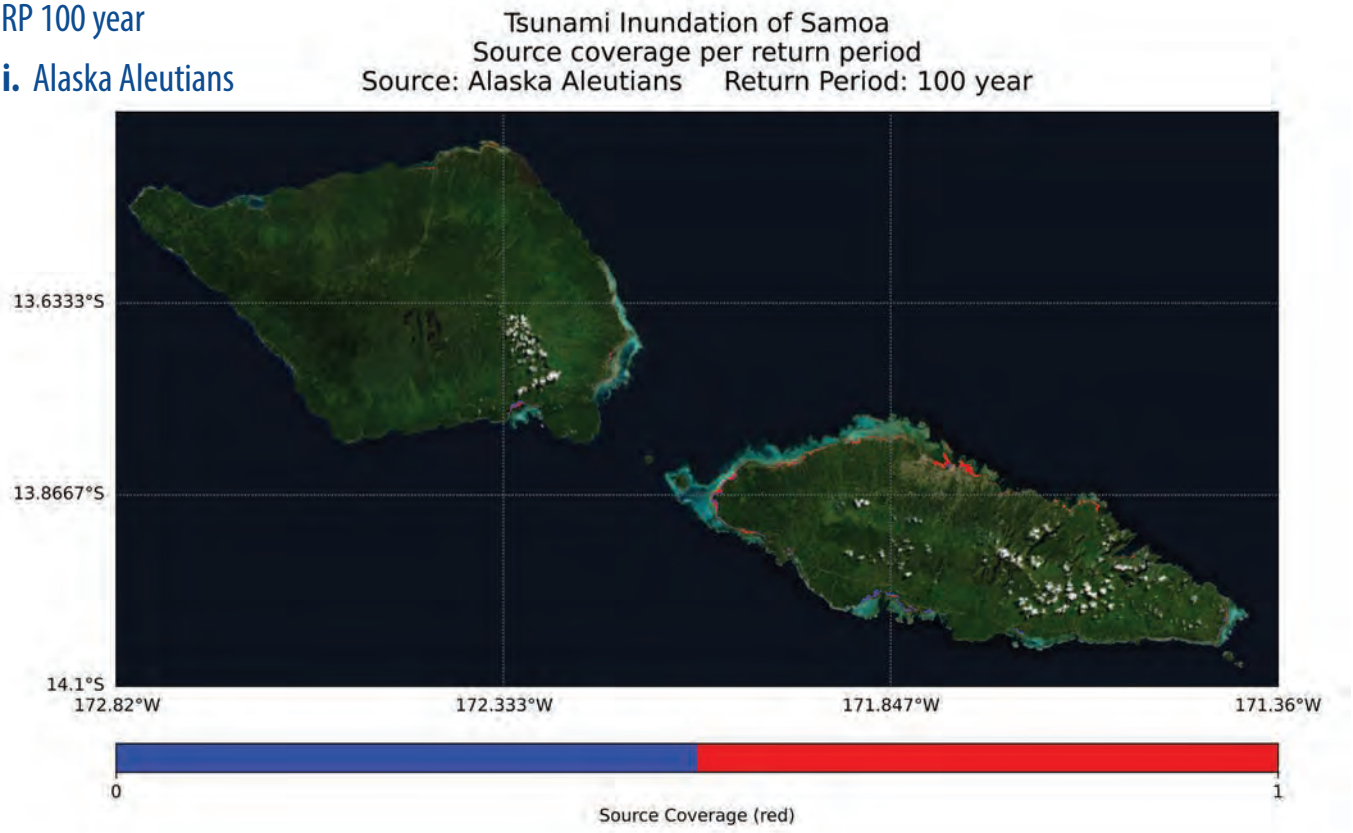

ii. Izu Mariana

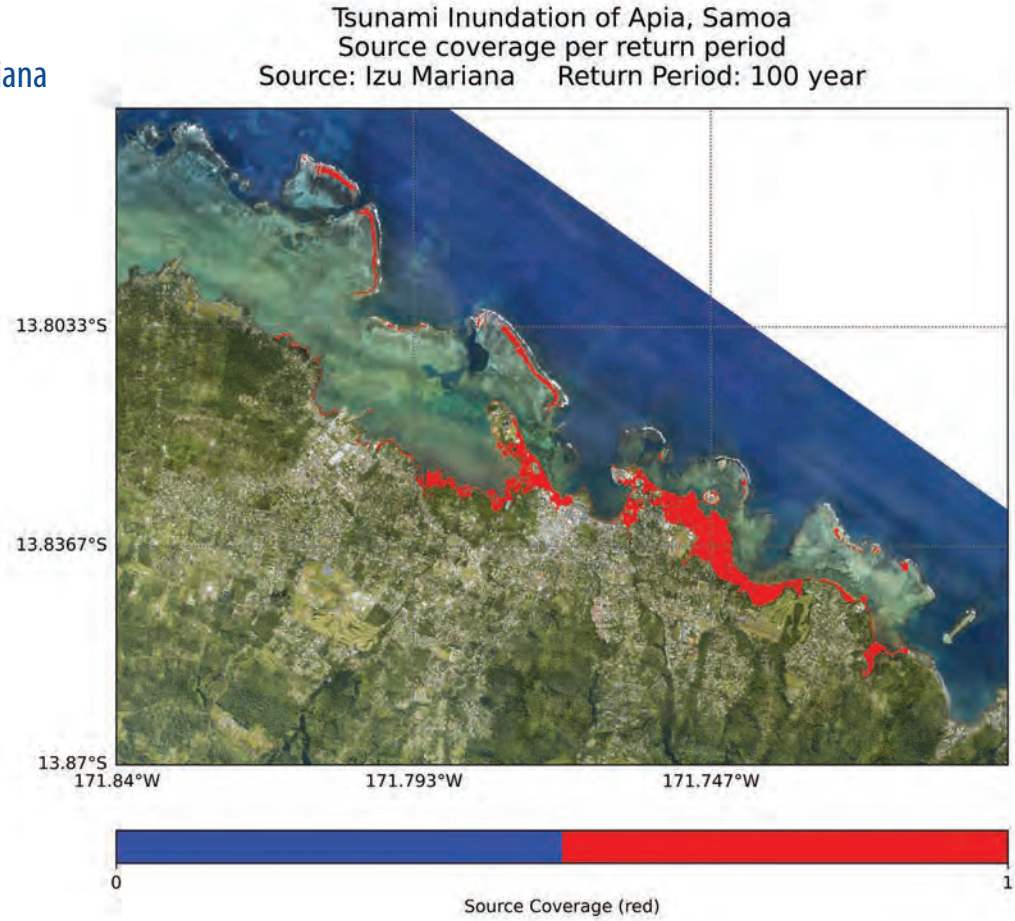

a. RP 100 year

ii. Izu Mariana

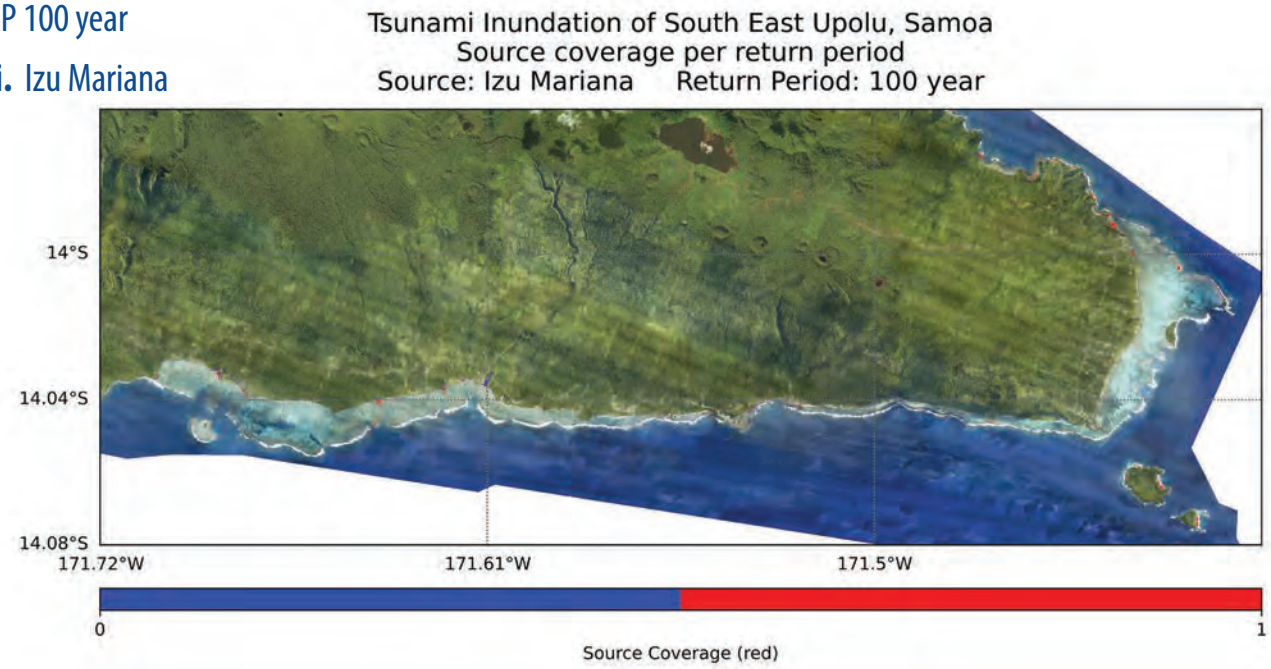

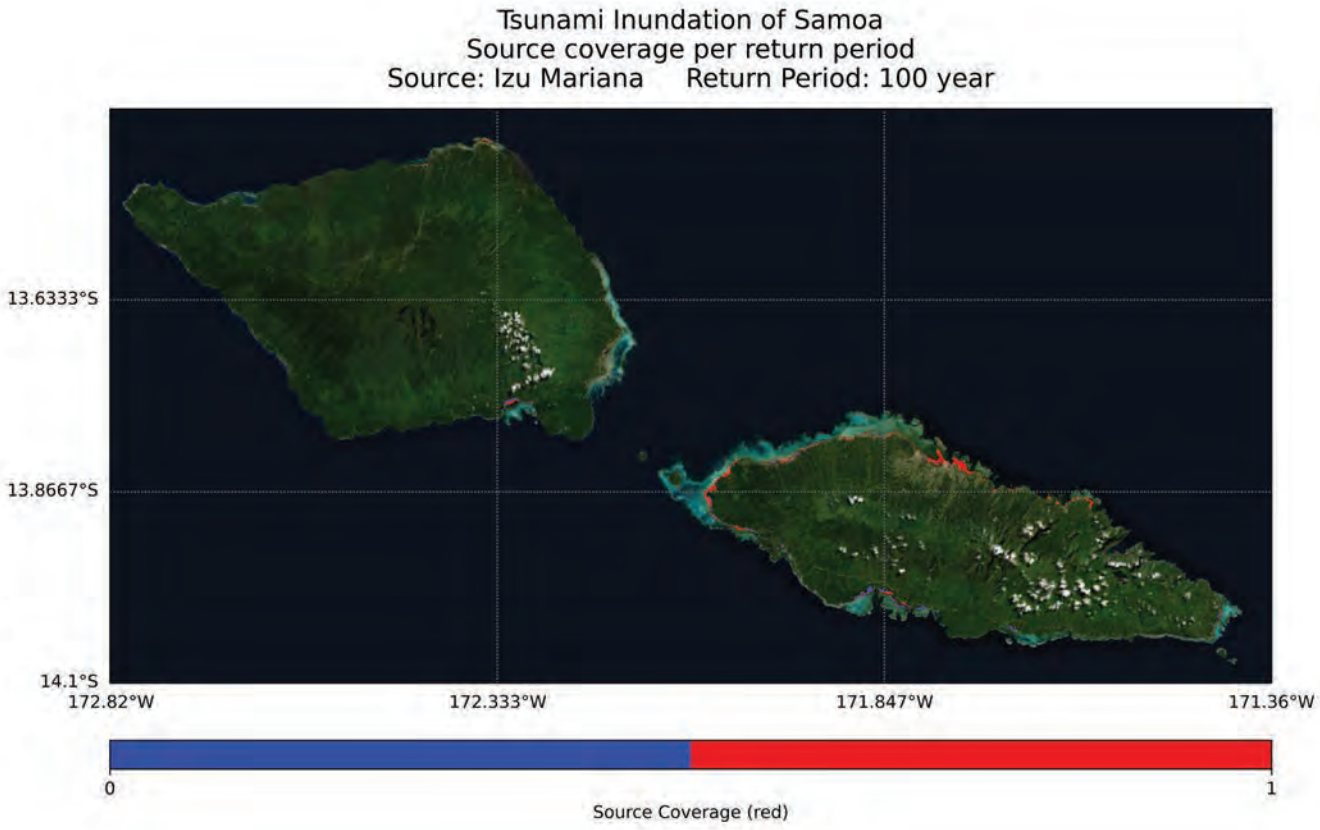

a. RP 100 year

iii. Kermadec-Tonga

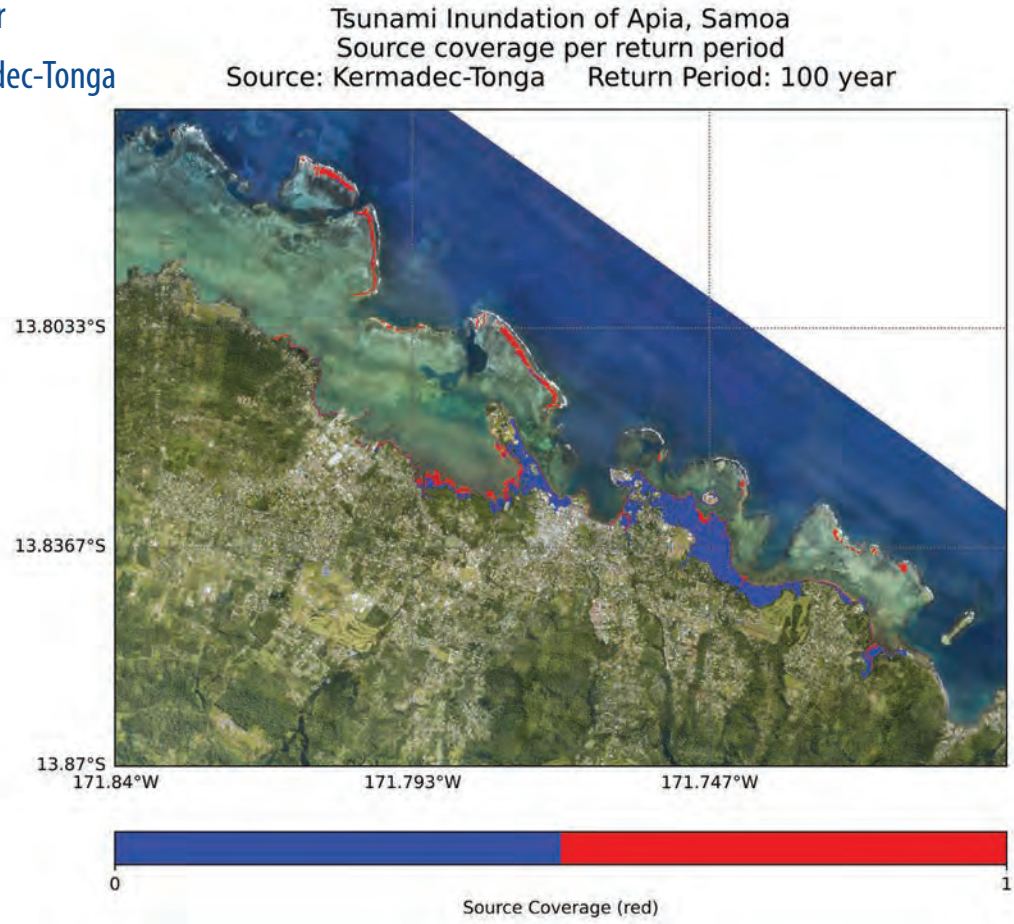

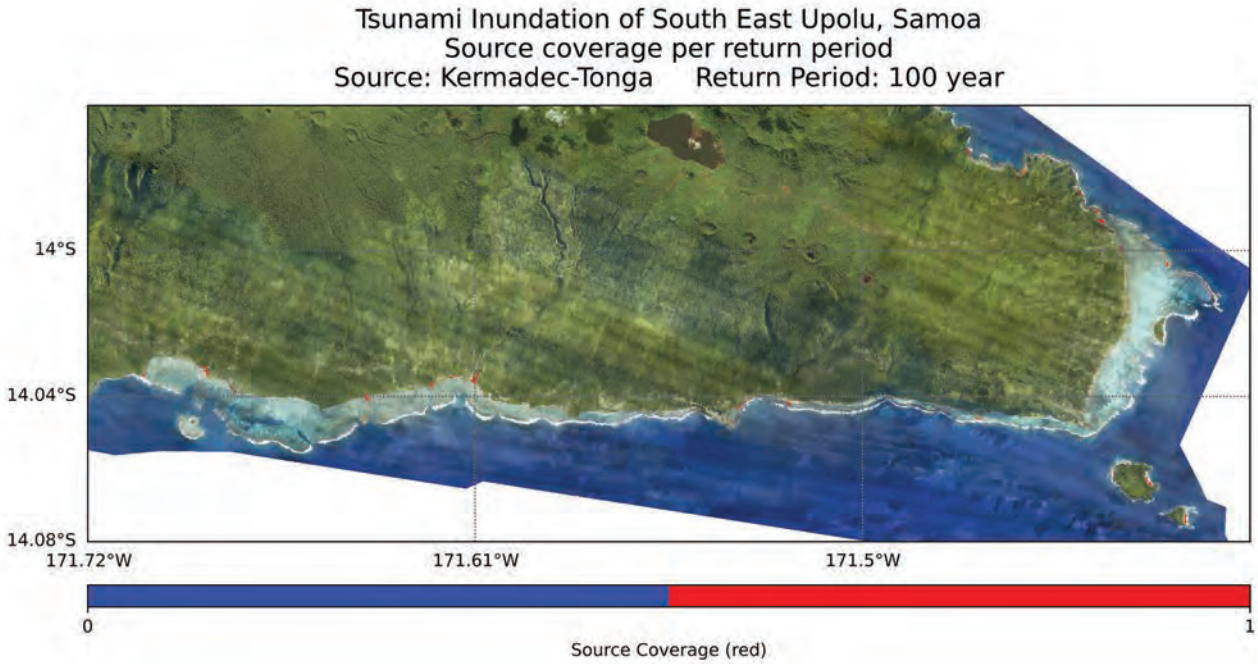

a. RP 100 year

iii. Kermadec-Tonga

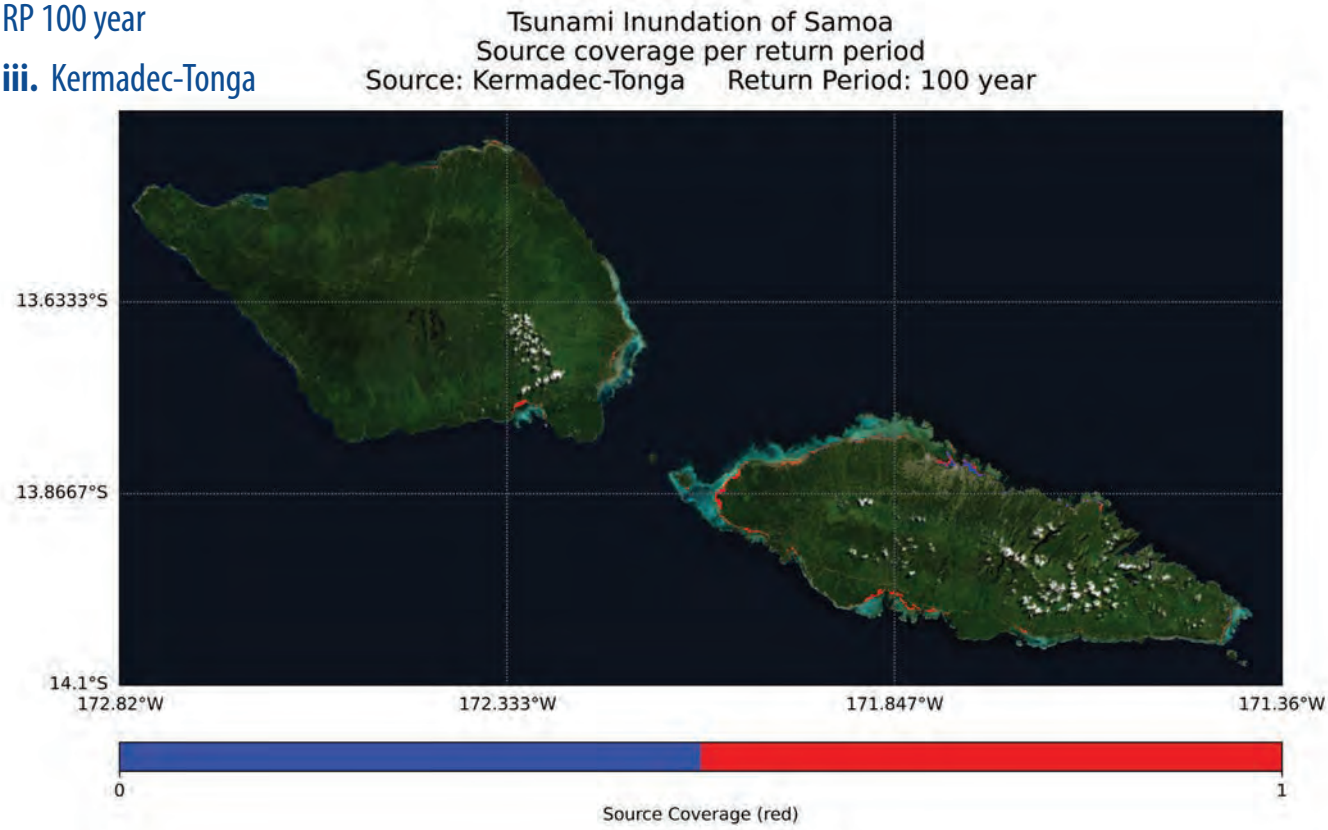

iv. Kurils Japan

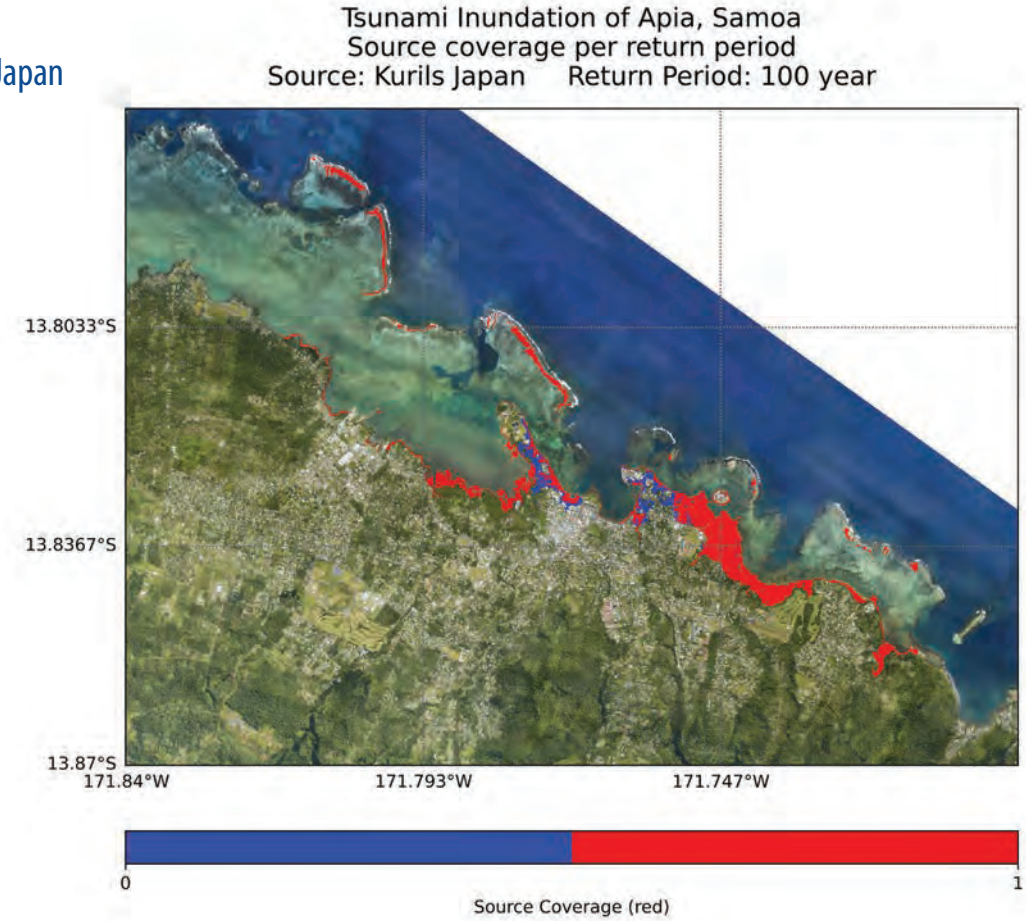

a. RP 100 year

iv. Kurils Japan

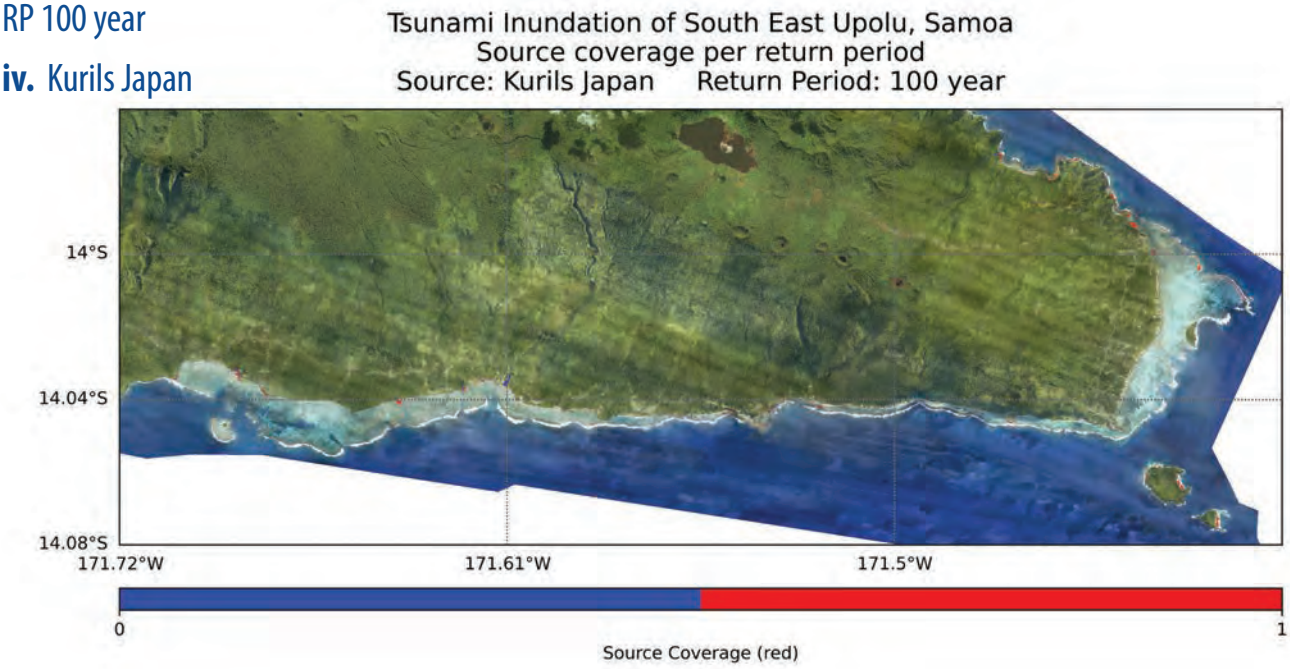

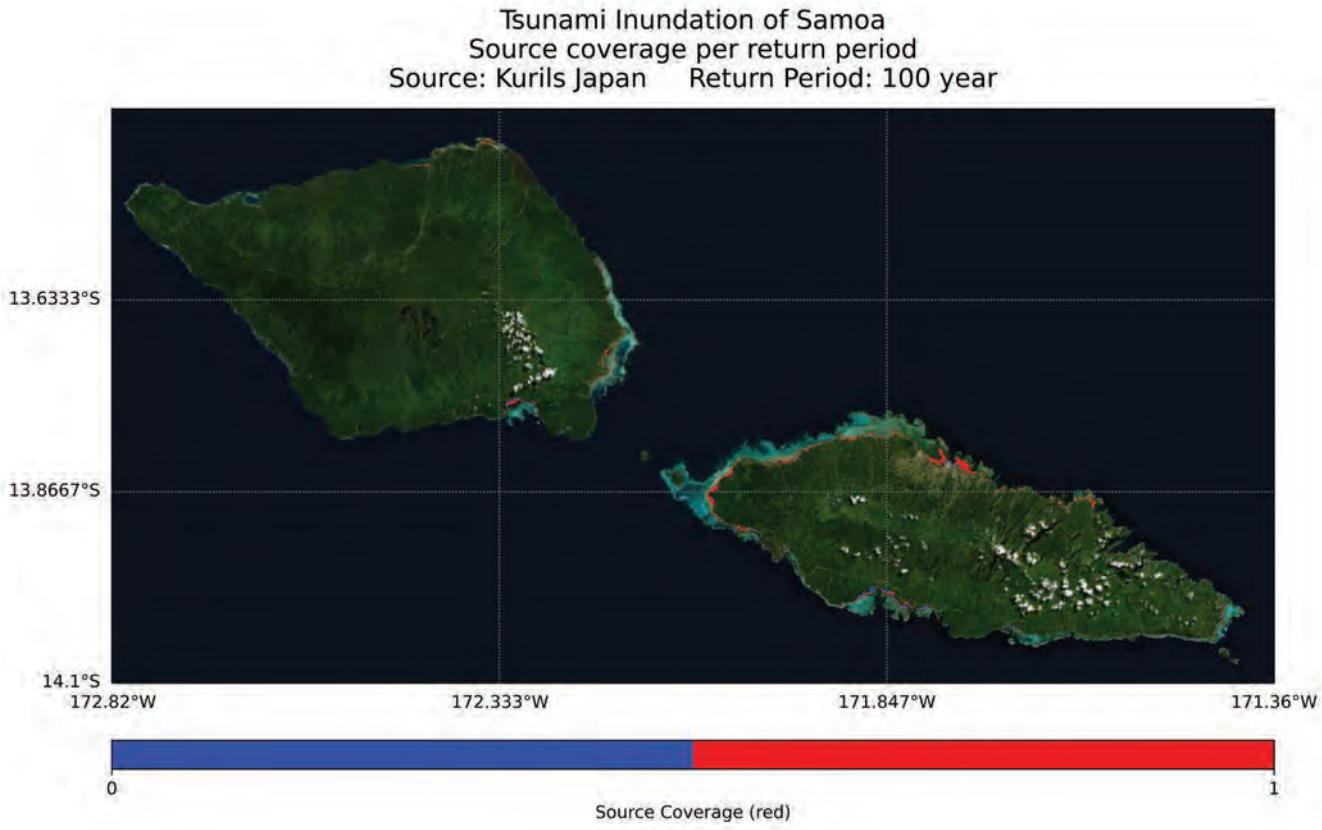

a. RP 100 year

v. Mexico

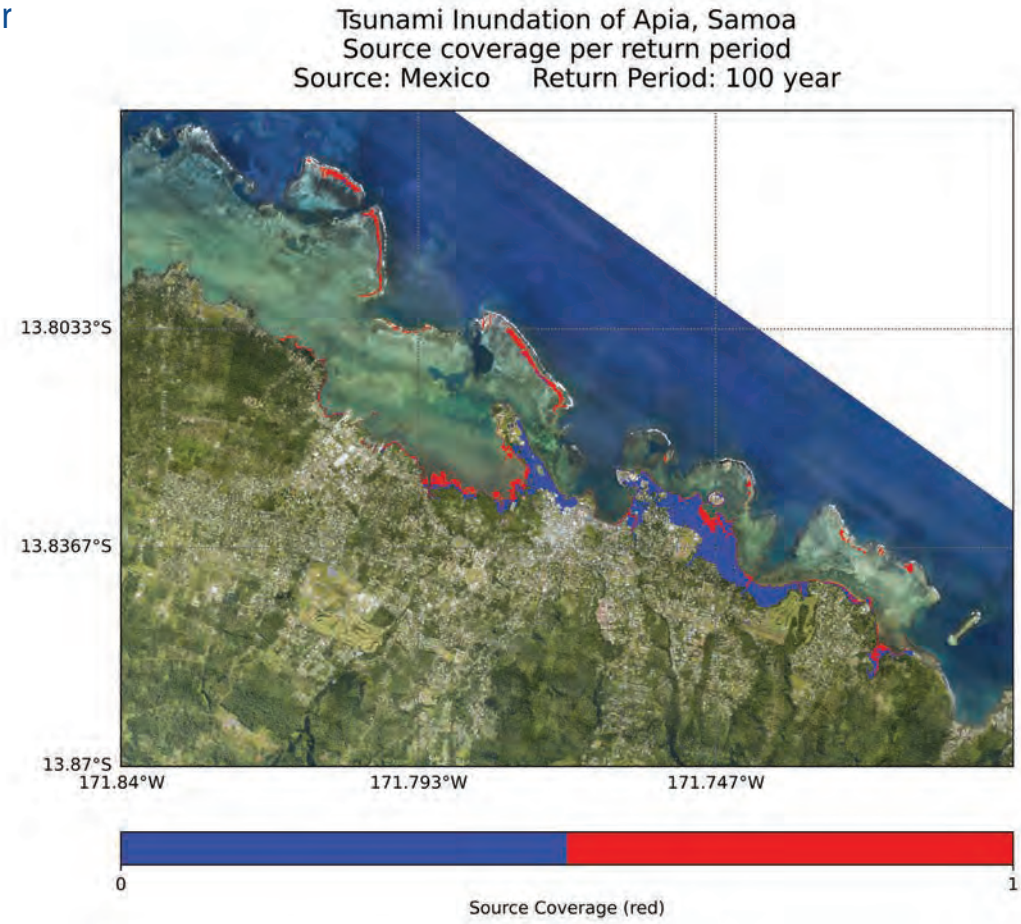

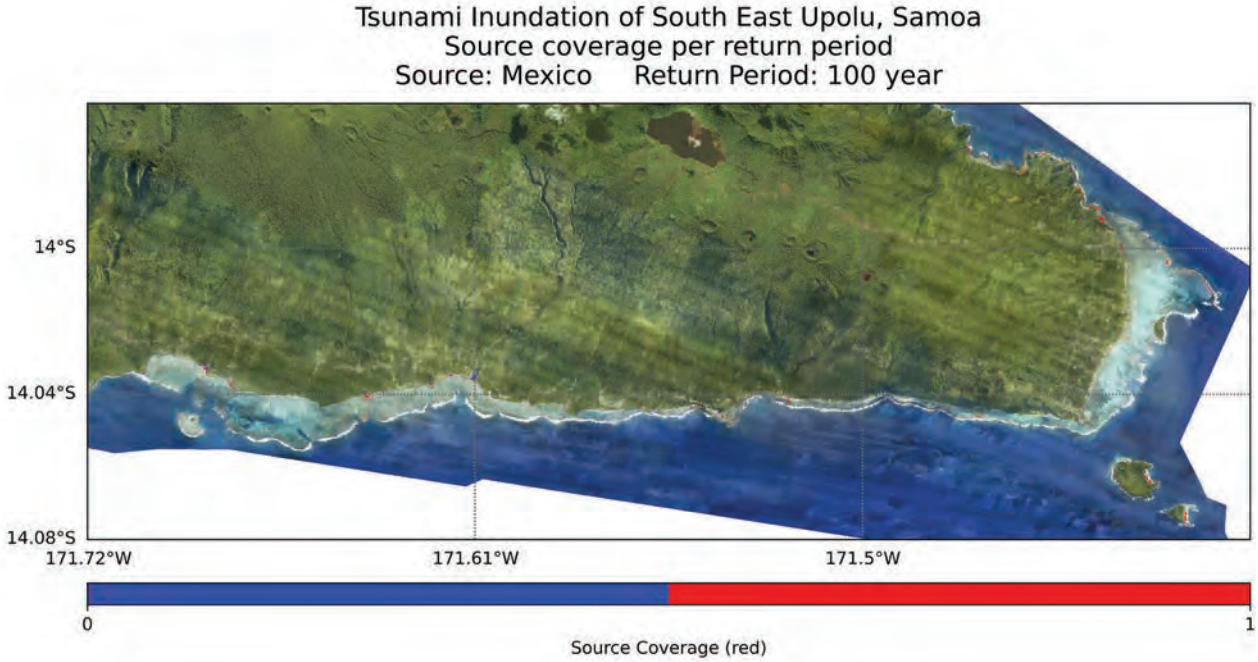

a. RP 100 year

v. Mexico

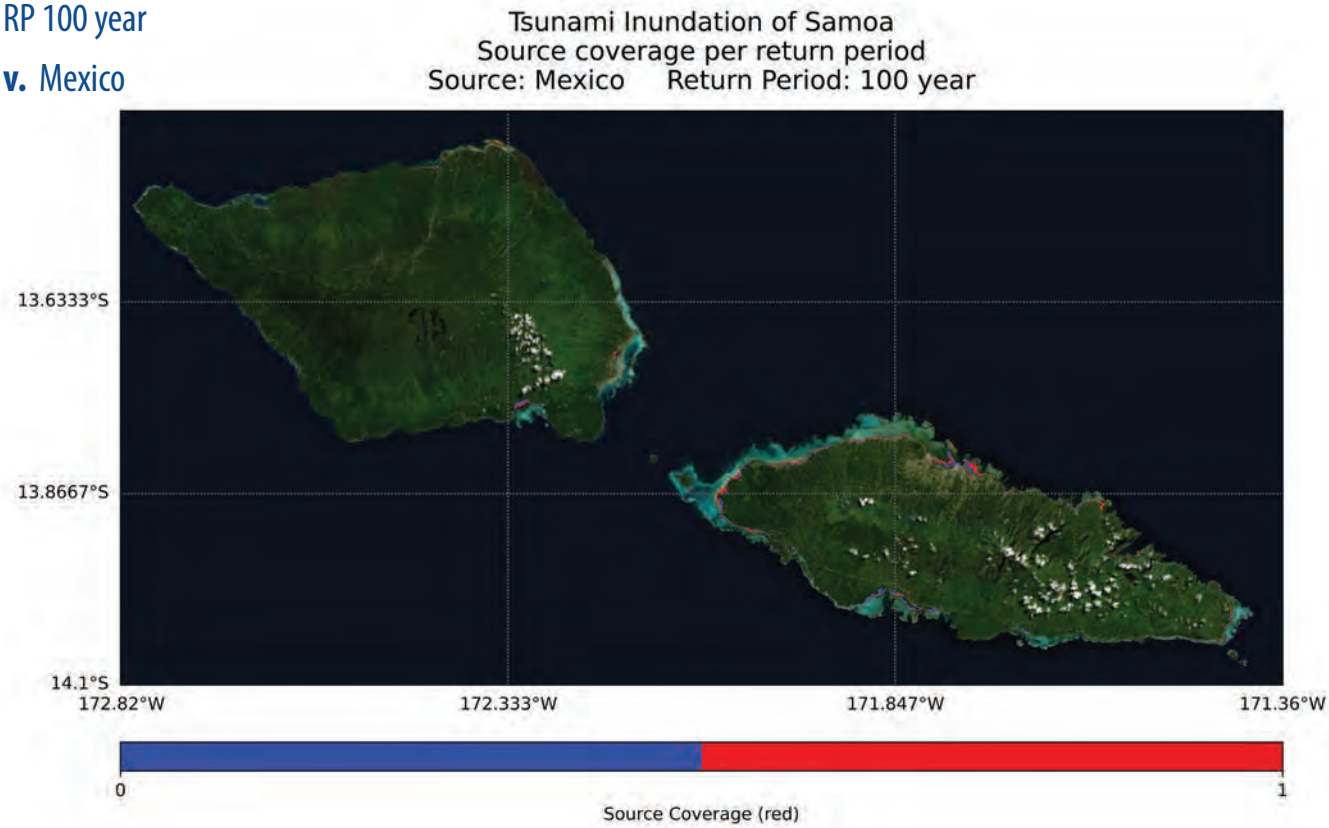

vi. South America

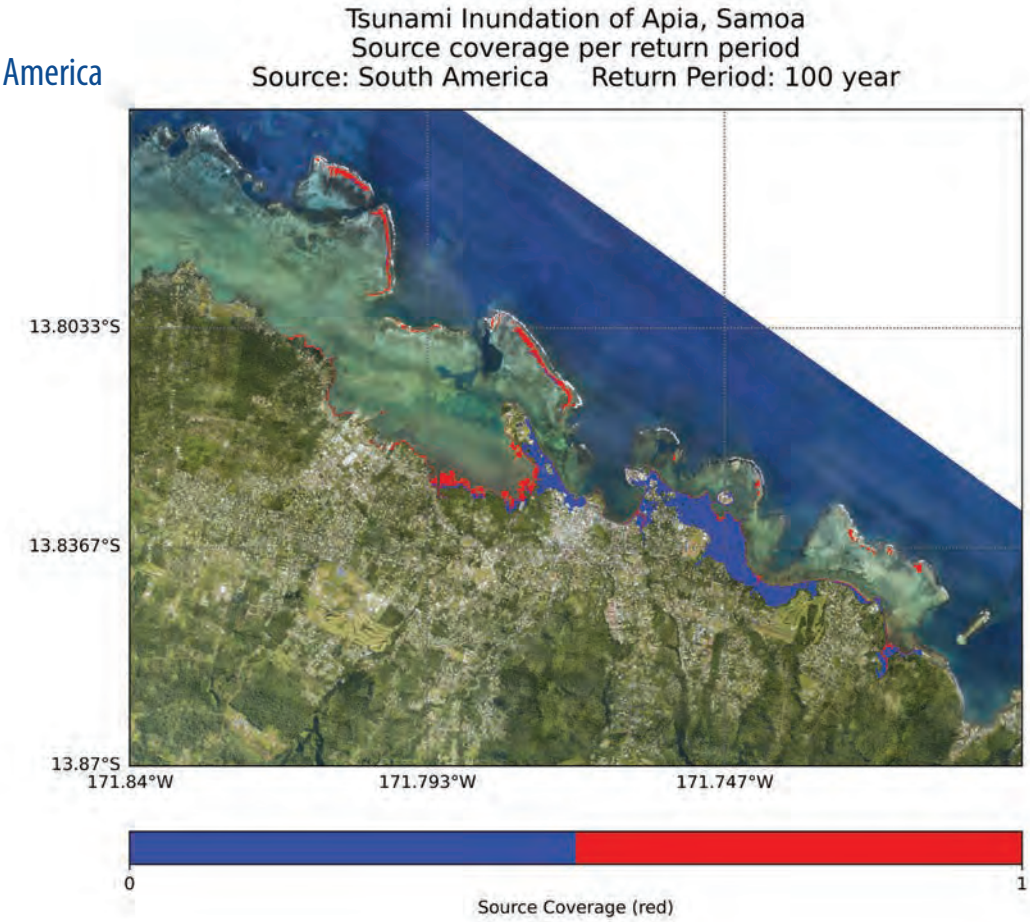

a. RP 100 year

vi. South America

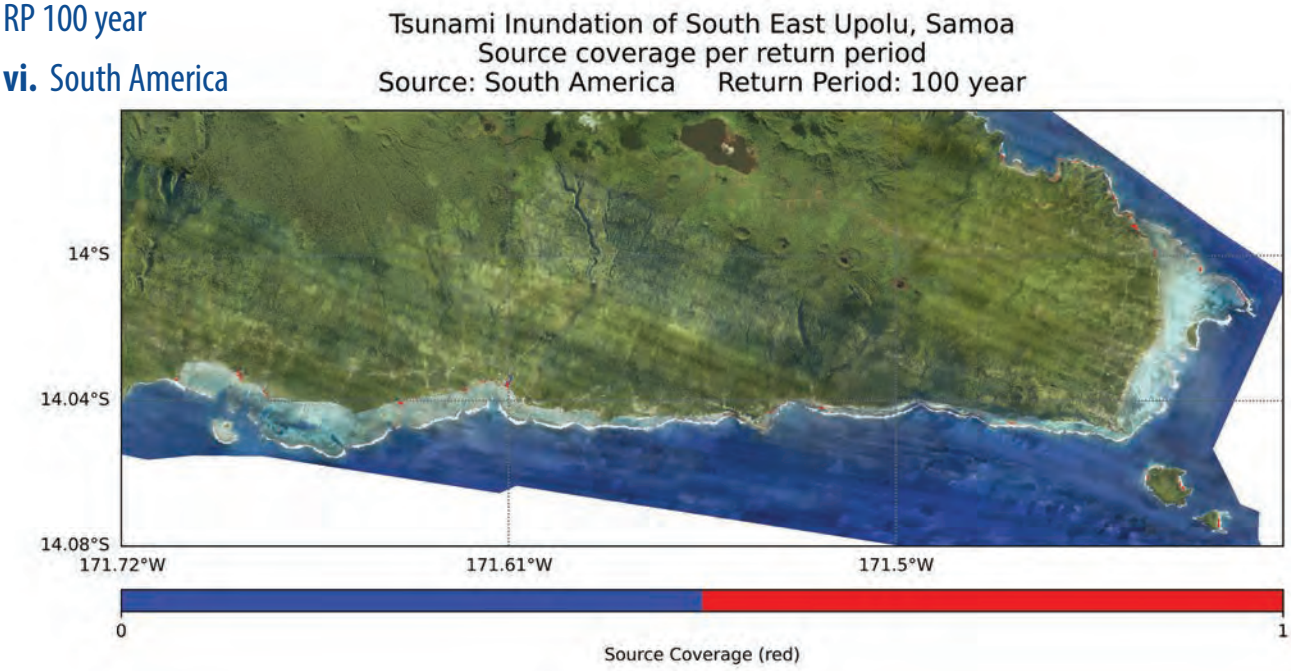

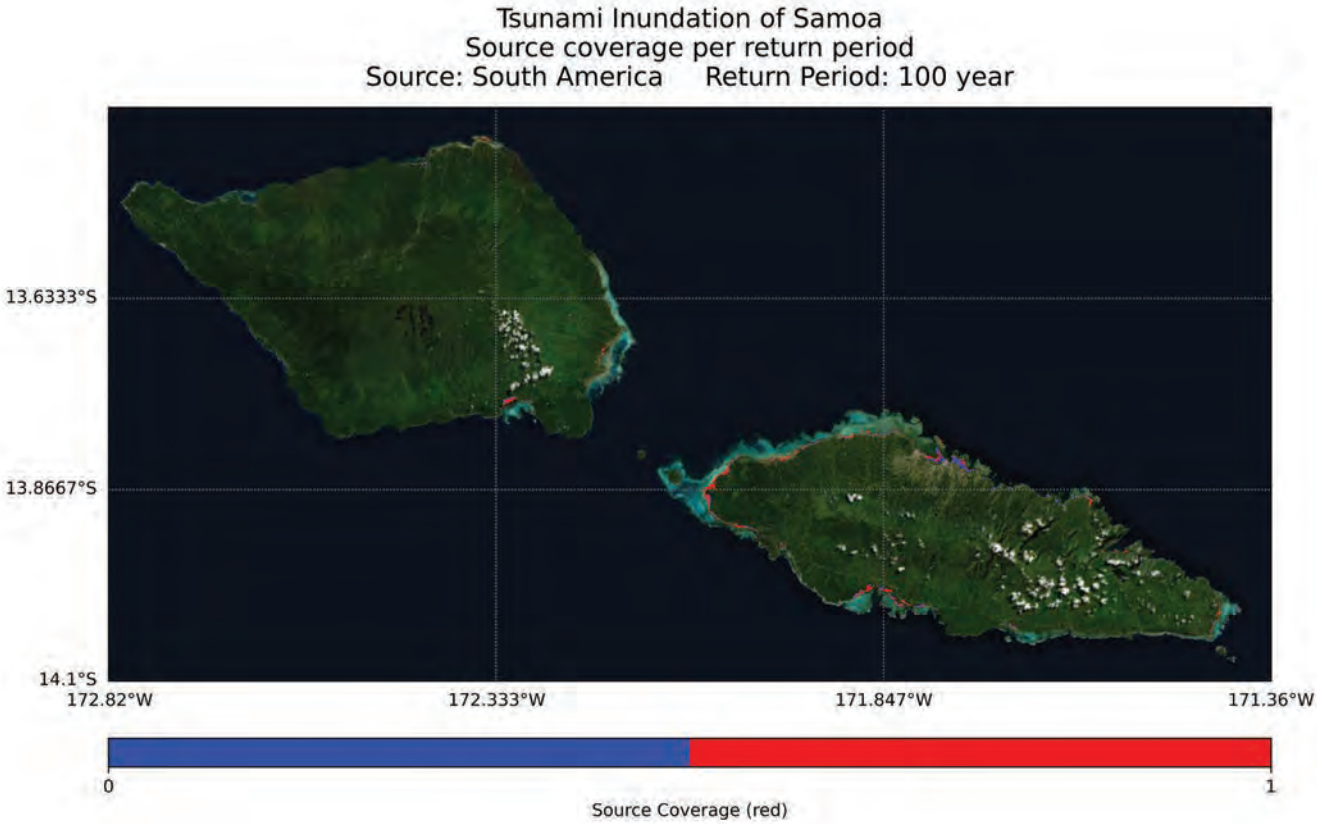

b. RP 500 year

i. Alaska Aleutians

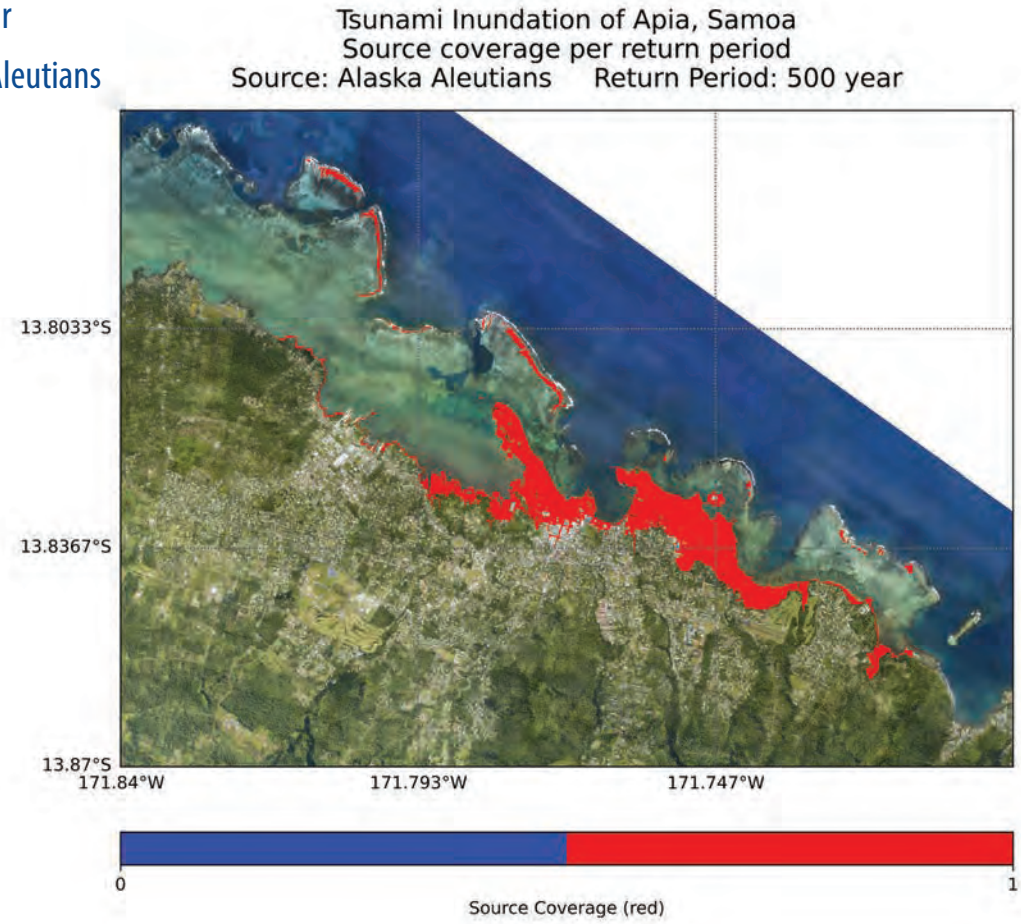

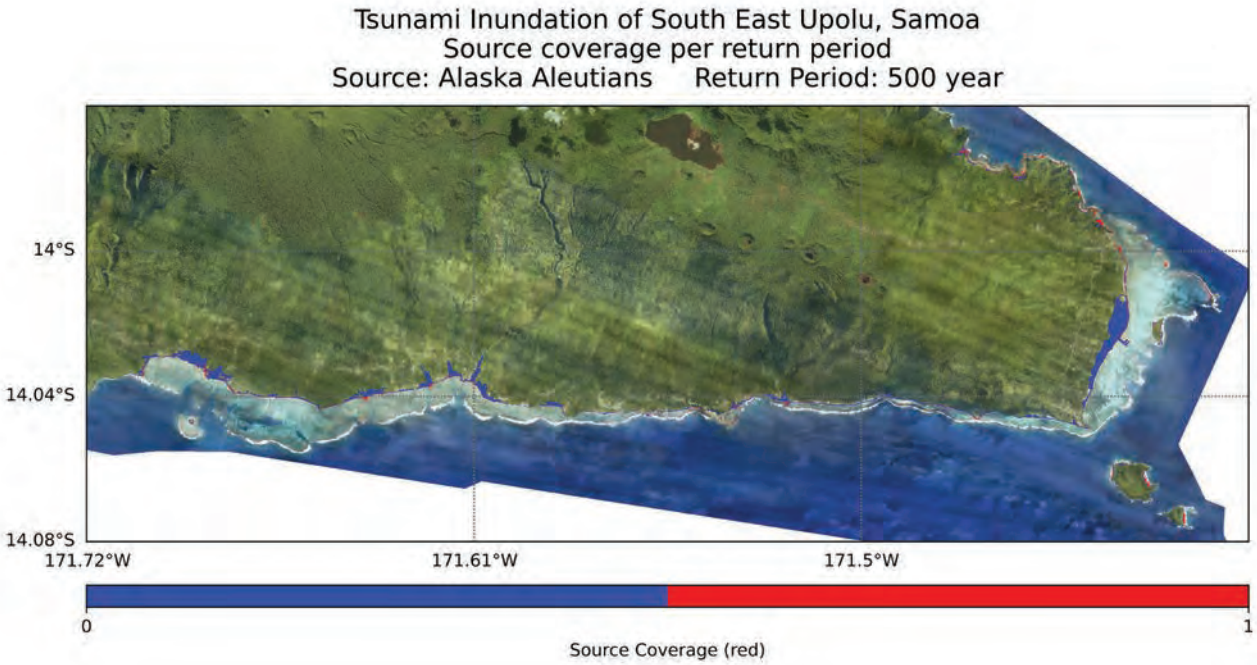

b. RP 500 year

i. Alaska Aleutians

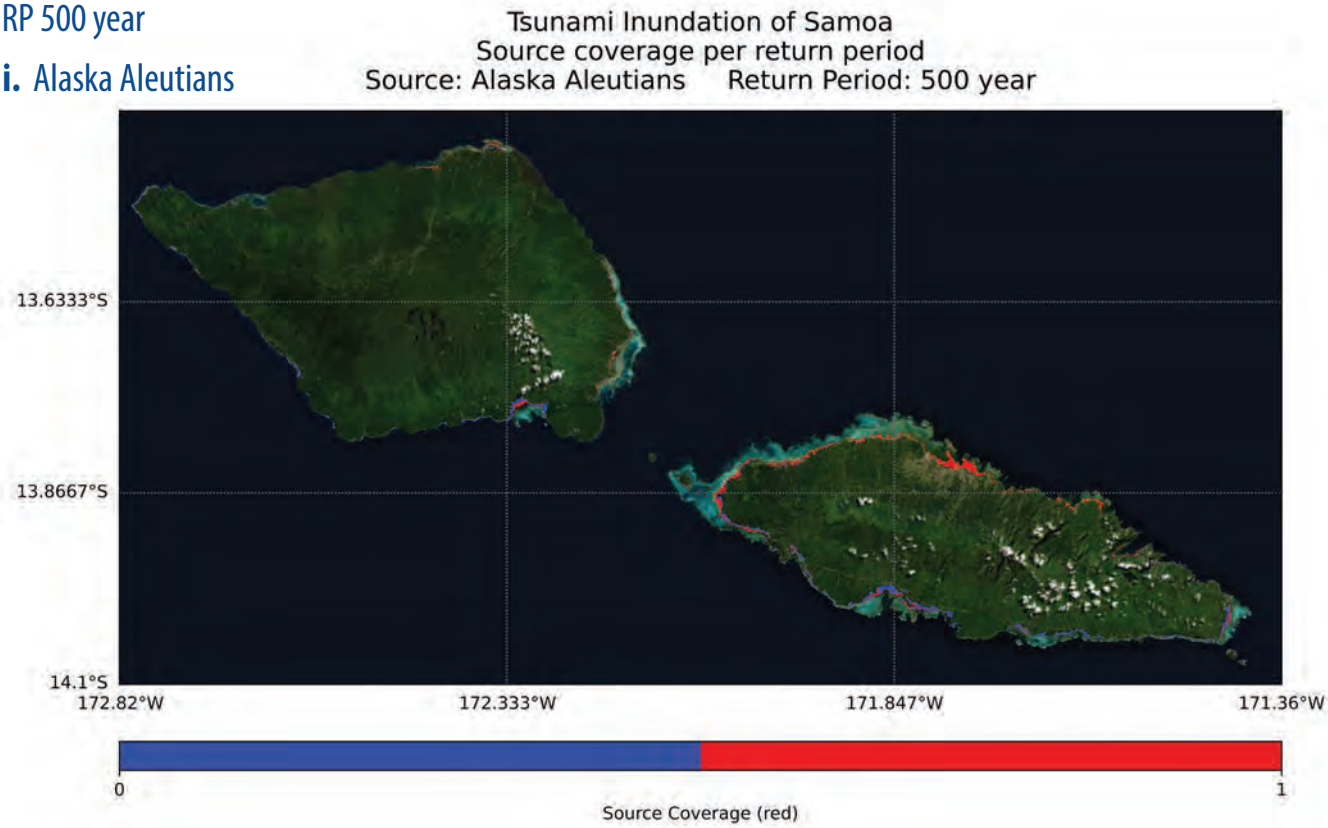

ii. Izu Mariana

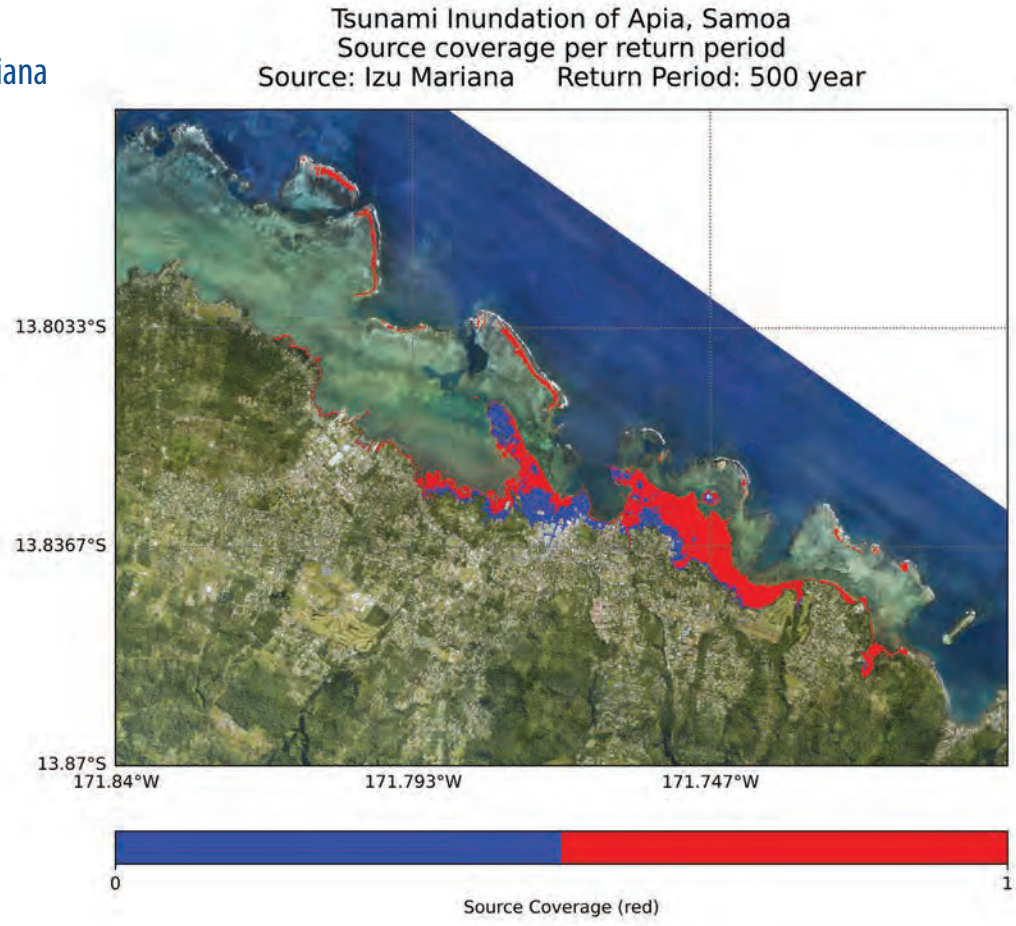

b. RP 500 year

ii. Izu Mariana

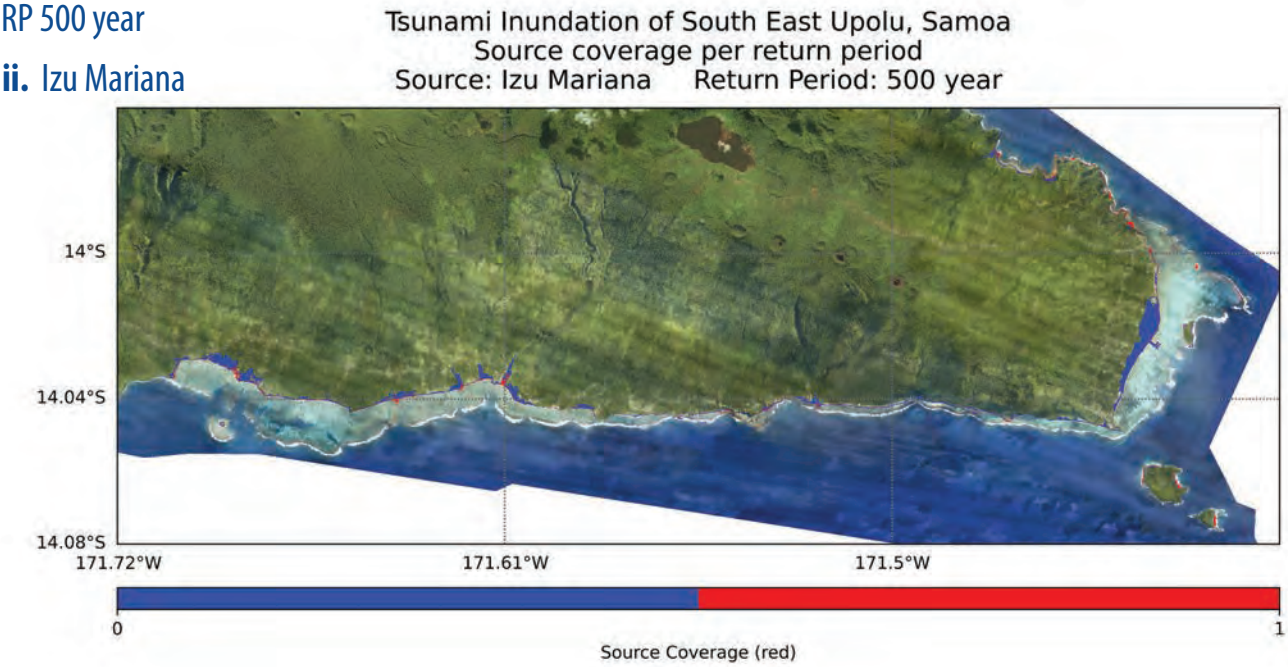

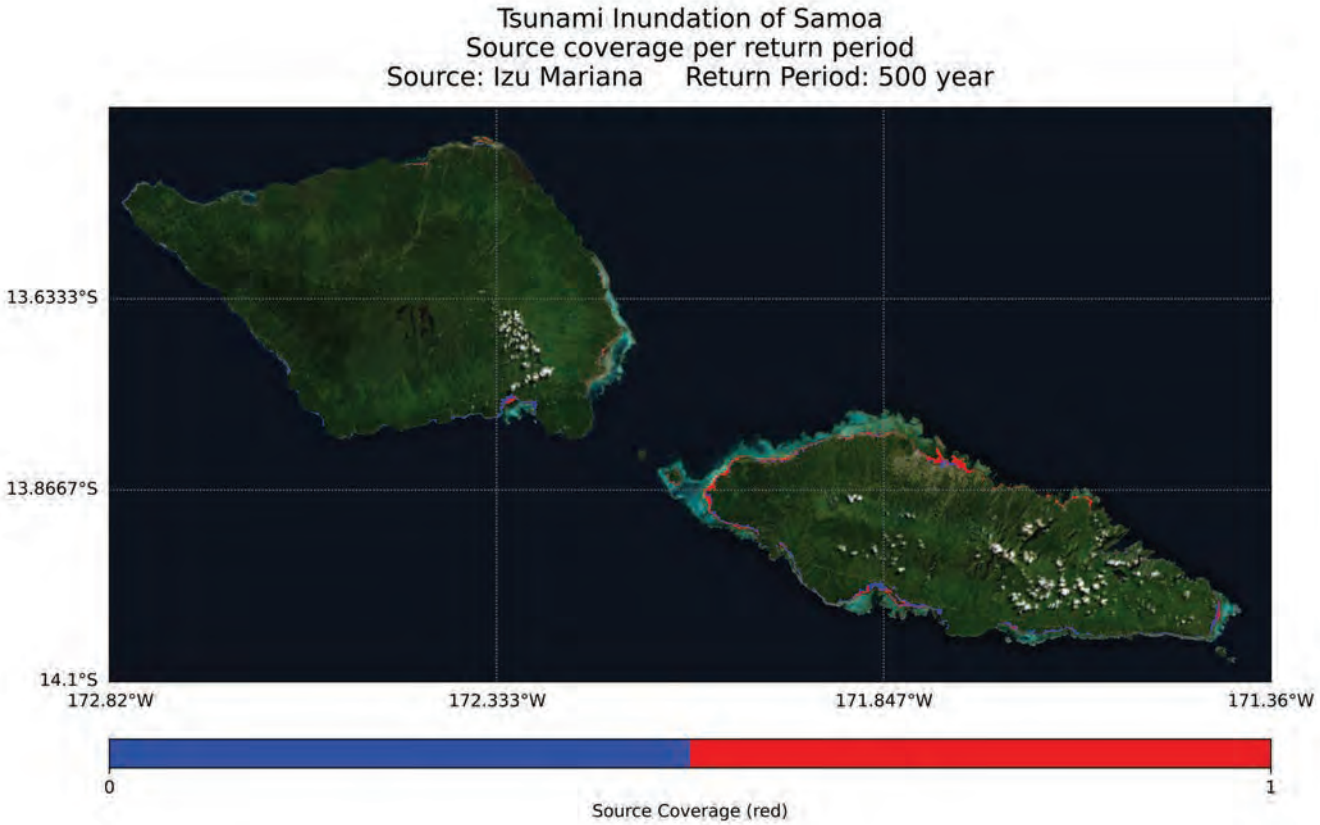

b. RP 500 year

iii. Kermadec-Tonga

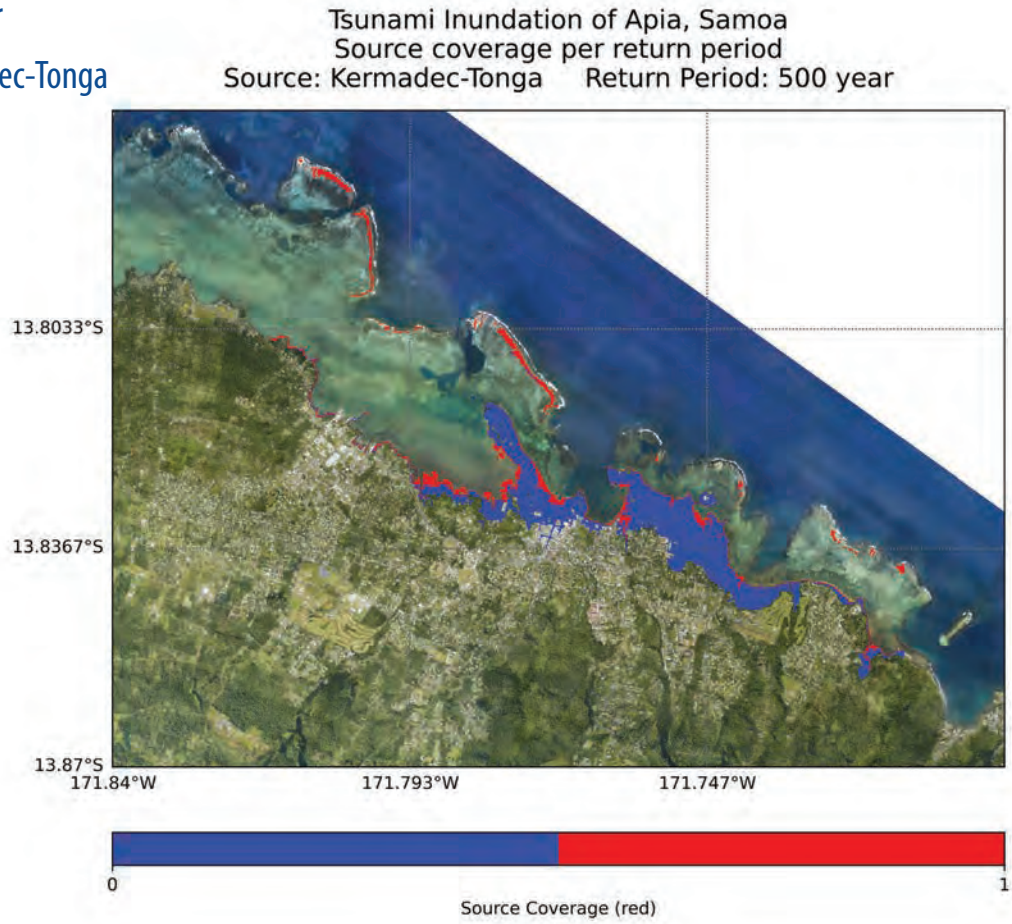

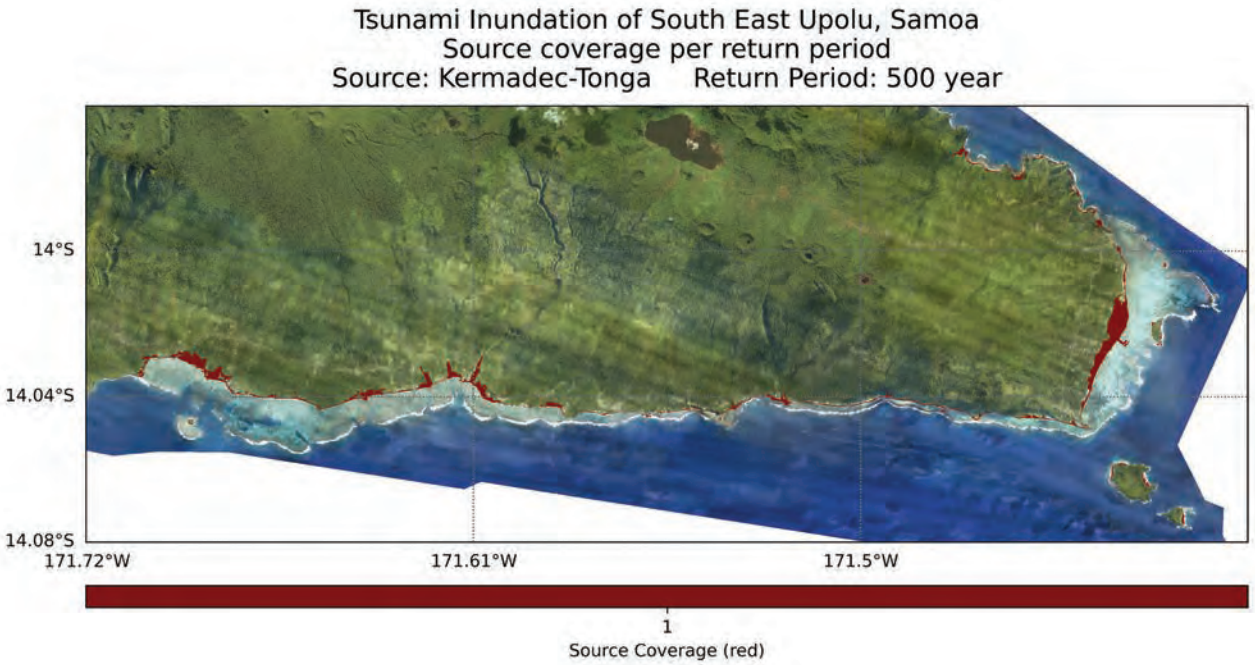

b. RP 500 year

iii. Kermadec-Tonga

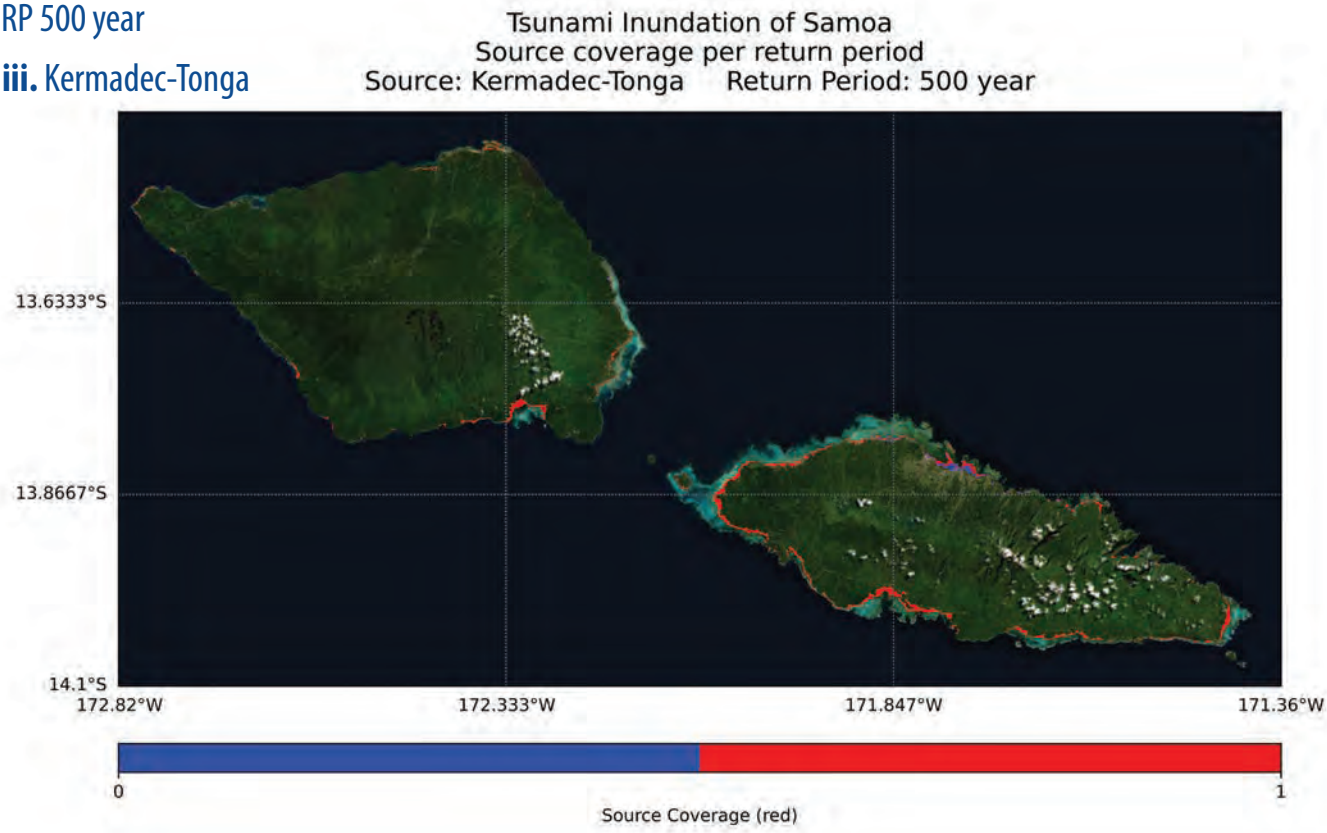

iv. Kurils Japan

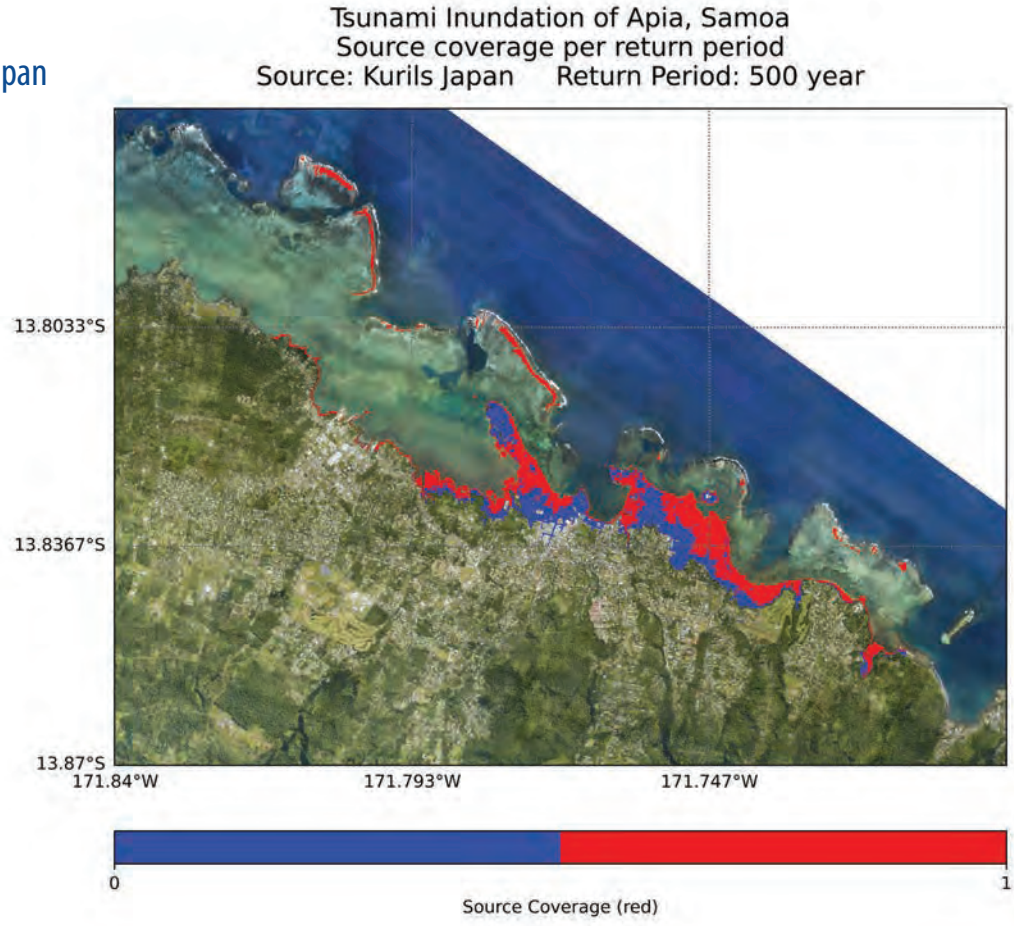

b. RP 500 year

iv. Kurils Japan

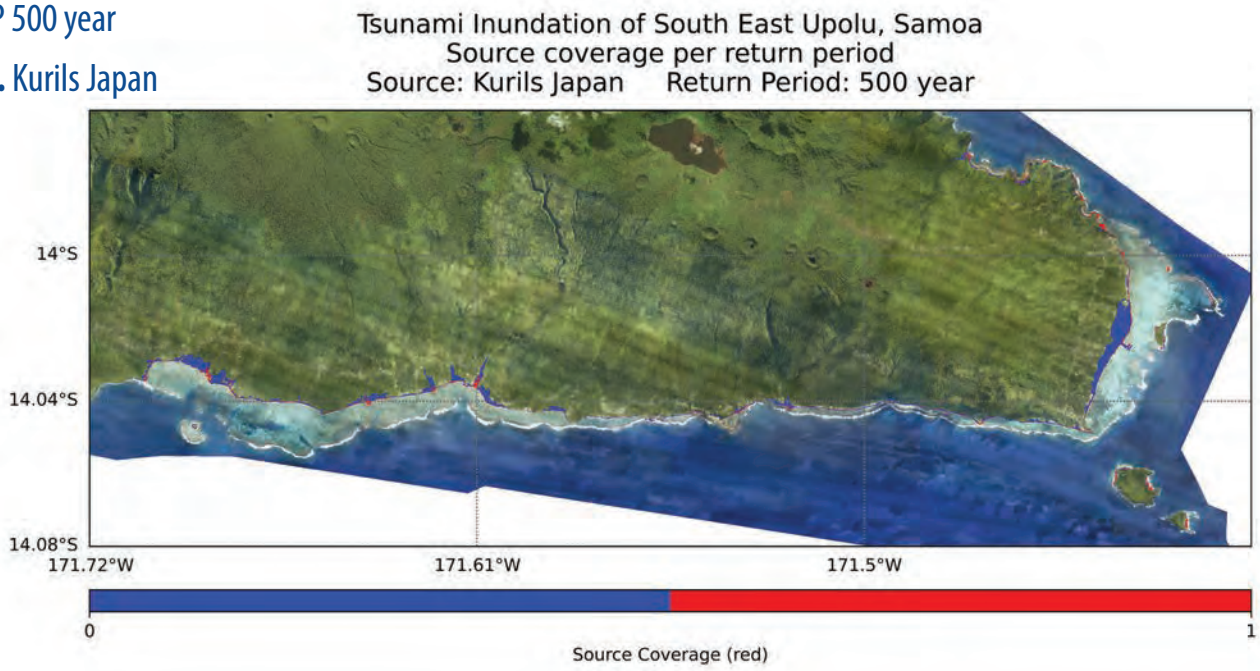

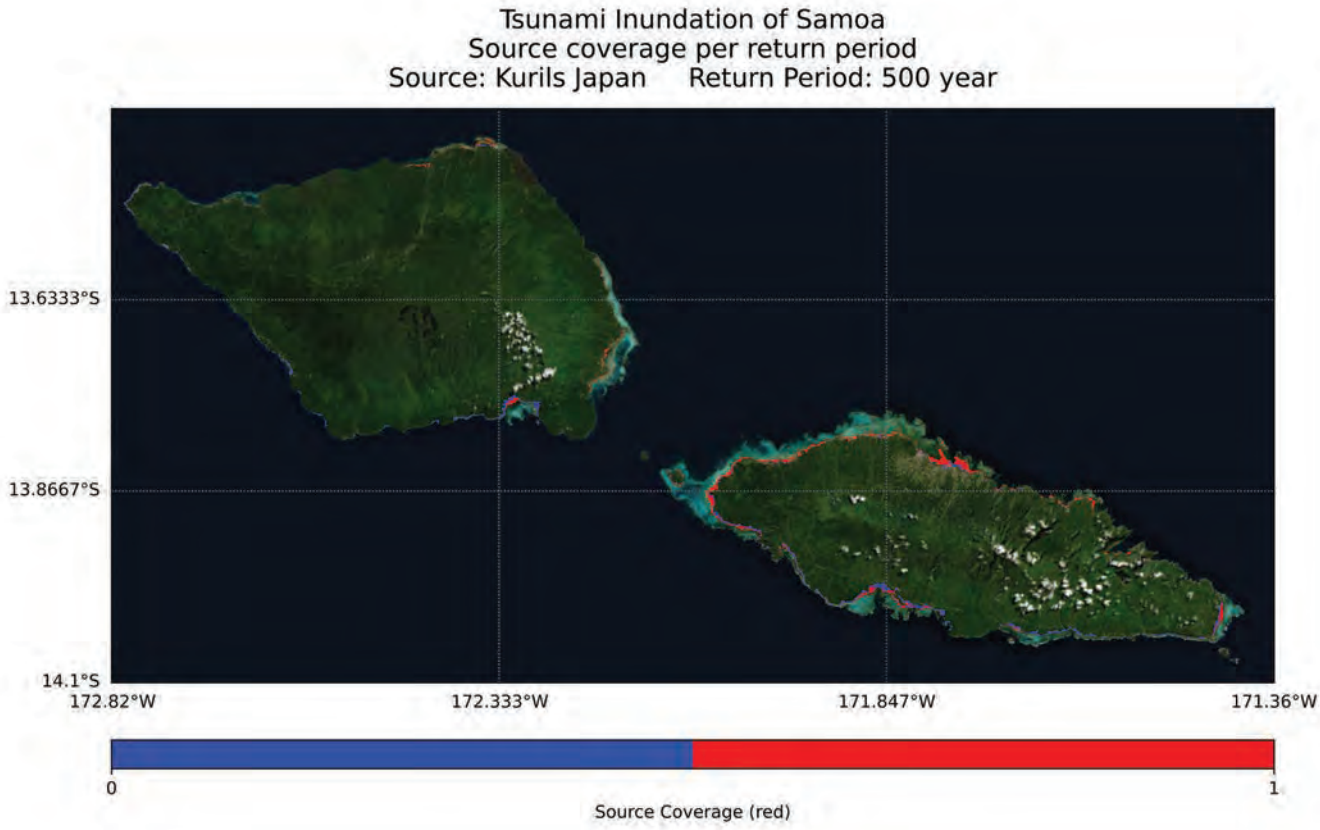

b. RP 500 year

v. Mexico

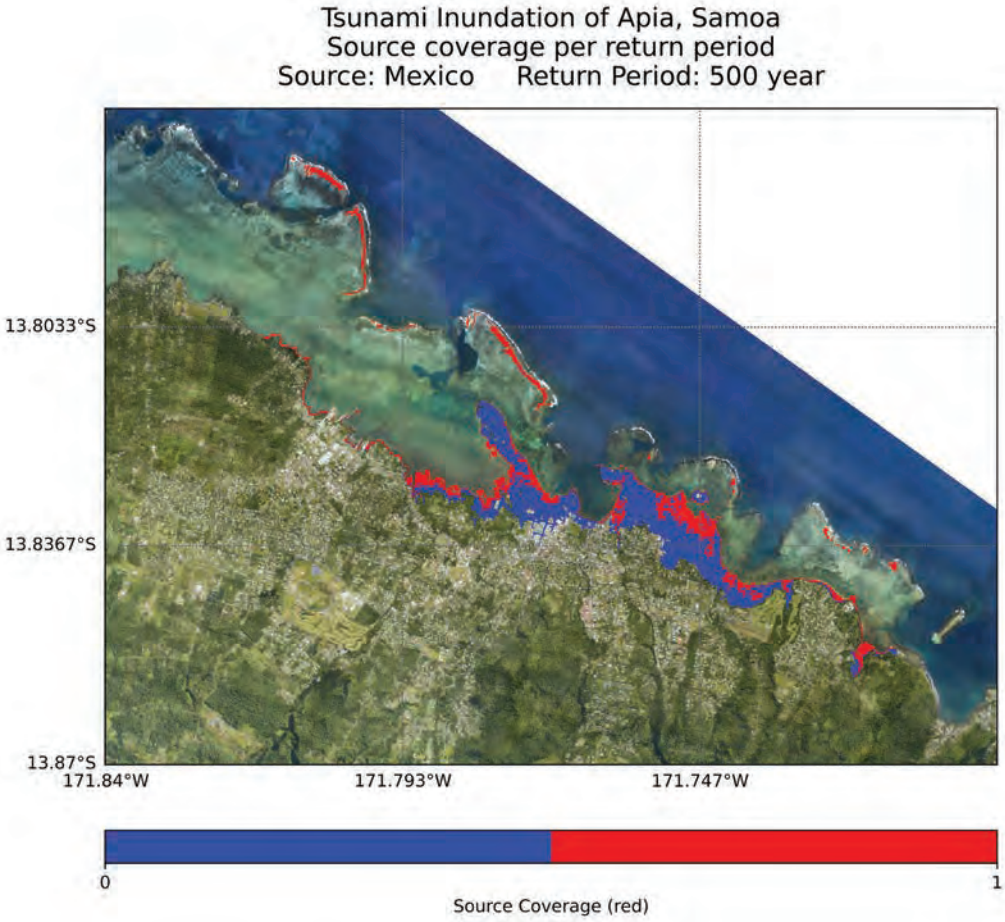

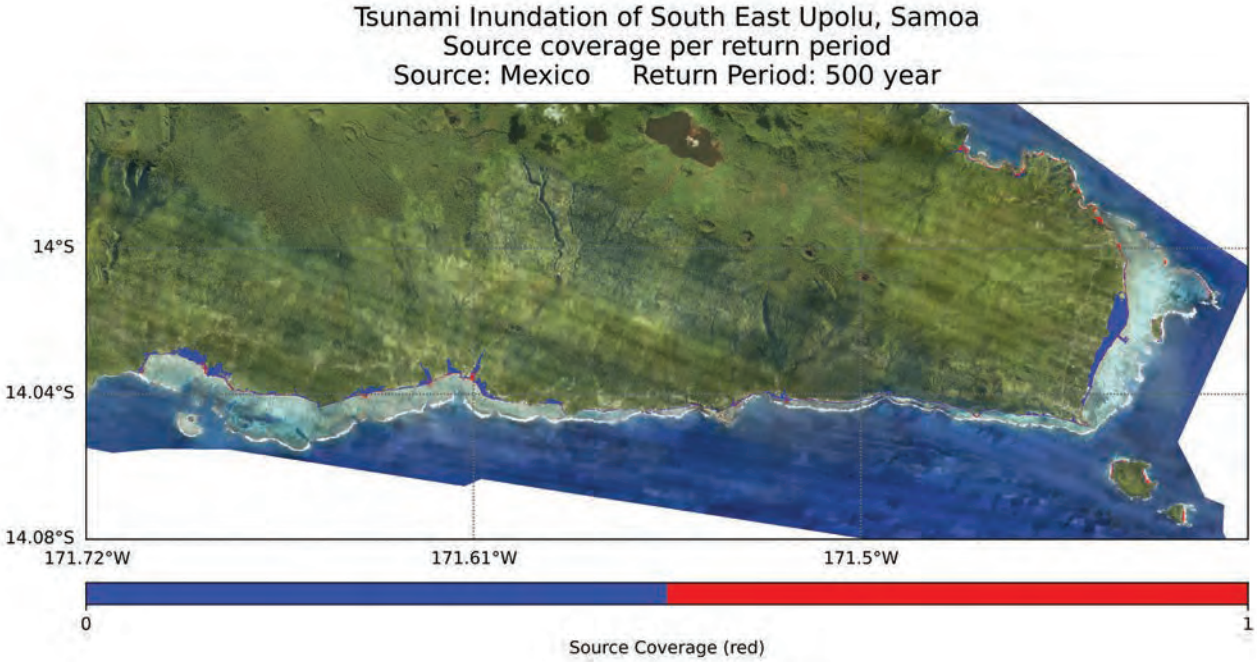

b. RP 500 year

v. Mexico

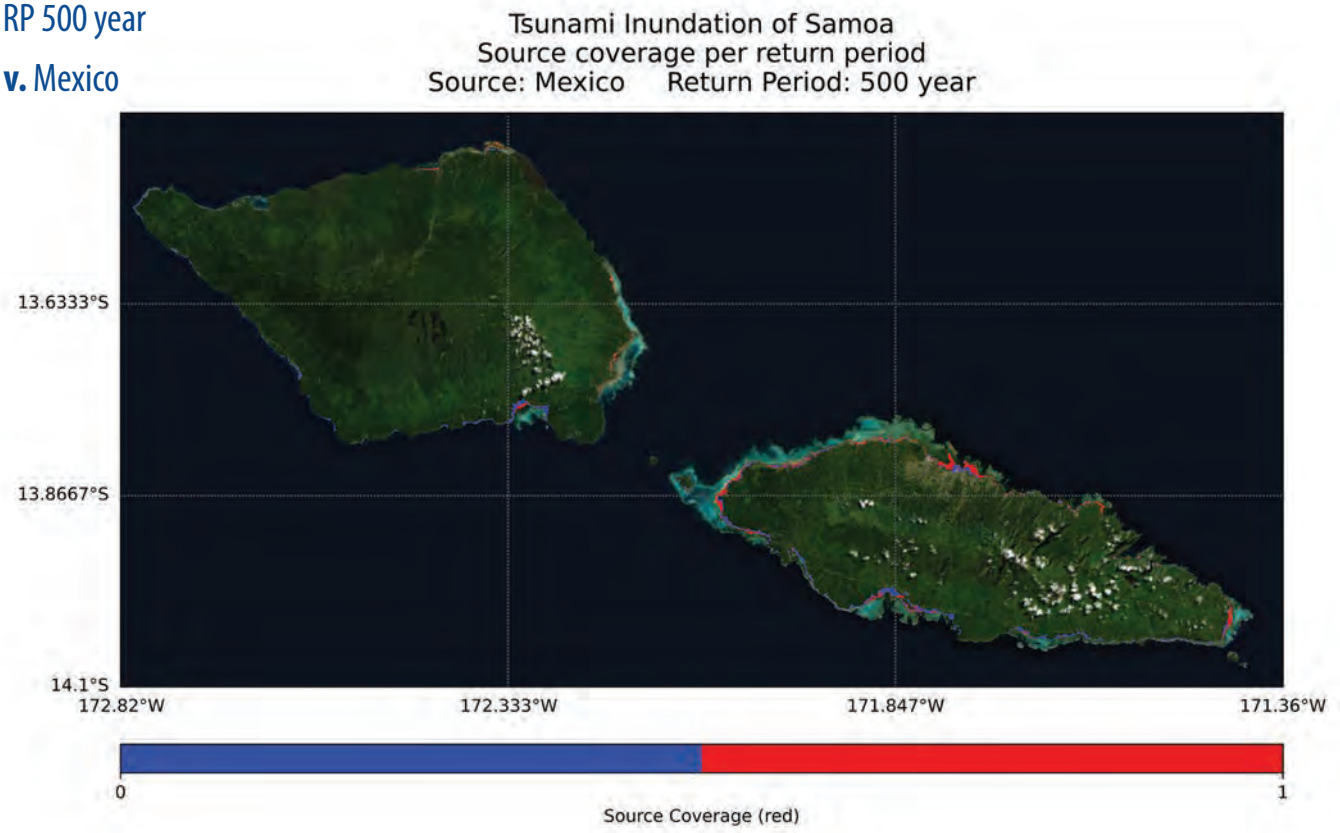

vi. South America

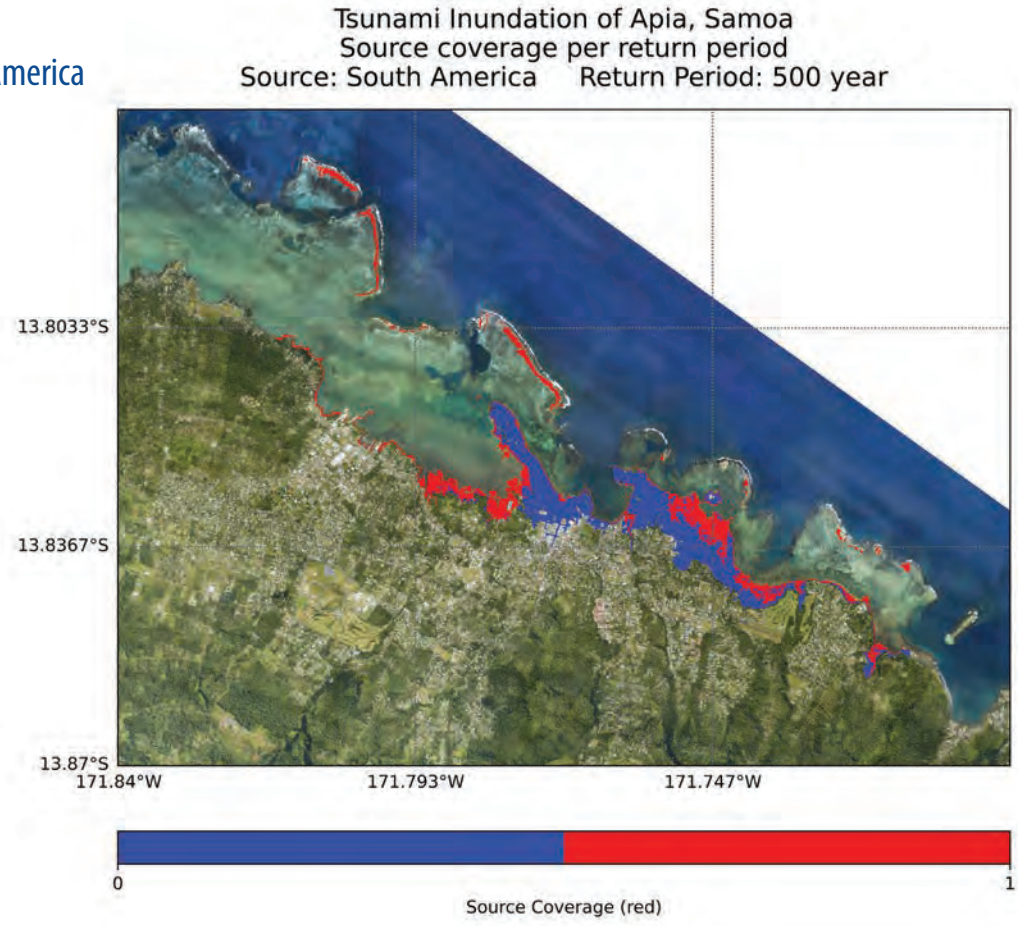

b. RP 500 year

vi. South America

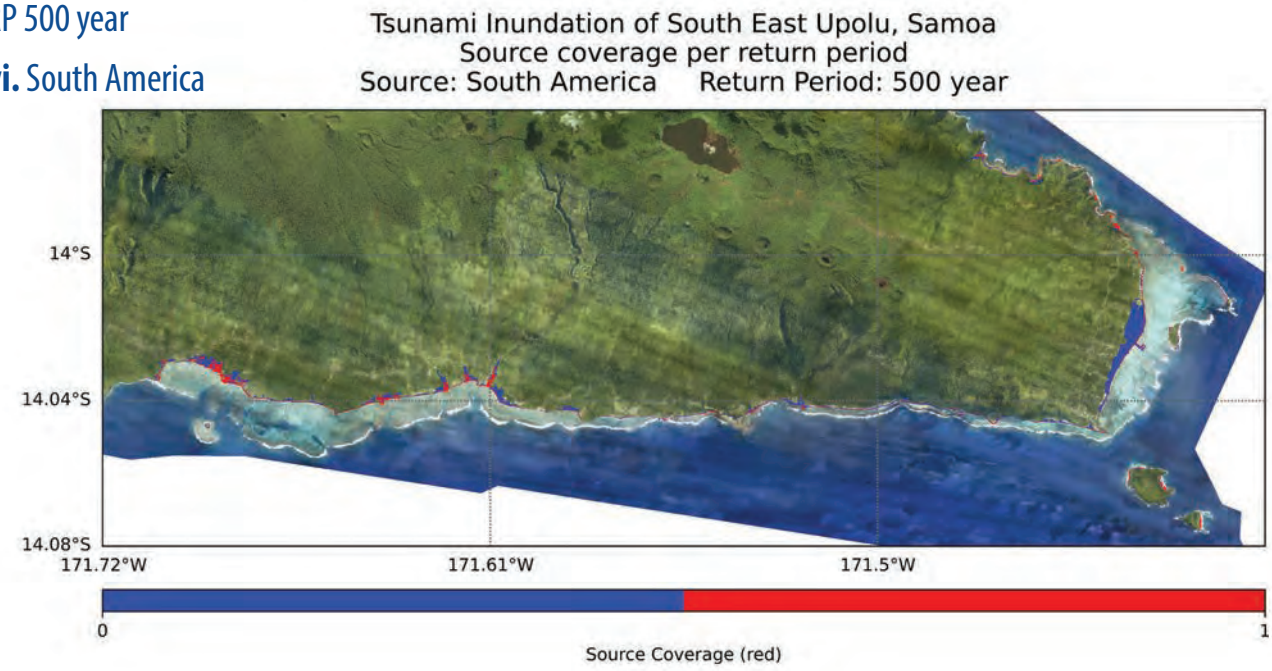

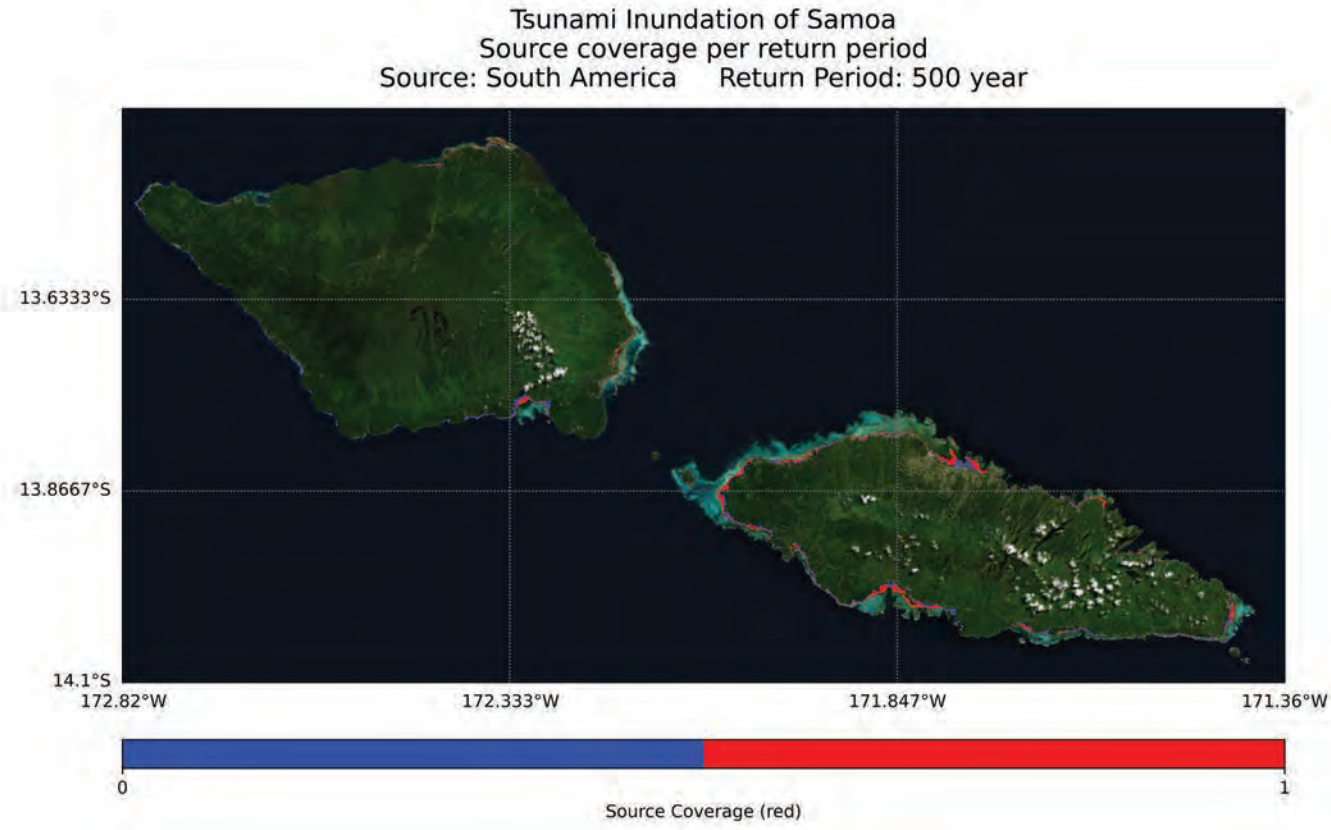

c. RP 1000 year

i. Alaska Aleutians

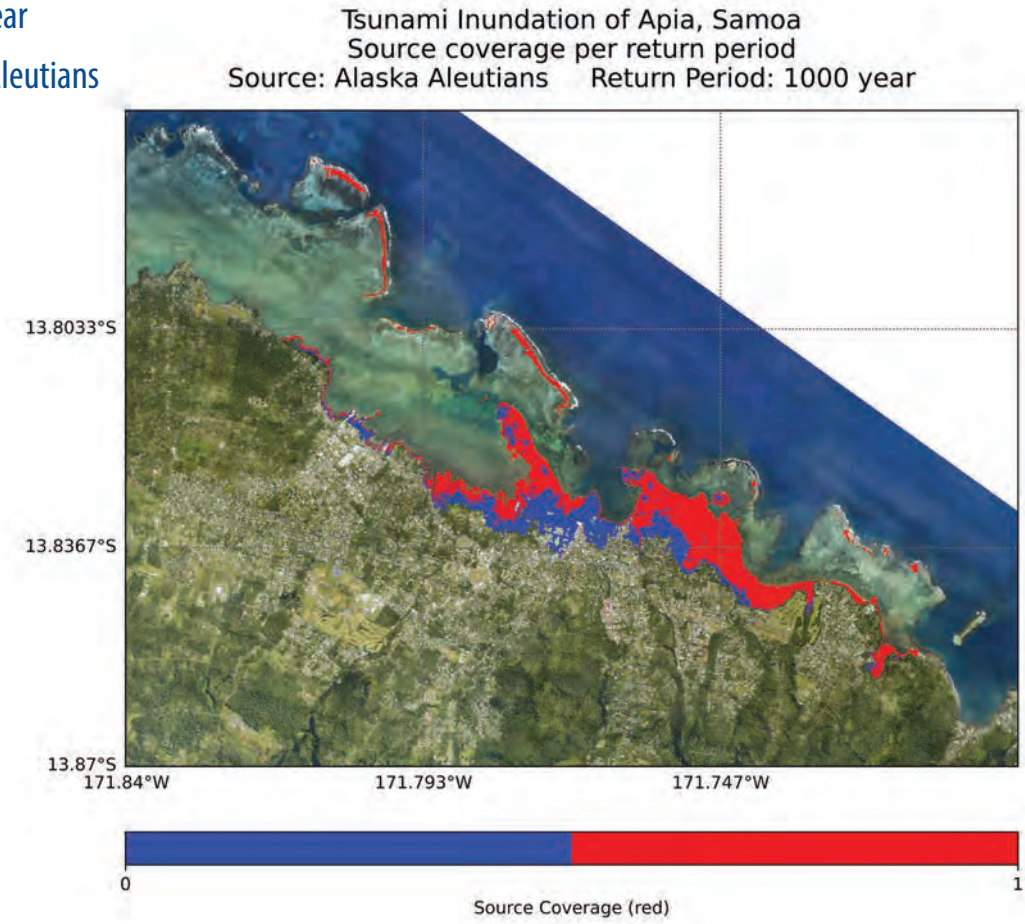

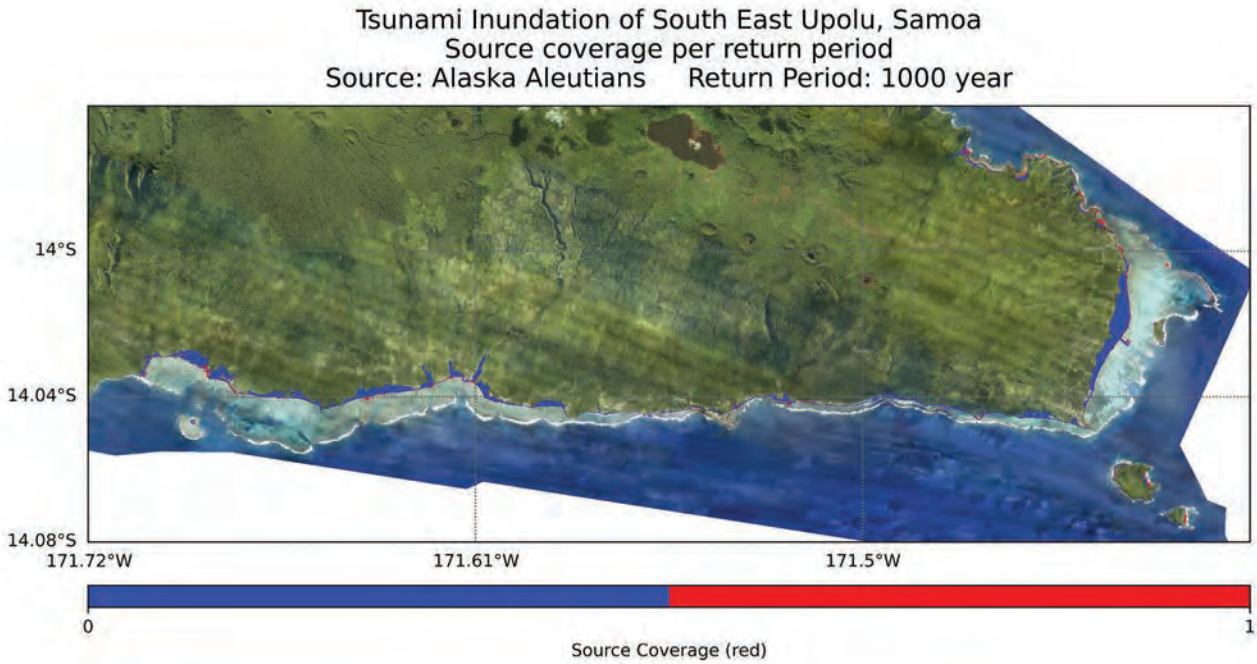

c. RP 1000 year

i. Alaska Aleutians

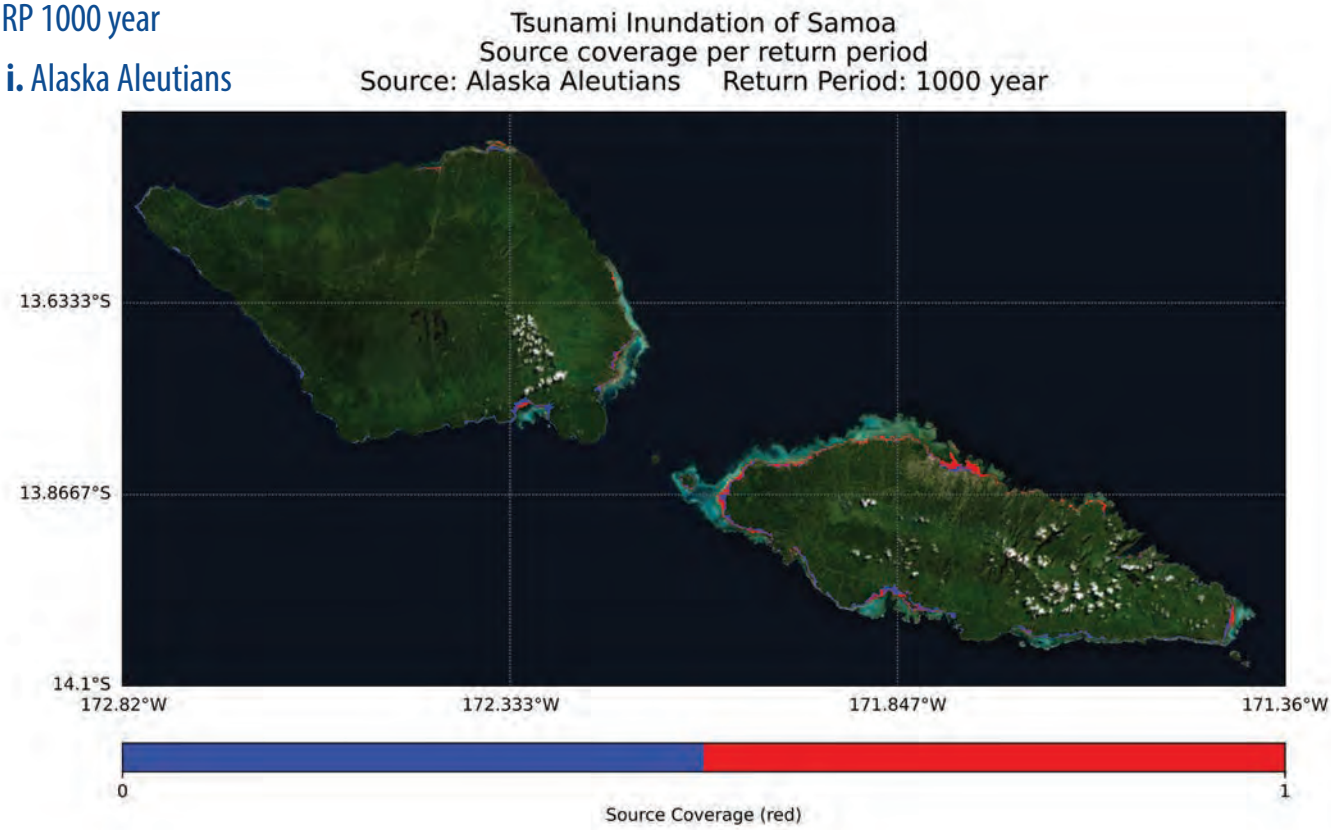

ii. Kermadec-Tonga

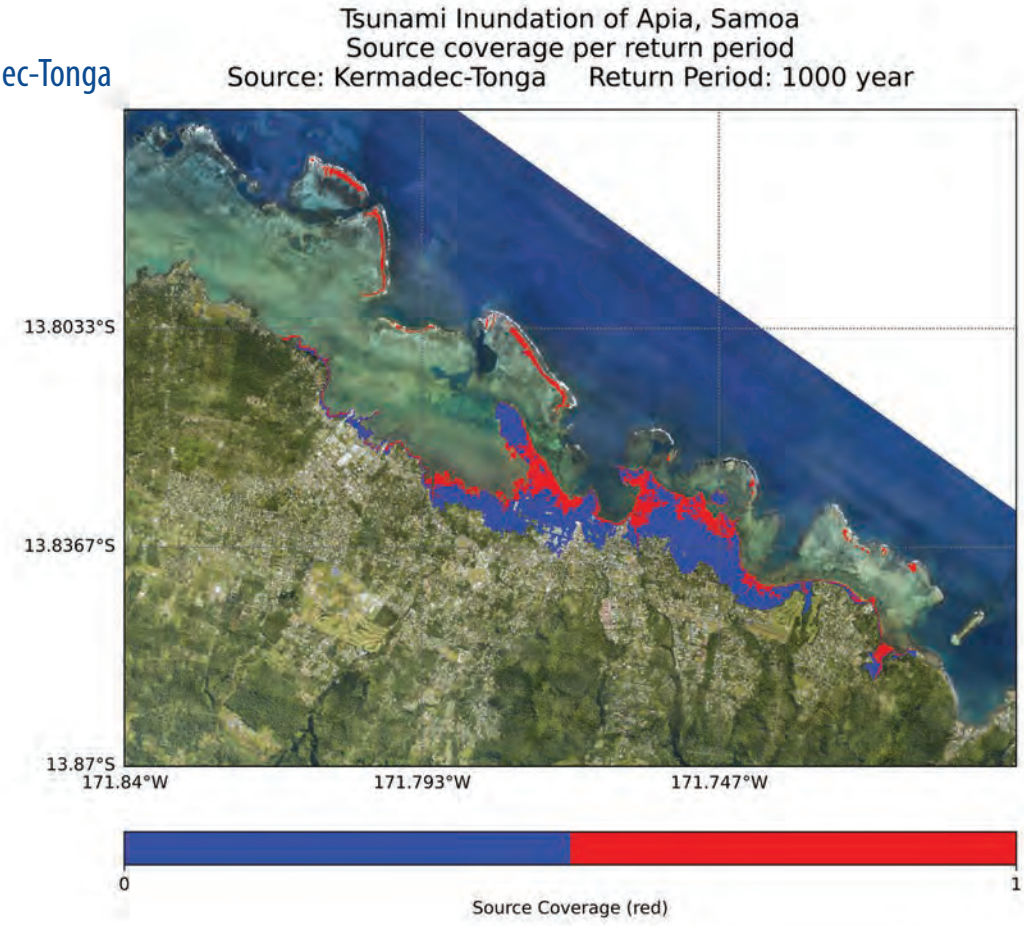

c. RP 1000 year

ii. Kermadec-Tonga

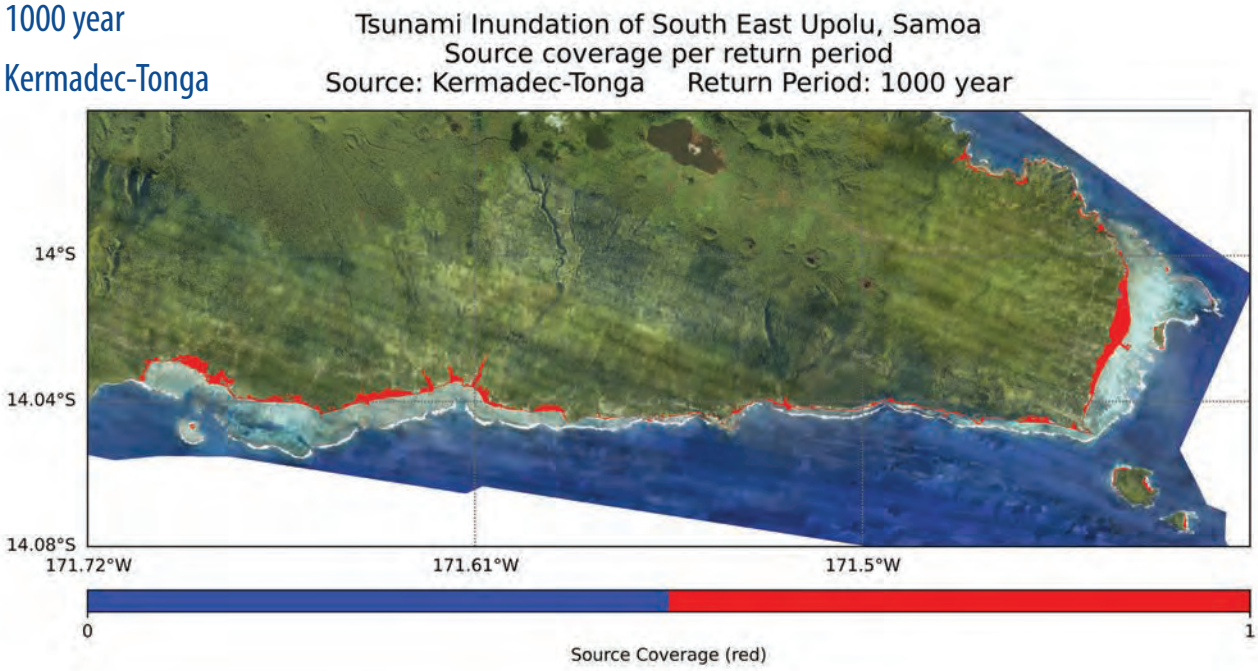

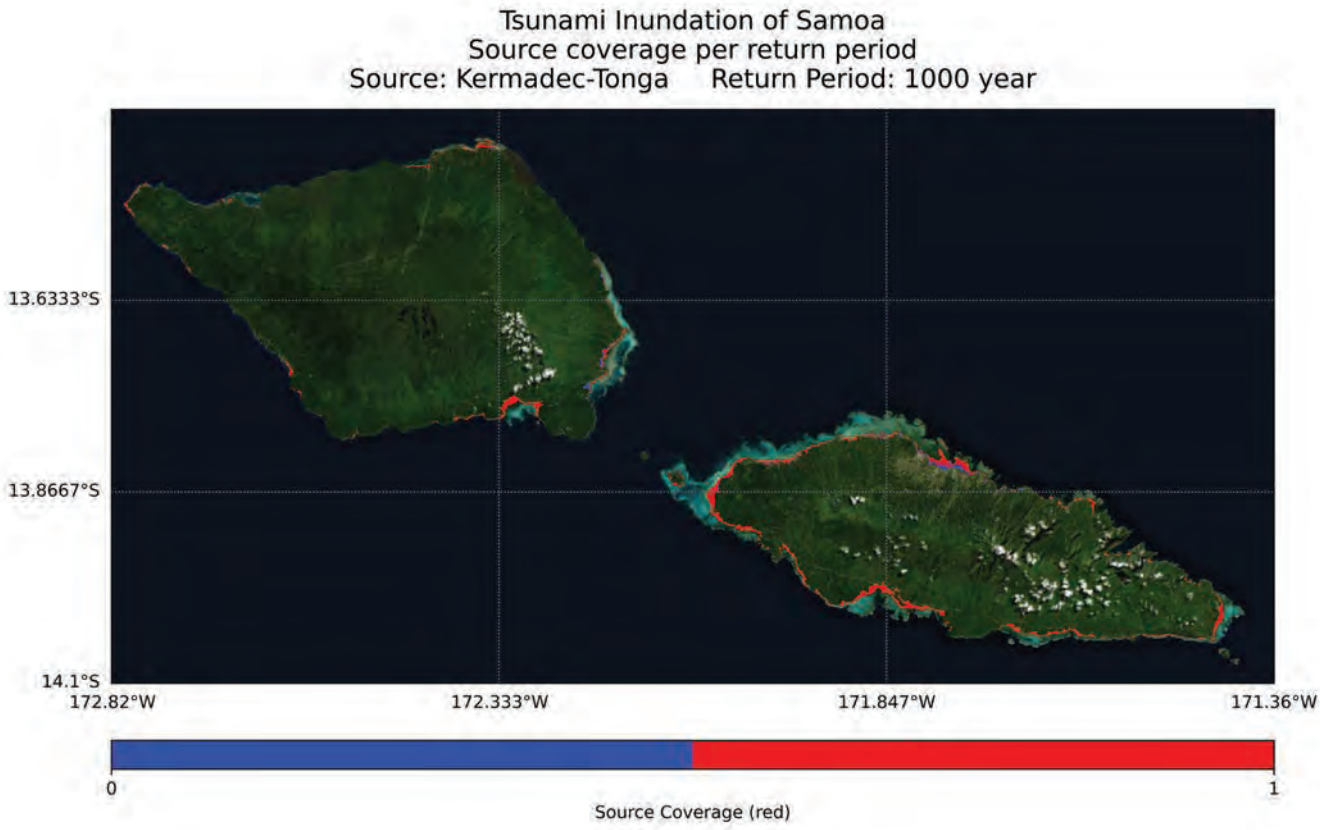

c. RP 1000 year

iii. Kurils Japan

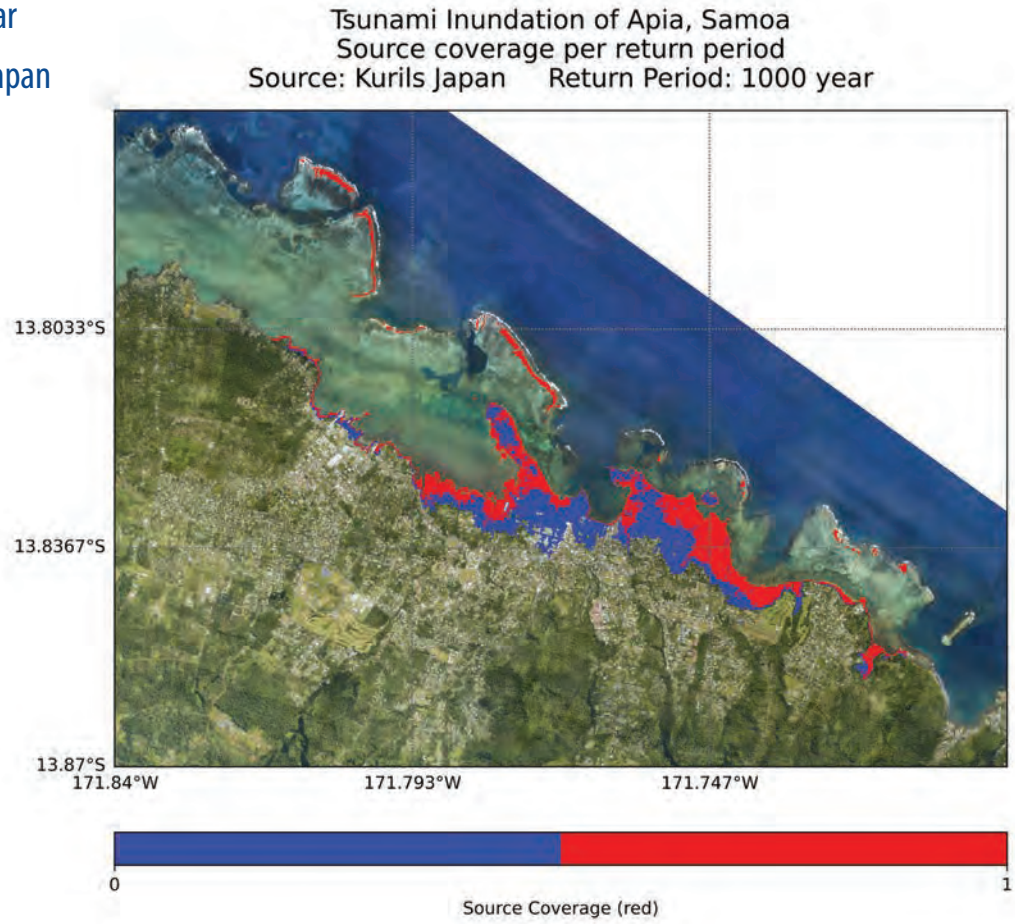

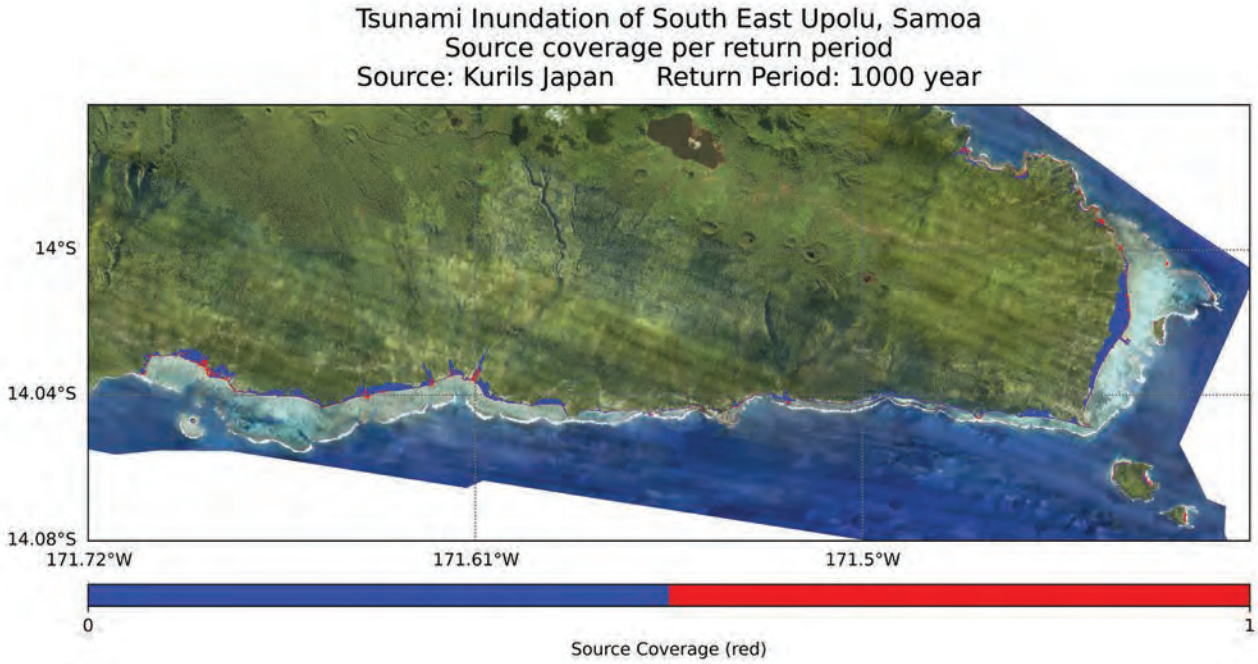

c. RP 1000 year

iii. Kurils Japan

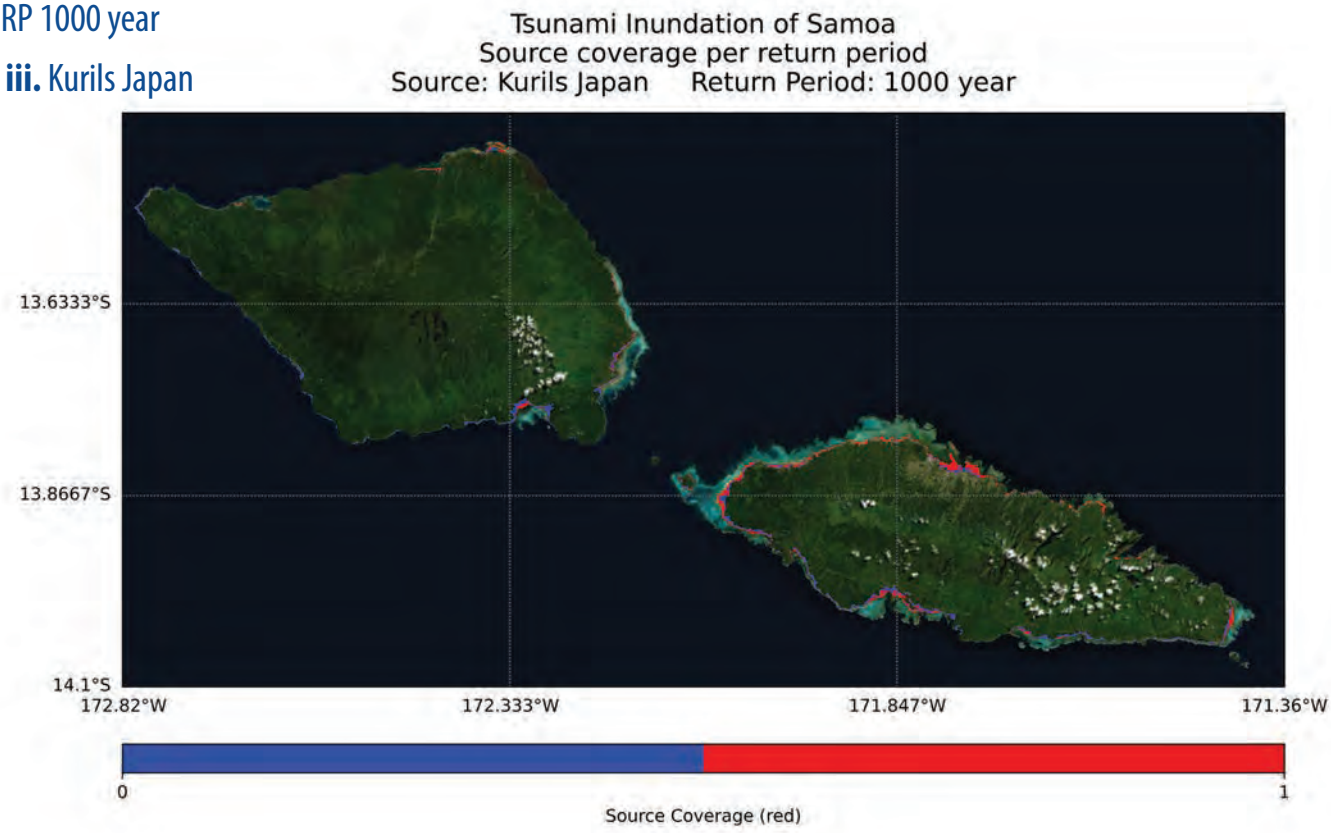

iv. South America

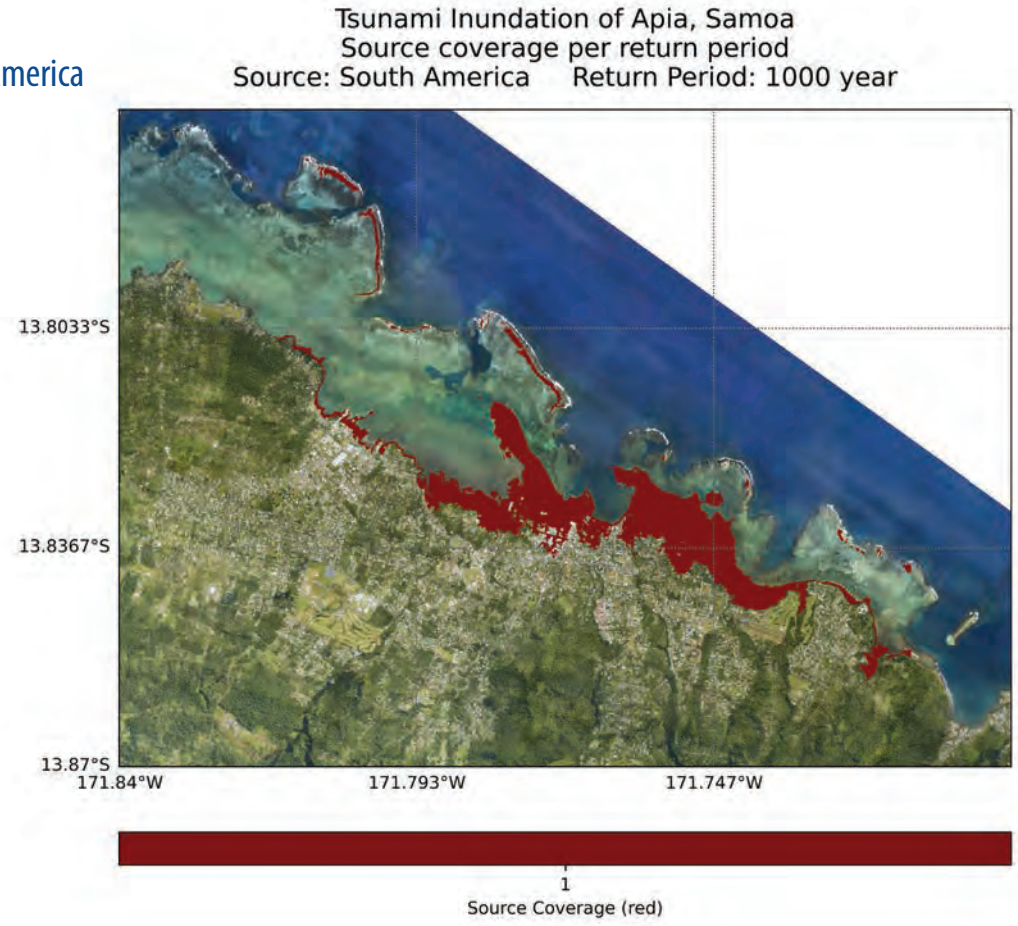

c. RP 1000 year

iv. South America

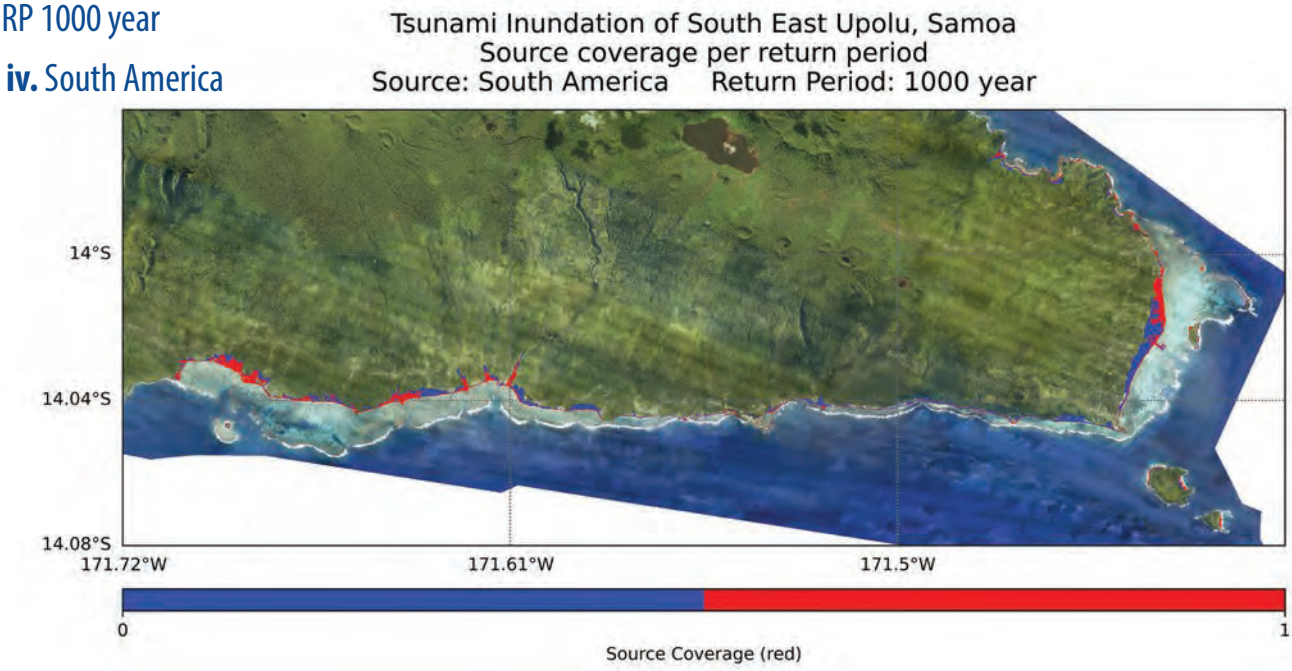

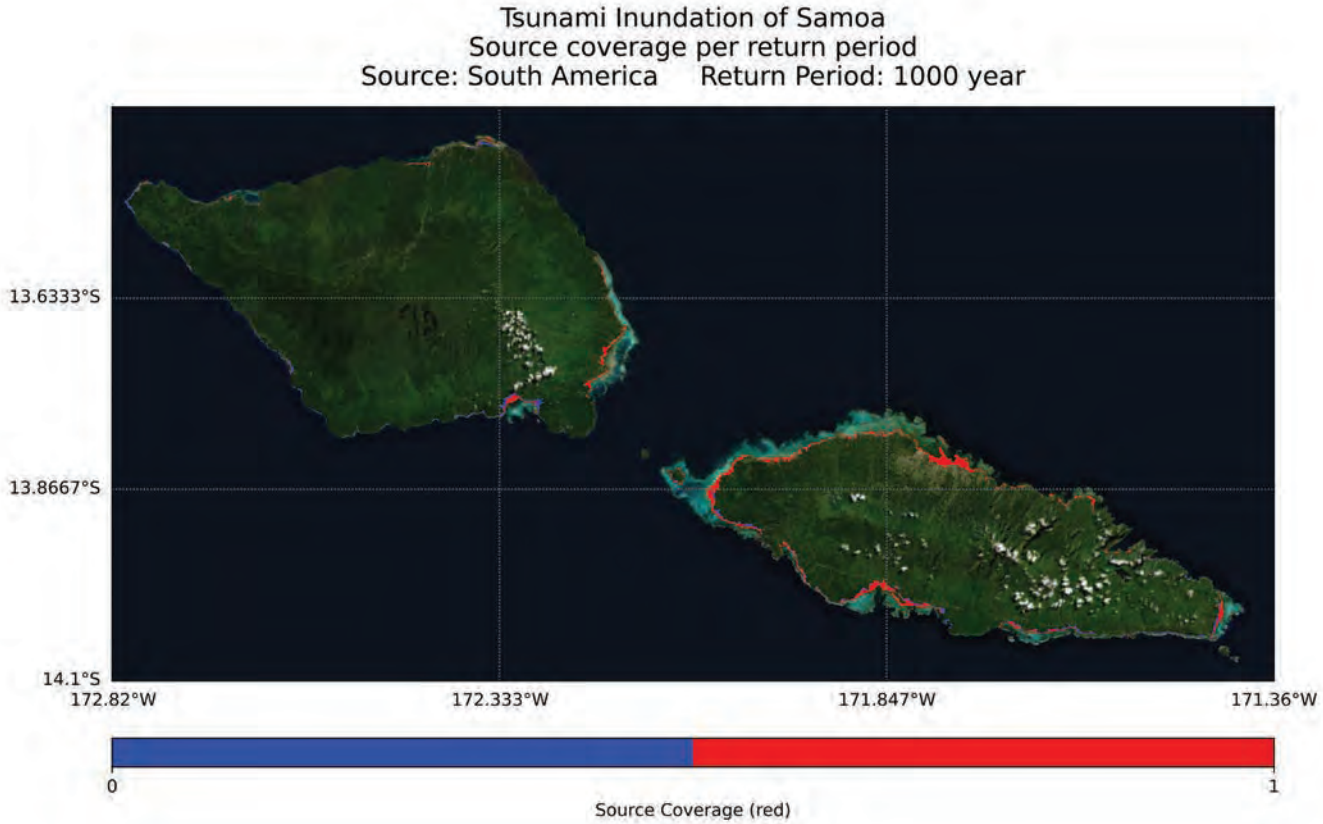

d. RP 2500 year 84th percentile

i. Alaska Aleutians

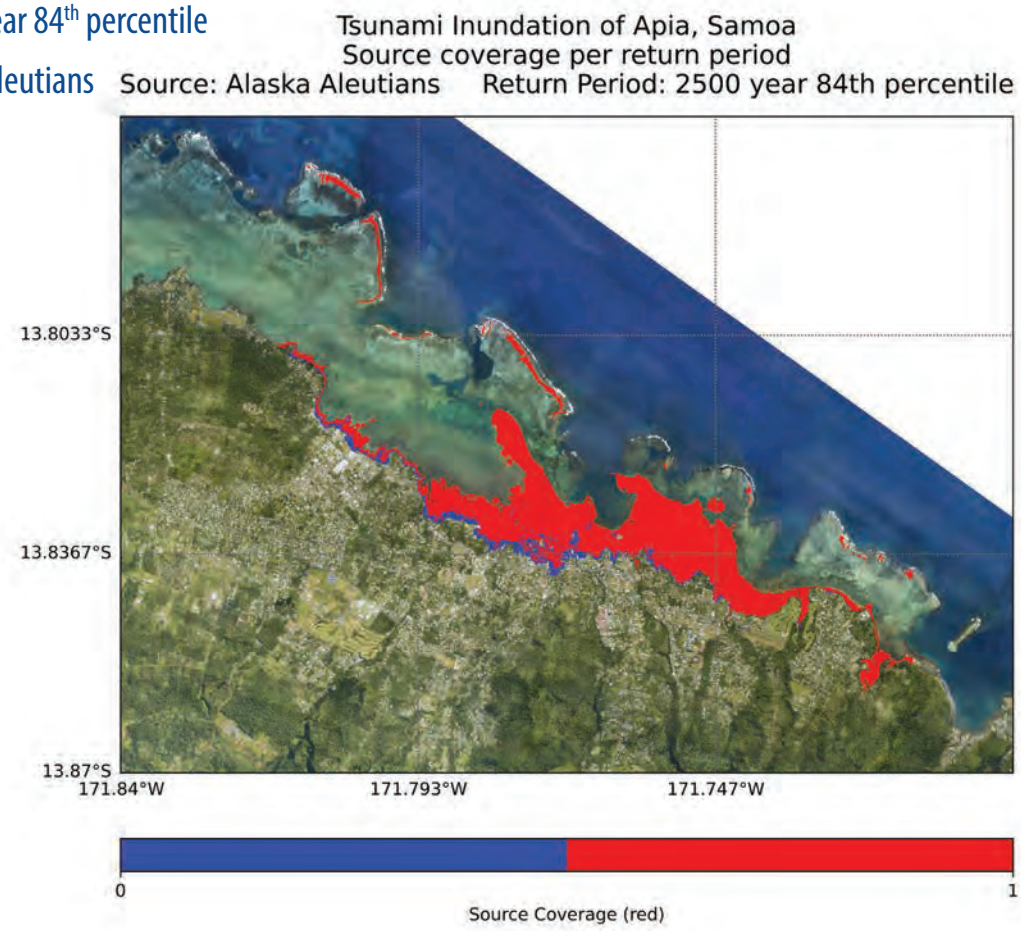

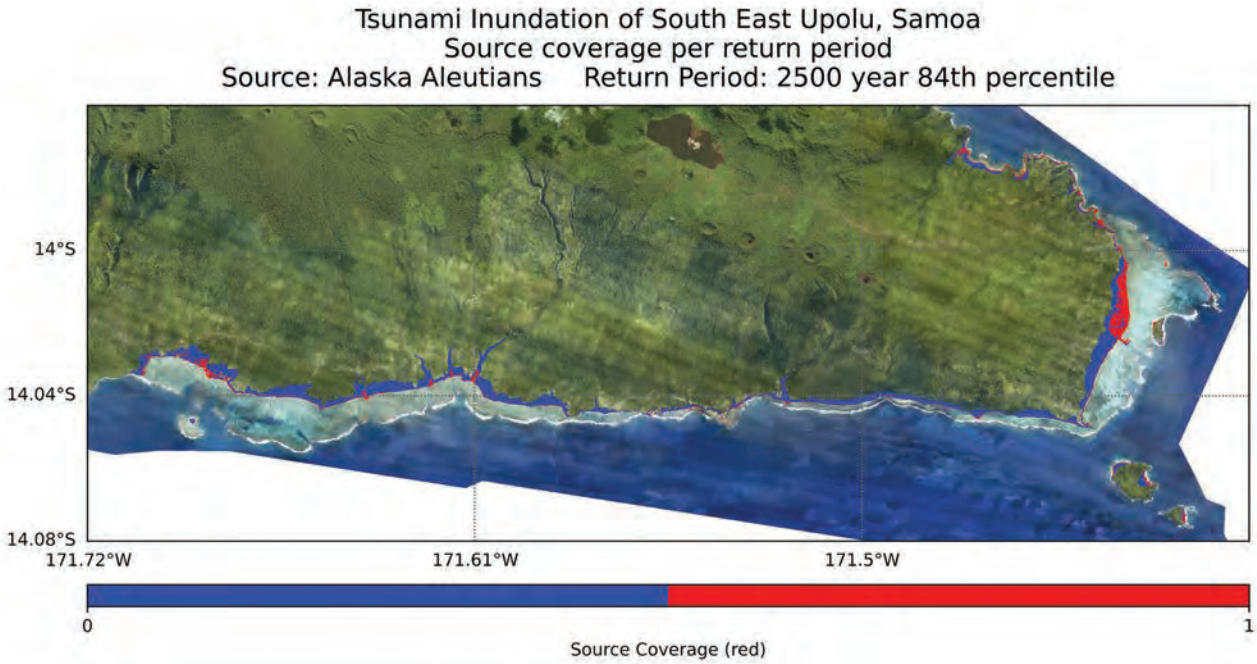

d. RP 2500 year 84th percentile

i. Alaska Aleutians

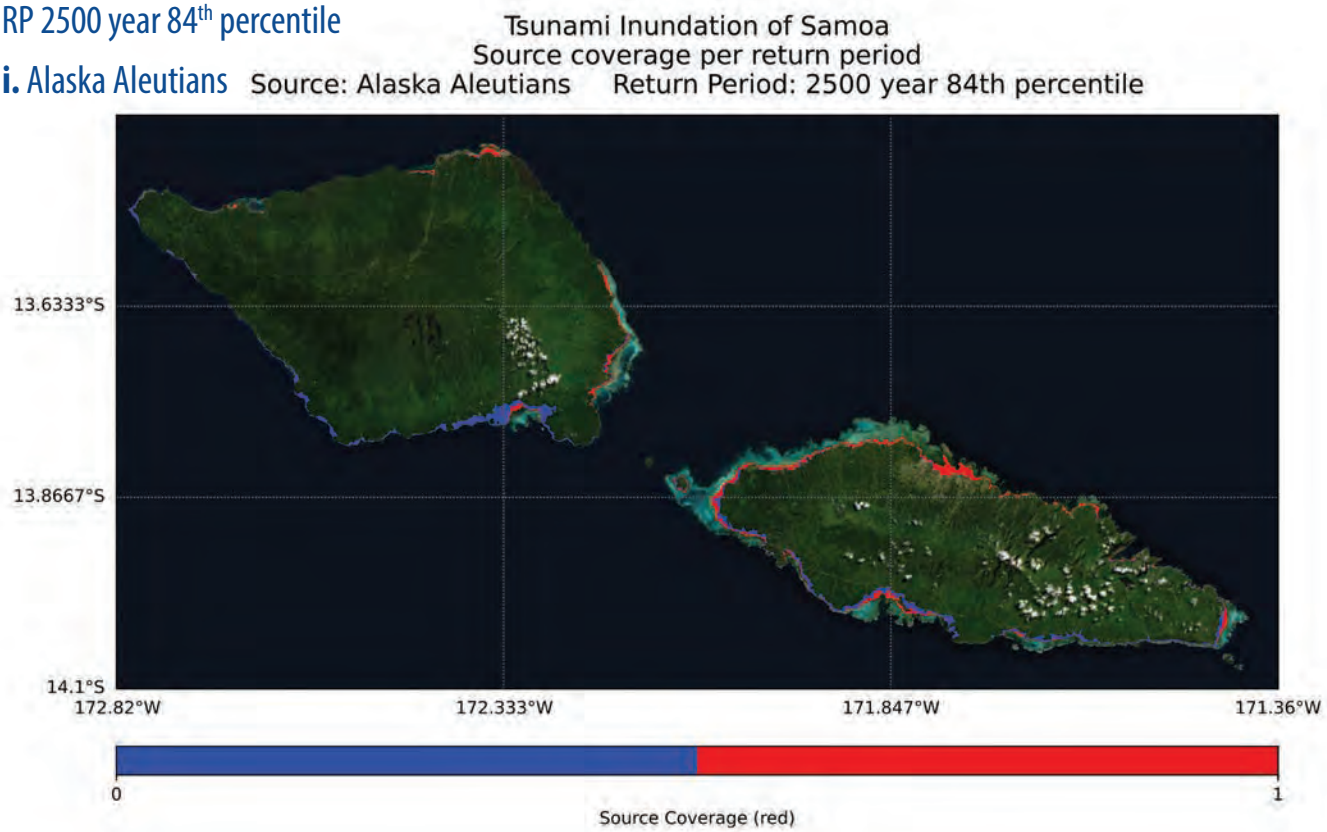

ii. Kermadec-Tonga

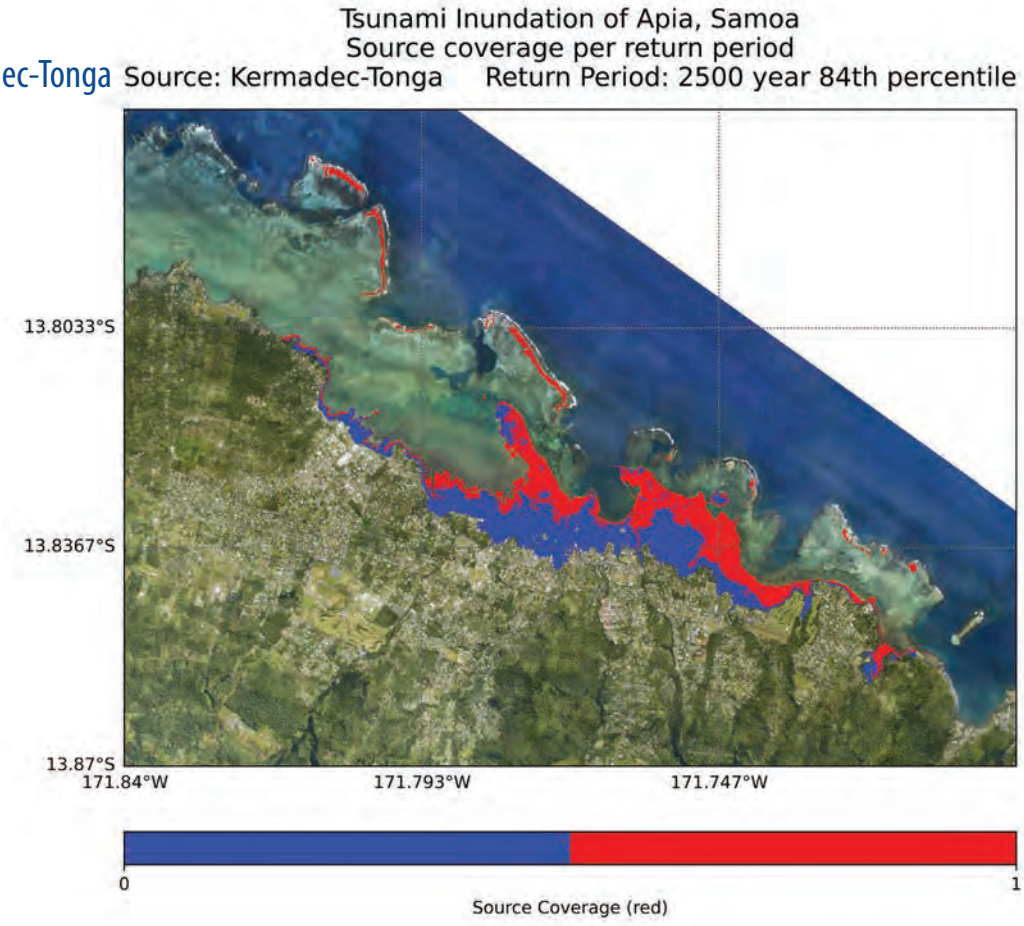

d. RP 2500 year 84th percentile

ii. Kermadec-Tonga

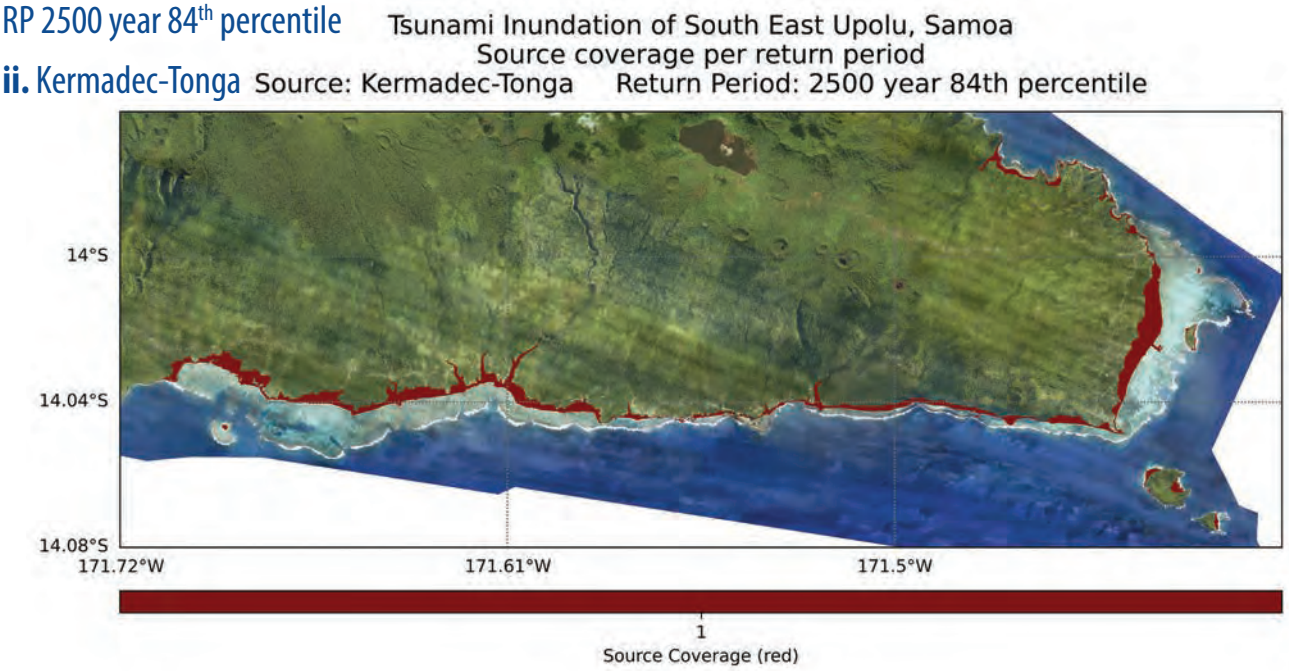

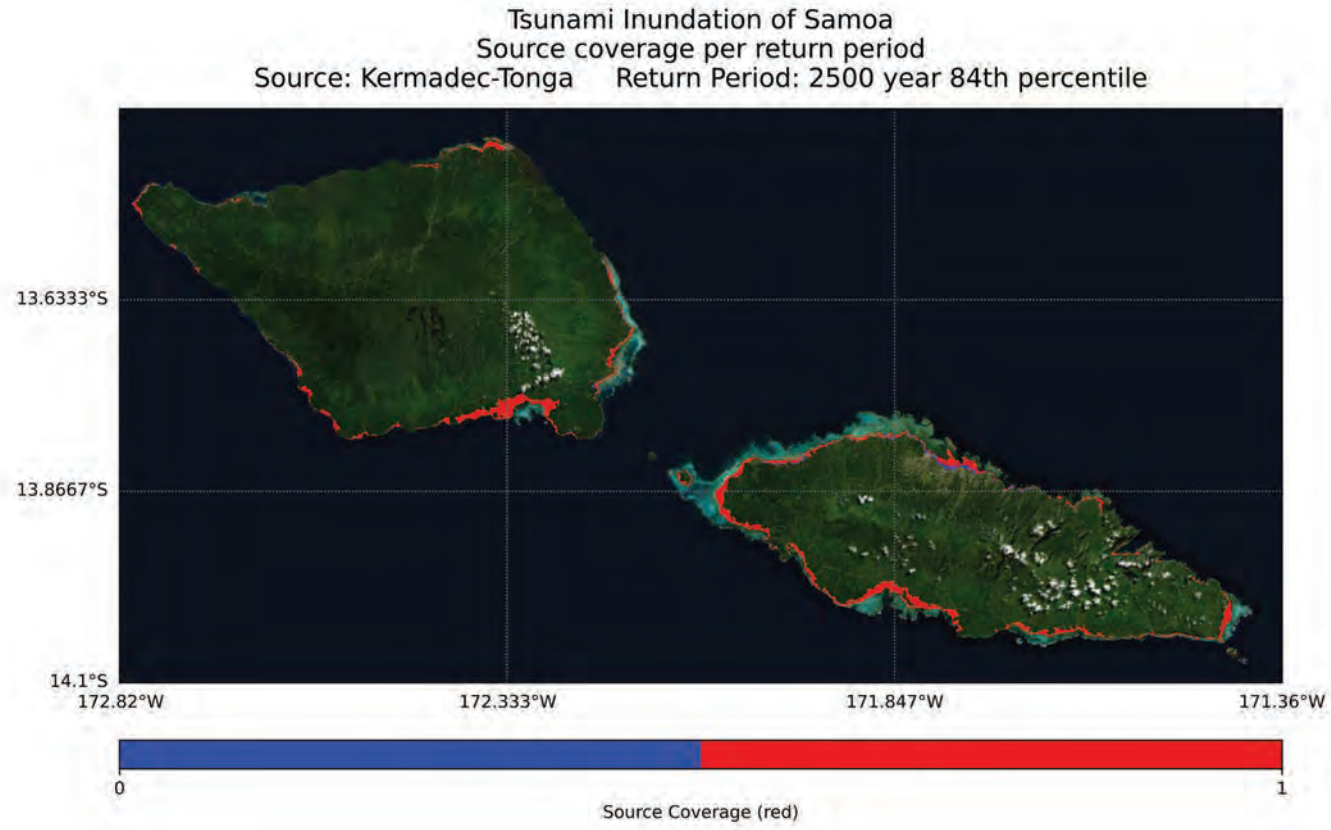

d. RP 2500 year 84th percentile

iii. South America

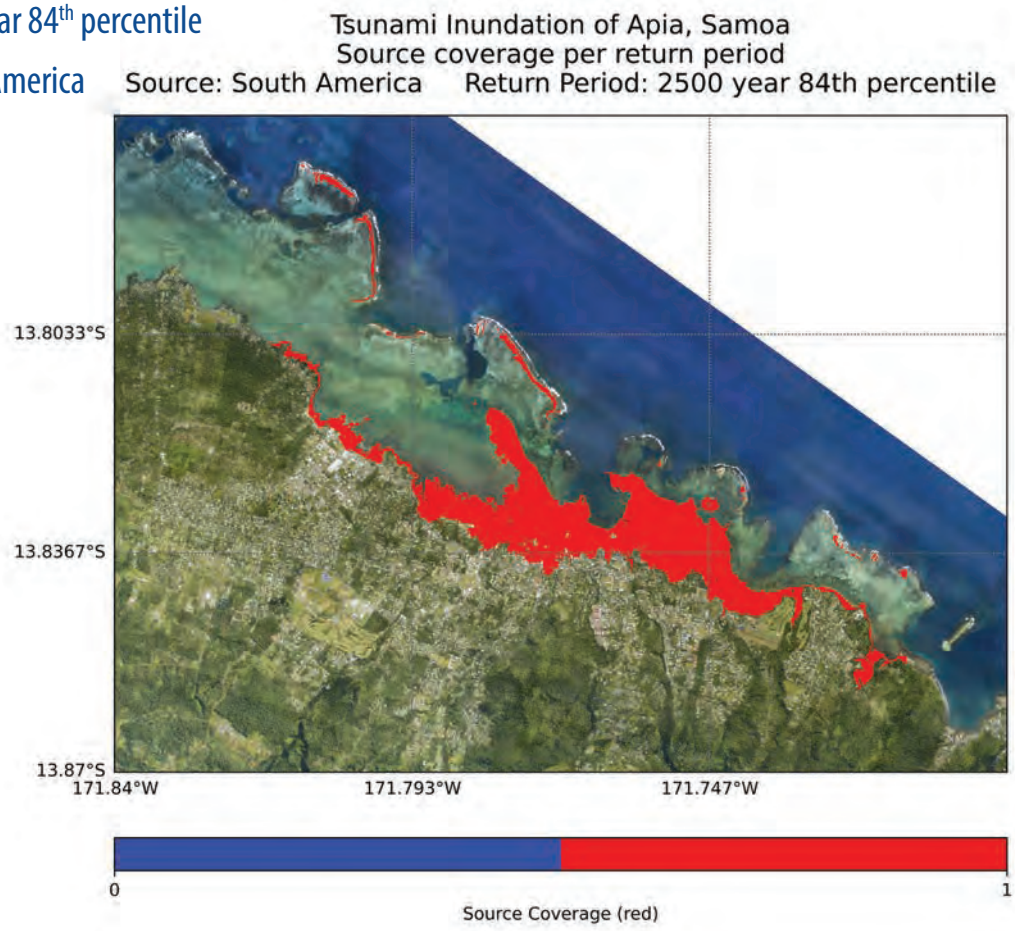

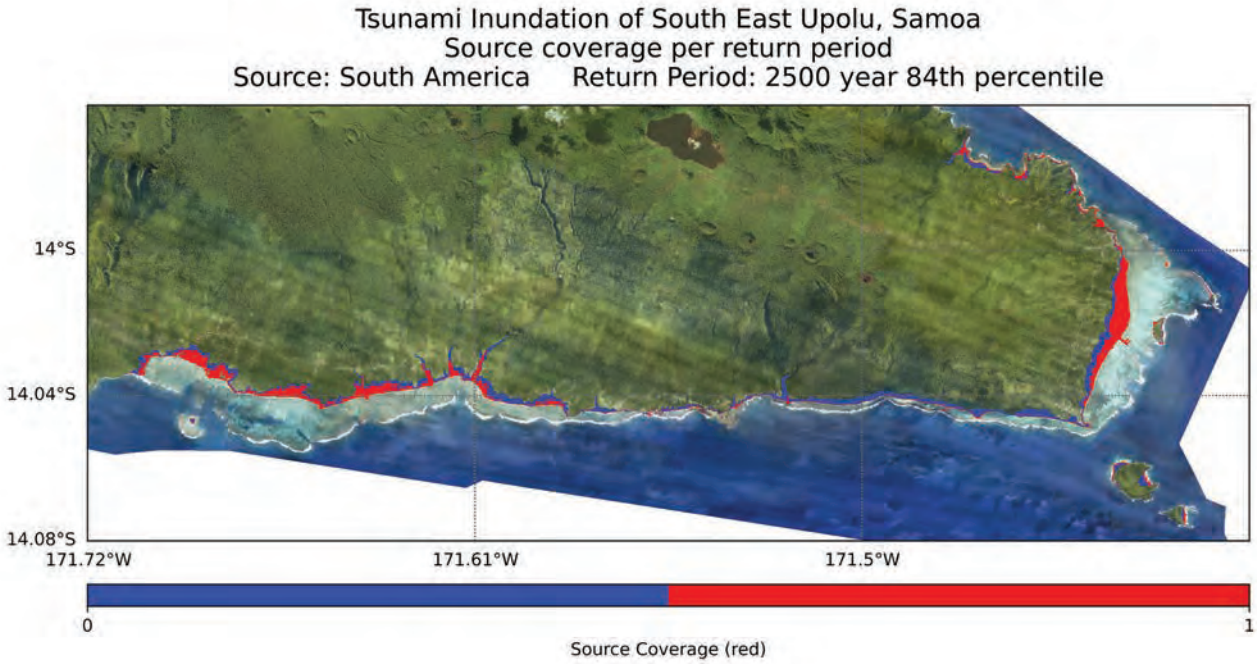

d. RP 2500 year 84th percentile

iii. South America

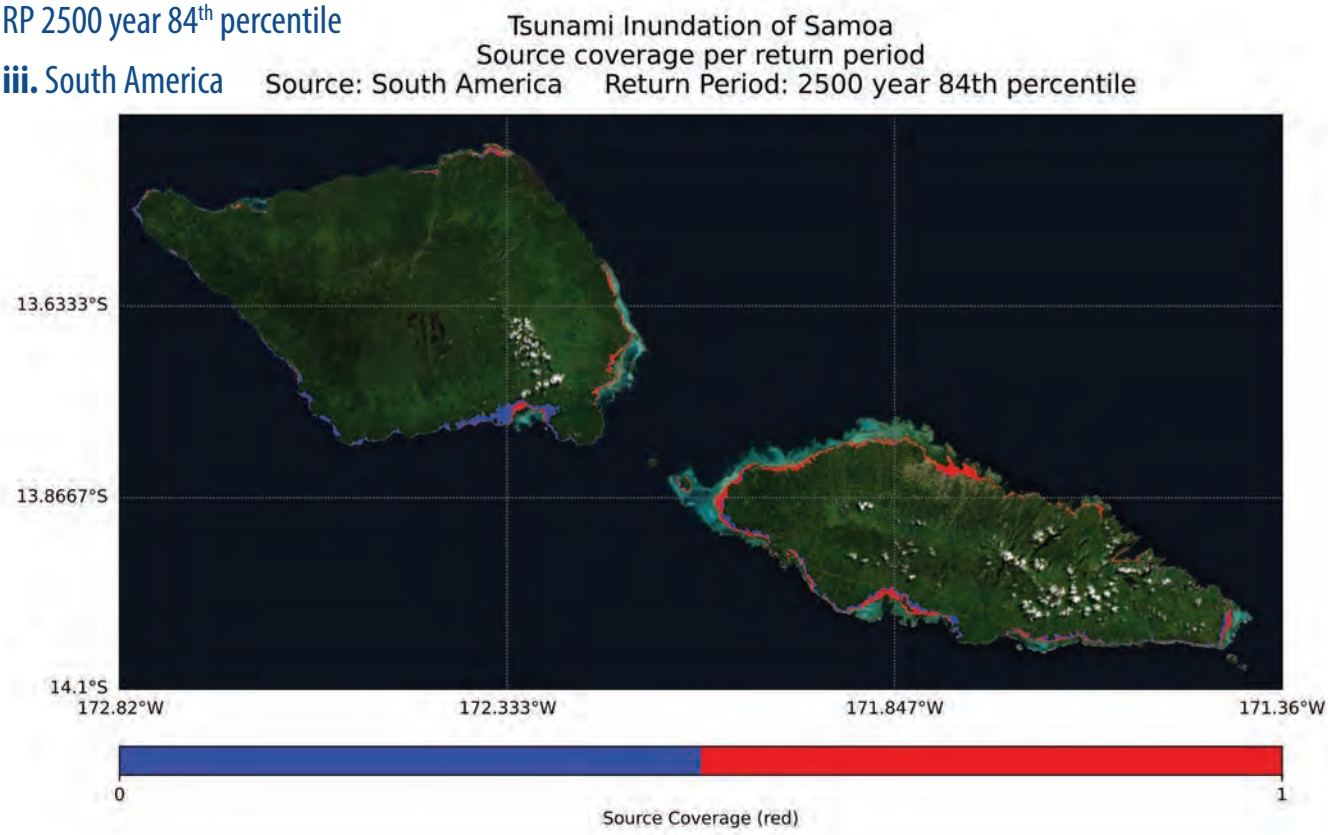

4.0 Building structure vulnerability (Tsunami Intensity Scale [ITIS]-2012)

a. RP 100 year

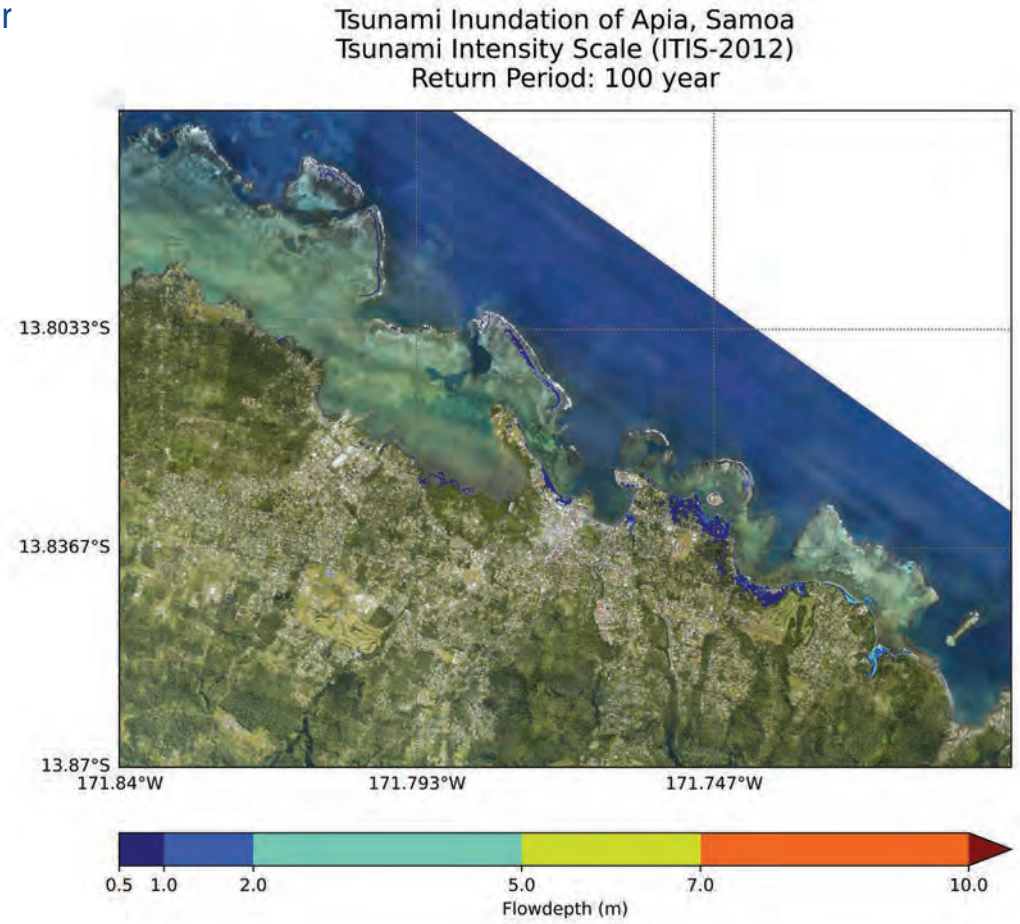

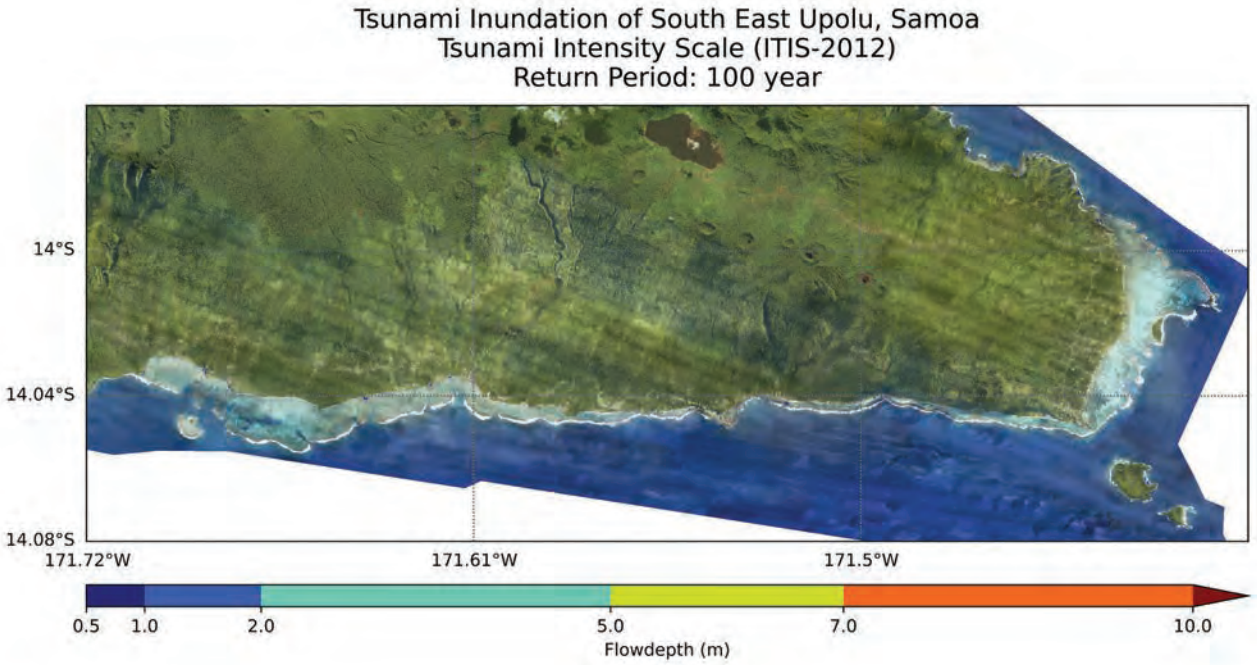

a. RP 100 year

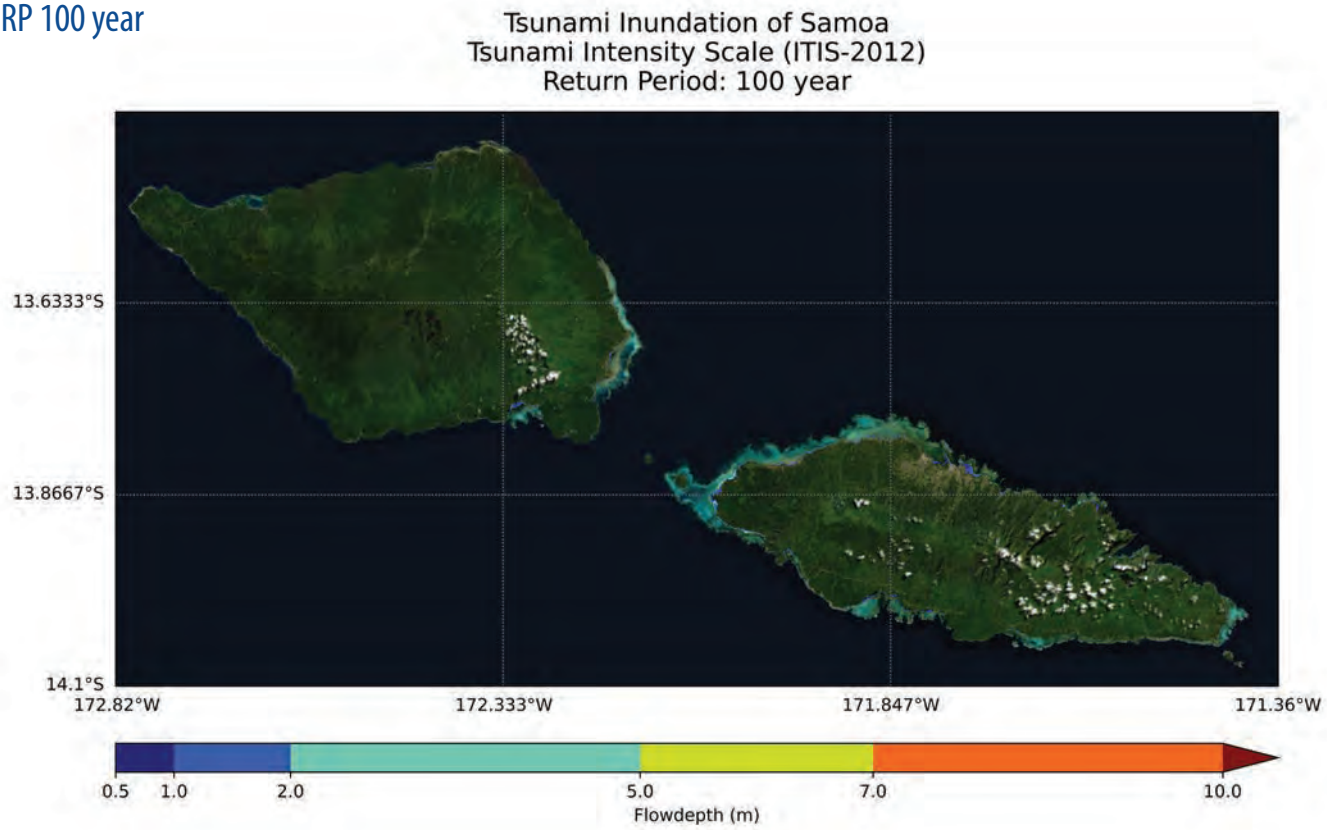

b. RP 500 year

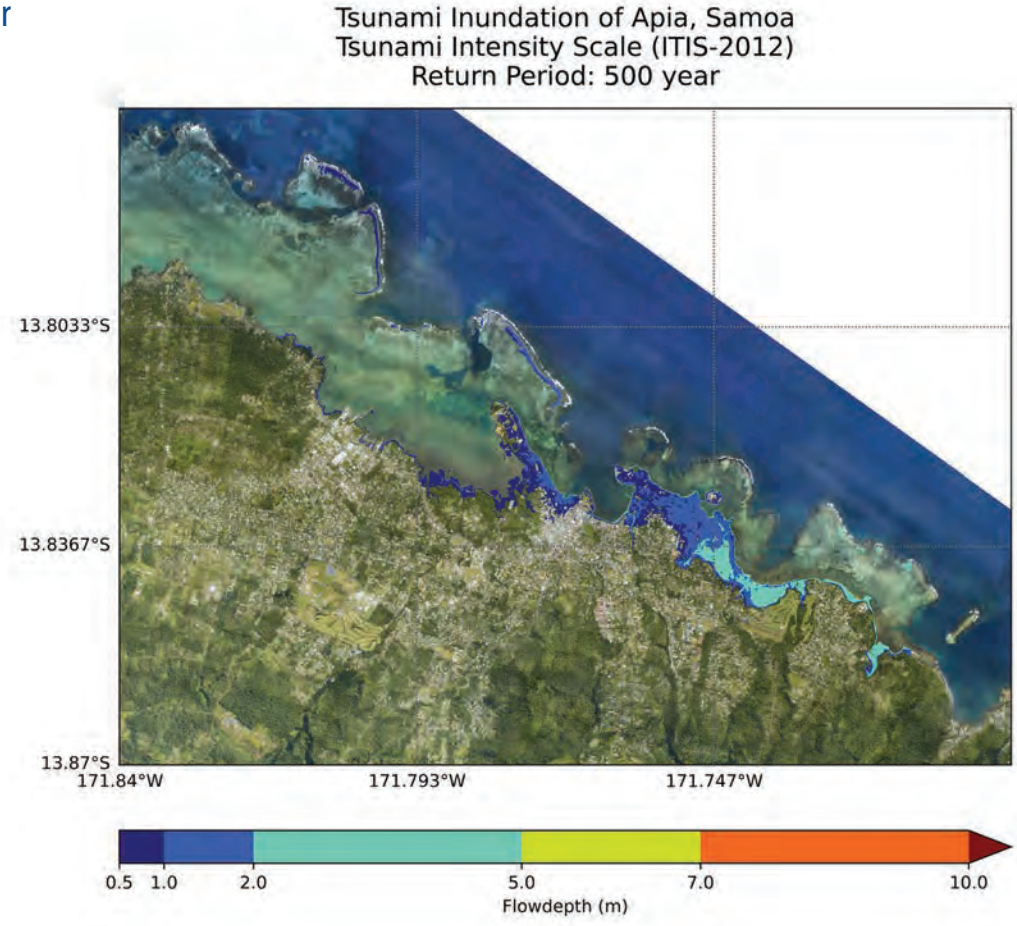

b. RP 500 year

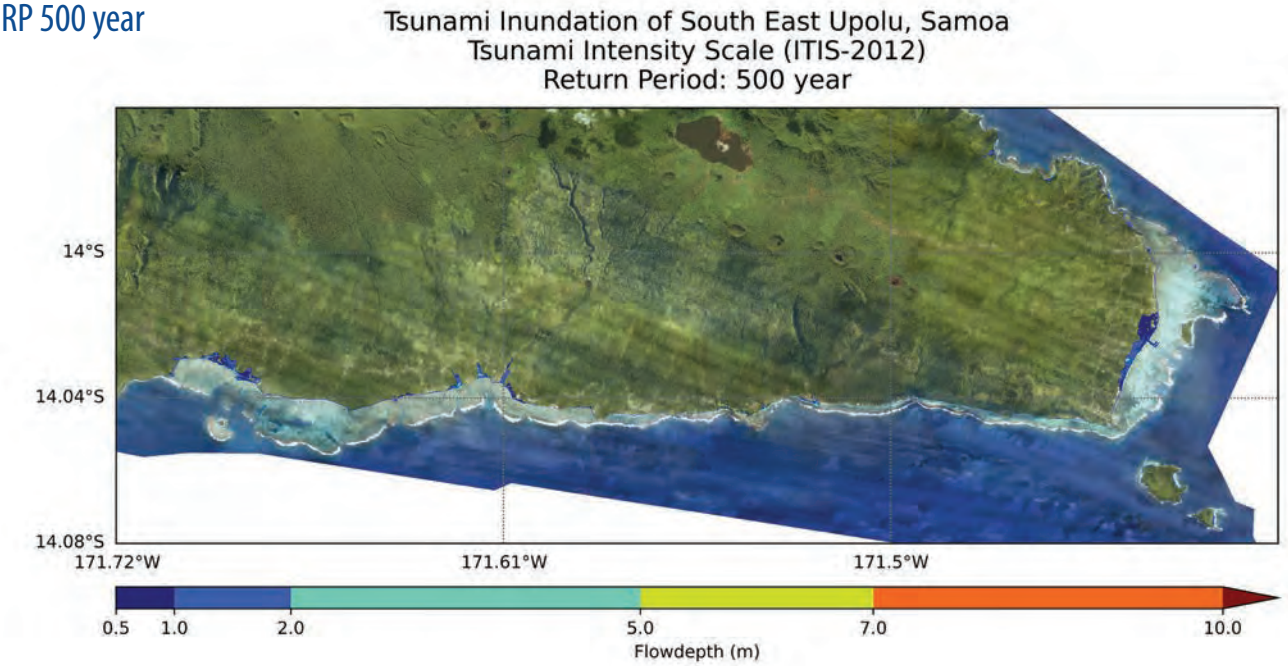
Tsunami Inundation of South East Upolu, Samoa
Tsunami Intensity Scale (ITIS-2012)
Return Period: 500 year
14°S
14.04°S
14.08°S
171.72°W
171.61°W
171.5°W
0.5
1.0
2.0
5.0
7.0
10.0
Flowdepth (m)

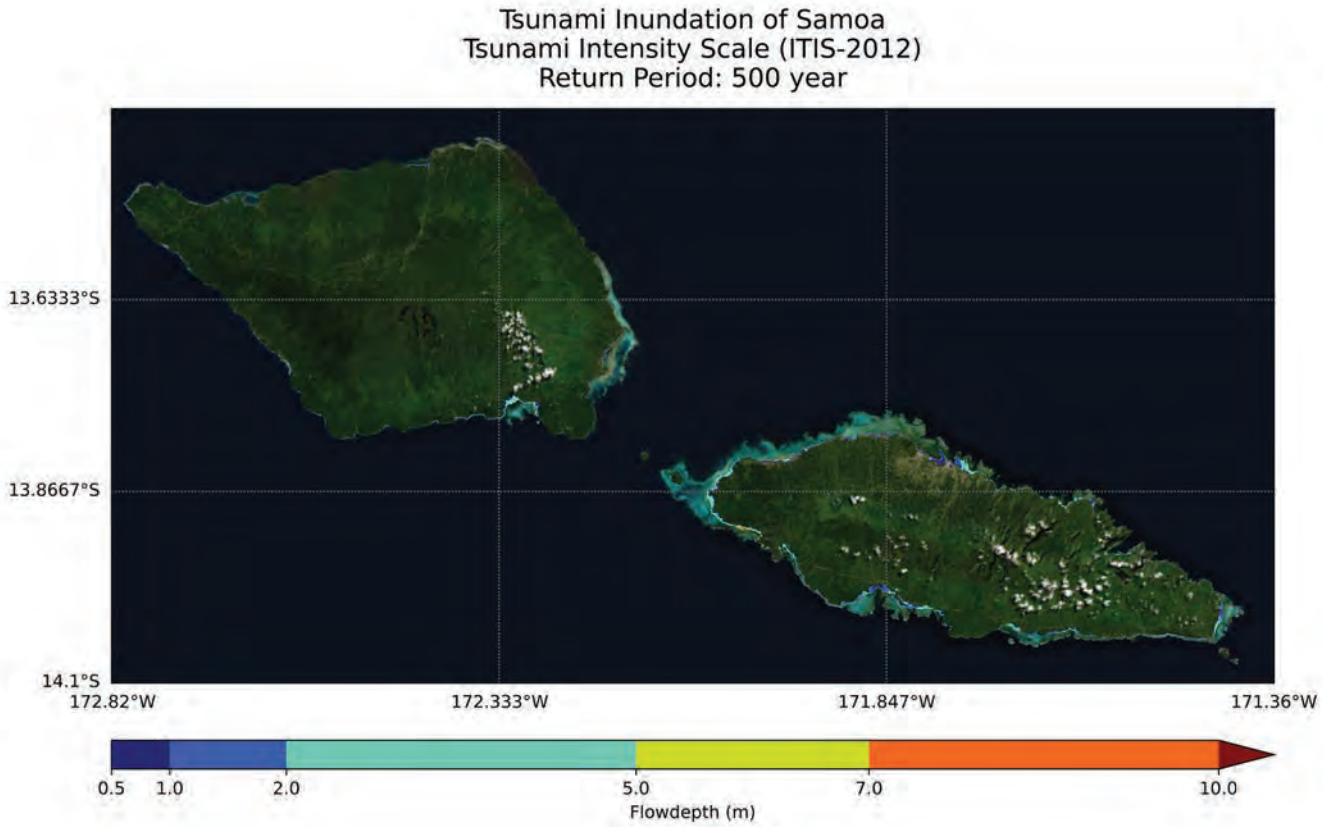
Tsunami Inundation of Samoa
Tsunami Intensity Scale (ITIS-2012)
Return Period: 500 year
13.6333°S
13.8667°S
14.1°S
172.82°W
172.333°W
171.847°W
171.36°W
0.5
1.0
2.0
5.0
7.0
10.0
Flowdepth (m)

c. RP 1000 year

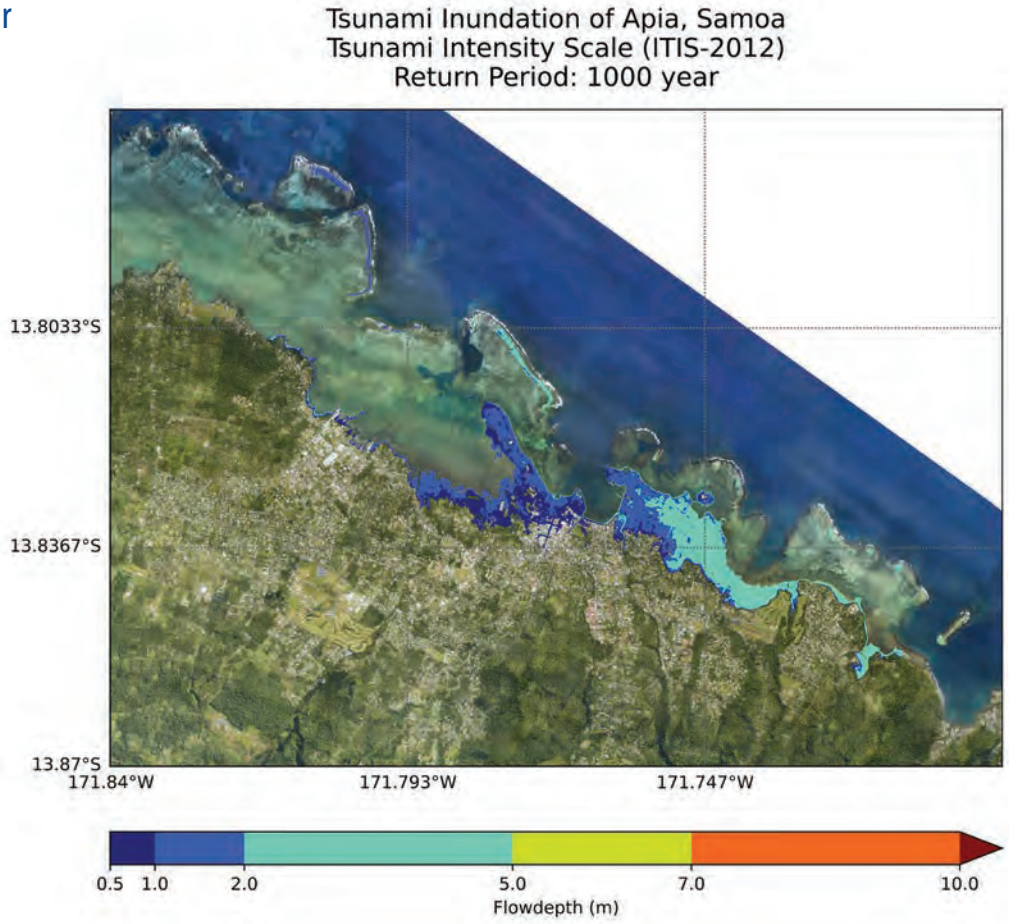

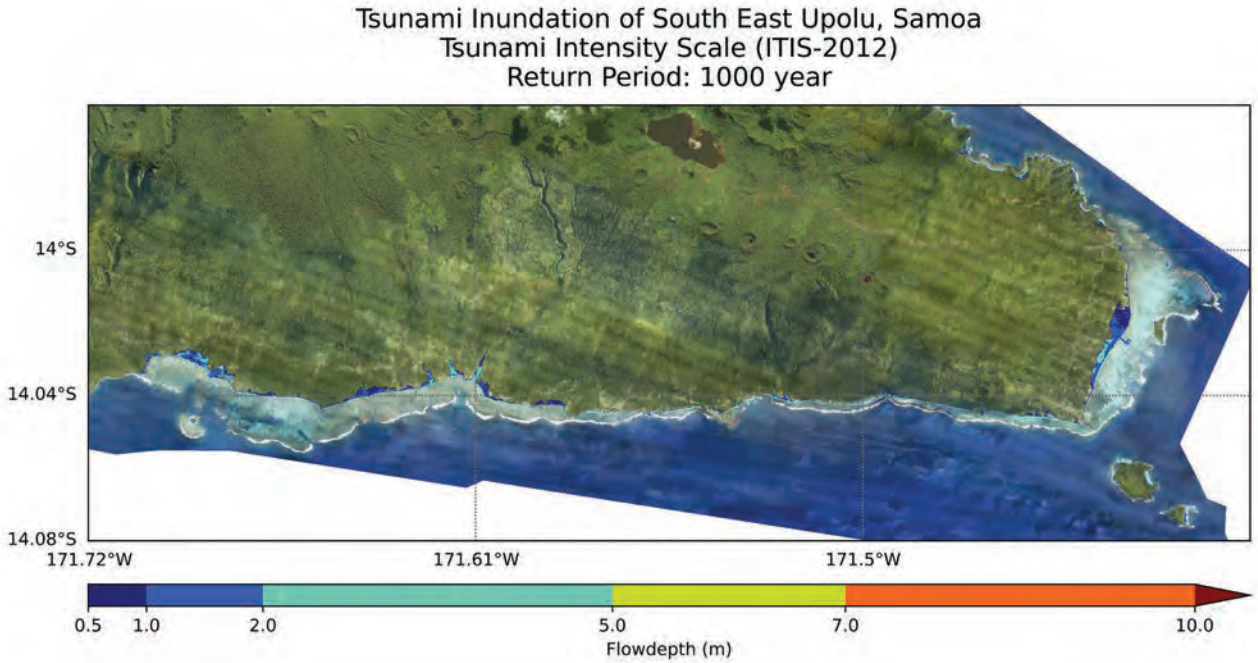

c. RP 1000 year

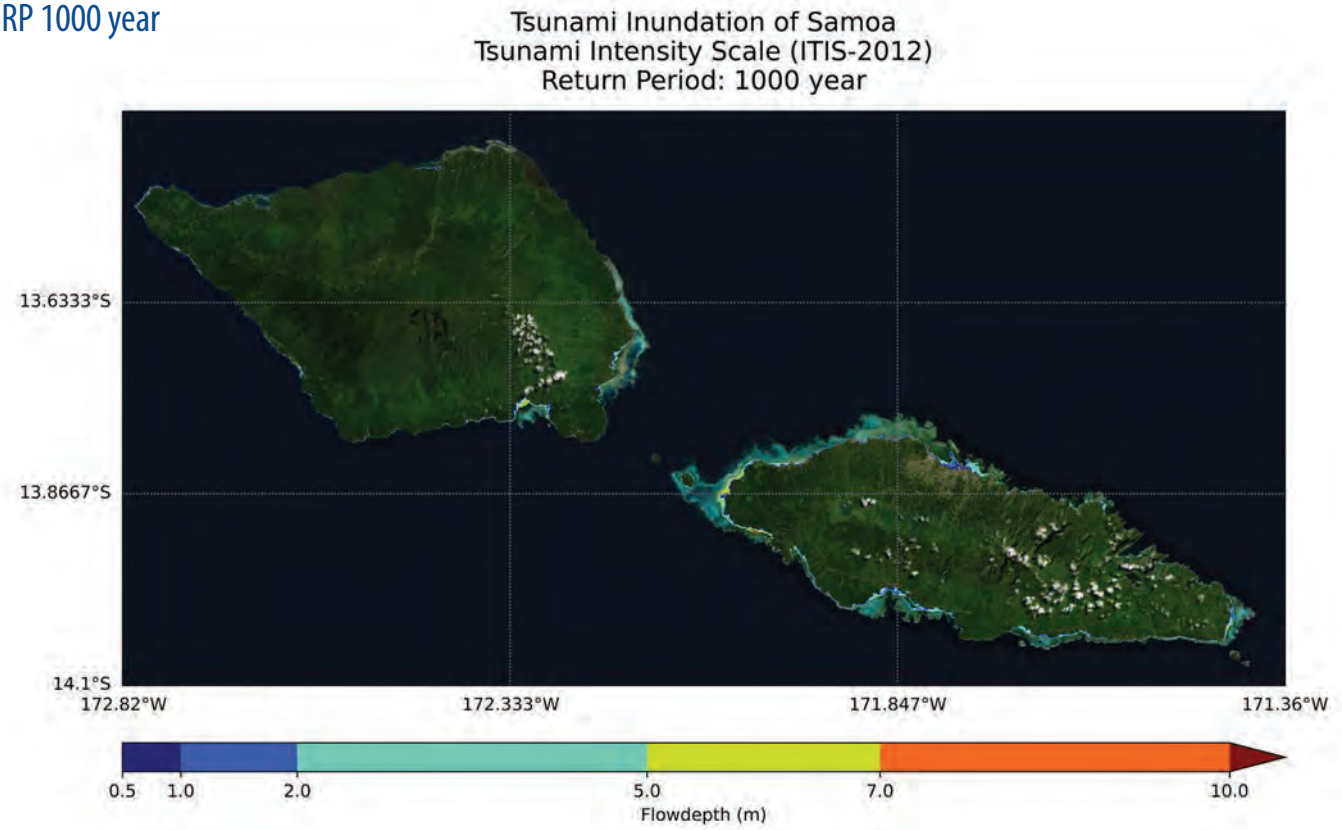

d. RP 2500 year 84th percentile

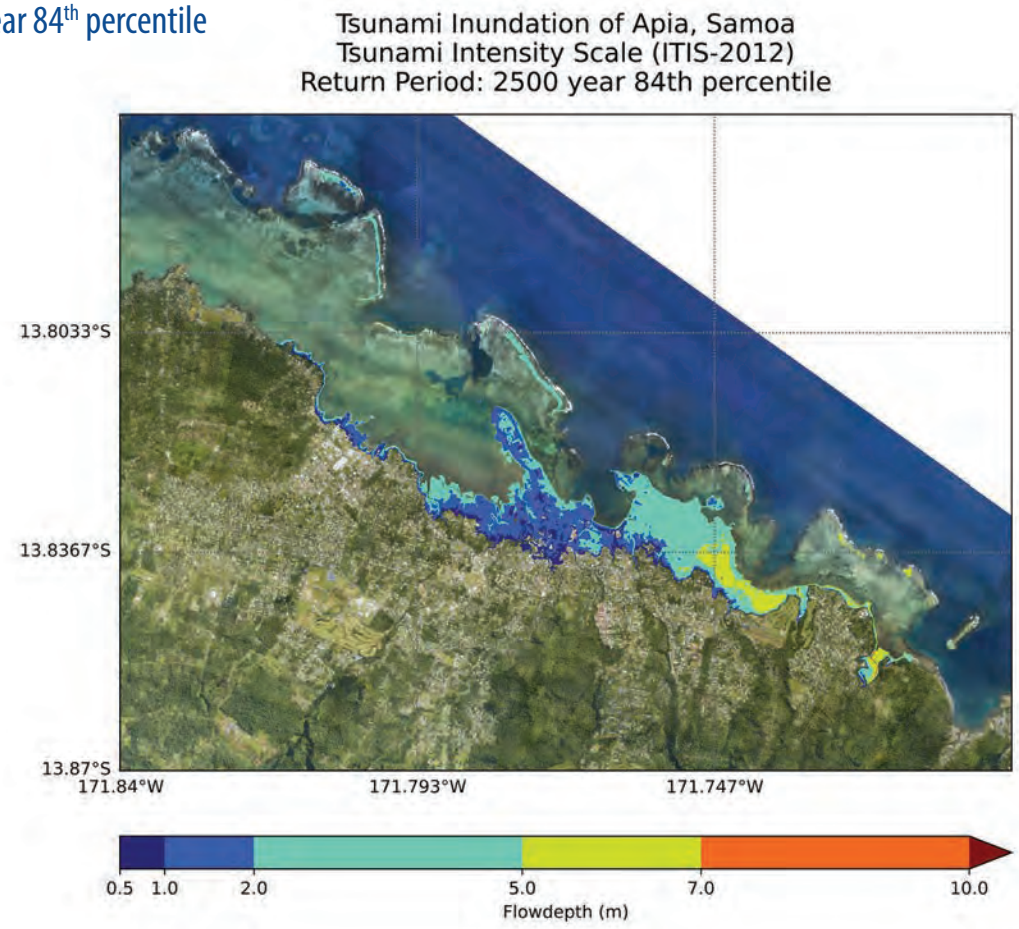

d. RP 2500 year 84th percentile

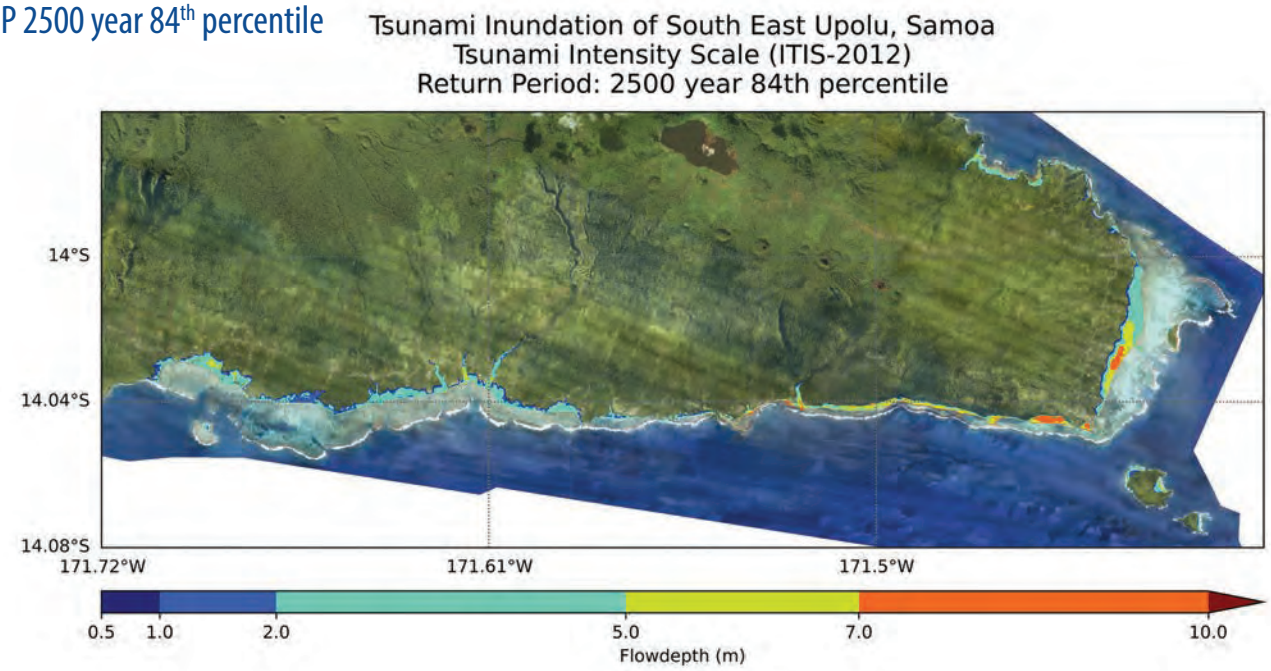

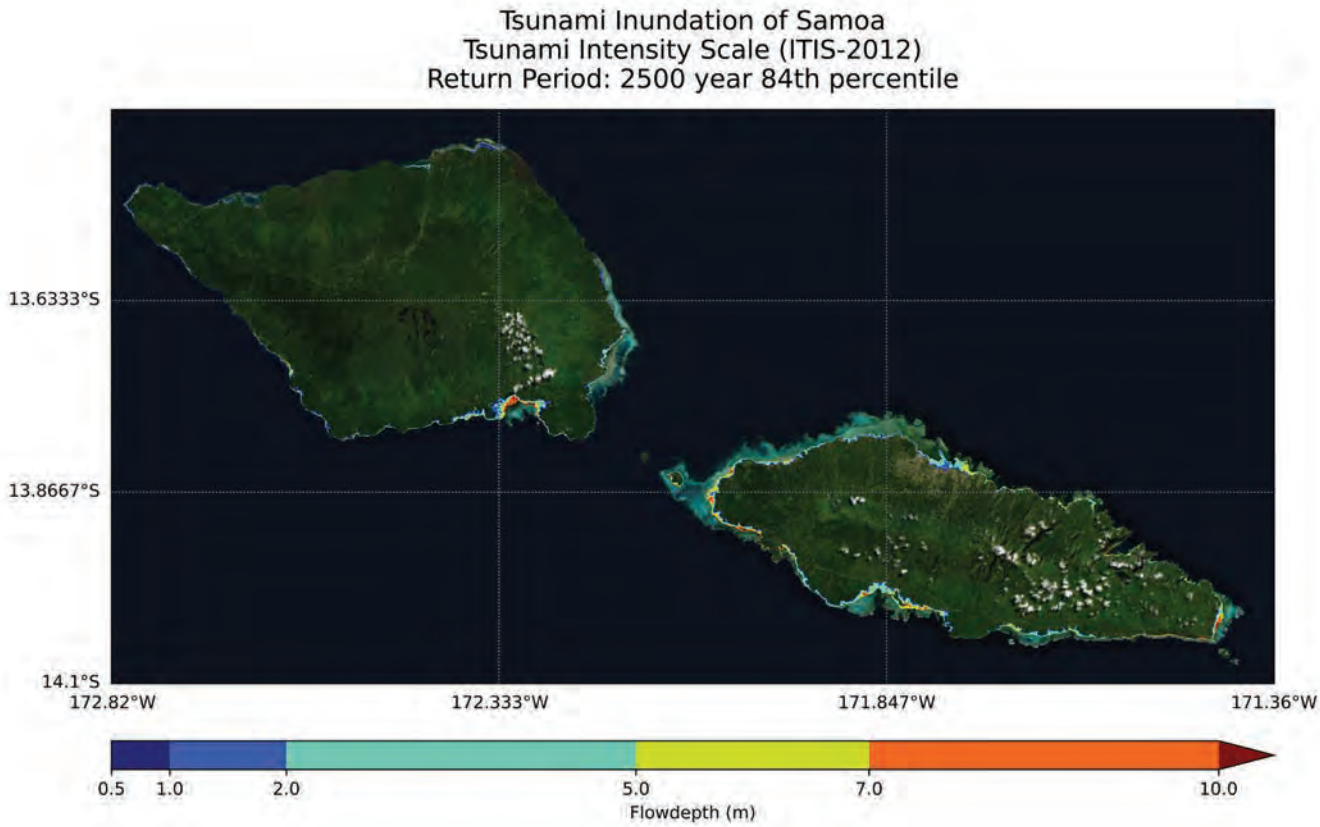

5.0 Event percent coverage per return period aggregation

a. RP 100 year

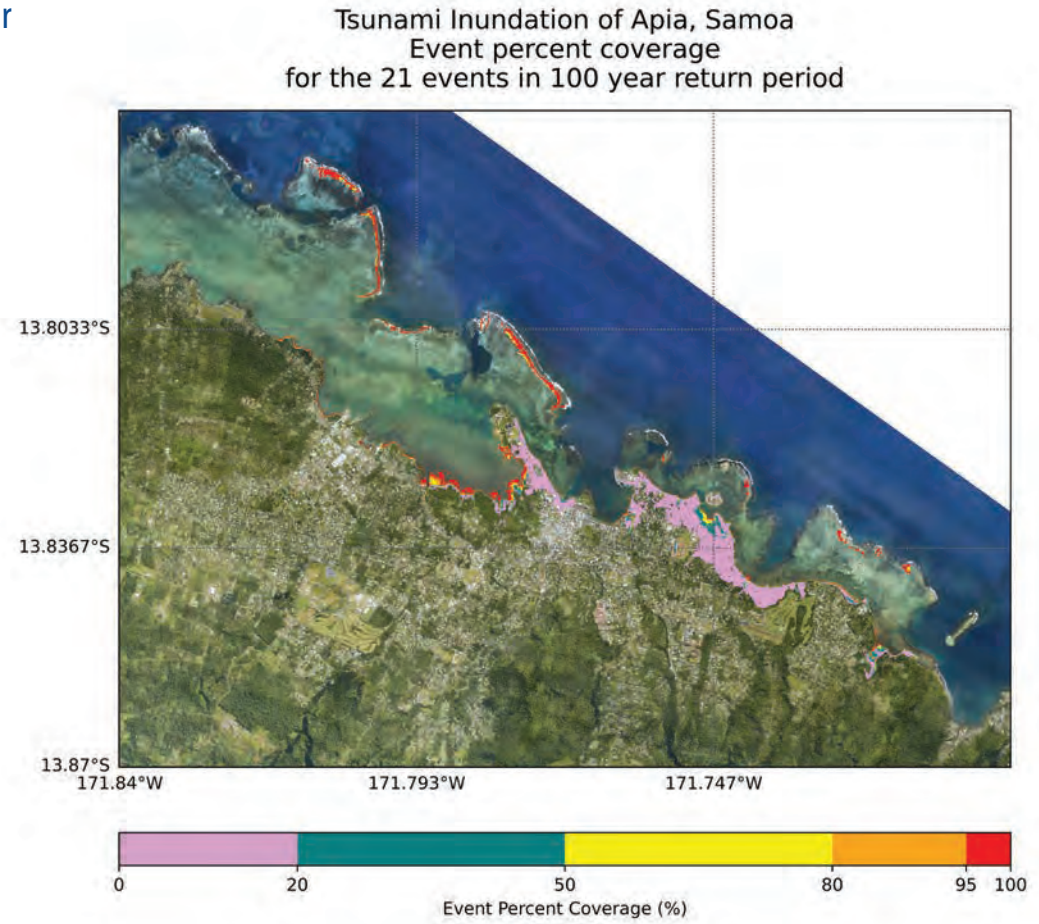

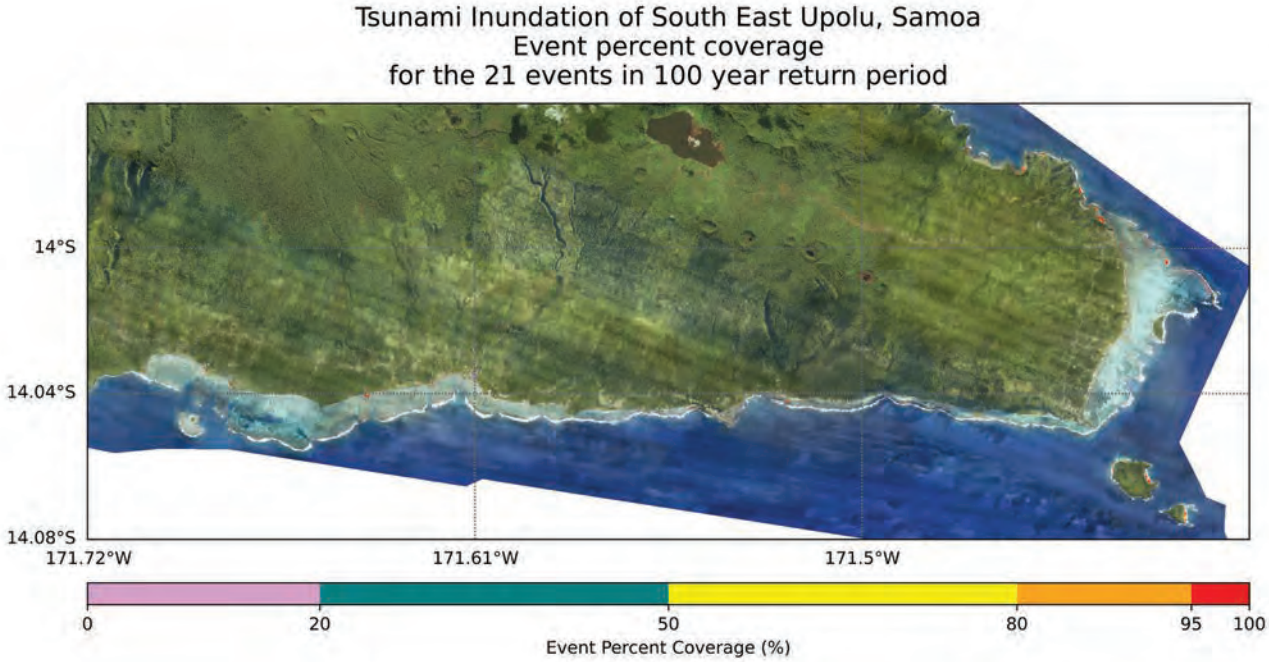

a. RP 100 year

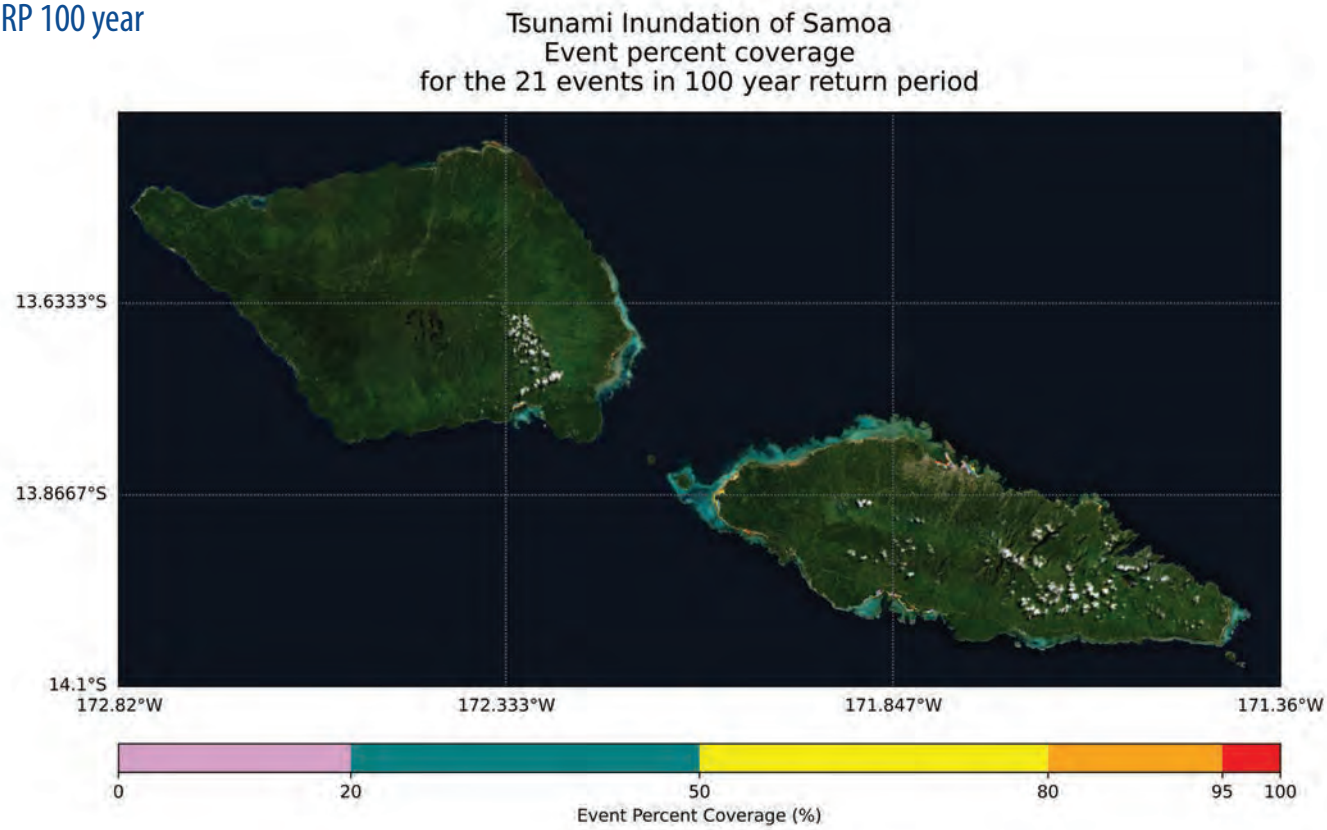

b. RP 500 year

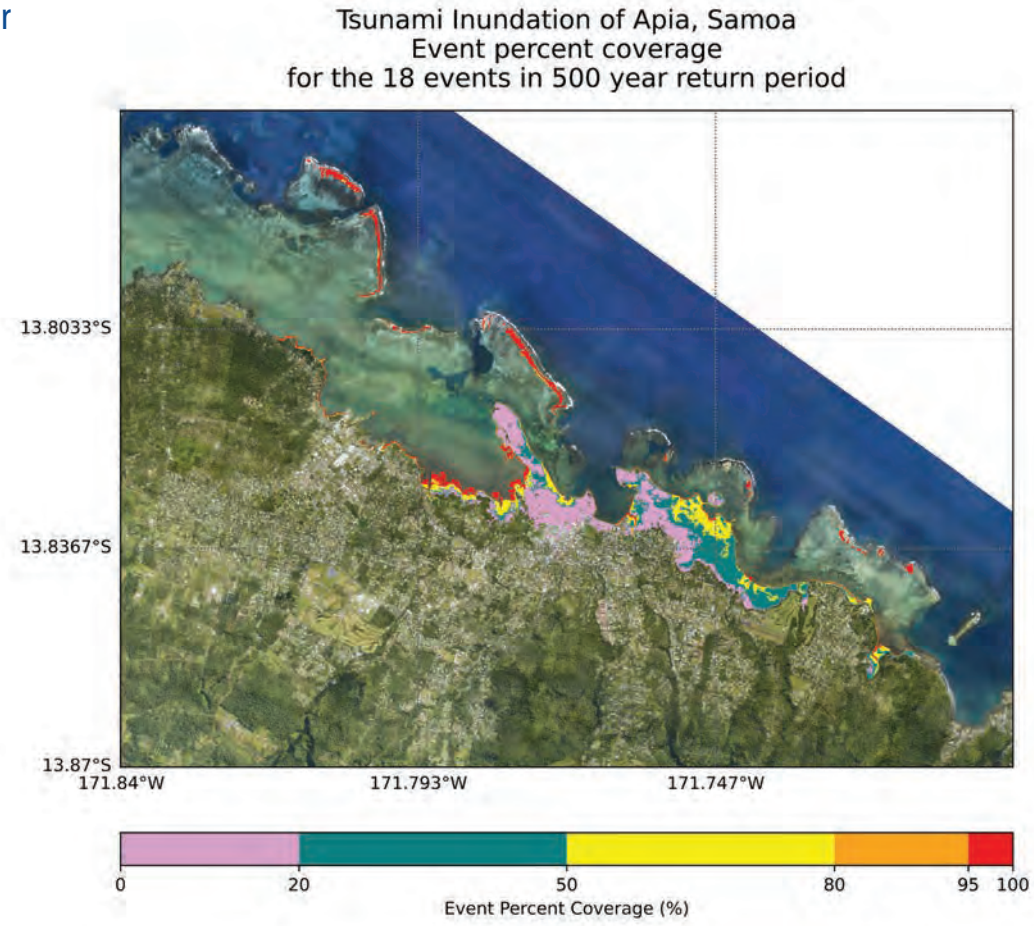

b. RP 500 year

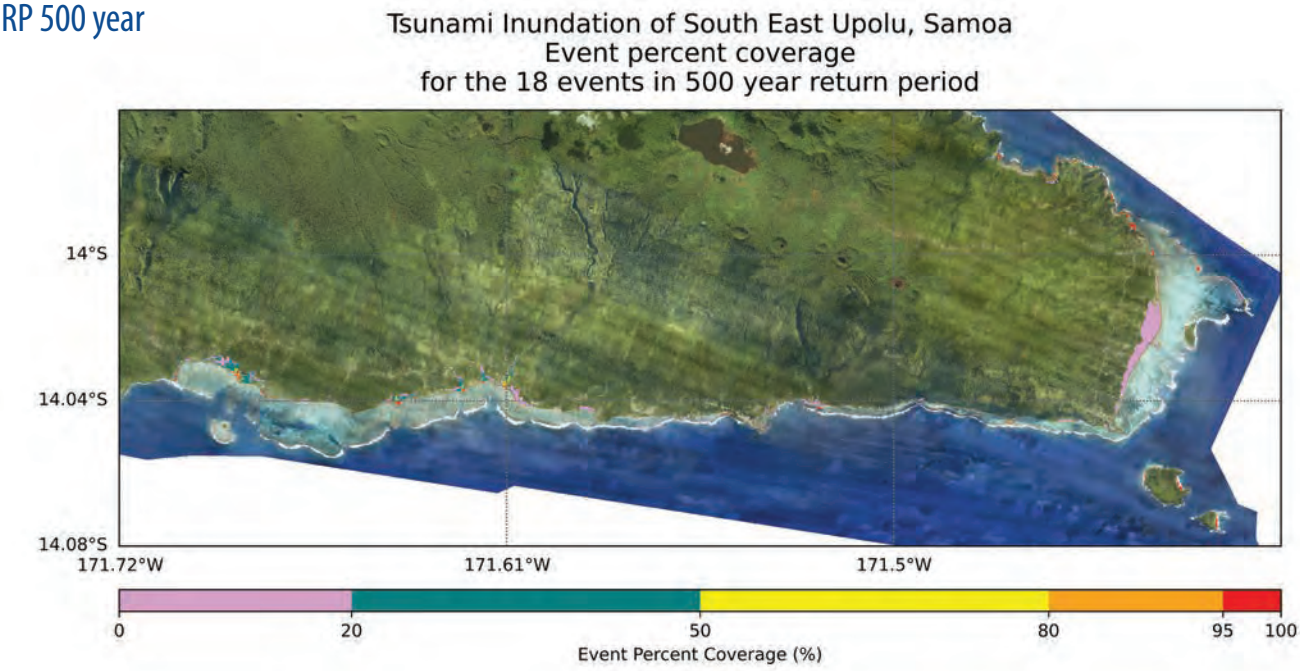
Tsunami Inundation of South East Upolu, Samoa
Event percent coverage
for the 18 events in 500 year return period
14°S
14.04°S
14.08°S
171.72°W
171.61°W
171.5°W
0
20
50
80
95
100
Event Percent Coverage (%)

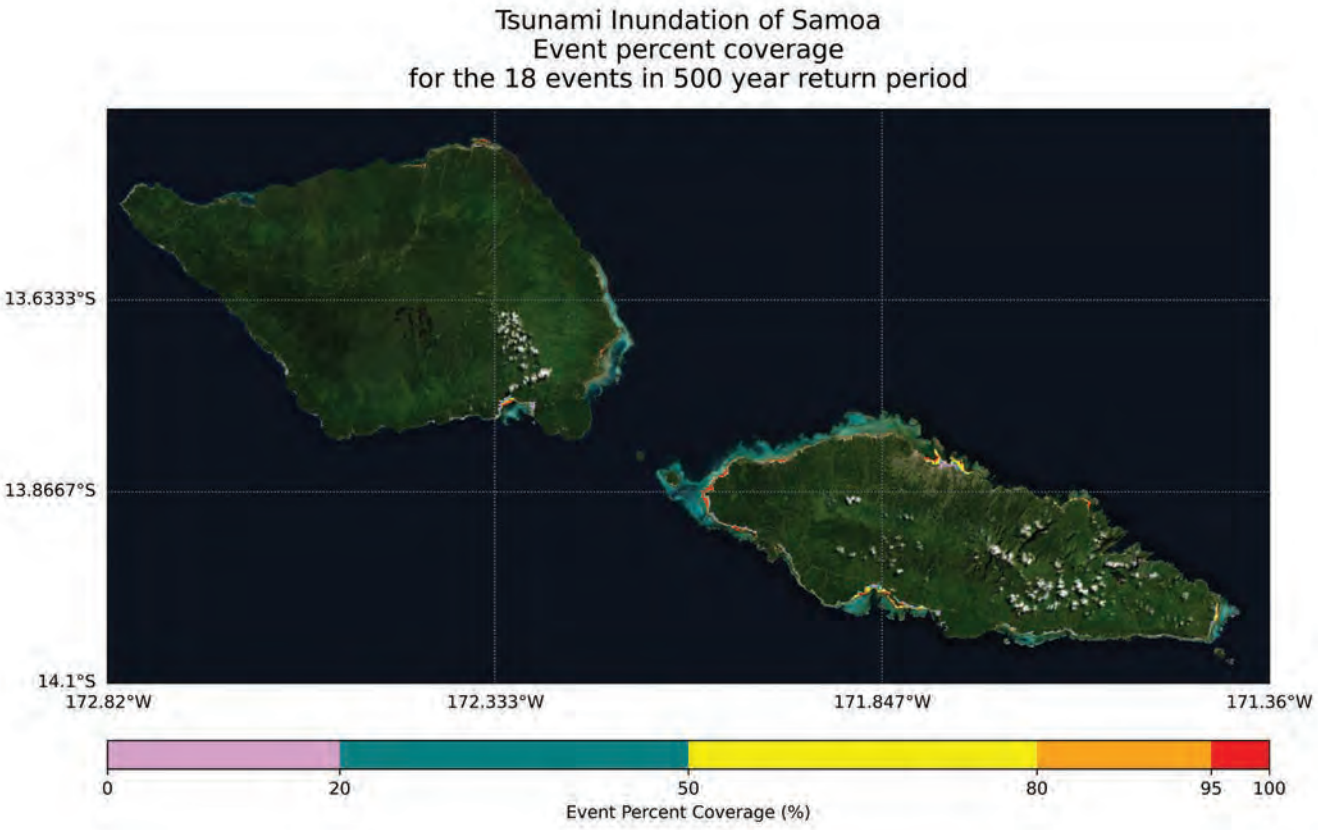
Tsunami Inundation of Samoa
Event percent coverage
for the 18 events in 500 year return period
13.6333°S
13.8667°S
14.1°S
172.82°W
172.333°W
171.847°W
171.36°W
0
20
50
80
95
100
Event Percent Coverage (%)

c. RP 1000 year

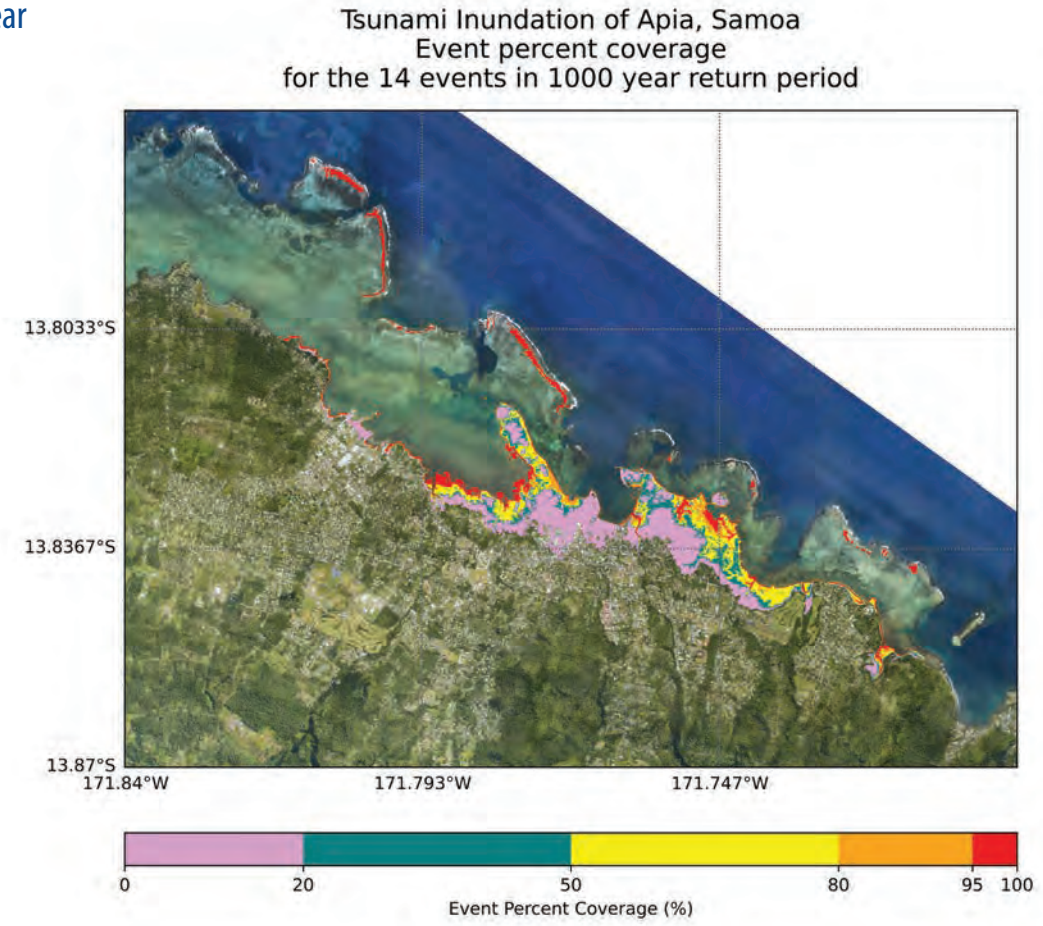

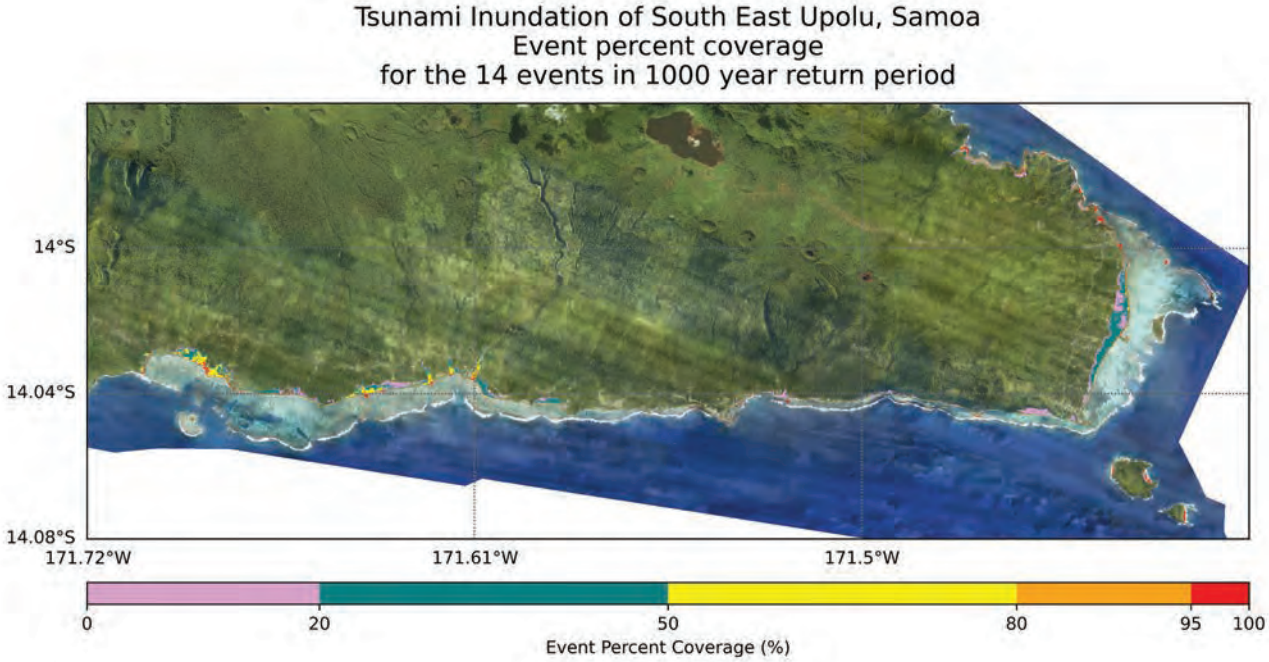

c. RP 1000 year

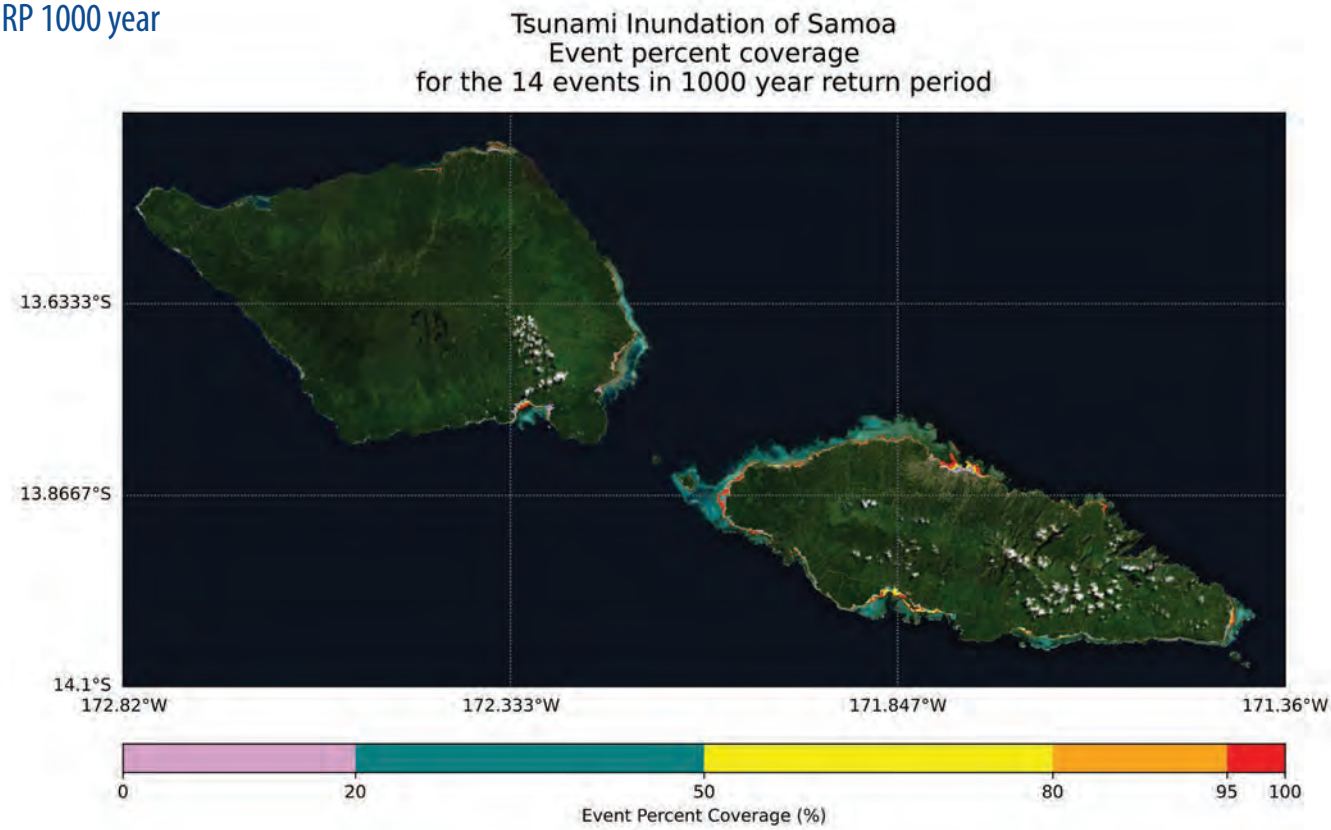

d. RP 2500 year 84th percentile

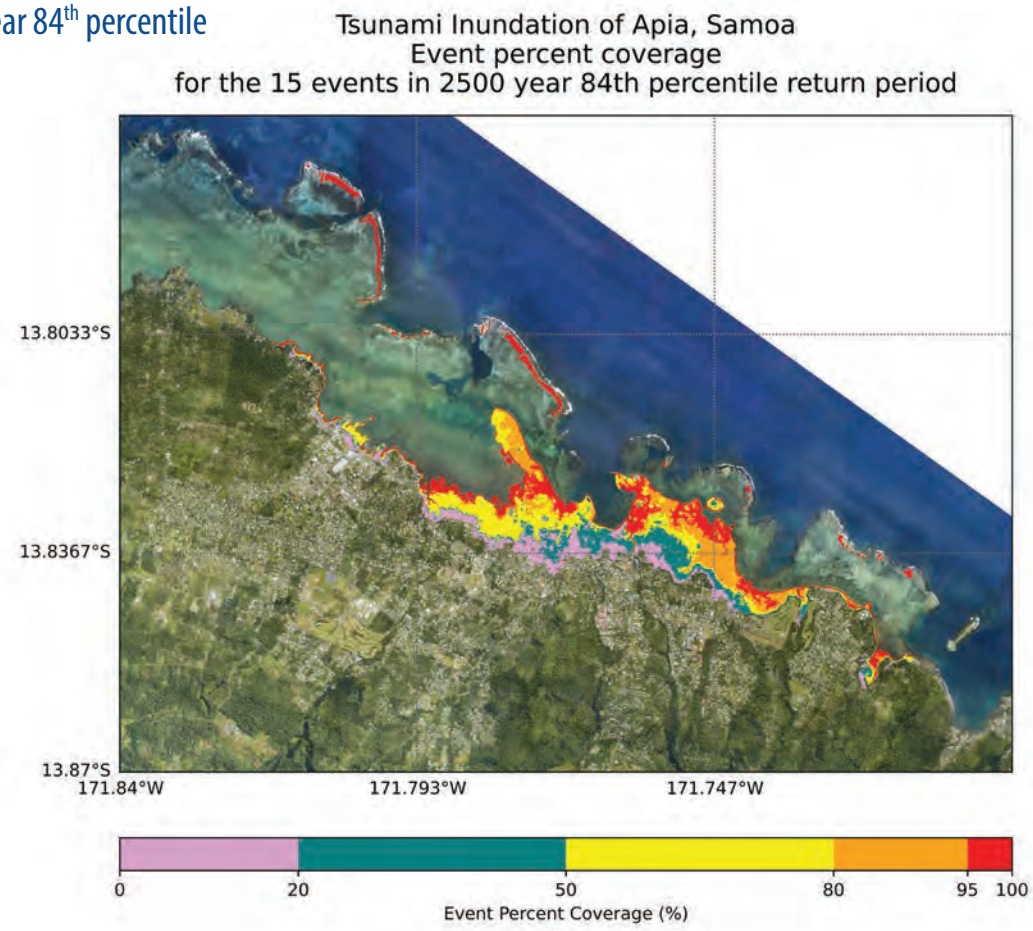

d. RP 2500 year 84th percentile

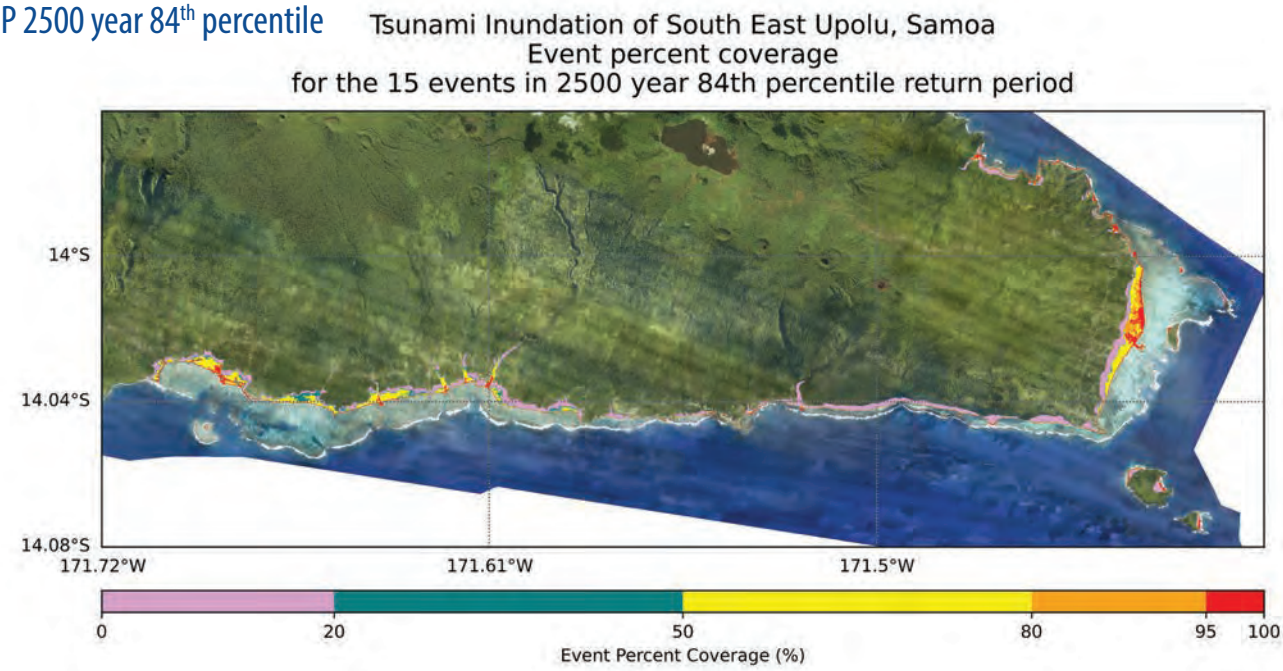

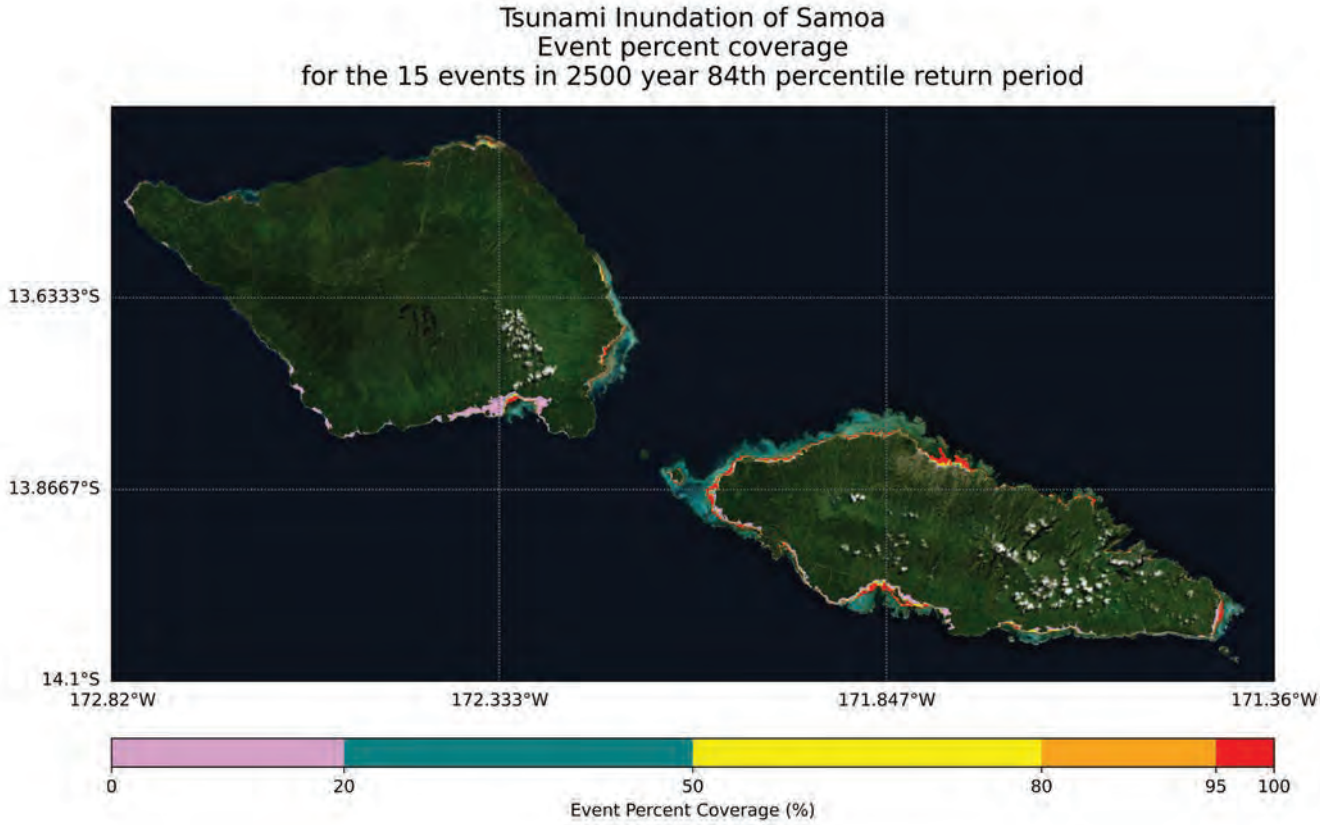

6.0 Maximum flux

a. RP 100 year

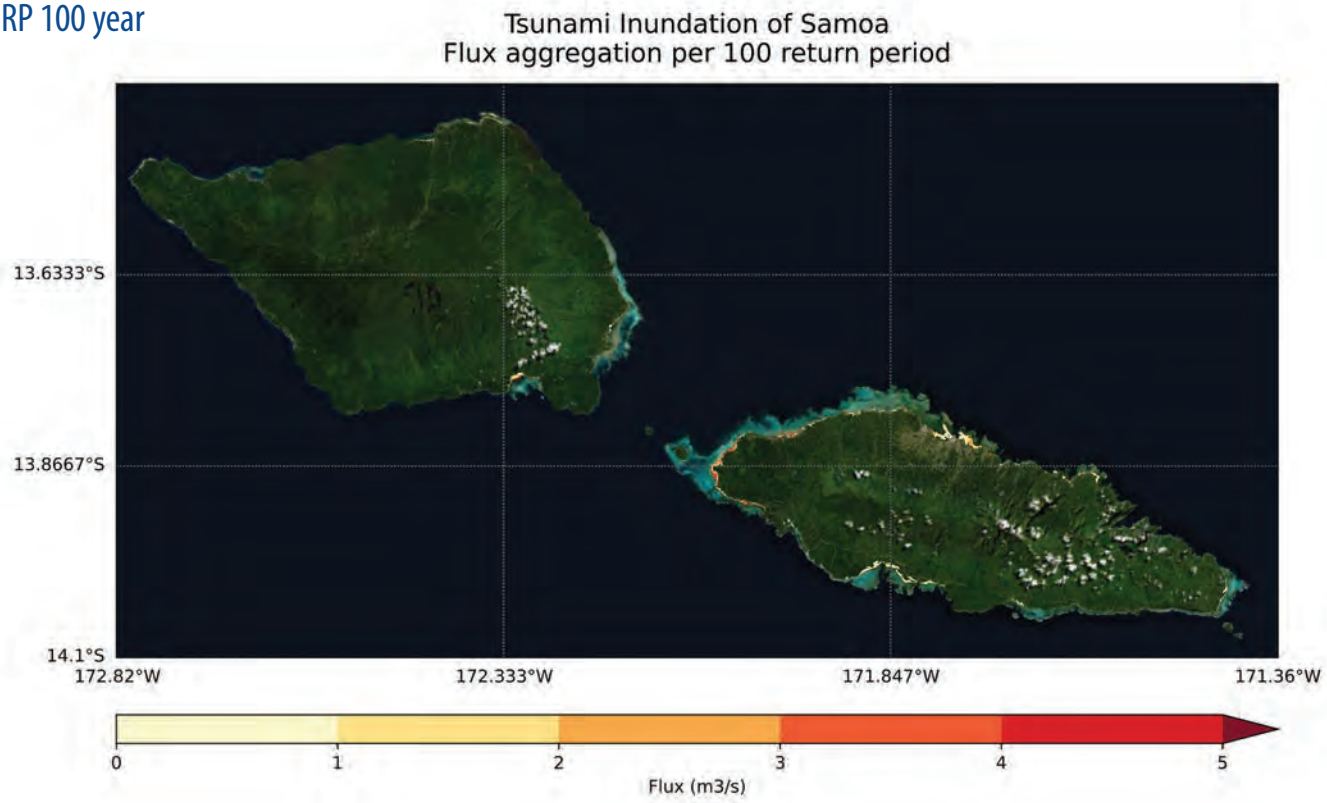

b. RP 500 year

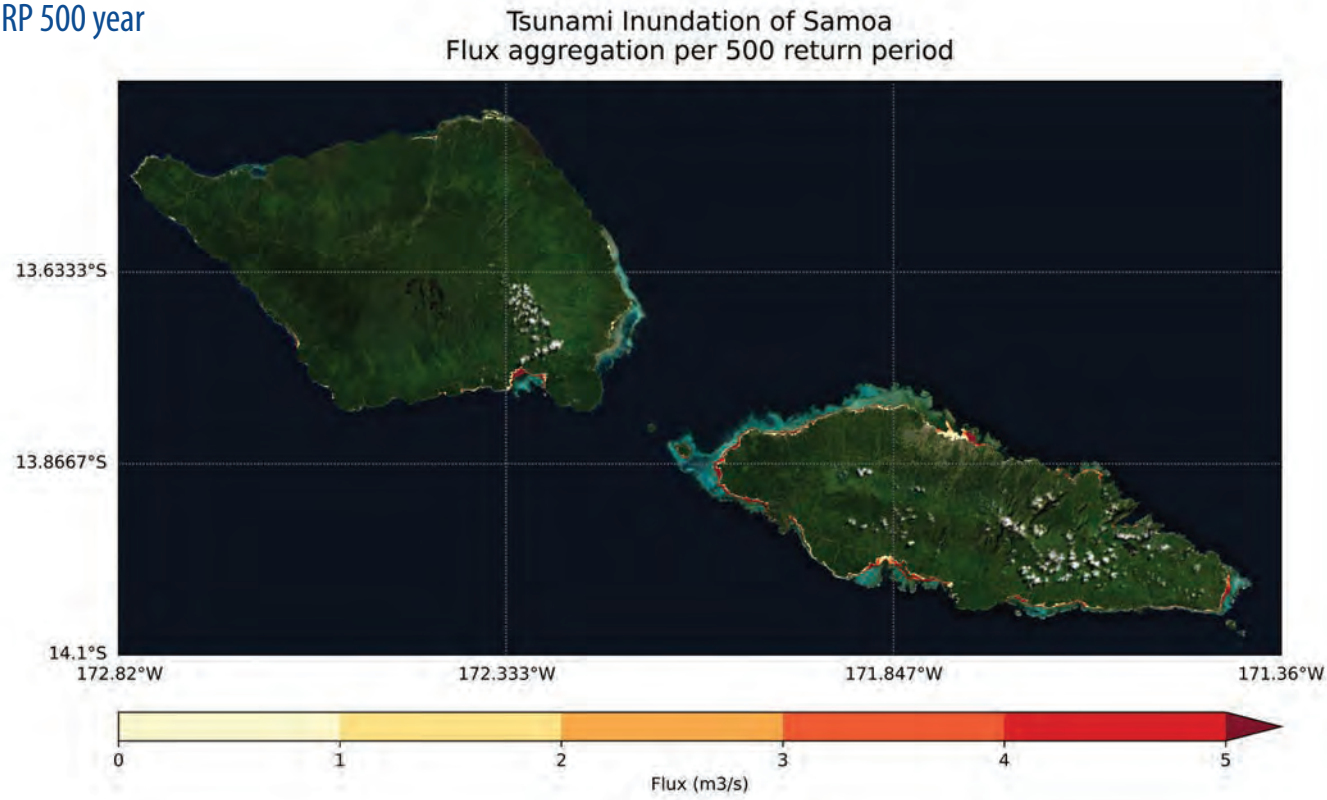

c. RP 1000 year

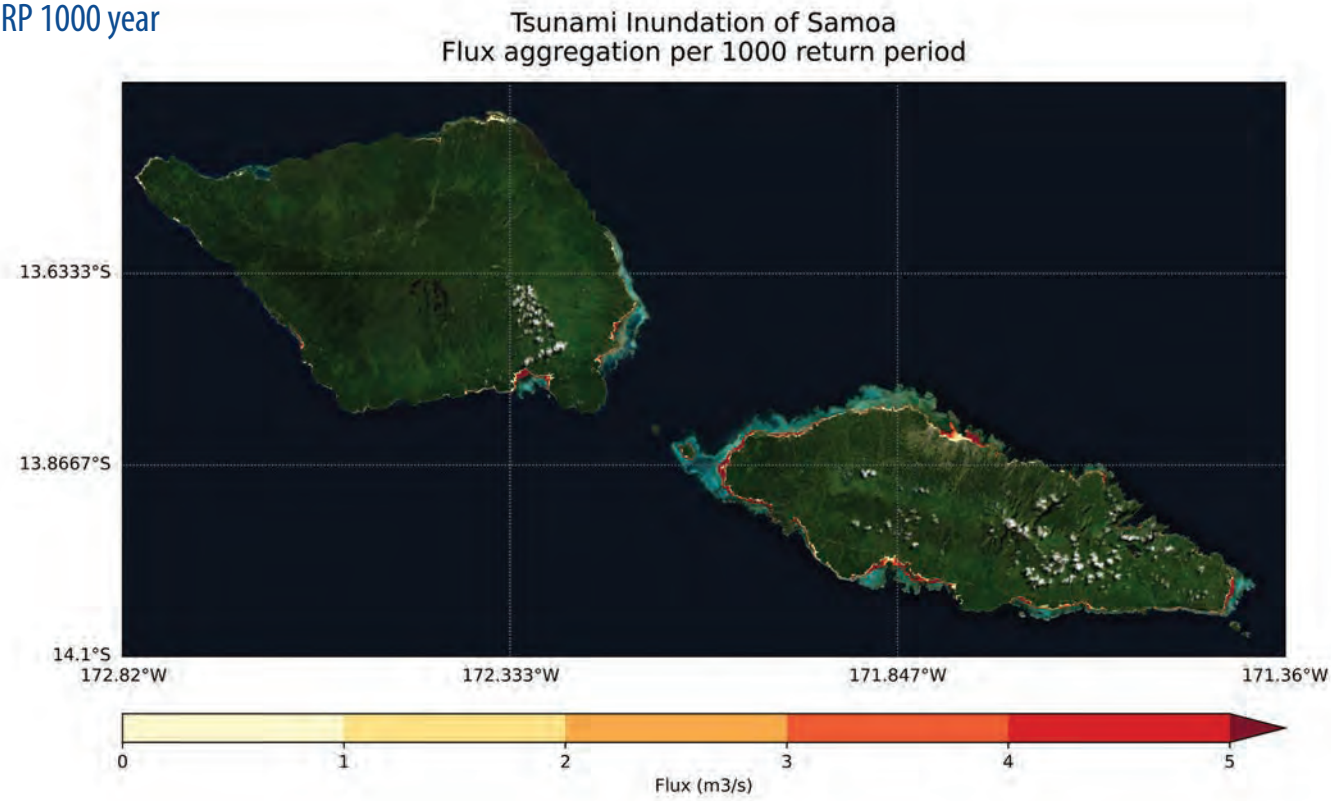

d. RP 2500 year 84th percentile

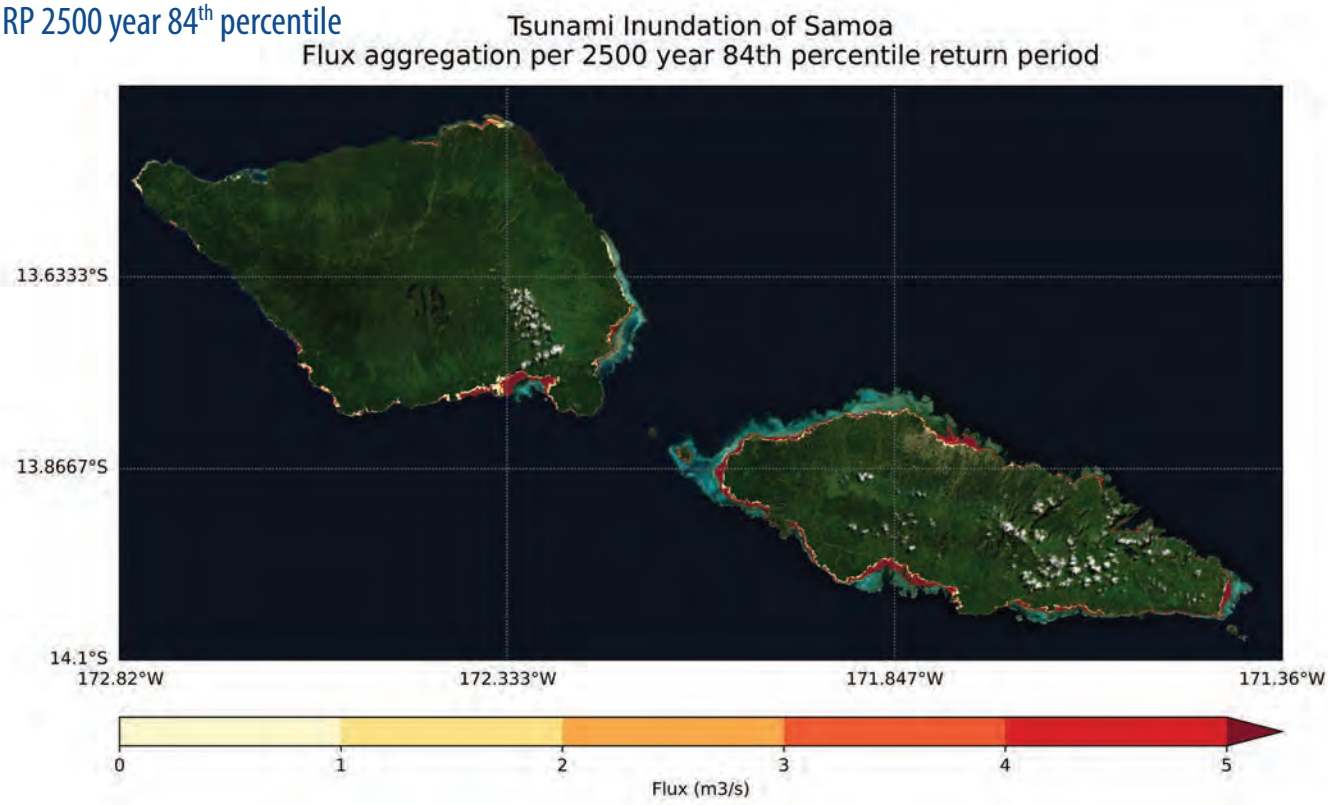

Produced by the Pacific Community (SPC)
Suva Regional Office
Private Mail Bag
Suva, Fiji
+679 337 0733
spc@spc.int | spc.int